Mitochondrial DNA as a biomarker for Bladder Cancer

Nana-Jane Chipampe

MIBMS, MRes, BSc (Hons)

This thesis is submitted for the degree of Doctor of Philosophy at Newcastle University.

Wellcome Centre for Mitochondrial Research, Newcastle Cancer Centre

September 2022

Author's Declaration

This thesis is submitted for the degree of Doctor of Philosophy at Newcastle University. The research was conducted across the Newcastle Cancer Centre and the Wellcome Trust Centre for Mitochondrial Research, Newcastle University, under the supervision of Prof Sir Doug Turnbull, Prof Rakesh Heer, Prof Rob Taylor, Prof Craig Robson, and Dr Helen Tuppen. I certify that none of the material presented here in this thesis has previously been submitted by me for a degree or qualification at this or any other university. This is my work unless stated otherwise.

COVID Impact Statement

I had made substantial progress with my PhD. However, COVID coincided with a particularly important part of my timetabled activity which was to take the optimisation work from the previous couple of years forward, into clinical material for a translation signal. As my PhD project relied on analysing patient bladder samples following Robotic cystectomy, with all routine planned surgery suspended this impacted the ability to collect data. I started a portion of the sequencing before lockdown, but the large majority of this remained to be completed, including a clinical cohort of urine along the bladder cancer tissue biopsies. This was a **major impact,** and we could not mitigate for this loss of work without extension. Moreover, with socially distant lab work and limited lab access, it was essential to have more time to meet the main objectives of my Studentship. I had my supervisor Professor Rakesh Heer's full backing and on-going support for an extension under these extenuating circumstances.

Abstract

Introduction

Although we take bladder function for granted, across the world ageing brings symptomatic lower urinary tract dysfunction to many individuals and risk of malignant transformation. Bladder cancer is the most prevalent urinary tract cancer and one of the most expensive cancers to manage on the NHS. The current diagnostic test, cystoscopy is **invasive** requiring lifelong patient monitoring.

The major clinical problem is a 40% risk of recurrence within 3 years. Associated with recurrence is the risk of stage progression to muscle-invasive, carrying a high mortality risk.

Herein, lies the unique translational opportunity of mitochondrial DNA (mtDNA). During ageing, mtDNA accumulates transformations that can lead to disease. Clonally expanded mtDNA variations have been observed in many tumours and I investigated whether clonally expanded mtDNA transformations are present in bladder tumours. Importantly, as tumour cells are readily shed into the urine, I explored the detection of clonally expanded mtDNA alterations in urine.

Methods

Following Radical Cystectomy, bladder tumour tissue, normal bladder tissue, matched urine, and blood were collected. DNA was extracted and PCR was performed to amplify mtDNA and mtDNA sequencing to detect mtDNA genotypes specific to the tumour. Bladder tissue sections were cut, stained with Haematoxylin and Eosin, and tumour content was determined by Pathologists.

Results

Tumour-specific mtDNA variants were detected in all patients with confirmed tumour tissue and were undetected or found at markedly lower or higher levels in the patient's normal bladder lining. These tumour-specific mtDNA genotypes were also identified within the patients' urine and formalin-fixed paraffin-embedded (FFPE) bladder tumour samples.

Conclusion

Bladder tumours possess a unique mtDNA genotype or barcode, that can be readily detected in patients' urine and FFPE bladder tumour material. Taking advantage of urine, a liquid biopsy of bladder tumour mtDNA offers a non-invasive paradigm to trace Bladder Cancer recurrence.

Acknowledgements

I would like to dedicate this thesis to my wonderful parents, who have always taught me that with hard work, dedication, determination, and motivation, I can achieve anything in life. Thank you for always supporting me, encouraging me, providing me with solid advice, and leading by example. I am who I am today, because of you. Thank you to my siblings Chabu, Aisha, and Natasha for the unending support, love, encouragement, and familial bond that will last for eternity.

I must thank my supervisor Professor Rakesh Heer for all his support, direction, encouragement, and valuable advice throughout this PhD journey. Particularly, your positivity, and compassion, coupled with your clinical and academic dedication, are a personal inspiration. Thank you to Dr Helen Tuppen for all your time, support, experimental guidance, advice, and kind nature. Professor Craig Robson, I am grateful for the opportunity you gave me to undertake a career in academic research and fruitful discussions. To Professor Rob Taylor, thank you for your input, guidance, suggestions, and invaluable advice throughout this project. I am grateful to pathologists Dr Amira El-Sherif and Dr Abed Zaitoun as your expert clinical opinion when assessing tumour content greatly assisted this research.

To Ana, seeing you in the corridor when performing long experiments out of hours continually motivated me, thank you for the many wonderful sociable times we had together. For all my friends, a sincere thank you for the kind words, elevation, and enjoyable times and listening ears. To Dr, Uncle Vincent for your personal inspiration, may your soul rest in heavenly peace. Salut to the ones here today, and to the ones that we lost on the way.

I am sincerely grateful to the NIHR, my funding body, and to all patients who consented and donated their tissue for research use within this project, as, without which, this work would not have been possible.

Table of Contents

Table of Figures

List of Tables

List of Abbreviations

APC	Allophycocyanin
ATP	Adenosine triphosphate
BC	Bladder Cancer
BCG	Bacillus Calmette Guérin
BioCOSHH	Biological Control of Substances Hazardous to Health
CIS	Carcinoma-in-situ
CK	Cytokeratin
cfDNA	Cell-free DNA
D-loop	Displacement loop
DMSO	Dimethyl Sulfoxide
DNA	Deoxyribonucleic acid
EMT	Epithelial-mesenchymal transition
ETC	Electron Transport Chain
EORTC	European Organization for Research and Treatment of Cancer
FACS	Fluorescence Activated Cell Sorting
FCS	Foetal Calf Serum
FFPE	Formalin-fixed Paraffin-Embedded
FSC	Forward Scatter
FSC-A	Froward Scatter Area
FSC – H	Forwards Scatter Height
H&E	Haematoxylin & Eosin
HG	High grade
ISPs	Ion Sphere particles
LCM	Laser Capture Microdissection
LG	Low grade
LUTS	Lower urinary tract symptoms
MET	Mesenchymal-Epithelial transition
MIBC	Muscle-Invasive Bladder Cancer
MMR	Mis match repair
Ms	Milliseconds

mtDNA	Mitochondrial DNA
NAT2	N-acetyltransferase
NGS	Next Generation Sequencing
NMIBC	Non-Muscle Invasive Bladder Cancer
OXPHOS	Oxidative phosphorylation
PCR	Polymerase Chain Reaction
PPE	Personal Protective Equipment
RBC	Red Blood Cell
ROS	Reactive oxygen species
RPM	Rotations per minute
rRNA	ribosomal RNA
SNPs	Single Nucleotide Polymorphisms
SOP	Standard Operating Protocol
SSC	Side Scatter
SSC-A	Side Scatter Area
tRNA	Transfer RNA
TURBT	Transurethral resection of the Bladder Tumour
UcfDNA	Urinary cell-free DNA
W/V	Weight/volume
µl	microlitre
µm	micromolar

Chapter 1: Introduction

Bladder cancer

1.1 Bladder cancer pathology

The urinary bladder is a hollow, distensible organ of the urogenital system. It is located inferior to the peritoneum and behind the pubic symphysis in the pelvis. The bladder has a capacity of 400–500 ml; it is made up of complex overlaps of smooth muscle fibres that enable the organ to carry out its primary function, which is efficient emptying of its contents. This urinary organ consists of three smooth layers of muscle known collectively as the detrusor muscle. The synergistic relaxation of the detrusor muscle and the contraction of the bladder and pelvic muscles enables humans to control bladder and bowel functions. This control is known as continence.

1.2 Molecular subtypes of non-muscle invasive bladder cancer

Non-muscle invasive bladder cancer (NMIBC) is observed within the tissue that lines the inner bladder surface. Urologists have observed that it comprises various clinical phenotypes, which are described below in Table 1 and visualised in Figure 1.

Carcinoma in Situ (CIS)
Ta – Non-invasive
T1 – Invasive high-grade phenotype
T2 – Superficial muscle infiltrate
T3 – Tumour has spread to perivesical fat
T4 – Tumour has spread to pelvic wall and surrounding organs

Table 1 – Diverse clinical phenotypes presented in NMIBC patients.

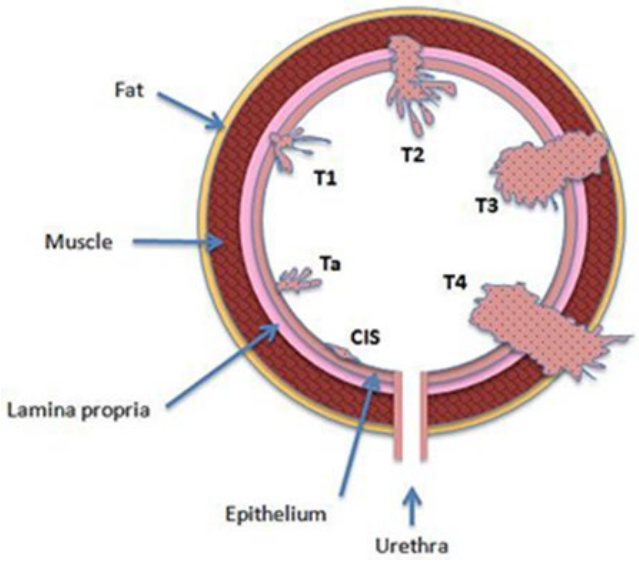

Figure 1 – Schematic illustration of various Bladder Cancer stages (Urology Today, UK).

CIS is a high-grade intraepithelial cancer, typically a high-grade (HG) flat tumour confined to the surface of the bladder lining. Ta indicates a non-invasive papillary carcinoma, often removed with Transurethral resection of the bladder tumour (TURBT). T1 the tumour has migrated to the connective tissue, T2 with a more migratory phenotype and the tumour is now situated within the muscle of the bladder. At stage T3 the tumour is embedded in the

perivesical fat layer of the bladder, and represented at stage T4, the tumour has now spread to lymph nodes and nearby organs such as the prostate in men and uterus in women.

Hedegaard and colleagues conducted an extensive transcriptional analysis of 460 primary-phase bladder adenocarcinomas. The authors reported that NMIBC could be sub-grouped into three major classes that showed basal and luminal-like characteristics and presence of which produced different clinical outcomes (Hedegaard et al., 2016). Variations in biological processes such as the cell cycle, epithelial-mesenchymal transitions (EMTs), and differentiation were importantly observed within urothelial carcinomas (Hedegaard et al., 2016).

Categorisation of molecular subtypes within NMIBC

Class	Histological Features	Classification
1	Luminal	Tumours with the greatest prognosis, characterised by early cell-cycle gene expression. Early stage, LG tumours, low likelihood of progression Modifications that activate fibroblast growth-factor receptor 3 (FGFR3) are prevalent.
2	Luminal	Tumours (particularly CIS) display increased expression of late-cycle genes. Associated with EMT markers. The greatest number of progression events observed. Perhaps because muscle-invasive cancers are thought to emerge from CIS, tumours within this group may have a genomic profile that identifies them as being at enhanced risk of advancement to muscle-invasive bladder cancer.
3	Basal	Tumours display features similar to those of basal tumours, advanced stage, high grade. Tumours are associated with primitive cytokines and increased expression of CD44, a bladder cancer stem cell marker identified by Volkmer et al., (2012). Activating modifications of FGFR3 are commonly found.

Table 2 - Molecular subtypes within NMIBC have been categorised by identifying variations in histological features, allowing the classification of urothelial tumours. The three classes identified are characterised in the table above. The author and colleagues reported luminal and basal histological featured subgroups within NMIBC, after a transcriptional investigation of 460 primary phase bladder adenocarcinomas (Hedegaard et al., 2016)*. Typically, three molecular subtype classes were found to be present, with variations observed and outlined above.*

The author and colleagues predicted markers of differentiation states in Bladder Cancer (BC) highlighting basal, intermediate, and umbrella cells that characterised cellular differentiation, from primitive cell stages to mature (Volkmer et al., 2012). As such, our understanding of mechanisms within BC that lead from normal tissue development to malignant transformation has been enhanced.

NMIBC is comprised of three main cellular features; basal, luminal, and, within luminal, a p53-like sub-class of cells as seen below in Figure 2. Basal cells have squamous features, which display similarities with lung, neck, and head cancers (J N Weinstein et al., 2014). The p53-like alterations appear to involve an infiltration of stromal fibroblasts (Lerner & Robertson, 2016). Luminal features are identified histologically as class two, high-risk encompassing tumours, with specific uroplakins that function as markers of terminal luminal differentiation (Wu et al., 2009).

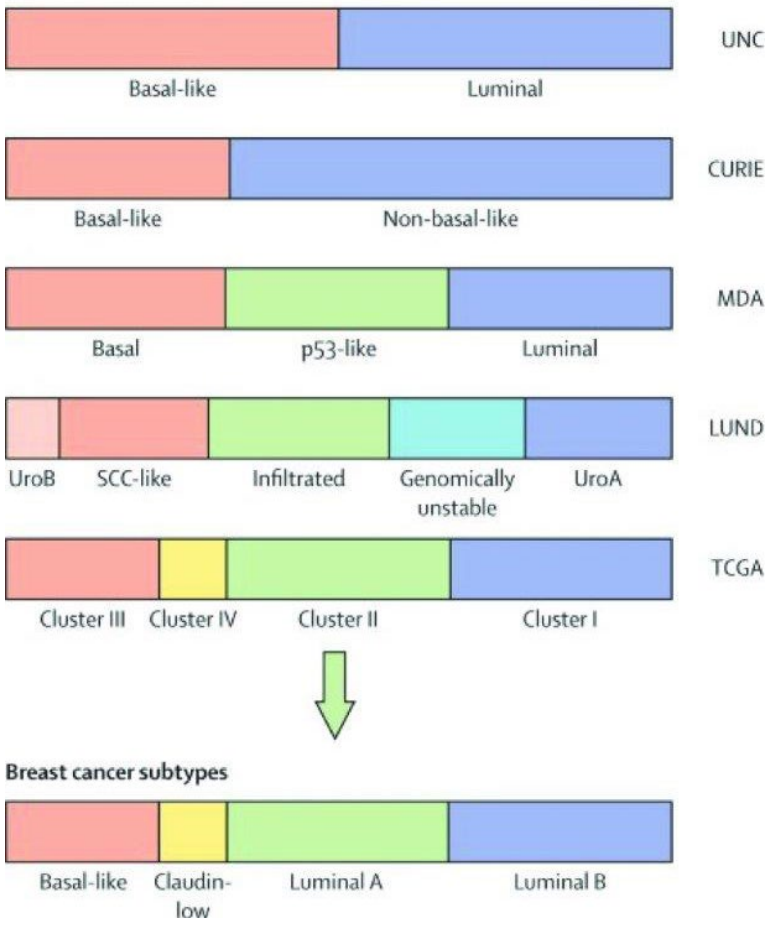

Figure 2 – Molecular subtype classification of NMIBC: UNC = University of North California, CURIE = Institute Curie, MDA = The University of Texas MD Anderson Cancer Centre, LUND = Lund University, TCGA = The Cancer Genome Atlas, SCC- Squamous Cell Carcinoma, UroA = Urobasal A (L Kamat, Lerner, et al Lancet, 2016; 388: 2796–810, Bladder cancer).

Various scientific studies have extensively reported the sub-classification of Muscle-Invasive Bladder Cancer (MIBC) into luminal and basal subtypes. Choi et al. (2014) in an investigation of MIBC, stated that differential expression of cytokeratin (CK) was a typical marker of muscle-invasive disease and a distinctive hallmark of the presence of chemo resistant luminal CK20 and aggressive basal CK5 subtypes in MIBC. Various combinations of the 20 cytokeratins are critical for cell integrity and are known to be expressed within the epithelia of BC tissue (Breyer et al., 2017).

CK5 is expressed within the basal urothelium and can be used as an identifier of progenitor stem cells (Moll et al., 1992). CK20 has been identified as a histological diagnostic marker in non-bladder cancers. Moll and colleagues reported that CK20 was entirely expressed in umbrella cells, and their work identified it as an exciting marker of luminal differentiation. Choi *et al*. (2014) also confirmed CK20 expression in umbrella cells within the superficial bladder layer and thereby identified a well-characterised hallmark of luminal subtypes. It has since been suggested that positive differential CK expression may be useful as a predictor in the diagnosis of T1 stage NMIBC.

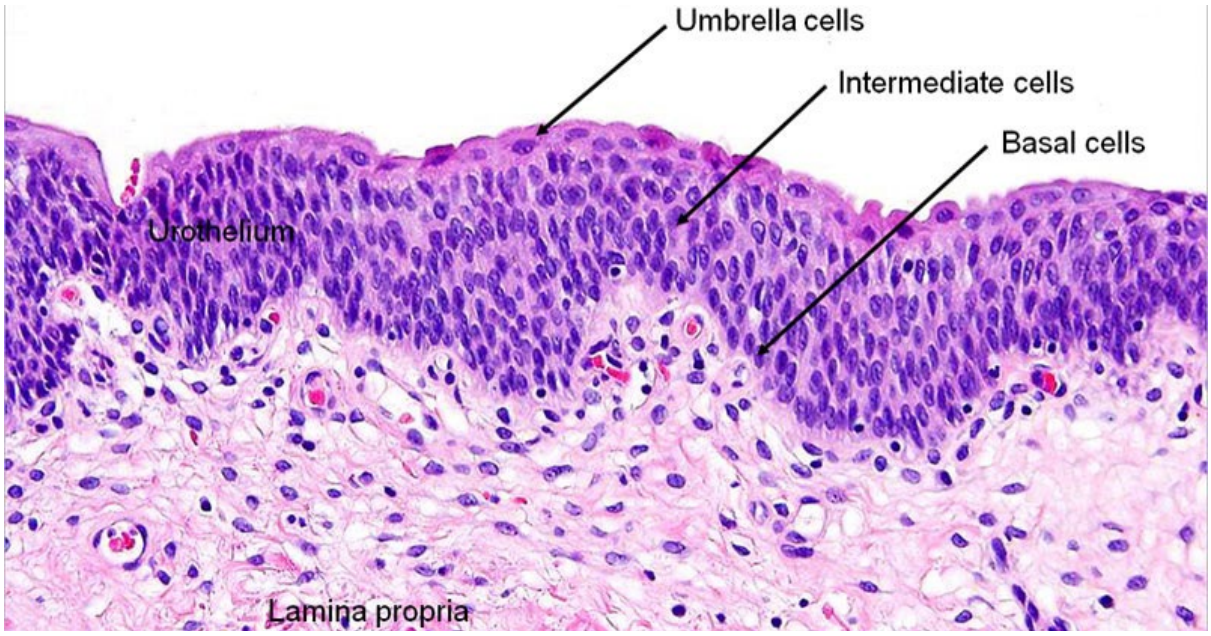

Figure 3 - Haematoxylin and Eosin stained normal urothelium, highlighting lamina propria, Umbrella, Intermediate and Basal cells, Bolla S.R et al 2023, Histology Bladder).

CK5 is expressed in basal cells of the bladder and prostate tissue. This author and colleagues have attempted to characterise sub-types further by stage through quantification of mRNA expression of CK20 and CK5 (Breyer et al., 2017). Findings reported an increased CK20 and

decreased CK5 mRNA expression in patients with stage T1 NMIBC, and therefore identified a potential predictive tool for NMIBC progression. The author and colleagues also indicated that expression of CK20 and ki67 (a marker of cellular proliferation) were positively correlated and confirmed that T1 tumours with luminal characteristics showed increased rates of proliferation and had the potential to be more aggressive. This finding was opposite to findings in MIBC, in which a luminal phenotype was associated with less aggressive behaviour post-chemotherapy (Choi et al., 2014).

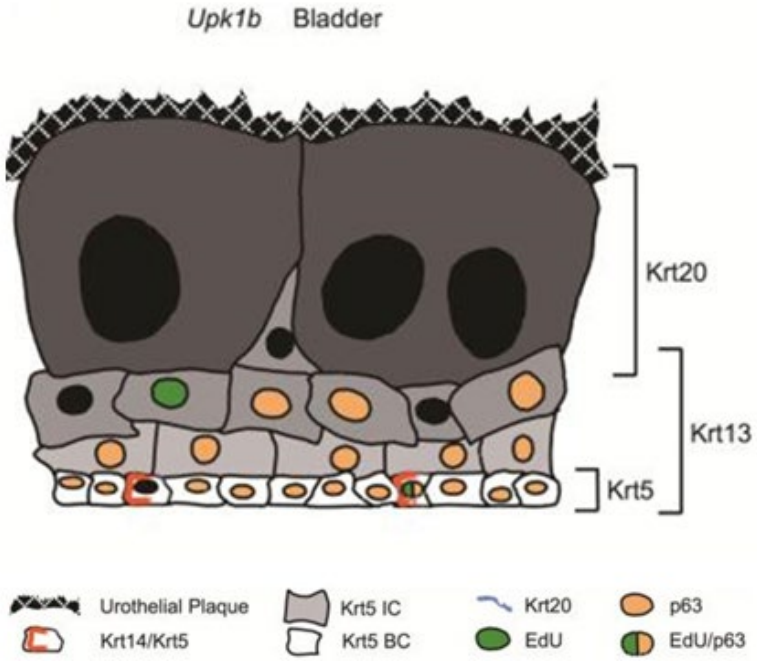

Figure 4 - A schematic diagram of urothelium urothelial organisation specifically represented by uroplakin 1b representation within the bladder. Urothelial protein differential expression is displayed for CK5, CK13, CK14, CK15, and CK20. EdU indicates proliferation. Source: (Carpenter et al., 2016).

Determination of the presence of keratin and cell surface markers supports current literature that stratifies NMIBC into subtypes and aids cancer cell detection within NMIBC. Throughout epithelial tissue differentiation, keratins are differentially expressed (Hedegaard et al., 2016). Normal, healthy urothelium exhibits an amalgamation of simple keratins that include CK20 and CK5, in which basal and intermediate cells express CK5 but not CK20. Terminal differentiation consists of the loss of CK5 and the increase of CK20 expression**.** As the stage and grade of BC increase, CK20 expression similarly increases (Choi et al., 2014)**.** This confirms that expression of CK20 and CK5 is prognostic for the prediction of NMIBC progression and recurrence, and therefore is an aid in the identification of patients who would benefit from early cystectomy.

1.3 Uroplakins and their potential application within bladder cancer

Urothelium-specific cell membrane proteins identified as uroplakins, construct components of urothelial plaques (Matuszewski et al., 2016). Plaques consist of four different uroplakins; UPIa, UPIb, UPII, and UPIII which cover the apical surface of urinary epithelium (J N Weinstein et al., 2014) as well as integral membrane proteins. Uroplakins have an important function to enhance the permeability barrier of the urothelium and act as a barrier to water, not to mention toxic materials within urine (Wu et al., 2009). Toxic materials from urine do not infiltrate back into the body, signifying the critical role of uroplakins in urinary bladder epithelium. In addition to this, increased uroplakin mRNA expression has been pinpointed in bladder cancer tissues and the peripheral blood of patients with primary and metastatic urothelial carcinoma (Lobban et al., 1998). Increased uroplakin Ia, Ib, II, III, and β-actin protein expression is observed in the bladder, (seen in Figure 5 below), with only uroplakin Ia expressed in the ventral prostate and no uroplakin expression noted in the posterior lateral prostate.

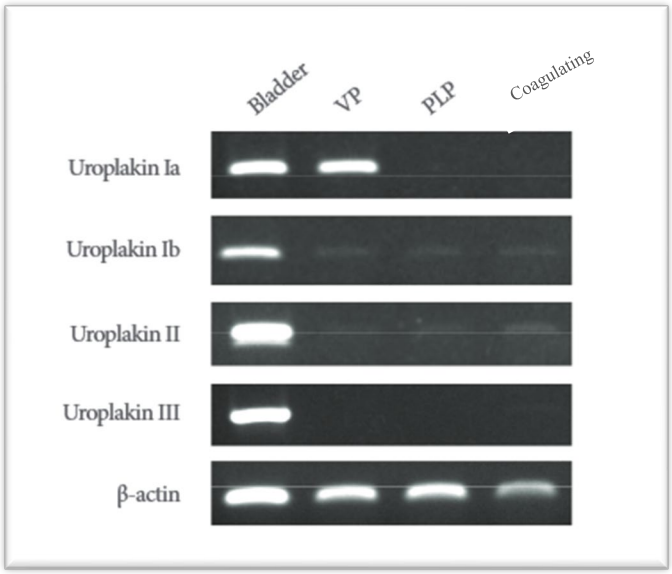

Figure 5 - Uroplakin and β-actin expression observed in bladder and prostate tissue. Uroplakin expression established in Bladder; VP ventral prostate; PLP posterior lateral prostate; Coagulating, coagulating gland. The above figure is a PCR experiment, and β-actin shows the loading control. Looking at specific bladder markers of Uroplakin Ia, Uroplakin Ib, II, and III was restricted to bladder expressions showing their specificity, whereas Uroplakin 1a was also seen in the ventral prostate. Source: Adapted from Lee, 2011, Uroplakins in the Lower Urinary Tract, International Urology Journal.

Uroplakins are a marker of urothelial differentiation and are synthesized in large quantities specifically by terminally differentiated urothelial cells. Importantly, within the normal bladder urothelium, differentiated superficial cells gradually develop from basal as well as

intermediate cells (Lee, 2011). Significantly, this identifies uroplakins as urothelium-specific markers of terminal differentiation in NMIBC. Class 1 and class 2 tumours, as defined in Figure 6 displayed a high expression of uroplakins, known to be mainly expressed in luminal and umbrella cells.

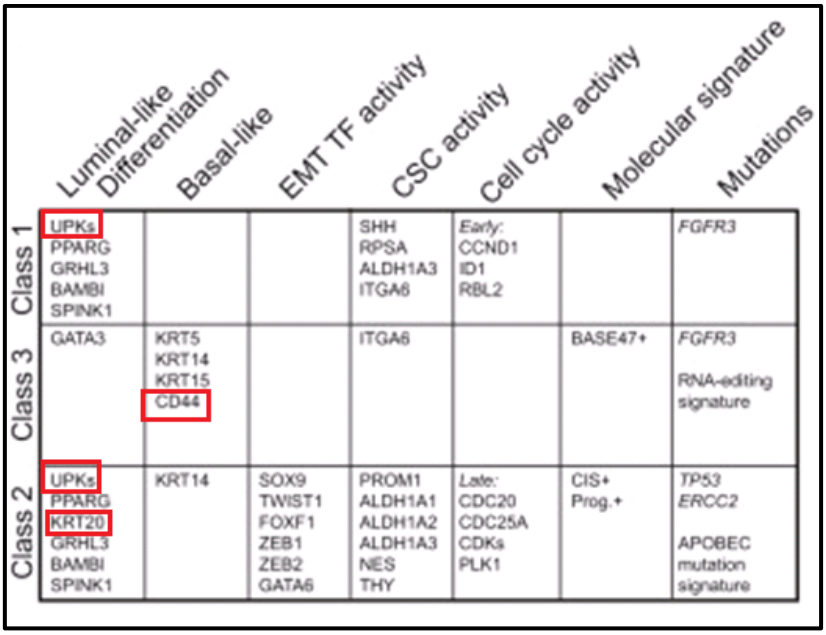

Figure 6 - A summary of representative molecular features for each tumour class representing NMIBC. Source: (Carpenter et al., 2016, Uroplakin 1b is critical in urinary tract development and urothelial differentiation and homeostasis, Kidney Int).

As members of the tetraspanin superfamily, uroplakins communicate with integrins and lineage specific proteins and perform by facilitating molecular events (Maecker et al., 1997). In two bladder cancer cell lines, KK47 non-invasive and YTS1 highly invasive, GM3 in glycosynapse 3 was found to regulate communications with CD9 an integral membrane protein associated with integrins (Mitsuzuka et al., 2005). Notably, depleted levels of GM3 increase bladder tumour motility coupled with invasiveness (Mitsuzuka et al., 2005), contributing to a more mesenchymal, migratory phenotype accelerating to muscle-invasive bladder cancer.

1.4 Clinical Presentation of Bladder Cancer

The classical presenting symptoms of patients presenting with a bladder tumour are painless haematuria, observable blood within urine, bladder-related pain, frequency, and dysuria. Non-visible, microscopic haematuria is also reported in patients with NMIBC. About 80% of BC sufferers emerge with this symptom, and approximately 20% that present with painless

haematuria will have urinary tract malignancy (Kamat et al., 2016). Patients with age-related bladder dysfunction clinically present with reduced bladder capacity, elasticity, and urinary flow. Other symptoms include irritative indicators such as painful discharge of urine, increased frequency, and urgency, pain when the bladder is full, and recurrent urinary tract infections (Kamat et al., 2017).

Lower urinary tract symptoms (LUTS) are described as frequent and severe abnormal voiding sensations that affect an individual's quality of life. Andersson *et al.* projected the age-exact incidence and severity of LUTS in a biased sample group, as only Swedish men were recruited for the study. Approximately 15–60% of these males aged over 40 years reported having LUTS, suggesting both occurrence and severity of BC significantly increase with age (S. O. Andersson et al., 2004). Further studies have supported this finding, although, in non-biased sample groups, suggesting BC is a urinary disorder correlated with age. With LUTS increased post-void residual urine is retained in the bladder after urination, increasing the likelihood of the interaction of potential carcinogens within the bladder urothelium and in urine. Additionally, increased bladder mass and wall thickening are observed in individuals presenting LUTS (Qie et al., 2016).

1.5 Clinical Burden - Recurrence, Progression, Follow up

Due to the heterogeneous nature of NMIBC, a major clinical problem is the 40% risk of recurrence within 3 years after transurethral resection of the initial tumour. Clinical predictive considerations for NMIBC bladder tumour recurrence and progression are tumour size, histopathological grade, stage, presence of CIS, and reaction to intravesical therapy (Van Der Heijden and Witjes, 2009).

Statistics highlight one-year recurrence rates at 15-61%, and five years at 31-78%, which mandates intensive invasive cystoscopic surveillance. This is life-long for many patients, making NMIBC a costly cancer to treat worldwide (Mowatt et al., 2011). Approximately 50% of all recurrence is known to reflect incomplete resection of the tumour, although additionally, tumour recurrence may be ascribed to a combination of missed tumours, reimplantation of tumour cells post resection, and *de novo* tumour incidence within high-risk urothelium (Van Der Heijden and Witjes, 2009). With recurrence, there is the risk of stage progression to MIBC, which carries a 50% risk of mortality at 3 years (Mowatt et al., 2011).

Skinner and colleagues reported the most reliable method to impair progressive BC disease is to identify tumours at the earliest stage and perform an early cystectomy. Pathological features of tumour size greater than 3cm and observance of lymph vascular invasion help to early detect the greatest risk patients with stage 1 cancers, likely to gain from early cystectomy. Early cystectomy is advantageous when there is accurate pathological staging and early staging of the disease, to allow a nerve-sparing cystectomy thus reducing the risk of late recurrences (Skinner, 2007).

Cystoscopy however is invasive, uncomfortable, time consuming, carries morbidity, and is a clinical burden on those patients that endure a lifetime of cystoscopies. Any reduction in cystoscopy would provide a major improvement in the patient experience (Kamat et al., 2017). Hospital Episode Statistical data (UK) shows that over 50,000 surveillance cystoscopies are performed annually, at an average cost of £441 per episode, with a cumulative cost of £22M/year (Qie et al., 2016). These substantial costs make BC the most expensive malignancy to manage, not just in the UK, but also in Europe and North America.

Blue light cystoscopy is offered to patients with MIBC with the view of increasing detection and decreasing recurrence or a form of enhanced cystoscopy known as narrow band imaging, also with the hope of increasing detection and decreasing recurrence (Van Der Heijden and Witjes, 2009).

1.6 The European Organization for Research and Treatment of Cancer

The European Organization for Research and Treatment of Cancer (EORTC) risk table provides a well-recognised model to predict bladder cancer recurrence and tumour progression within NMIBC patients. EORTC allows the probability of recurrence and progression to be predicted based on tumour number, grade, size, CIS, and previous recurrence rate (Sylvester et al., 2006). Stage 1 and HG tumours, CIS, and high EORTC risk scores were observed more frequently in class 2 and 3 tumours (Lerner & Robertson, 2016).

Critically, the EORTC risk table is known to mismeasure risk and have poor discrimination for prognostic outcomes. Incorporating additional prognostic factors into the EORTC risk table, namely depth of lamina propria invasion and molecular biomarkers would improve the predictive accuracy when assessing the risk of NMIBC.

1.7 Clinical Management

1.7.1 TURBT

Transurethral resection of the bladder tumour (TURBT) remains the gold standard for the management of NMIBC. The current clinical process involves patients with suspected BC undertaking a pipeline where they receive a diagnosis, undergo TURBT, and then proceed to cystectomy. After histopathological assessment of suspected cancer within the bladder, patients endure initial TURBT, where a clinician should accurately excise all visible tumours. Additionally, the histological type and grade of the tumour, as well as presence, depth, and type of the tumour invasion should be determined. TURBT quality affects the diagnosis, treatment, and even prognosis of NMIBC (Qie et al., 2016). A repeat TURBT is recommended within four to six weeks of the primary urological procedure (Sfakianos et al., 2014).

1.7.2 Adjuvant Intravesical Chemotherapy of NMIBC

Guidelines recommend induction intravesical therapy with Bacillus Calmette Guérin (BCG) or mitomycin C for patients with multifocal and/or large low-grade Ta tumours (Baltaci et al., 2015). The high requirement of adjuvant therapy in NMIBC patients indicates incomplete TURBT or high recurrence rates.

A valuable intravesical treatment for NMIBC, BCG can delay the progression of MIBC (Babjuk et al., 2008). Long term efficacy results of patients with low risk and intermediate BC were treated with BCG. Intravesical instillations of epirubicin reported a significant decrease in BC progression and recurrence (Sfakianos et al., 2014). Such a highly encouraging response driving a reduction in BC progression and recurrence was observed in papillary and CIS lesions (Mowatt et al., 2011). This confirms that effective therapy with BCG is seemingly considerably superior in preventing recurrences than chemotherapy, while unfortunately, BCG produces substantially greater side effects (Baltaci et al., 2015). Mitomycin C, epirubicin, and pirarubicin all displayed favourable impacts on decreasing BC advancement (Baltaci et al., 2015).

Existing Bladder Cancer biomarkers

1.8 Urine Biomarkers

Presently, the typical non-invasive bladder tumour examination is voided urine cytology. Although cytology has high selectivity and specificity for the detection of high-grade urothelial carcinoma, (Kamat et al., 2014) confirmed cytology sensitivity decreases when detecting low-grade tumours. In contrast to NMIBC, detecting MIBC sensitivity is of utmost importance due

to the muscle invasive nature of the disease. If a false-positive result is reported, a patient may have to undergo an unnecessary endoscopy or upper urinary tract investigation, which is invasive, unpleasant, time consuming, and costly on the NHS. A false negative result has the potential to dramatically impact the patient, thus an assay with high sensitivity for high-grade tumours is essential.

The ideal bladder cancer screening and monitoring test would be non-invasive, fast, objective, easy to perform and interpret, and have high sensitivity and specificity. A urinary biomarker to detect either macroscopic residual disease or early growth from microscopic residual disease presenting over the subsequent months and years would transform clinical practice by reducing recurrence and relieving the reliance on surveillance cystoscopy.

Tumour cells are shed readily into urine and provide an easy and accessible source for tumour cell surveillance. Urinary biomarkers provide a non-invasive paradigm for detecting tumour recurrence and current literature confirms the requirement to exploit the unique benefit of highlighting exfoliated urine cells for specific cell surface antigen detection.

Nuclear Matrix Protein 22

Nuclear Matrix Protein (NMP22)is a diagnostic marker representing the mitotic activity from urothelial cells attaining ~65% sensitivity in the detection of urothelial carcinomas (Hwang et al,.2011), compared to 44% sensitivity with urine cytology when identifying LG 1 and 2 tumours. An amalgamation of NMP22 and cytology improves the diagnosis and monitoring of BC recurrence in the clinical setting.

ImmunoCyt

The ImmunoCyt test identifies by fluorescence three monoclonal antibodies M344, LDQ10 and 19A211 present in exfoliated urothelial cells. Sensitivity of the ImmunoCyt test is high, however specificity is low. Increased numbers of exfoliated cells are required to perform the examination, therefore only when combined with cytology, ImmunoCyt improves diagnostic accuracy and amplifies clinical performance in the detection of LG bladder tumours (Yang, M et al., 2014).

Bladder Tumour Antigens

Bladder tumour antigens (BTA) stat and TRAK are urine biomarkers utilised in the diagnosis of urothelial carcinomas. The BTA stat test is a immunochromatographic assay detecting human complement factor-H related protein, a Bladder Cancer specific antigen. The test is quick and can be completed within five minutes. Furthermore, as direct voided urine is utilised for the test, the requirement of pre-treating the urine specimen is not necessary offering further advantages to this urine biomarker (Raitanen, 2008). The nature of the urine sample for the BTA stat test is diverse, samples can be provided fresh and the refrigeration or freezing the urine specimen does not compromise the performance or quality of the test.

Overall one sixth of recurrent bladder tumours undetected by cystoscopy, were identified by positive BTA stat test (Raitanen, 2008) and increased sensitivity of the BTA stat examination compared to cytology in the initial diagnosis and recurrence of urothelial carcinomas is evident.

Mitochondria

Mitochondria are small cytoplasmic organelles found in all nucleated cells. Each cell contains approximately 100 mitochondria, and each mitochondrion contains approximately 10-100 mtDNA molecules. Each cell can therefore contain between 1,000 and 10,000 molecules of mtDNA. Mitochondria are present in multiple copies of each cell, according to the bioenergetic need for each tissue (Ju, 2016). As mitochondria are constantly changing tubular networks, undergoing fusion and fission, exact quantities of mtDNA molecules per mitochondrion are unknown (Vyas et al., 2016).

Mitochondria play a significant role in energy production, by producing >90% of adenosine triphosphate (ATP) with a cell, allowing normal metabolic function to be carried out. Mitochondria synthesize ATP through oxidative phosphorylation. The ‘powerhouses’ of the cells additionally perform a significant role in immune responses and cellular signalling (Stefano & Kream, 2015).

1.9 Mitochondrial Function

Due to the oxidative microenvironment of mitochondria, mtDNA is vulnerable to oxidative damage from reactive oxygen species (ROS). Influencers are the close proximity of mitochondria to the ETC, the lack of protective histones in the mtDNA, and the limited efficiency of the mtDNA repair mechanisms compared to nuclear DNA. A lack of protective histones and limited repair mechanisms enhance susceptibility to changes in mtDNA sequences (Suzuki et al., 2011). Although nucleoid composition may affect this, the mtDNA modification rate is estimated at 5-50 times higher than nuclear DNA (Li et al., 2010). High mtDNA variation rate creates heteroplasmy and the process of cell division causes random segregation of both mutant and wild-type mtDNA (Blokzijl et al., 2016).

MtDNA inheritance is uniparental, and as mtDNA is maternally inherited, fathers with mtDNA variants are not at risk of transmitting the variant to their offspring. Numerous studies focus on identifying specific mtDNA modifications through germline blood to determine the likelihood of transmission of mtDNA alterations. MtDNA variant m.16069T>C identified after the analysis of blood, malignant and benign tissue of BC patients was found to be linked with BC as well as mitochondrial variants m.10464T>C and m.4918A>G (Shakhssalim et al., 2013).

1.10 Mitochondrial DNA

The human mitochondrial genome circular genome is only 16.6 Kb containing 37 genes of those, 13 are protein-coding, and 24 used for translation of those 13 codes for polypeptides, electron transport chain (ETC) subunits (Suzuki et al., 2011). Within the 24 genes, 2 consist of ribosomal RNAs (rRNAs) and 22 transfer RNAs (tRNAs). Although the mitochondrial genome is small and accounts for approximately 0.0006% of the human genome, mitochondrial variants are correlated with many cancer types throughout tumour development (Hertweck & Dasgupta, 2017a).

The thirteen mitochondrial protein-coding proteins instruct cells to generate protein subunits within the oxidative phosphorylation (OXPHOS) system. Variations in genes encoding subunits of the OXPHOS complex can contribute to mitochondrial disorders required for their translation and assembly (Suzuki et al., 2011). MtDNA is essential for ETC complex transcription, and the amount of mtDNA within cells can affect OXPHOS (Williams et al., 2015). Studies identified energy-demanding tissues such as cardiac and skeletal muscle comprised of 4000 - 6000 copies of mtDNA per cell, while liver, kidney, and lung tissues

averaged between 500 and 2000 copies (D'Erchia et al., 2015). Bladder tissue requires energy for contraction, although decreased mtDNA is present in bladder tissue (Hertweck & Dasgupta, 2017a).

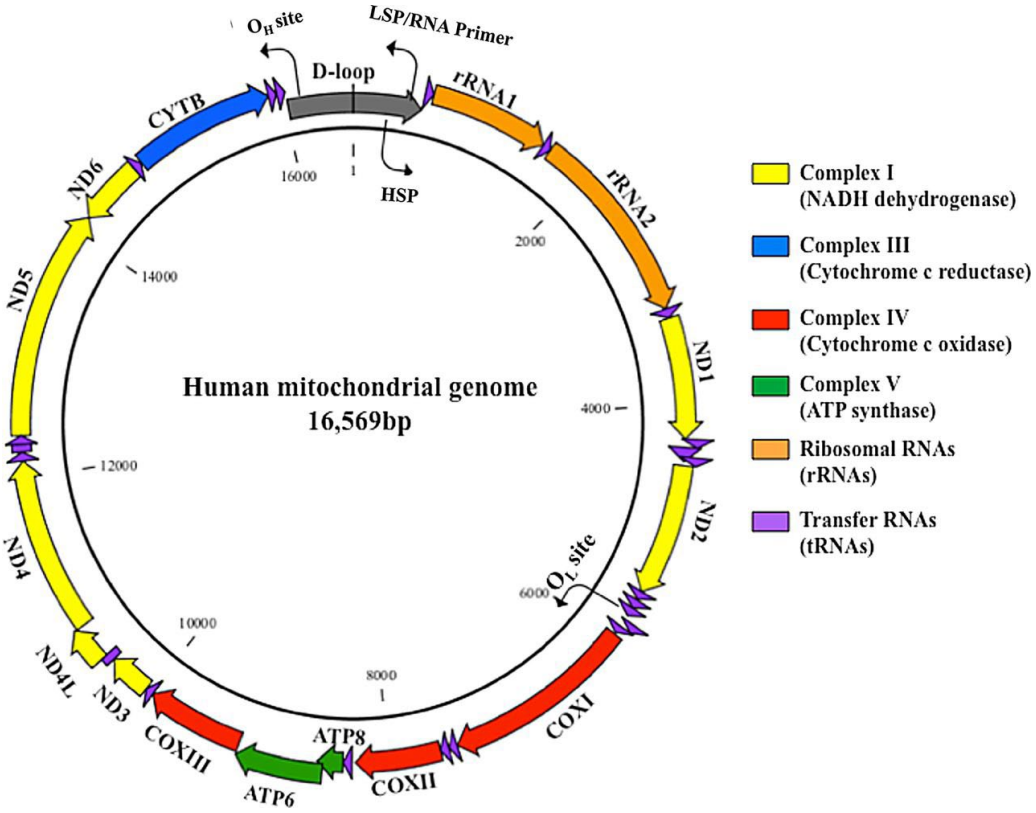

Figure 7 - The human mtDNA is a 16,569-bp, double-stranded, circular molecule encoding 13 polypeptides. All mtDNA-encoded polypeptides include seven subunits of complex I (yellow), one subunit of complex III (blue), three subunits of complex IV (red), and two of complex V (green). Besides protein-coding genes, mtDNA codes for 22 tRNAs (purple) and two ribosomal RNAs (orange). Source: (Sun and St. John, 2016).

1.11 Mitochondrial Dysfunction

Cancer cells typically have high rates of proliferation and energy requirements, suggesting mitochondria have a crucial role in inducing cancer and its development. Due to the role mitochondria play in cancer, the cytoplasmic organelles are essential in the resistance to treatment. Increased glycolysis results from cancerous cells having a high proliferation index and high energy request (Antonella Cormio et al., 2017).

In investigating cancer cell metabolism, mitochondria were characterised as an essential facilitator of aerobic glycolysis by Otto Warburg due to the presence of oxygen, and glucose fermentation occurs, producing pyruvate (Hanahan & Weinberg, 2011). The proximity of ROS produced increases the risk of mtDNA disruption, instability, and damage (Hertweck &

Dasgupta, 2017b) Consequently, this results in decreased repair mechanisms within the mitochondrial genome, hence a higher rate of mtDNA alterations. Contributors to the distribution and a high number of transformations in mtDNA are the existence of thousands of mitochondrial copies in each cell and heteroplasmy effects of multiple mitochondrial copies per cell (Vyas et al., 2016).

Cancer cell energy production is reliant on the glycolytic pathway due to ROS stress, oncogenic signals, and mitochondrial dysfunction resulting in mtDNA variants (Ishikawa et al., 2008). Nevertheless, it is still unknown if mitochondrial transformations or mitochondrial dysfunction occurs first, initiating replicative advantage by relying on glycolysis. Alternatively, mitochondrial modifications and dysfunction occur as a result of other cellular abnormalities, and the reliance on glycolysis is perhaps a coping mechanism of the cell containing dysfunctional mitochondria (Vyas et al., 2016).

1.12 Mitochondrial Mutations

Patients with mtDNA defects are known to display features that mimic alterations in nuclear genes, with point alterations or DNA duplications, deletions, or inversions being the main contributor to primary mtDNA diseases. Such modifications stimulate tumour survival to have a direct impact on the downregulation of OXPHOS function (Suzuki et al., 2011). OXPHOS disorders exhibit respiratory chain deficiency displaying reduced enzymatic function in the respiratory chain complexes thus resulting in reduced ATP synthesis and oxygen consumption. Dysfunction in OXPHOS is reported to contribute to activating the AKT cell survival pathway. Activation of this pathway is driven by NADH, resulting in the downregulation of apoptosis (Sun & St. John, 2016). Contrary to previous belief, it is reported that a normal amount of OXPHOS function is required within cancerous cells for tumours to be viable (Suzuki et al., 2011).

Clonal mtDNAs are known to accumulate during our existence, particularly in post-mitotic brain, cardiac and muscular tissues (Schon et al., 2012). Such clonal mtDNAs exist as the result of somatic variations and have the ability to expand clonally (Oldfors et al., 1992). This is particularly evident in muscles of aged people (Blokzijl et al., 2016) and as clonal-mtDNA species accumulate, during ageing in bladder tissue rich in sphincter muscles surrounding the urethra helping urine to be kept in the bladder (Braakhuis et al., 2003). If these cells become transformed, these alterations serve as inherent lineage tracing marks. Published data

confirms that mtDNA variations are common in NMIBC and these are tumour specific and absent from cells in the patient's normal bladder lining (Shakhssalim et al., 2013).

1.13 Heteroplasmy

The diversity and existence of both mutant and wild-type genomes within a cell is known as heteroplasmy, and every person is characterised by a population of mtDNA genomes (Hertweck & Dasgupta, 2017a). The existence of multiple copies of mitochondrial DNA (mtDNA) per cell is a defining characteristic of the mitochondrial genome, as well as its polyploid makeup. Heteroplasmy and homoplasmy can be mitochondrion specific, cell specific, and tissue specific.

Within normal tissue, the frequency of heteroplasmic variants varies within the same individual, as reported by Li *et al.,* with extensive heterogeneity found within mtDNA of unremarkable cells and additional homoplasmic and heteroplasmic alterations in cancer cells (He et al., 2010). Heteroplasmies occur at locations with increased transformation rates indicating transformation and drift are the leading forces determining heteroplasmy (Li et al., 2010).

As mitochondria contain multiple copies of mitochondrial DNA within the mtDNA genome, cells are homoplasmic or heteroplasmic. Altered mtDNA copies spread through the mitochondrial network through fission and fusion, and dominant mtDNA alterations are found in a clonal cell population (Vyas et al., 2016).

Mitochondrial variations within aged cells are known to be caused by replication errors early in life and not oxidative damage. These modifications may undergo polyclonal expansion and cause respiratory chain dysfunction in different tissues (Sun & St. John, 2016).

MtDNA variants can act as single base pair variants, contributing to mtDNA population variability with non-protein altering variants being more common. MtDNA deletions are associated with disease, these can often be single large-scale mtDNA deletions or multiple, usually smaller mtDNA deletions (Kirches, 2017).

As inter-tumour heterogeneity research has further developed, diverse molecular groups outside of typical histopathological categorisation have been identified by transcriptional

genome expression assessment, thus impacting clinical outcomes. Variants within particular genes and molecular pathways within NMIBC, have also been identified.

1.14 tRNA

The unique folded structure of tRNAs particularly their three hairpin loops that appear like a three-leafed clover, uniquely identifies tRNAs from cytoplasmic tRNAs. Mitochondrial disorders are often the result of point transformations affected by the predisposition of genes encoding mitochondrial tRNAs (Suzuki et al., 2011). If a point modification occurred in one of the anticodon bases essential for codon recognition, this would destroy tRNA function directly (Suzuki et al., 2011). Primarily the D-loop (Displacement loop) region is where mtDNA replication occurs. If a transformation within a mitochondrial tRNA gene does not affect this region, alterations within mitochondrial tRNA may have an undesirable effect on the biogenesis and functioning of tRNAs after their transcription. Resulting in posttranscriptional modification.

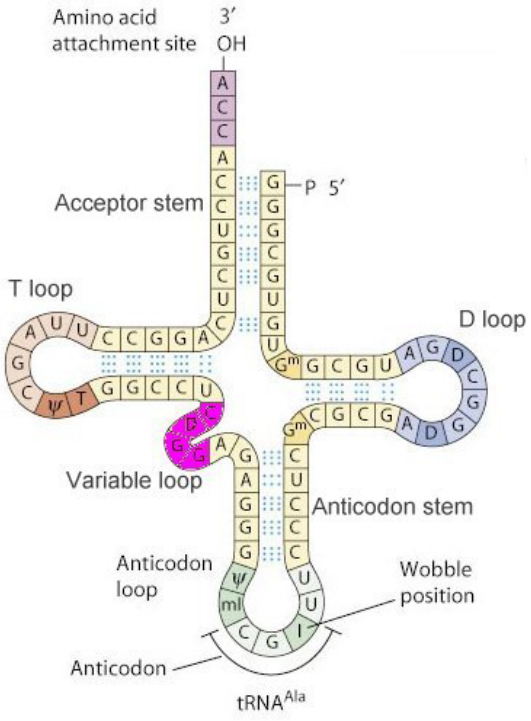

Figure 8 - Schematic diagram of tRNA secondary structure. The 'clover leaf' secondary structure results in a complex three-dimensional folding of the molecule. The hydrogen-bonded stems stabilize the tertiary structure. (Source: Figure modified from Becker, et al., 8th edition, The World of the Cell).

1.15 Mitochondria and Cancer

Mitochondria are complex organelles that influence cancer initiation, growth, survival, and metastasis. Various mitochondrial biology including mitochondrial mass, dynamics, cell death regulation, redox homeostasis, metabolic regulation, and cell signalling contributes to tumorigenesis (Antonella Cormio et al., 2017). Genomic instability, a typical feature of the majority of cancers has been described as an emerging hallmark of cancer. Hanahan and colleagues identified genomic instability driving variant accumulation as an underlying principle of cancer progression (Hanahan & Weinberg, 2011).

Single nucleotide polymorphisms (SNPs) are a prevalent type of genetic variation, and every SNP embodies a difference in a single nucleotide. SNPs are the stable substitution of a single base (Erichsen & Chanock, 2004) and ordinarily occur within the human genome. In BC a high correlation of polymorphisms in N-acetyltransferase 2 (NAT2) are identified. This is also demonstrated in colon cancer, where NAT2 encodes enzymes crucial for the biotransformation of carcinogens. Moreover, there was an increased risk of developing BC in the slowest NAT2 acetylator phenotype (Erichsen & Chanock, 2004).

1.16 Mitochondrial function in other cancers

Mitochondrial dysfunction performs numerous roles in cancer (Schon et al., 2012). Respiratory functions occurring in the mitochondria may be compromised, facilitating tumour growth due to the accumulation of NADH and pyruvate within the cytosol resulting in surplus cytosolic pyruvate converted to lactate-by-lactate dehydrogenase. Such explains excessive lactic acid found in patients with mitochondrial diseases, particularly children. (Stefano & Kream, 2015).

Ishikawa *et al.* confirmed mtDNA dysfunction results in the overproduction of ROS affecting the ETC, which contributes to tumour cell metastasis (Ishikawa et al., 2008). ROS is produced at low levels during normal mitochondrial respiratory chain function and causes the development of somatic modifications in mtDNA as reported by (Harman, 1992). The hypothesis of ageing was extensively described with mitochondria playing a significant role. Such alterations can impair respiratory chain function, resulting in enhanced ROS assembly, thus an accumulation of mitochondrial variants. Particular pathogenic variations, for example, m.8993T>G, results in enhanced ROS production (Robert W. Taylor & Turnbull, 2005). ROS is known to be the source of oxidative impairment during ageing, subsequently affecting

apoptosis, replicative senescence, and energy reduction all contributing to a loss of tissue and cellular function.

Colorectal cell lines and mtDNA alterations were investigated by Vogelstein and authors who found most transformations were somatic and homoplasmic (Polyak et al., 1998). As a result of diversity within the mitochondrial genome, as well as mtDNA heterogeneity, the presence of an mtDNA variant may assist in detecting tumour recurrence (He et al., 2010).

1.17 Mitochondrial function in Bladder Cancer

mtDNA alterations affect tumorigenesis, while little is known about the functional consequences of mtDNA alterations, particular transformations arise in ETC genes and may cause an increase in oxidative stress as a result of ETC dysfunction, thus enhancing tumorigenesis (van Gisbergen *et al.,* 2015). Replication occurs within the D-loop region of the mitochondrial genome and in 57% of BC cases substitutions, insertions and deletions are observed. Decreased mtDNA is noted in bladder tumour tissue compared to normal urothelium, summarised in Table 3 below.

Tumour type	D-loop variants	Variants occurring frequently in genes	MtDNA content relative to normal tissue
Bladder	Substitutions and indels in 57% of cases.	Substitutions and indels in ribosomal RNA and protein-coding genes ND3, ND4, ND5, and CYTB.	Decrease

Table 3 - A Table displaying well characterised mtDNA variations in Bladder Cancer and mitochondrial copy number variation relative to normal tissue are displayed. Bladder cancer is reported to have decreased mtDNA content relative to normal bladder tissue. (Source: Hertweck and Dasgupta, 2017a, The landscape of mtDNA Modifications in Cancer: Frontiers in Oncology).

1.18 Mitochondrial Copy Number

Depending on tissue type, studies have measured mtDNA copy number per cell and compared mtDNA content with normal tissue. After mtDNA sequence analysis of bladder tumour tissue mostly including stromal and immune cell infiltration sample areas, bladder tumour cells are reported to have decreased mtDNA copies (Reznik et al., 2016)

Variations in mtDNA content are associated with tumorigenesis (Reznik et al., 2016). Some mtDNA in cancer studies do not focus on mtDNA copy number variation within tumour development and progression but focus on the analysis of transformations and heteroplasmy (Reznik et al., 2016). Bladder tissue particularly is reported to have a decreased mtDNA content. This was characterised by bladder samples defined by the existence of reduced mtDNA copy number modifications.

This implies bladder tumours have a decreased dependence on mitochondrial metabolism to proliferate, directing mitochondrial therapies at enabling passenger modifications in genes such as DNA polymerase gamma needed for mtDNA copy number maintenance (Kamat et al., 2017).

1.19 Mitochondrial DNA a Unique Translational Opportunity

Herein lies the unique translational opportunity of mtDNA as:

(i) mtDNA alterations accumulate at much higher frequencies than genomic DNA.

(ii) mtDNA is much more abundant than genomic DNA and its small size permits full length sequencing reads.

Such are features that profoundly increase the sensitivity in the detection from urine. Unlike other approaches, benchmarking mtDNA modifications that are unique to the tumour provides excellent diagnostic specificity in surveillance for recurrence through lineage tracing.

Ageing

1.20 Non-Muscle Invasive Bladder Cancer is strongly associated with advancing age.

Worldwide, there are over 350, 000 new Bladder Cancer diagnoses each year, thus tumours of the Urinary Tract considerably contribute to the overall human cancer burden (Van Der Heijden and Witjes, 2009). Of all newly diagnosed cases, 80% of sufferers are diagnosed with Non-Muscle Invasive Bladder Cancer and ~ 20% of patients present a more migratory, mesenchymal, invasive phenotype of Muscle-Invasive Bladder Cancer (Kassouf et al., 2015).

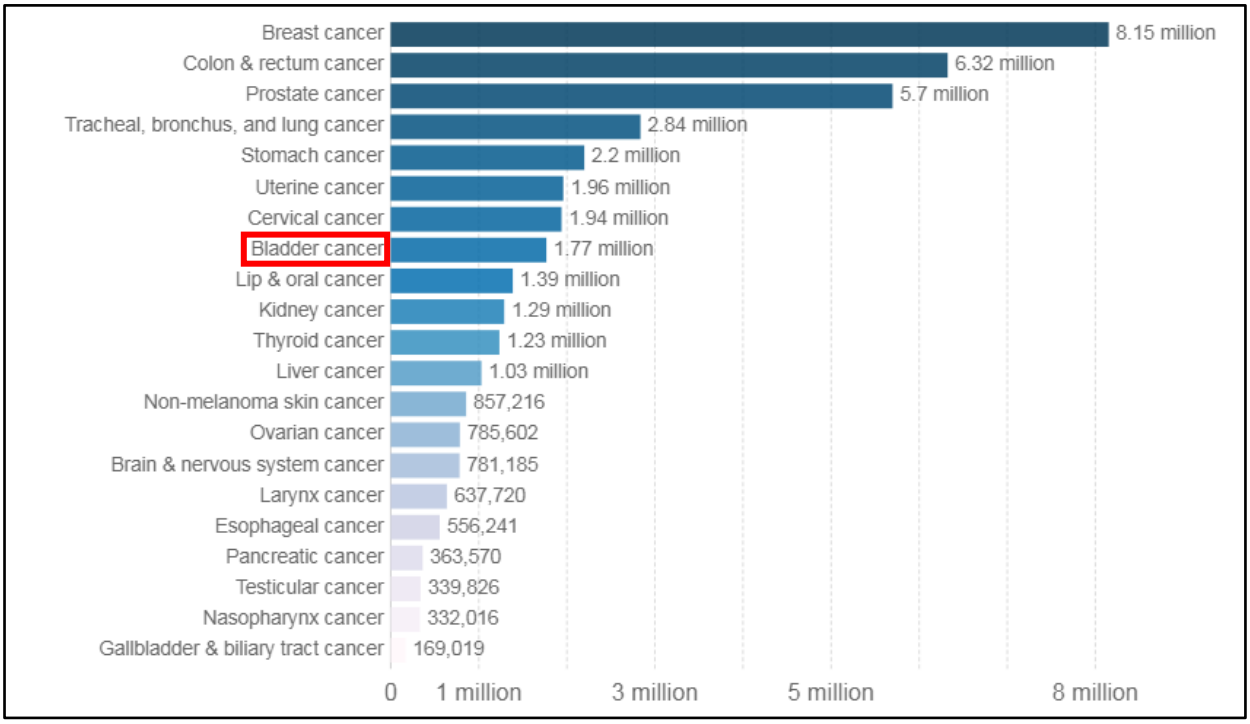

Figure 9 - Number of people with cancer differentiated by cancer type. Bladder Cancer is the eighth most common cancer when distinguished among various cancers, highlighted in red. 1.77 million people worldwide were affected by the disease in 2018. (Source: IHME, Global Burden of Disease).

Despite significant advances in screening, surgical interventions, and treatment, BC incidence is strongly associated with advancing age. As patients over 70 years old more frequently present with aggressive disease, age is the biggest risk factor for BC development. Such association between age and BC incidence is well documented (A. Cormio et al., 2018). As represented by the blue line in Figure 10, BC incidences are higher in men than women and men have a higher mean age of diagnosis ~ 75 years compared to ~ 70 years in women.

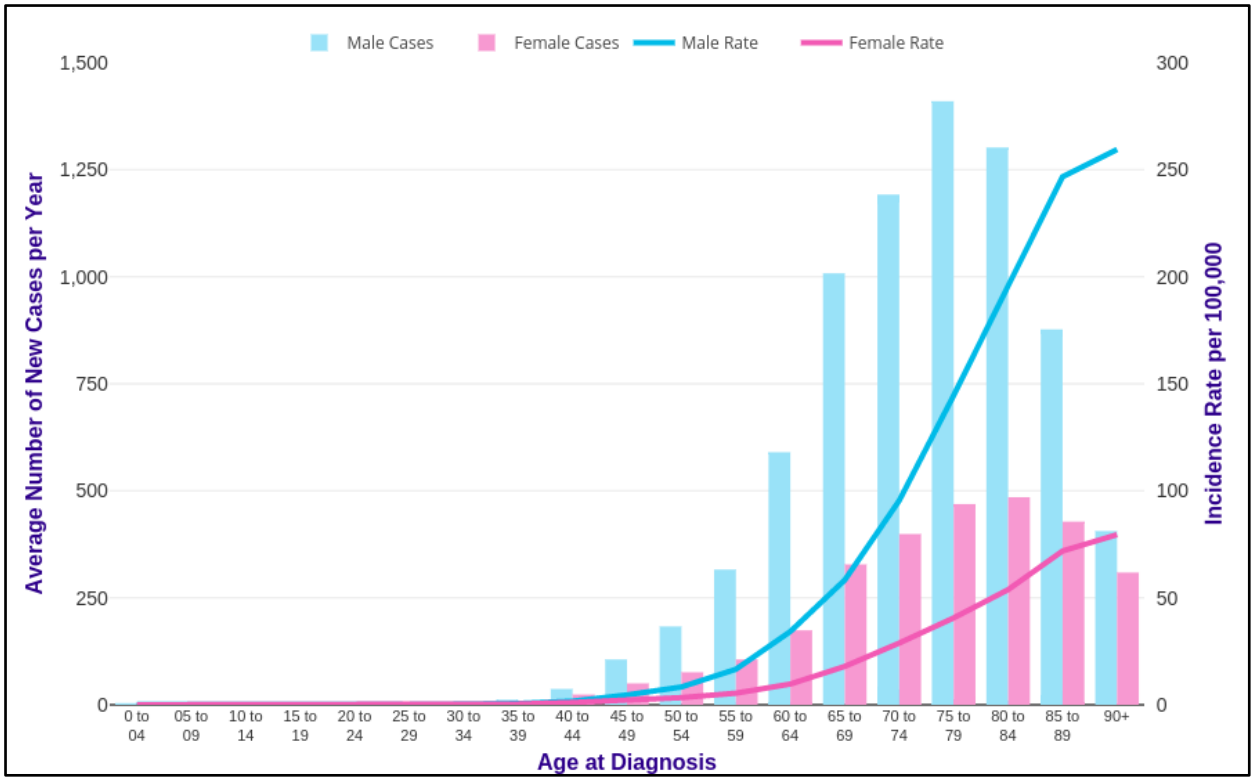

Figure 10 – A graph displaying male and female Bladder Cancer incidence statistics, displaying rate and age at diagnosis. BC incidences are higher in men (represented by the blue line) than women (indicated by the pink line). Men have a higher mean age of diagnosis ~ 75 years compared to ~ 70 years in women. (Source: Cancer Research UK).

1.21 Mitochondrial dysfunction is a Hallmark common to both ageing and cancer.

Ageing has been associated with several molecular hallmarks, principally identifying nine candidate hallmarks contributing to the ageing phenotype. An equivalent set of hallmarks remained established for cancer (Hanahan & Weinberg, 2011) with mitochondrial dysfunction identified as a hallmark common to both ageing and cancer (López-Otín et al., 2013). Together, this suggests a link between ageing and Bladder Cancer, thus identifying the necessity to look across both the Hallmarks of ageing and the Hallmarks of Cancers. Subsequently, within this project, I investigate age-related mitochondrial biology and naturally occurring tumour barcodes to trace BC recurrence.

Figure 11 - Schematic diagram indicating the nine Hallmarks of Ageing: Mitochondrial dysfunction, deregulated nutrient sensing, loss of proteostasis, epigenetic alterations, telomere attrition, genomic instability, altered intercellular communication, stem cell exhaustion, and cellular senescence. The red circle highlights the Hallmark of ageing of particular interest: Mitochondrial Dysfunction. (Source: Otin et al 2013, The Hallmarks of Aging, Cell).

Mitochondria are complex organelles that influence cancer initiation, growth, survival, and metastasis. Various mitochondrial biology including mitochondrial mass, dynamics, cell death regulation, redox homeostasis, metabolic regulation, and cell signalling contributes to tumorigenesis (Antonella Cormio et al., 2017). Genomic instability is a characteristic of most cancers and has been described as an emerging hallmark of cancer. Hanahan and colleagues, identified genomic instability driving transmutation accumulation as an underlying principle of cancer progression (Hanahan & Weinberg, 2011).

Variations steadily accrue throughout life in ageing tissues as characterised by (Blokzijl et al., 2016) with the age-dependent accumulation of cellular damage being a general cause of ageing (John N. Weinstein et al., 2014). Ageing is believed to be multifactorial, and the mitochondrial theory of ageing suggests the inevitable decrease in fully functional mitochondria is a result of alterations in mitochondrial DNA in a variety of tumour types.

Naturally occurring mtDNA transformations stochastically accumulate in normal ageing cells (Harman, 1992) and mitochondrial modifications within aged cells are known to be attributed to replication errors early in life and not exclusively due to oxidative damage (López-Otín et al., 2013). Whilst increased levels of specific mtDNA alterations accrue triggering mitochondrial oxidative metabolism deficiencies (Elson et al., 2001), specifically it is when the quantity of mutant mtDNA greatly surpasses a critical threshold level that results in weaknesses within mitochondrial oxidative phosphorylation (R W Taylor et al., 2001). Mitochondrial DNA variations may endure polyclonal expansion, causing respiratory chain dysfunction in numerous tissue types (Sun & St. John, 2016). Whilst there are difficulties in calculating exact totals of mutant DNA in intact living cells, advances have published displaying models of cellular mitochondrial genetics showing random genetic drift contributes to the clonal accumulation of mutant mtDNA in postmitotic cells (Elson et al., 2001).

1.22 Mitochondrial theory of ageing

The mitochondrial theory of ageing suggests the inevitable decrease in mitochondrial function is a result of a progressive accumulation of somatic transformations within mtDNA. Naturally occurring mtDNA alterations stochastically accumulate in normal ageing cells (Harman, 1992).

Advances in the knowledge of molecular bladder function mechanisms have aided our understanding that bladder dysfunction appears to be driven by altered sensation in the urothelium bladder lining. Mitochondria generate cellular ATP and specifically, ATP release from the urothelium upon bladder distension activates afferent nerves signalling bladder contraction. As ageing is associated with oxidative stress and subsequent urothelial dysfunction, mechanisms relying on mitochondria and age-related mtDNA variations are critical (Stefano & Kream, 2015).

The stochastic nature of mtDNA provides a unique tumour-specific mark as chances of the same alteration occurring in the same individual are estimated at 1 x10^{29} moreover, this then provides a unique approach of lineage tracing (Blanpain & Simons, 2013).

1.23 Cell-free DNA (cfDNA)

cfDNA signifies DNA fragments not found in cells, however within bodily fluids including plasma, urine, and cerebrospinal fluid. cfDNA is thought to arise from apoptotic cells and

particularly necrotic cells. Within this project I will investigate cfDNA mtDNA within urine as tumour cell-free DNA extracted from the urine of NMIBC patients has a higher tumour genome burden and allows greater detection (90%) of key nuclear genomic biomarkers than the intact cellular fraction (61%) (Togneri et al., 2016). Published data has not confirmed if the detection of mtDNA in urine demonstrates comparable features.

Variations in *RAS* genes within cancer sufferers were some of the initial variations described in the cfDNA, with cfDNA investigated as a prospective biomarker for assessing tumour progression, recurrence, and response to therapy (Schwarzenbach, Hoon, and Pantel, 2011). Levels of low cfDNA in plasma and serum are largely indicative of good health within individuals, although during pregnancy, illness, and extensive physical activity or tissue damage, cfDNA quantities mostly increase. One theory could be the unplanned release of DNA by proliferating cancer cells as the spontaneous release of DNA by human blood lymphocytes has been demonstrated *in vitro* (Stewart et al., 2018).

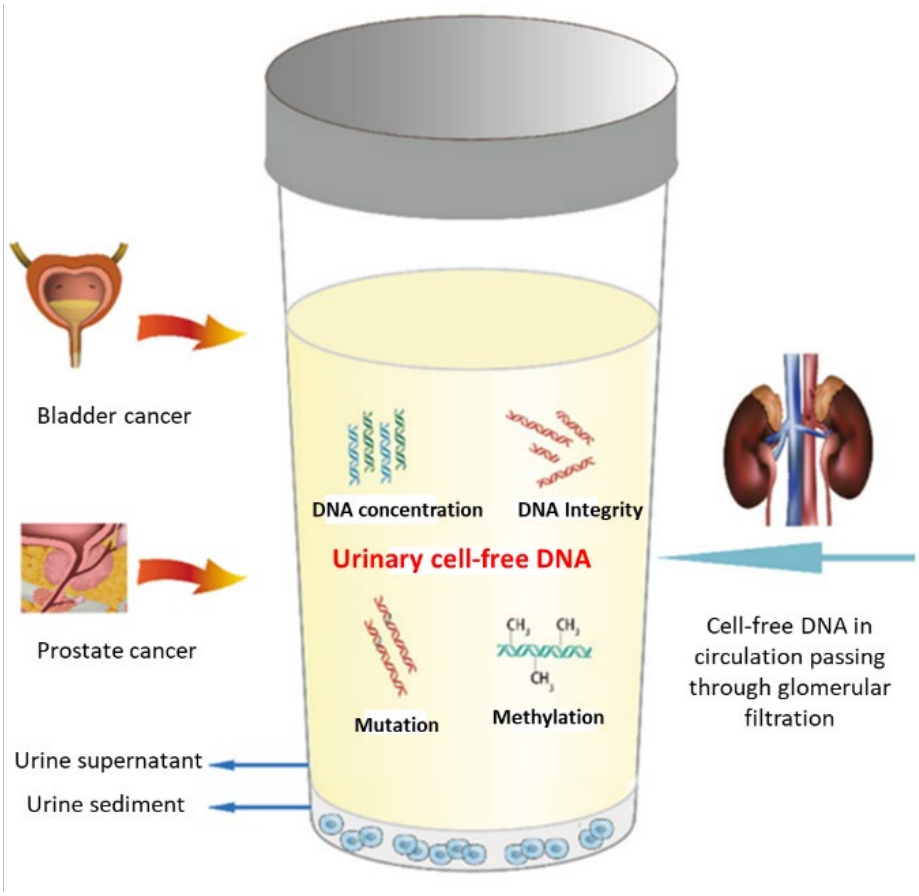

Figure 12 – Urinary cell-free DNA (Source: Lu, Tian et al (2017), Clinical applications of urinary cell-free DNA in cancer: current insights and promising future. American journal of cancer research).

1.24 Field Characterisation

Throughout ageing transformations accrue, some tissues become tumourigenic and modifications drive the formation and phenotypic evolution of a field of mutant cells. Before a lesion grows to become malignant, a normal cell lineage can acquire pro-tumourigenic genetic variations. The mutant lineage has the potential to grow into fields of cells being likely to evolve to a neoplasm, known as a cancerised field (Curtius et al., 2017).

A cancerized field of cells has acquired some but not all malignant phenotypic alterations and this altered phenotype is the result of an underlying transformation. The underlying variant may be the result of DNA replication errors during ageing by mutagenic insult. Such phenotypic alterations may include increased growth rate, enhanced immune evasion, and decreased death rate. Such phenotypic changes will be the result of alterations in important cancer linked genes that are independent or co-dependent on the altered microenvironment. This cancerised field of cells can vary in size and can be microscopically and morphologically described as normal, hyperplastic.

Transformations accumulate in ageing tissue and it is believed that the neutral drift amongst adult stem cells which maintain the tissue, directly triggers the clonal expansion of mutants (Blanpain & Simons, 2013).

Microsatellites are short tandem repeating sequences of 2-6 base pairs of DNA. Pathogenic variants within microsatellite sequences are increasingly used to identify the clonal evolution of tumour cells, suggesting a promising marker for the detection of BC. Abnormalities in microsatellites and a loss of heterozygosity are commonly found in tumour cells, particularly bladder cancer cells, and can be detected by polymerase chain reaction (PCR). Microsatellite instability transpires as a result of defects in mismatch repair (MMR) genes, including human mutL homolog 1 and 2. Reduced expression of MMR protein is reported to be correlated with microsatellite instability in BC and may potentially be applied as a new biomarker for the detection of BC (Wadhwa *et al.,* 2013). To subclassify varying stages and grades of BC, various combinations of chromosomal lesions and expression tumour markers can be employed. Chromosome imbalance and mis segregation occur in cancers contributing to DNA breaks. Interpreting the effect of chromosomal instability will aid the identification of early BC recurrence or later recurrence occurring from ‘field change’ transformation (Braakhuis et al., 2003).

1.25 Hypothesis

Urinary mitochondrial DNA presents a new concept for longitudinal lineage tracing of specific transformational marks from the primary bladder tumour. Sequencing of voided bladder cancer cells (or cell-free) mtDNA defines the presenting index lesion and allows lineage tracing to confirm tumour clearance and clonal recurrence.

1.26 Aim

This body of work aimed to identify novel diagnostic urinary biomarkers of bladder cancer recurrence by characterising tumour-related mitochondrial DNA within the ageing bladder.

1.27 Objectives

I investigated patient samples from the Bladder Cancer cohort undergoing cystectomy, and then explored their matched TURBT samples within the objectives of this study. The main objectives for this body of work were to:

(1) Identify epithelial, urothelial, and basal specific cell populations within urine using a representative model of non-muscle invasive Bladder Cancer.
(2) Perform a histological assessment confirming the presence of tumour in each patient bladder tumour sample, in preparation for downstream whole mtDNA genome sequencing analysis.
(3) Reliably amplify the mitochondrial genome in Bladder Cancer patients undergoing Robotic Cystectomy.
(4) Detect tumour-specific mtDNA pathogenic variants by performing mtDNA sequencing in primary bladder tumour samples following Radical Cystectomy.
(5) Confirm the presence of tumour-specific mtDNA variants in non-invasive patient matched samples, by analysing stored patient's matched cellular and cell-free urine to determine matched correlations of mtDNA variants between the primary tumour sequences and urine PCRs.

Within the introduction, I have described the major clinical problems associated with Bladder Cancer and the evidence gaps are rates of recurrence, biomarkers for recurrence, and accessibility within urine. I will take each of these components in turn and discuss them within the subsequent chapters of this thesis.

Chapter 2: Materials and Methods

All laboratory procedures were carried out in accordance with the departmental safety policy as outlined in the Newcastle Cancer Centre and Wellcome Trust Mitochondrial Research Group's safety policies. The Standard Operating Protocol (SOP) for each respective technique was followed, and Personal Protective Equipment (PPE) was worn. All BioCOSHH (Biological Control of Substances Hazardous to Health) forms and risk assessments were read and signed before the commencement of each procedure.

2.1 Human bladder Transitional Cell Carcinoma cell lines

To represent the most common types of NMIBC, experiments were conducted on T24, and RT112 bladder cancer cell lines spiked in urine. T24 and RT112 human bladder transitional carcinoma cell lines represent robust *in vitro* bladder tumour cell models. The rationale for the use of the T24 and RT112 cell lines in this project was, they both reflected the most common type of bladder cancer, transitional cell carcinomas, providing a representative cell line for optimisation and validation before use on valuable human patient tissue. T24 cell line, was isolated from the urinary bladder of an 81-year-old female and purchased from American Type Culture Collection. RT112, a slow growing human bladder carcinoma epithelial cell line, was supplied by the European Collection of Authenticated Cell Cultures. LNCaP cells were grown in addition, for use as an appropriate control due to the proximity of the prostate to the bladder.

2.2 Cell culture

2.2.1 Subpassaging

Cell culture was performed in a Class II microbiological safety cabinet [Bioflow 2] under aseptic conditions. Prior to all cell culture work, tissue culture hoods and reagents were sprayed with 70% ethanol. T24, RT112, and LNCaP cells were initiated from -80°C cell stocks and grown for several passages in standard growth medium RPMI-1640 [Thermo Scientific, FisherScientific] at 37°C, 5% CO_2. 45 ml 10% foetal calf serum (FCS) [Dutscher Scientific] and 5ml 1% antibiotics (Penicillin/Streptomycin) [GIBCO/Invitrogen] were added to RPMI media. Cell lines were grown in T175 flasks in a thermally controlled incubator, and at 70% confluency, by standard trypsinisation, cells were detached. Cell lines were resuspended in 4ml media and spun at 1500 rpm for 5 minutes. The supernatant was discarded, and the cell

pellet was resuspended in 1ml fresh media. The cell suspension was split into T175 cell culture flasks (Fisher-Scientific) and incubated with growth media changed every two to three days.

2.2.2 Counting Cells

After trypsinisation, cell pellets were resuspended in 1ml media, and a 30 µl total cell suspension was added to the haemocytometer [Neubauer]. Gentle pressure in small circular motions ensured the coverslip was placed accurately and cells spread over the haemocytometer by capillary action. Cells were counted as Total number counted / Number of quadrants x Cell Dilution Factor. Counted cells ensured correct seeding density and determined the precise volume of cells required when splitting to new flasks. Cells were seeded in a T175 flask at 80% confluency at a density of 2-4 x 10, 000 cells/cm^2 per flask.

2.2.3 Freezing Cells

Cryopreservation ensured a reserve of cells were available for future experiments. Once 80% confluency had reached monolayer cultures were frozen to ensure available working stock. After trypsinisation cell pellets were suspended in 1ml freezing media (300 µl FCS and 200 µl growth media with 10% Dimethyl Sulfoxide (DMSO)) Hybri-Max™ [Sigma-Aldrich]. DMSO acted as a cryoprotective agent and slowly reduced the media freezing point preventing the formation of ice crystals, a potential contributor to cell damage and apoptosis. Cells were immediately added to a sterile labelled cryotube and incubated on ice for 20 minutes. Cryotubes were placed in a -80^oC freezer for future use, and cells were initiated when required for further downstream analysis.

2.2.4 Spiking cells in urine

Cell lines were routinely incubated in standard growth medium, trypsinised to detach adherent cells (as described in section 2.2.1) and counted (as explained in section 2.2.2). Cells were washed in 1x PBS spun at 1500 rpm for 3 minutes to remove residual media and repeated three times. 15ml urine specimens were collected from healthy volunteers into a universal containing preservative to mimic urine samples received as part of the PHOTO-T trial, the largest national Bladder Cancer clinical trial. Such reflected home urine collection and 150 000 RT112, T24, and LNCaP cells/cm^2 were added respectively to each urine sample and left at room temperature for two days.

2.3 Flow Cytometry

Flow cytometry is a laser-based analysis technology that characterises cells in a fluid. Cells for analysis flow in a liquid stream through a laser beam, and using an array of detectors, a measurement is provided (Giaretti, 1997). Notably, this technique offers advantages as numerous particles can be measured, and each measurement is completed for every cellular event, recorded and cellular subpopulations determined (Mack, 2007). A valuable tool in biomarker research and clinical practice, multiple parameters are measured at single cell level, providing tremendous insight into cellular subpopulations (Barlogie et al., 1983).

Fluorescence-activated cell sorting (FACS) is quantitative and informative. Furthermore, in conjunction with the use of specific markers, a quantitative measurement can distinguish cell types within urine. Detailed analysis of the cellular composition of urine is provided by flow cytometry DNA analysis, offering an alternative platform to cytology to detect bladder cancer cell types with high specificity. Although flow cytometry is not routinely performed during the screening of urothelial carcinomas, cell sorting has been advocated for patients with the presence or suspected presence of a bladder tumour.

Identifying specific cell populations in urine to further understand the molecular makeup of cells in patients with NMIBC was performed using a conventional BD FACS Flow Cytometer. Setup controls, gating controls, and biological comparison controls were completed to optimise Flow Cytometry. The cytometer detected a voltage pulse per cell, producing two pulses that were measured and one pulse was calculated.

Forward Scatter (FSC) was roughly proportional to each cell size, Side Scatter (SSC) determined the granularity of each cell. Doublet cells had double the area and width of single cells, therefore, disproportions between cell height, width and area identified doublets. Consequently, the SSC area (SSC-A) was plotted as the channel is more sensitive to changes in cases of doublet discrimination which affects fluorescence, against the FSC area (FSC-A) for doublet discrimination. Doublet discrimination was scaled linearly as their presence was a function of random distribution as some cells ended up close enough to one another producing a doublet.

Setup controls comprised of gating to select specific cells for analysis on the scatter plot enabling positive and negative boundaries for data collection and analysis to be set. Above

all, this ensured cellular debris was excluded from analysis and allowed essential parameters to be set. Gating enabled the reliable determination of positive or negative CD49f, EpCAM, and uroplakin 1b staining within transitional cells, in addition to the exact proportions of cells to be known.

Further setup controls included 'height', which changed in photomultiplier tube voltage-based intensity of the signal and was regulated by the optimal correlation with the highest signal. 'Width' gating control was the time taken for each cell to pass over the laser beam, which correlated with cell size and provided the best correlation to cell size. The 'area' gating control was calculated from all height measurements and displayed the signal and expression, which correlated to cell size (height of cells x width of cells). Biological comparison controls were applied to differentiate specific from non-specific binding using relevant secondary antibodies, and LNCaP control cells identified cellular marker populations in a nearby organ to the bladder.

FSC-A events were plotted against SSC-A to identify the viable urine cell population of interest, cell surface marker against SSC-A determined non-specific binding, and the cell surface marker against SSC-A identified cell-specific marker positive cells within each population. Properties of transitional bladder cancer cells from urine were quantified, and surface antigen expression within distinct cell types were characterised one cell at a time. Additionally, gating controls were applied to differentiate specific from non-specific binding, ensuring accurate setting of gates allowing the determination of positive and negative cell identification (Mack, 2007) from scattergrams.

2.3.1 Epithelial and basal cell detection – EpCAM and CD49f staining

T24, RT112, and LNCaP urine cell suspension were centrifuged according to the PHOTO-T Urine processing SOP (detailed in section 2.6.2), pelleted cells were re-suspended in 4ml RPMI media and transferred to a sterile FACS tube. Cells were washed three times with 1ml 1x PBS by centrifugation of 15000rpm for 5 mins at 4^{o}C and placed in 5ml blocking buffer (4% serum/BSA) at 4^{o}C for 1 hour. Varying dilutions of epithelial marker EpCAM and basal cell marker CD49f were prepared in blocking buffer with samples incubated in primary antibody at room temperature for 1 hour. Cells were washed in cold, sterile 1ml PBS and spun at 15000 rpm for 5 minutes. Cell washes were repeated three times, and all samples were kept in the dark and protected from light from this stage.

Although EpCAM and CD49f were directly conjugated antibodies to 488nm and APC, respectively, a secondary antibody was added to demonstrate non-specific binding. T24, RT112, and LNCaP cell lines were incubated at 4°C for 15 mins and thoroughly washed three times in cold sterile PBS. Cells were left in 3ml fresh PBS added and samples were then ready for flow cytometric analysis. Cells were resuspended before running through the BD FACS Calibur ™ Flow Cytometer [342975]. Gentile agitation ensured cells were not shattered before running through the flow cytometer, such prevented clumping and ensured single cell suspensions were analysed.

2.3.2 Urothelial cell detection – Uroplakin 1b staining

After trypsinisation (as described in section 2.2.1), cells were fixed before use in 4% paraformaldehyde for 1 hour. Due to the intracellular nature of Uroplakin 1b, fixed cells were permeabilised in 0.2% Triton X-100 and washed twice in 1x BD Perm/Wash buffer following a 15-minute incubation. Fixed permeabilised cells were centrifuged at 1500 rpm for 15 minutes and thoroughly resuspended in varying dilutions of Uroplakin 1b [Sigma-HPA 031799] prepared in 1x BD Perm buffer. Cells were left to incubate for 1 hour at room temperature and washed twice in 1x BD Perm/Wash buffer. A secondary antibody was added for 15 minutes to T24, RT112, and LNCaP cell lines at 4°C to display non-specific binding. Samples were thoroughly washed three times in cold, sterile PBS, 3ml fresh PBS was added and repeated three times. Cells were then ready for flow cytometric analysis.

Each healthy volunteer provided ~15ml urine that was spiked individually with 150, 000 cells/cm^2 either Transitional Cell Carcinoma (RT112/T24) or prostate (LNCaP) cells. EpCAM, Uroplakin 1b, and CD49f contents within T24, RT112 and LNCaP cells were plotted on bivariate dot plots. Population means were not compared for statistically significant differences as cell sorting was undertaken to gain an appreciation of the molecular subtypes within urine. Urine cellular analysis was repeated three times for reliable insight into the molecular subtypes within transitional cell carcinoma models. Dot plots were analysed using FlowJo single cell analysis software (version. 10), with the flow cytometry detecting 30,000 cellular events in each experimental arm meeting the minimum analysis requirements for flow cytometry (Hedley et al., 1993).

Gating was performed to select specific cells for analysis on scatter plots enabling positive and negative boundaries to be set for data collection and analysis. Primarily, this ensured

cellular debris was excluded from analysis and allowed essential parameters to be determined. Gating enabled the reliable determination of positive or negative CD49f, EpCAM, and Uroplakin 1b staining within transitional and prostate cells, in addition to the exact proportions of cells to be known.

2.4 Tissue Preparation for tumour assessment

Clinical samples were collected from NMIBC patients within the Urology department at Freeman Hospital, Newcastle, UK, undergoing Radical Cystectomy. These samples were selected for use in this study as patients were already undergoing the invasive, cystectomy procedure as part of treatment for Bladder Cancer. Additional samples from the Radical Cystectomy collection ensured no further discomfort was experienced by patients. The samples provided a primary source of relevant material in order to address the aims and objectives of the research project. Similar clinical material: blood and urine from patients diagnosed with bladder cancer had been previously collected as part of a larger national clinical trial, and this study acted as a feasibility and proof of principle before using the precious clinical trial material. Additionally, a cohort of FFPE blocks from Royal Victoria Infirmary, Newcastle, from NMIBC patients who had previously undergone Radical Cystectomy, were received, including TURBT, benign bladder, and bladder tumour FFPE blocks. An anonymous database of patients' clinical details was accessed at Freeman Hospital, and all samples were securely stored according to good clinical laboratory practice guidelines.

FFPE sections of bladder tumour and benign tissue were cut at 4 µm using a standard microtome [Microm] for H&E staining. Fresh frozen bladder tumour and benign bladder tissue mounted onto filter paper embedded with OCT (as described in section 2.6.1) were cut at 4 µm for H&E staining and 15 µm thickness for laser capture microdissection.

2.4.1 Haematoxylin and Eosin Staining

Tissue sections were air-dried for 1 hour, stained in Mayer's haematoxylin for 5 mins, and rinsed with tap water until the water ran colourless. Sections were subsequently blued in Scott's Tap Water (0.2% (w/v) Sodium Bicarbonate, 2% (w/v) Magnesium Sulphate) for 30 seconds and washed with running tap water. Sections were soaked in Eosin for 2 minutes, rinsed thoroughly in tap water, and agitated through a series of gradient ethanol solutions (70%, 95%, 2x 100%) for 1 minute in each. Sections were dehydrated and cleared in 100% xylene twice, for a minute each, and mounted in DPX with a coverslip.

Slides were given to Consultant Histopathologists at Royal Victoria Infirmary Hospital (Newcastle), North Tyneside Hospital (North Shields), and Queens Medical Centre (Nottingham), and tumour assessment was performed by determining the total percentage of tumour in each representative section of TURBT, tumour and benign H&E sections.

2.5 Laser Capture Microdissection

Tumour rich regions were captured using a PALM MicroBeam laser micro-dissection microscope [Leica Microsystems]. Areas of interest were isolated from a 10 µm section of heterogenous bladder tissue and mounted on membrane slides (1.0 PEN). Sections were dehydrated in 100% xylene for 45 minutes to fully remove paraffin wax following 70% and 100% ethanol immersion for 10 minutes each and subsequently air dried.

Settings for laser energy and focus on the MicroBeam system were optimised for FFPE cut bladder tissue. The Laser Capture Microdissection (LCM) system was set to the following parameters: 52 ms energy, 12dB analogue gain, and 75 ms focus. As sections to be laser capture microdissected were unstained; a higher laser cutting energy was required due to a lower absorption of laser energy. 50 large cell areas ~ 250.000 μm^2 each in size were selected, which generated ~ 12.5 mm^2 pooled tissue in each cap. Tumour rich regions were cut and catapulted into the cap containing lysis buffer. A focussed infrared laser was fired which stuck onto the wet inner surface of the cap during the lifting procedure. After microdissection, the cap containing the microdissected sample was removed from the collector and placed on ice.

2.5.1 Laser Capture Microdissection Optimisation

On bladder tumour and benign 10 µm sections, parameters were optimised to ensure optimal settings were selected for use on patient tissue. A compromise between a high energy laser setting, but sufficient not to disrupt and damage the DNA were chosen. Annotation elements were drawn, and tissue was lifted into lysis buffer, as seen in Figure 13 below. Drawing tools outlined the area to be cut and catapulted whilst the UV laser ensured the selected area was cut and catapulted into the cap.

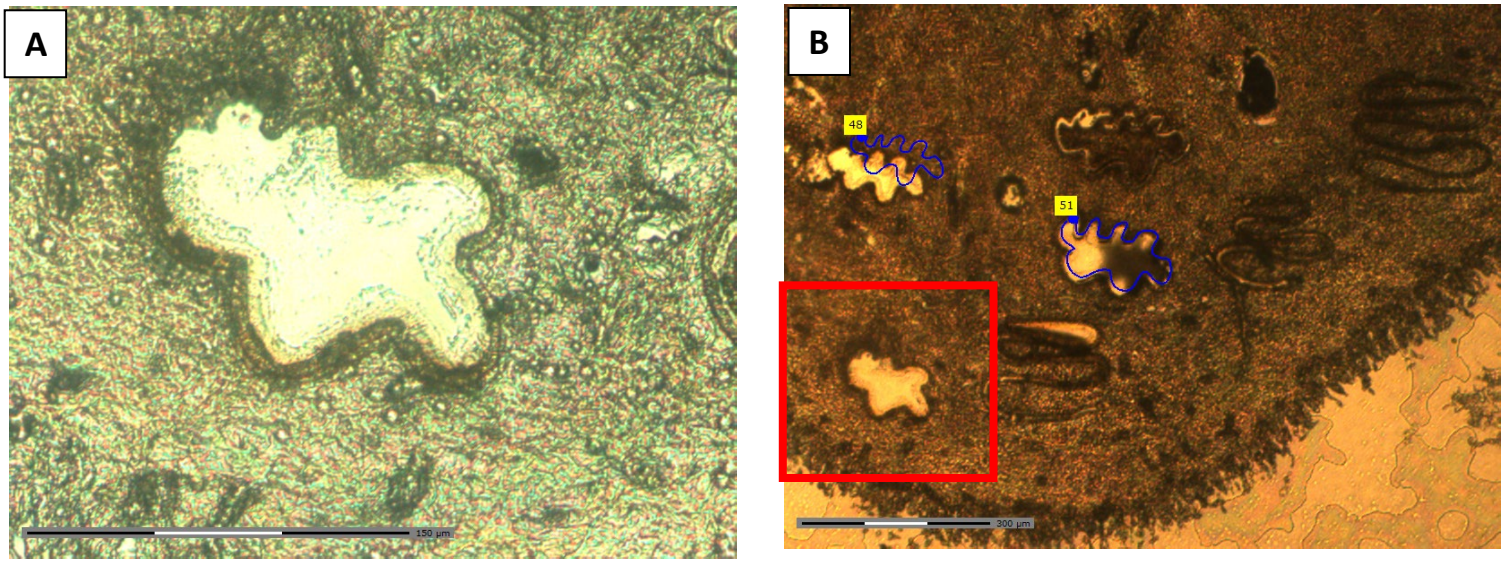

Figure 13 -Parameters were optimised on 10 µm bladder tissue sections to precisely microdissect tumour-specific regions for analysis. The images were taken directly on the Laser Capture Microdissection microscope and have not been edited to display a true representation of specific tumour region removal.. A) Representative section at 150 µm B) Representative section at 300 µm. .

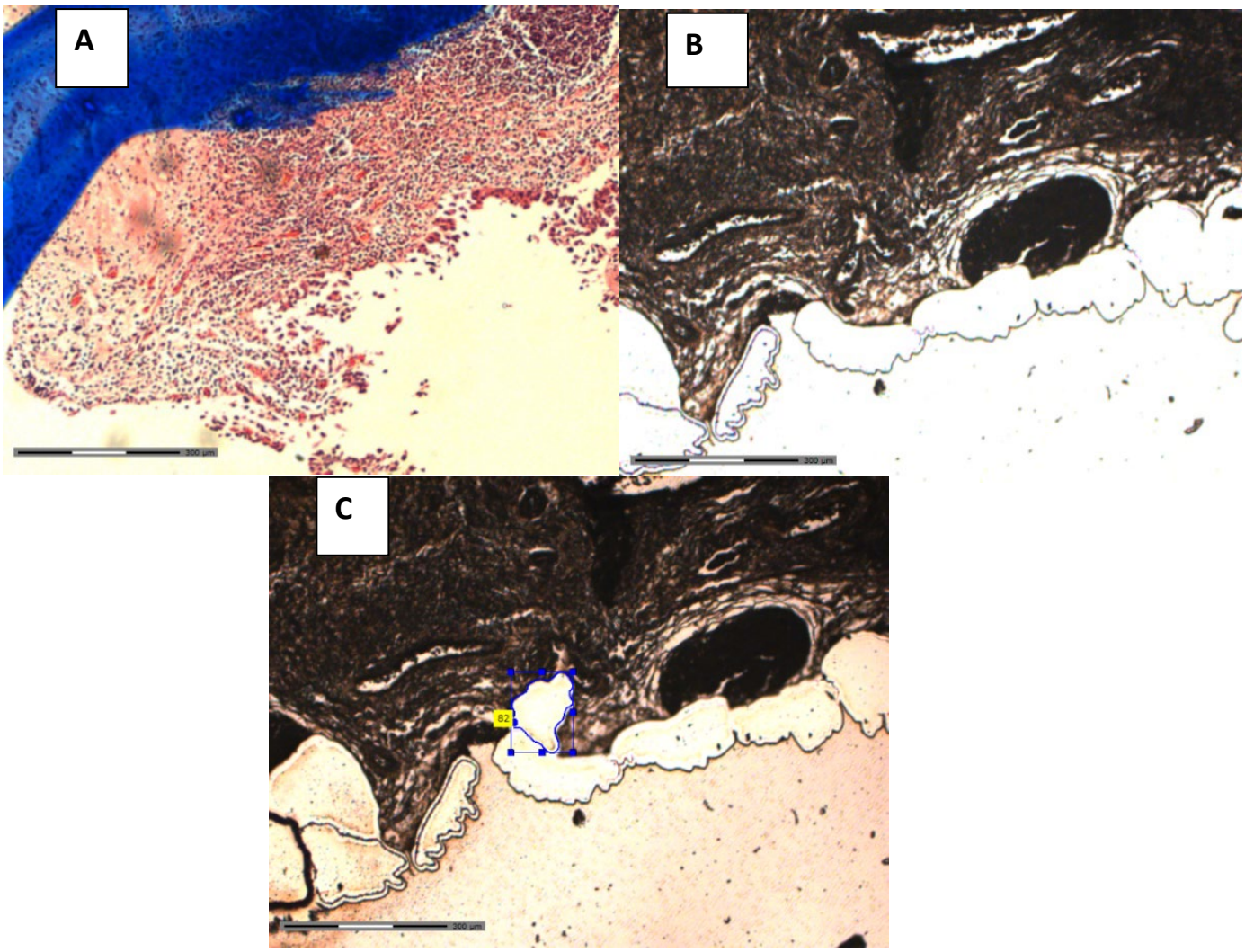

Figure 14 - A) Tumour rich areas marked on a representative H&E section by Pathologist B) Tumour rich region to be microdissected C) Tumour rich region post microdissection.

After histological assessment, tumour rich regions were marked by the Pathologist as shown in Figure 14 A). After histological assessment patient 13's representative H&E stained section of bladder tumour FFPE tissue, was described as suggestive of a potential non-invasive papillary tumour with an overall tumour content of 10%. This 10% tumour was microdissected resulting in 100% tumour content to be prepared for mtDNA sequencing. A demonstration of bladder tissue captured and lifted for analysis can be seen in Figure 14 C).

Tumour rich regions were analysed in single cell lysis buffer (250 µl 1% Tween 20, 195 µl dH_20, 45 µl TRIS-HCL, 5 µl Proteinase K) and 20 µl lysis buffer placed into the cap to improve tumour rich tissue adhesion. Tissue was lysed at 55°C for 3 hrs, 95 °C for 10 mins, stored at -20°C for mtDNA amplification and 1 µl cell lysate was added to PCR mastermix as listed in Table 4.

Component	Volume
10 x LA Taq Buffer	5 µl
dNTPs (2.5 µm)	8 µl
Genomic DNA	1 µl
10 µM Forward Primer	1 µl
10 µM Reverse Primer	1 µl
LA Taq polymerase	0.5 µl
Nuclease free water	33.5 µl
Total	**50 µl**

Table 4 - Reagent components for the Mastermix prepared for mtDNA amplification from microdissected bladder tissue.

Whole genomic DNA was amplified under cycling conditions listed in Table 5 below.

Stage	Step	Temperature (°C)	Time
Activate	Activate the enzyme	94	30 secs
Cycle (35 cycles)	Denaturation	94	30 secs
	Anneal	68	15 mins
	Extension	72	10 mins
Hold	Final hold	4	∞

Table 5 - PCR Cycling conditions for mtDNA amplification from microdissected bladder tissue.

PCR products were run on a 0.7% agarose gel with a 1Kb ladder to confirm the presence of amplified amplicons and determine the size. Amplicons were purified as detailed in section 2.10 and subsequently prepared for fragmentation and whole mtDNA sequencing (as described in section 2.11).

2.6 Tissue Processing

Bladder tissue was processed through a series of dehydration and clearing steps carried out on the automated tissue processor (Leica). Water from tissue was removed by dehydration through a series of ethanol: 70% to 95% to 100%. Clearing with xylene removed the dehydrant and finally, tissue was infiltrated with paraffin wax the embedding agent. Tissues were correctly orientated and embedded into cassettes ready for microtomy.

Position	Reagent	Routine Overnight Programme
1	70 % Ethanol	1 hr
2	95 % Ethanol	30 mins
3	95 % Ethanol	1 hr
4	100 % Ethanol	1 hr
5	100 % Ethanol	1 hr
6	100 % Ethanol	1hr 30
7	Xylene	30 mins
8	Xylene	1 hr
9	Xylene	1 hr
10	Xylene	1 hr
11	Wax	2 hr
12	Wax	2 hr
Total Time		**13 hrs**

Table 6 - Bladder Tissue Processing schedule utilised for automated tissue processing.

2.6.1 Primary Bladder Sample Tissue Processing

Bladder tumour and benign tissue were collected from patients following Radical Cystectomy at Freeman Hospital, Newcastle UK with approval from Newcastle Upon Tyne NHS trusts ethics committee. Primary tissue was cut in half transversely with every attempt at preserving the mucosa, submucosa, and muscularis bladder wall layers (if present) in each piece. Half of the tissue was snap frozen in isopentane and liquid nitrogen and stored at -80 °C. The other

tissue half was fixed in 4% paraformaldehyde, processed, and embedded into an FFPE block. One tissue half was fixed in 4% paraformaldehyde, with fixative penetrating the tissue for 48 hrs, and the other tissue half mounted in OCT embedding compound onto filter paper. Isopentane was frozen in liquid nitrogen at -150 ^{o}C and tissue attached to filter paper was fully immersed in isopentane to ensure fully frozen.

2.6.2 Urine Supernatant and Urine Cell Pellet Preparation

Urine samples were processed according to the PHOTO-T SOP for processing PHOTO-T collected Blood and Urine Samples in the Newcastle Cancer Centre. Currently, PHOTO-T the largest bladder cancer trial in the North East is looking at improving tumour clearance through better tumour visualisation during surgery. For each participant, blood and 50ml urine samples were collected serially at baseline, 3, 12, 24, and 36 months or recurrence. Ethical approval has been obtained to use samples collected for PHOTO-T, which provides an excellent source of human primary cellular samples.

Urine was kept at room temperature, as when chilled precipitates may form which can interfere with downstream DNA purification. 1ml of whole urine was transferred into a sterile bijou, and the rest of the urine sample was centrifuged at 1900xg for 5 minutes at room temperature. The supernatant was decanted, placed into a sterile Eppendorf tube, and labelled. The lid was parafilmed and frozen immediately at -20 °C for 25 minutes before moving to -80 °C storage. 1 ml sterile PBS was added to the cell pellet and resuspended gently to avoid vigorous cellular disruption, and centrifuged at 3500 rpm for 5 minutes. The supernatant was discarded without disrupting the cell pellet, the lid parafilmed, and the sample frozen immediately at -20 °C for 25 minutes before moving to -80 °C storage.

2.6.3 Buffy Coat sample preparation

Blood samples were centrifuged at 4 ^{o}C at 1900xg for 10 minutes on the lowest deceleration brake setting to avoid disrupting the buffy coat layer. Plasma supernatant was pipetted without disturbing the middle buffy coat layer into Eppendorf tubes and centrifuged for 10 minutes at 13,5000 rcf at 4 ^{o}C. Plasma supernatant was pipetted into cryotubes and stored immediately at -80 ^{o}C. Pushing through the buffy coat layer to the bottom of the red blood cell layer, 2x2ml was pipetted into cryotubes. 200 µl (10% volume of freezing media [FCS + 10% DMSO]) was added, and cryotubes were labelled and stored immediately at -80 ^{o}C.

Remainder buffy coat and red blood cell volume were pipetted into a fresh cryotube, and 10% freezing media added. All cryotubes were labelled and stored immediately at -80 ^{o}C.

2.7 DNA Extraction

DNA was extracted from clinical bladder tissue, urine, and buffy coat samples using the QIAamp DNA Mini Kit [Qiagen]. To achieve standardisation samples were extracted using the automated DNA extractor Qiacube [Qiagen] according to the manufacturer's instructions according to each specimen type and uploaded onto the machine.

DNA was eluted in 50 µL of molecular biology water. DNA quantity and quality were assessed using the Nanodrop [Life Technologies] according to the manufacturer's instructions. 1 ng/µl of DNA was used for whole mtDNA amplification.

2.7.1 Bladder Tumour, Benign, Urine, and Buffy Coat tissue lysis

The sample pellet was resuspended in 180 µl Buffer ATL 20 µl proteinase K added, mixed, vortexed, and incubated at 56 ^{o}C for 1 hour and 90 ^{o}C for 1 hour. From this stage, the next steps were placed on the Qiacube for automated DNA extraction. The steps were as followed. 200 µl Buffer AL was added to each sample and mixed thoroughly to bind the DNA. 200 µl 99% ethanol was added, and the entire lysate was transferred to the QIAamp MiniElute column. The column was centrifuged at 6000 xg for 1 min and placed into a clean 2ml collection tube. The collection tube containing the flow-through was discarded, and 500 µl Buffer AW1 was added and centrifuged at 6000 xg for 1 minute. The flow-through was again discarded, and the column placed into a sterile collection tube. 500 µl Buffer AW2 was added to the column, centrifuged at 6000 x g for 1 minute, and the flow through discarded. The sample was centrifuged at 10 000 x g for 3 minutes to dry the membrane, and the column was placed in a sterile microcentrifuge tube. The flow-through was discarded, and 50 µl Buffer AE was added to the centre of the membrane and incubated at room temperature for 1 minute. The sample was centrifuged at full speed for 1 minute and placed on ice, ready for quantification.

2.7.2 DNA Extraction for FFPE bladder biopsies

Excess paraffin wax was trimmed off the FFPE block, and 10 x 10 µm sections were cut using the microtome and placed in a sterile Eppendorf. An additional section cut at 4 µm was stained by H&E to confirm the presence of tumour within the tissue taken for DNA extraction.

1ml xylene was added to the sample, vortexed vigorously for 1 minute, and centrifuged at full speed for 2mins. The supernatant was discarded, and this was repeated twice. 1 ml 99% ethanol was added to the pellet and the above steps were repeated twice. The tube was opened and incubated at 37 ^{o}C for ~ 10 minutes until all excess ethanol has evaporated. The pellet was resuspended in 180 µl Buffer ATL and 20 µl proteinase K added, mixed and vortexed, and incubated at 56 ^{o}C for 1 hour and 90 ^{o}C for 1 hour. From this stage, the next steps were placed on the Qiacube for automated DNA extraction and automated steps were as follows: 200 µl Buffer AL was added to each sample and mixed thoroughly to bind the DNA. 200 µl 99% ethanol was added and the entire lysate was transferred to the QIAamp MiniElute column. The column was centrifuged at 6000 xg for 1 min and the column was placed into a clean 2ml collection tube. The collection tube containing the flow-through was discarded and 500 µl Buffer AW1 was added and centrifuged at 6000 xg for 1 minute. Flow through was again discarded and the column placed into a sterile collection tube. 500 µl Buffer AW2 was added to the column, centrifuged at 6000 x g for 1 minute, and the flow through discarded. The sample was centrifuged at 10 000 x g for 3 minutes to dry the membrane, and the column was placed in a sterile microcentrifuge tube. The flow-through was discarded, and 50 µl Buffer AE was added to the centre of the membrane and incubated at room temperature for 1 minute. The sample was centrifuged at full speed for 1 minute and placed on ice, ready for quantification.

2.8 DNA Quantification

The NanoDrop® ND-100 spectrophotometer was used for the quantification of 1µl samples of DNA. 1µl of Buffer AE was used to blank the sample and lowered onto the lower pedestal replicating the buffer the nucleic acids were dissolved in. Both pedestals were wiped to remove the blank, and 1µl sample was applied to the lower measurement pedestal and the nucleic acid amount, and quality were measured in ng/ µl.

2.9 PCR Amplification

2.9.1 Long Range PCR - Two Primer Pair Sets

To exclude the possibility of nuclear pseudogene amplification, DNA (20-50ng) was amplified with two overlapping primer pair sets, generating two ~9kb amplicons using GoTaq Long PCR Master Mix [Promega] according to the manufacturer's protocol.

Two Overlapping Primer Pairs used to amplify the human mitochondrial genome. Working concentration 10 µM			
Oligo Name	**Sequence (5' > 3')**	**Nucleotide Positions (bp)**	**Amplicon Size (bp)**
1**A**_F	AACCAAACCCCAAAGACACC	550-569	9289
1**A**_R	GCCAATAATGACGTGAAGTCC	9839-9819	
1**B**_F	TCCCACTCCTAAACACATCC	9592-9611	7622
1**B**_R	TTTATGGGGTGATGTGAGCC	645-626	

Table 7 -Two Oligonucleotide primer pairs used to amplify the whole mitochondrial genome.

2.9.2 Long Range PCR - Five Primer Pair Sets

To confirm the presence of mtDNA genotypes, five primer pair sets were used, and ~4,000 bp amplicon sized fragments obtained as a targeted area of the mitochondrial genome was amplified from matched samples from the Radical Cystectomy Cohort.

Each of the five primer pairs used to amplify the whole of the mitochondrial genome is described in Table 8 below.

Five Overlapping Primer Pairs used to amplify specific regions of the mitochondrial genome. (Working concentration 10 µM)				
Primer Pair	**Oligo Name**	**Nucleotide Positions**	**Sequence (5' > 3')**	**Amplicon Size (bp)**
1	D4F-6R	323-3574	TGTAAAACGACGGCCAGTGCCACAGCACTTAAACACATC - CAGGAAACAGCTATGACCGGAGGGGGGTTCATAGTAG	3251
2	6F-13R	3017-6944	TGTAAAACGACGGCCAGTCAGCCGCTATTAAAGGTTCG - CAGGAAACAGCTATGACCAAGAAAGATGAATCCTAGGGC	3927
3	13F-20R	6358-10147	TGTAAAACGACGGCCAGTTAGCAGGTGTCTCCTCTATC - CAGGAAACAGCTATGACCTAGCCGTTGAGTTGTGGTAG	3789
4	20F-28R	9607-13859	TGTAAAACGACGGCCAGTCATCCGTATTACTCGCATCAG - CAGGAAACAGCTATGACCGTTAGGTAGTTGAGGTCTAGG	4252
5	28F-D4R	13365-771	TGTAAAACGACGGCCAGTCGGGTCCATCATCCACAAC - CAGGAAACAGCTATGACCTGCTGCGTGCTTGATGCTTG	3975

Table 8 - Five Oligonucleotide primer pairs used to amplify the whole mitochondrial genome.

2.9.3 Long Range PCR - Eighteen Primer Pair Sets

To specifically amplify a targeted area of the mitochondrial genome from a cohort of formalin fixed samples from patients undergoing TURBT and Radical Cystectomy, eighteen overlapping primer pair sets ~1,000 bp spanning the whole circular genome were used (displayed in Table 9) to amplify the entire 16, 000 bp mitochondrial genome.

Eighteen Overlapping Primer Pairs used to amplify specific regions of the mitochondrial genome. (Working concentration 10 µM)

Primer Pair	Oligo Name	Nucleotide Positions	Sequence (5' > 3')	Amplicon Size (bp)
1	1F-2R	721 -1709	TGTAAAACGACGGCCAGTTCACCCTCTAAATCACCACG – CAGGAAACAGCTATGACCCTGGTAGTAAGGTGGAGTGGG	988
2	3F-4R	1650 - 2644	TGTAAAACGACGGCCAGTAACTTAACTTGACCGCTCTGAG – CAGGAAACAGCTATGACCTCGTGGAGCCATTCATACAG	994
3	5F-6R	2549 - 3574	TGTAAAACGACGGCCAGTCAGTGACACATGTTTAACGGC - CAGGAAACAGCTATGACCGGAGGGGGGTTCATAGTAG	1025
4	7F-8R	3505 - 4577	TGTAAAACGACGGCCAGTACCATCACCCTCTACATCAC - CAGGAAACAGCTATGACCGTTTATTTCTAGGCCTACTCAG	1072
5	9F-10R	4518 - 5481	TGTAAAACGACGGCCAGTACACTCATCACAGCGCTAAG- CAGGAAACAGCTATGACCTGTAGGAGTAGCGTGGTAAGG	963
6	11F-12R	5367 - 6430	TGTAAAACGACGGCCAGTACCTCAATCACACTACTCCC - CAGGAAACAGCTATGACCATGGCAGGGGGTTTTATATTG	1063
7	13F-14R	6358 - 7396	TGTAAAACGACGGCCAGTTAGCAGGTGTCTCCTCTATC - CAGGAAACAGCTATGACCCATCCATATAGTCACTCCAGG	1038
8	15F-16R	7272 - 8301	TGTAAAACGACGGCCAGTGGCTCATTCATTTCTCTAACAG - CAGGAAACAGCTATGACCTACAGTGGGCTCTAGAGGG	1029
9	17F-18R	8196 - 9201	TGTAAAACGACGGCCAGTACAGTTTCATGCCCATCGTC - CAGGAAACAGCTATGACCGTTGTCGTGCAGGTAGAGG	1005
10	19F-20R	9127 - 10147	TGTAAAACGACGGCCAGTATCCTAGAAATCGCTGTCGC - CAGGAAACAGCTATGACCTAGCCGTTGAGTTGTGGTAG	1020
11	21F-22R	10085 - 11109	TGTAAAACGACGGCCAGTCAACACCCTCCTAGCCTTAC - CAGGAAACAGCTATGACCATGATTAGTTCTGTGGCTGTG	1024
12	23F-24R	11010-12054	TGTAAAACGACGGCCAGTTATCCAGTGAACCACTATCAC - CAGGAAACAGCTATGACCCGTGTGAATGAGGGTTTTATG	1044

13	25F-26R	11977 - 13009	TGTAAAACGACGGCCAGTCTCCCTCTACATATTTACCAC - CAGGAAACAGCTATGACCCTGATTTGCCTGCTGCTGC	1032
14	27F-28R	12940 - 13859	TGTAAAACGACGGCCAGTGCCCTTCTAAACGCTAATCC - CAGGAAACAGCTATGACCGTTAGGTAGTTGAGGTCTAGG	919
15	29F-30R	13790 - 14857	TGTAAAACGACGGCCAGTACCTAAAACTCACAGCCCTC - CAGGAAACAGCTATGACCAAGGAGTGAGCCGAAGTTTC	1067
16	31F-32R	14797 - 15896	TGTAAAACGACGGCCAGTATTCATCGACCTCCCCACC - CAGGAAACAGCTATGACCTACAAGGACAGGCCCATTTG	1099
17	D1F-D2R	15758 - 129	TGTAAAACGACGGCCAGTATCGGAGGACAACCAGTAAG - CAGGAAACAGCTATGACCAGATACTGCGACATAGGGTG	940
18	D3F-D4R	16548 - 771	TGTAAAACGACGGCCAGTCCTTAAATAAGACATCACGATG - CAGGAAACAGCTATGACCTGCTGCGTGCTTGATGCTTG	792

Table 9 - Eighteen Oligonucleotide primer pairs used to amplify the whole mitochondrial genome.

2.9.4 PCR cycling conditions

Forward and reverse PCR primers listed in Tables 7, 8, and 9, Go Taq Long Range PCR mix and genomic DNA were thawed when required and placed on ice. For each amplicon generated PCR mastermix listed in Table 10 and all components listed were added to a 0.2mL strip sterile strip tube on ice and thoroughly mixed.

Component	**Volume**
Go Taq Long Range PCR Mix	12.5 µl
20-50ng genomic DNA	1 µl
10 µM Forward Primer	1.25 µl
10 µM Reverse Primer	1.25 µl
Nuclease free water	9 µl
Total	**25 µl**

Table 10 - PCR Mastermix for long range mtDNA sequencing.

2.9.5 PCR Thermal Cycling Conditions Fresh bladder, Urine, Buffy Coat samples

Samples were loaded into a thermal cycler and the following programmes highlighted in Table 11, were run to amplify mitochondrial genomic DNA.

Stage	Step	Temperature (°C)	Time	2 Primer Pairs	5 Primer Pairs	18 Primer Pairs
Hold	Activate the enzyme	94	2 min			
Cycle (35 cycles)	Denaturation	94	30 sec			
		65	30 sec			
	Anneal	71	1 min/1kb	N/A	4 mins	1 min
	Extension	71	1 min/1kb			
Hold	Final hold	4	∞			

Table 11 -PCR Thermal Cycling Conditions Fresh bladder, Urine, and Buffy Coat samples.

Stage	Step	Temperature (°C)	Time	2 Primer Pairs	5 Primer Pairs	18 Primer Pairs
Hold	Activate the enzyme	94	2 min			
Cycle (35 cycles)	Denaturation	94	30 sec			
		65	30 sec			
	Anneal	68	1 min/1kb	8 mins	4 mins	N/A
	Extension	71	1 min/1kb			
Hold	Final hold	4	∞			

Table 12 -PCR Thermal Cycling Conditions FFPE bladder samples.

2.9.6 PCR Thermal Cycling Conditions Targeted Sequencing

Stage	Step	Temperature (°C)	Time
Hold	Activate the enzyme	94	2 min
Cycle (35 cycles)	Denaturation	94	30 sec
		65	30 sec
	Anneal	68	2 mins 30 secs
	Extension	71	2 mins 30 secs
Hold	Final hold	4	∞

Table 13 - PCR Thermal Cycling Conditions Targeted Sequencing.

2.9.7 Gel Electrophoresis

Varying amounts of agarose depending on the applicable percentage gel required (see Table 14) were weighed in 100ml of 1x TAE Buffer and heated on high. 4 µl SYBR Safe (10, 000 x concentrate in DMSO) [ThermoFisher] was added to the molten agarose and poured into the gel rig with combs and left to completely set. Once the gel was completely solidified 4 µl DNA ladder [New England Biolabs] 100 µg/ml was added to the first row and 5 µl sample to each preceding well. The electrodes were hooked up so negatively charged DNA would run toward the positive electrode at 65 V for 90 minutes. Gels were imaged using the ChemiDoc GelDoc system selecting the illuminator which could excite SYBR Safe.

Percentage Agarose Gel (w/v)	DNA Size Resolution (kb = 1000)
0.5 %	1 kb to 30 kb
0.7 %	800 bp to 12 kb
1.5 %	200 bp to 3kb

Table 14 - A Table to show agarose gel concentrations prepared when confirming mtDNA amplification from generated amplicons.

2.10 Purifying amplicons

PCR products were purified with AMPure XP Reagent [Beckman Coulter, High Wycombe, UK] and the sample volume was made up to 50 µl with nuclease-free water. AMPure XP reagent beads were left at room temperature for ~30 mins, pulse-vortexed spun, resuspended and 90 µl added to the sample. The bead and DNA suspension were thoroughly mixed and left to incubate for 5 mins at room temperature. Each tube was placed on a DynaMag -2 magnet for 3 mins at the solution turned clear. The supernatant was discarded without disturbing the pellet and after 70% ethanol was freshly prepared, 500 µl was added to each tube. Samples were incubated for 30 secs and tubes were turned twice in the magnetic rack to rotate the beads and thoroughly purify the DNA. Once the solution had cleared, the supernatant was discarded without disturbing the pellet, and this was repeated. The tube was pulse vortexed and after placing back on the magnet, the remaining supernatant was removed with a 20 µl pipetted and discarded to remove residual alcohol, again without disturbing the pellet. After leaving the tubes on the magnet, beads were air-dried for 4 mins and tubes were removed from the magnetic rack, and 25 µl nuclease-free water was added directly to the pellet to disperse the beads. The suspension was pipetted five times and vortexed for 10 secs to ensure the sample was thoroughly mixed.

2.11 Preparing amplicon libraries requiring fragmentation

2.11.1 Bioanalyser

After mtDNA amplification, amplicons were purified (as described in section 2.10 purifying amplicons), and the molar concentration of each amplicon was determined using Agilent 2100 Bioanalyzer and DNA 12 000 kits. Before the chip was prepared, the chip priming station and bioanalyzer were optimally calibrated and ready for use.

2.11.2 Agilent 12 000 Kit

Blue-capped DNA dye concentrate and red-capped DNA gel matrix were left to equilibrate to room temperature for 30 minutes and vortexed. Ensuring samples were thoroughly thawed 25 µl blue-capped vial was pipetted into the red-capped DNA gel matrix vial and vortexed. The gel-dye mix was transferred to the top receptacle spin filter and centrifuged at room temperature for 10 minutes at 4000 rpm. 9 µl gel-dye mix was pipetted into wells of the chip, and 5 µl marker was added to each of the 12 sample wells, 1 µl DNA, and 1 µl ladder into each representative well as seen in Figure 15. The chip was placed on the IKA vortex mixer for 1

minute at 2400 rpm. The 12 000 DNA chip was inserted into the Agilent 2100 Bioanalyser, and the molarity of each sample was determined.

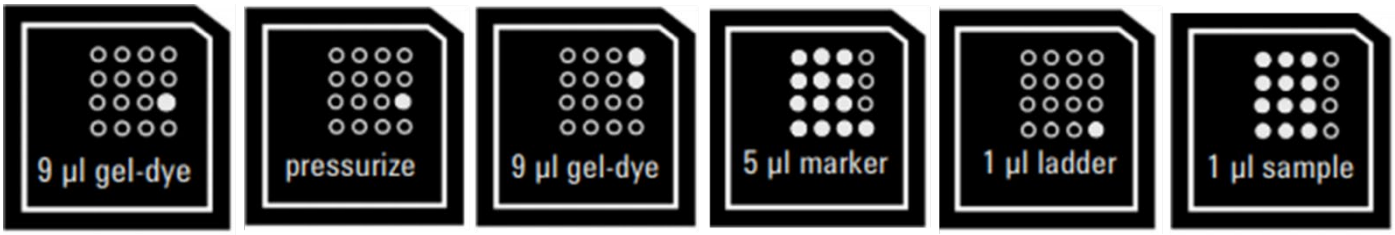

Figure 15 – A schematic illustration to show components loaded onto a 12 000 DNA chip ready to be inserted into the Agilent 2100 Bioanalyser for sample analysis.

The results of a successful DNA sample run resembled the electropherogram of the ladder well, as shown in Figure 16, and the molarity was determined from 1 µl of each sample.

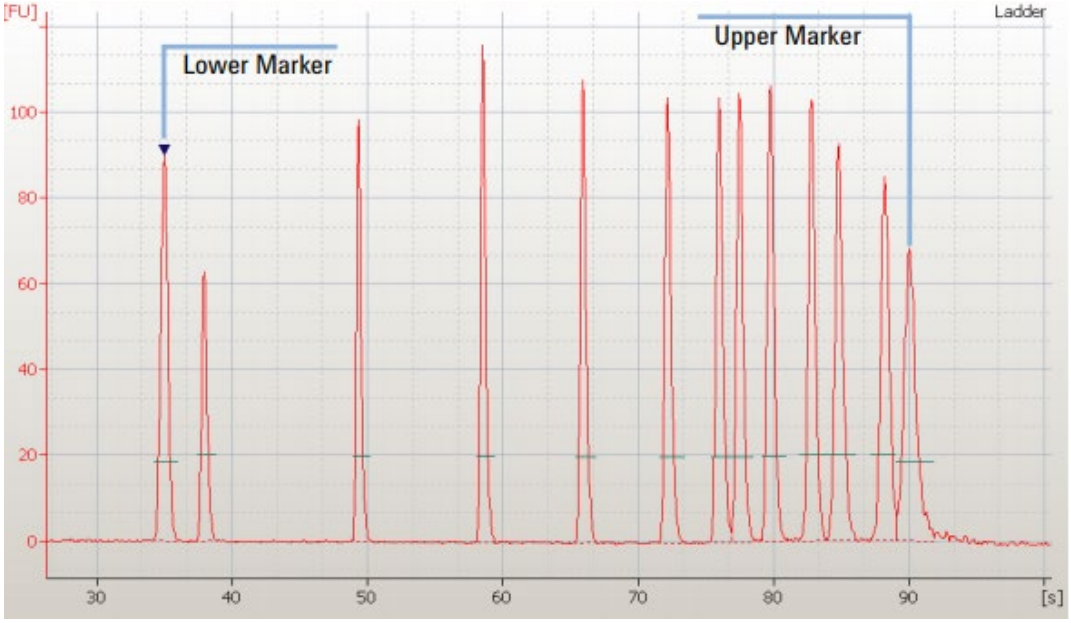

Figure 16 - Electropherogram of a well-run DNA 12 000 Agilent kit ladder indicating a good run. The electropherogram displays the lower ladder marker at 35bp and the upper ladder marker at 90bp. The DNA sample peaks were evident within the lower and upper mark ladder regions.

2.11.3 Agilent High Sensitivity Kit

The chip was primed, and the bioanalyser was set up and ready for use. Blue-capped DNA dye concentrate, and red-capped DNA gel matrix were left to equilibrate to room temperature for 30 minutes and vortexed before use. Ensuring samples were thoroughly thawed 15 µl blue-capped vial was pipetted into the red-capped DNA gel matrix vial and vortexed. The gel-dye mix was transferred to the top receptacle spin filter and centrifuged at room temperature for 10 minutes at 6000 rpm. 9 µl gel-dye mix was pipetted into wells of the chip, 5 µl marker was added to each of the 12 sample wells, and 1 µl DNA to each and 1 µl ladder into each

representative well. The chip was placed on the IKA vortex mixer for 1 minute at 2400 rpm. The high sensitivity chip was inserted into the Agilent 2100 bioanalyser and the molarity of each sample was determined.

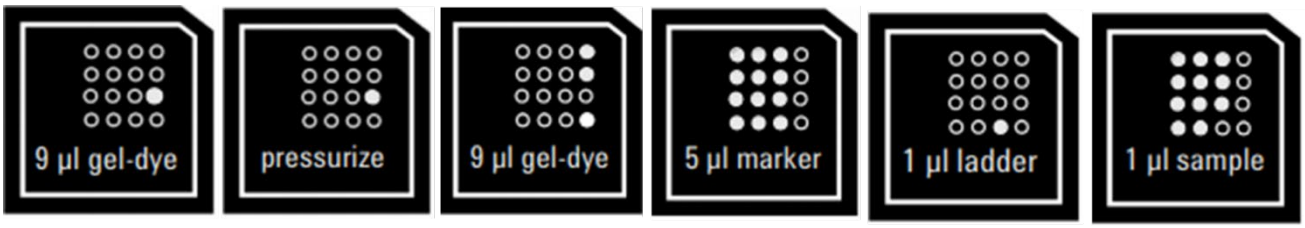

Figure 17 - A schematic illustration to show components loaded onto a High Sensitivity DNA chip ready to be inserted into the Agilent 2100 Bioanalyser for sample analysis.

The results of a successful DNA sample run resembled the electropherogram of the ladder well as seen in Figure 18, and the molarity was determined from 1 µl sample.

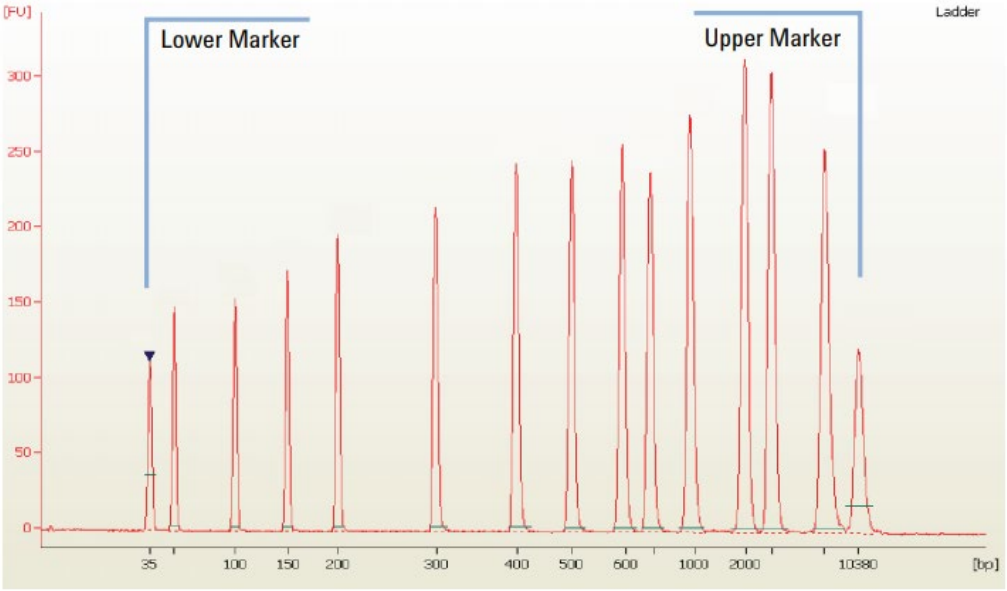

Figure 18 - Electropherogram of a well-run DNA High Sensitivity kit ladder indicating a good run. The electropherogram displays the lower ladder marker at 35bp and the upper ladder marker at 10, 380 bp. The DNA sample peaks were evident within the lower and upper mark ladder regions.

2.12 Pooling amplicons

To ensure even coverage of the mitochondrial target regions, amplicons were pooled in equimolar amounts for Ion library construction by combining 100ng equimolar amount of each amplicon stock after performing the following calculations:

100 ng equimolar volume = 100 / concentration (ng/ µl)

Total ng in combined pool = SUM (equimolar volume adjusted x concentration (ng/ µl)

2.12.1 Fragmenting Amplicons

Fragmentation conditions were selected according to the desired 200 bp target length read and ~260 median insert size. All components listed in Table 15 were vortexed for 5 secs, pulse-spun, and placed on ice. Components were added in the order listed above to a sterile 1.5-mL Eppendorf LoBind tube and mixed vigorously by vortexing for 5 seconds. 10 µl Ion Shear Plus Enzyme Mix II was added, and the enzyme mix, DNA, and buffer were mixed rapidly and incubated in a pre-heated 37 °C heat block for 15 mins, and a 200-300 base read median fragment sized library was obtained. 5 µl Ion Shear Stop Buffer was added immediately and mixed thoroughly and vortexed for 5 secs, and stored on ice.

Samples were purified (as detailed in section 2.10) with 99 µl Agencourt AMPure XP Reagent beaded to the sheared DNA sample, and DNA was eluted into 25 µl Low TE ready for ligation.

Component	Volume
Pooled amplicons, 100ng	Y µl
Ion Shear Plus 10x Reaction Buffer	5 µl
Nuclease-free Water	35 -Y µl
Total	**40 µl**

Table 15 -Reagents required for pooling equimolar 100ng amplicons. The total volume of 100ng pooled amplicons is indicated by Y, and this amount was deducted from 35 µl nuclease-free water.

2.12.2 Ligate adaptors, nick repair

In a sterile 0.2-mL PCR tube, the reagents listed in Table 16 were combined and mixed well.

Barcoded Libraries (Total 100 µl)			
Component	**Volume**	**Component**	**Volume**
10 x Ligase Buffer	10	Nick Repair Polymerase	8
Ion Xpress Barcode	2	DNA	25
Ion P1 Adapter	2	dNTP Mix	2
DNA Ligase	2	Nuclease-free water	49
Total 100 µl			

Table 16 -Reagent components for barcoded libraries Mastermix.

Tubes containing barcoded library mastermix were placed in a thermal cycler and run on the following program listed in Table 17.

Stage	Temperature	Time
Hold	25 °C	15 min
Hold	72 °C	5 min
Hold	4 °C	Up to 1h

Table 17 - Thermal Cycler programme for ligation and nick repair barcoded libraries library.

The reaction mixture was transferred into a 1.5-mL Eppendorf sterile LoBind Tube for purification. Samples were purified (as described in section 2.10) with 120 µl Agencourt AMPure XP Reagent beaded to the sheared DNA sample, and DNA was eluted into 23 µl Low TE for size selection.

2.12.3 Size Selection

The E-Gel SizeSelect 2% agarose gels [ThermoFisher Scientific, Paisley] cassette was inserted securely into the E-Gel electrophoresis device, and all wells were filled with 50 µl dh_20. Samples listed in Table 18, were prepared in a total volume of 25 µl and loaded onto the e-gel. 25 µl ladder was loaded into marker well, and the size select 2% run started on the electrophoresis device for 16 mins the expected migration time of our 200bp target fragment size according to the reference line. Gel status was checked using the backlight, and the UV-protected filter screen used to ensure the 200bp library had not missed the recovery well.

Component	Volume
Sample	22.5 µl
10x sample loading buffer	2.5 µl
Total	**25 µl**

Table 18 - A table listing reagents required for a 200bp product.

Ladder components	Volume
DNA Ladder	12.5 µl
Nuclease Free Water	10 µl
Loading Buffer	2.5 µl
Total	**25 µl**

Table 19 -DNA Ladder components required for size selection.

2.12.4 DNA Collection

Once the reference band of the DNA ladder had reached 1 minute before the reference line, the gel was paused, excess solution removed, and fresh 50 µl dH_20 added to each recovery well. The run was resumed, and once the reference band at 350 bp target library peak had completely entered the top edge of the collection well the run was stopped. The sample was recovered using a pipette ensuring the agarose was not pierced during collection.

2.12.5 Library Amplification and Purification

Reagents were combined in the order listed in Table 20 and mixed thoroughly. The reaction was split into two 0.2-mL PCR, each containing ~65 µl. The tubes were placed in the thermal cycler and run on the thermocycling program described in Table 21.

Component	Volume
Platinum PCR SuperMix High Fidelity	100 µl
Library Amplification Primer Mix	5 µl
Unamplified library {size selected by E-gel agarose gels}	25 µl
Total	**130 µl**

Table 20 -Reagents required for generating 200bp size selected amplicons.

Stage	Step	Temperature	Time
Hold	Denature	95 °C	5 min
Cycle (8 cycles)	Denature	65 °C	15 sec
	Anneal	58 °C	15 sec
	Extend	70 °C	1 min
Hold	-	4 °C	Hold up to 1hr

Table 21 -A Thermal cycling conditions of 200bp size selected amplicon required for mtDNA sequencing.

Once amplification was complete, split PCRs were combined into a sterile 1.5-mL Eppendorf LoBind tube. Samples were purified (as detailed in section 2.10) with 195 µl Agencourt AMPure XP Reagent beaded to the sheared DNA sample, and DNA was eluted into 20 µl Low TE for mtDNA sequencing.

2.13 Preparing amplicon libraries without fragmentation

Targeted mtDNA PCR amplicons were prepared (as detailed in section 2.9.2) and amplified accordingly. Samples were purified, and molar concentrations of each amplicon were determined (as previously described in section 2.10).

2.13.1 End Repair

100 ng pooled amplicons were prepared (as listed in section 2.12), and the end repair reaction was prepared as described in Table 22 and incubated for 20 minutes at room temperature.

Component	Volume
10-100ng pooled amplicons	79 µl
5x End Repair Buffer	20 µl
End Repair Enzyme	1 µl
Total	**100 µl**

Table 22 -Reagents required for End Repair amplicon Mastermix.

Samples were purified (as described in section 2.10) with 180 µl Agencourt AMPure XP Reagent beaded to the sheared DNA sample, and DNA was eluted into 25 µl Low TE for size selection.

Samples were ligated (as described in section 2.12.2), purified, amplified, barcoded, size-selected, and amplified using the IonXpress Plus Fragment Library kit, Ion Xpress Barcode Adapters 1-16 kit, and E-Gel SizeSelect 2% agarose gels [ThermoFisher Scientific] as per the manufacturer's instructions. Barcoded libraries were assessed on the 2100 Bioanalyzer using the Agilent High Sensitivity DNA kit and subsequently pooled in equimolar concentrations.

2.14 Loading barcoded libraries onto a chip

Molar concentrations of the library pool were determined and diluted to a concentration of ~100pM and further diluted to ~20 pM**.** Clonal amplification of 20 pM pooled amplicon libraries enrichment was loaded onto an Ion 316 v2 BC sequencing chip with sequencing

performed on the Ion Torrent Personal Genome [Life Technologies] and Ion Torrent S5 [ThermoFisher Scientific] machines.

2.15 Variant Caller Analysis

Tumour-specific mtDNA genotypes were detected in samples absent from the patients' benign urothelium when aligned both to the revised Cambridge mtDNA reference sequence NC_012920.1 and the hg19 human genome sequence. Sequence alignment to mtDNA and hg19 human reference genome data analysis was conducted using the variant caller plug-in Torrent Suite Variant Caller (TVC). v5.10.1.20 (mtDNA custom settings). Analysis was performed on Torrent Suite version 5.10.2, utilising the Coverage Analysis and Variant Caller plug-in.

The Torrent Suite Variant caller pipeline was applied to sequenced data to ensure true mtDNA variants were identified, coupled with setting stringent filtering thresholds manually using the mtDNA alignment pipeline. For quality control the minimum allele frequency was set to 0.05 for insertion and deletion of bases, and 0.005 for single and multiple nucleotide polymorphisms, which was greatly improved and refined compared to a previous threshold of 0.02 bases for the latter. Data quality was assessed by the probability of variant allele frequency being greater than, or below the minimum allele frequency. 6.5 minimum relative read quality was applied and additional strand bias and homopolymer filters to ensure data quality stringency. Updated TVC software ensured false positives were accurately and not excessively reported and manual assessment of uniformity of coverage and sequencing quality using a 1000 cut-off, strengthening the robustness of confidence when variant calling. A heteroplasmy threshold of 5% was set as the same as the Wellcome Centre diagnostic mitochondrial service, Newcastle, which identifies mtDNA variants in clinical patient samples. In addition, various published papers similarly detect mtDNA pathogenic variants from a heteroplasmy level of 5%.

All detected mtDNA variants were manually reviewed with the Integrative Genomics Viewer [v2.4.19, Broad Institute, Cambridge, Massachusetts, US]. Sequence coverage of this depth confidently detected variants that are only present in the tumour and not within benign and Buffy Coat samples.

Chapter 3: Does the characterisation of molecular subtypes using cell markers aid Bladder Cancer cell detection and stratify transitional cell carcinomas?

3.1 Urine provides a valuable non-invasive biopsy of bladder tumour

Urine is a valuable tool to indicate suspected bladder cancer, as ~85 % of NMIBC patients initially present with haematuria (Kamat et al., 2016), in addition to experiencing painful urination. Fundamentally a liquid biopsy of bladder tumours (Kamat et al., 2014), urine is an abundant source of bladder tumour material (Satyal et al., 2019). The accessibility and non-invasive nature of urine are particularly advantageous, coupled with the ongoing search for a urinary biomarker. A non-invasive urinary biomarker would profoundly relieve the reliance on surveillance cystoscopy, thus dramatically improving the NMIBC patient experience.

Urine comprises various cells, including leukocytes, squamous cells, erythrocytes, transitional cells, erythrocytes, and renal tubular cells (Khan et al., 2017). Typical proportions of cells in urine vary depending on patients' disease type, condition and treatment, hence national reference ranges for amounts of cells in urine are variable. For instance, in leukopenia, a reduction in the total number of white blood cells may be observed in the urine of patients prescribed antibiotics, undergoing radiation therapy, or chemotherapy. Typically increased cellular counts detected in urine are confirmed with additional microscopy culture, sensitivity, and cytological tests. UK standards for Microbiological Investigations advise >100 lymphocytes per µl of urine indicative of infection and >25 erythrocytes per µl considered microscopic haematuria (Public Health Guidance SMI B 41: Investigation of urine). Urinary single-cell profiling captured natural helper immune cells, macrophages, lymphocytes, and several kidney cell types, including proximal tubule cells, Loop of Henle cells, umbrella, intermediate, and basal layer cells. Comparative single-cell transcriptomics confirmed representative gene expression parallels (Abedini et al., 2021) with the cell types identified.

Epithelial cells line a variety of body surfaces (Wiggins et al., 2009) yet naturally slough off from various sites within the body (Pisitkun et al., 2006). Furthermore, transitional epithelial cells line the urinary tract and are shed into urine, in addition to renal epithelial tubular cells, which migrate from the kidney and are similarly shed into urine (Pisitkun et al., 2006). Squamous cells are the largest cell type derived from both the vagina and urethra and are found in high abundance in females compared to males (Wiggins et al., 2009).

Bladder tumour cells are shed readily into urine providing an easily accessible source for bladder tumour cell surveillance (Shariat et al., 2008). Shed cells only make up a proportion of the tumour as the shedding of tumour cells is determined by tumour size, cancer stage, grade, and several cell types found in urine (E. Andersson et al., 2014). Detectable tumour cells from Grade I bladder tumours are low (20-40% sensitivity (Goodison et al., 2013)) as only a small number of cancer cells are exfoliated into the urine, whereas shed cells from Grade II bladder tumours can be pathologically diagnosed as malignant (Pathol, 1981) when evaluated by urine cytology. Enrichment of shed tumour cells in urine can be achieved by size-based capturing methods as lymphocytes are greater in size than epithelial cells, thus utilising filters to isolate cells based on size (E. Andersson et al., 2014). Scanning Electron Microscopy was highlighted as a sensitive application to detect specific cells within shed urine (Croft & Nelson, 1979). Urinary cell-free DNA (U-cfDNA) typically represents the tumour genome, and an increased tumour burden observed compared to DNA from exfoliated whole urine cells (Togneri et al., 2016). Tumour cells with U-cfDNA have higher rates of necrosis compared with normal urothelium. This proposes U-cfDNA as a potential tumour-specific BC biomarker for use within clinical applications.

Identification of distinct molecular subtypes (Lerner & Robertson, 2016) derived from various urothelial progenitor cells (Czerniak et al., 2016) inform patients' clinical phenotypes, therefore informing BC patients' treatment plan. Filtration of voided BC patients' urine increased the proportion of tumour cells captured, enhancing the accuracy, detection, and sensitivity of identifying BC (E. Andersson et al., 2014) by a non-invasive approach.

75% of BC patients present with NMIBC (Babjuk et al., 2017), and despite transurethral resection and adjuvant intravesical immunotherapy or chemotherapy offered, high recurrence rates of 50% within 3 years after transurethral resection of initial tumour, is anticipated. Regardless of treatment, 45% of NMIBC patients experience muscle invasive progression, MIBC (van der Heijden & Witjes, 2009). Clinical prognostic factors for NMIBC recurrence and progression are tumour size, histopathological grade, stage, presence of CIS, and reaction to intravesical therapy (Van Der Heijden and Witjes, 2009).

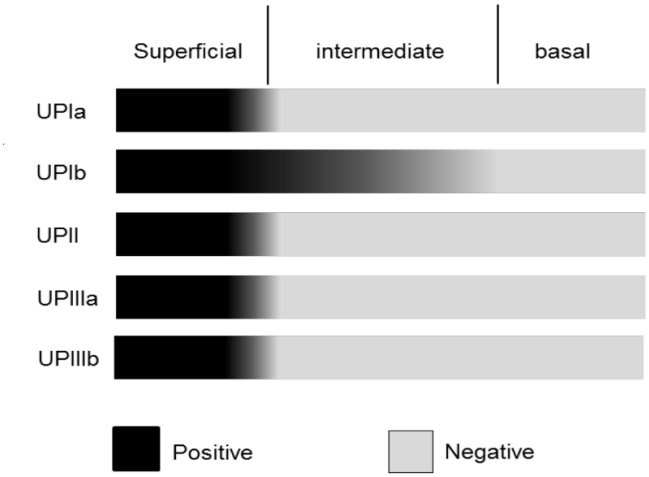

Figure 19 - Distribution of uroplakins within the superficial, intermediate, and basal urothelium layers. UPIb is observed within the intermediate and superficial layers of the bladder and UPIa, UPII, UPIIIa, and UP111b is found within the superficial bladder layer only. Source: (Moad et al., 2017).

The distribution of uroplakins within the urothelium layers is illustrated in Figure 19 above. Uroplakin Ib was earmarked for flow cytometry analysis within this study as a marker of both the superficial and intermediate layer of the bladder. Importantly, such methodology would offer the ability to capture urothelial cells found in both the superficial and intermediate layers of the bladder of transitional cells within urine.

3.2 Cellular markers

Urinary biomarkers offer a non-intrusive paradigm for detecting bladder cancer (Chakraborty et al., 2019) coupled with current literature confirming the requirement to exploit the unique advantage of identifying exfoliated cells in urine, for the detection of bladder cell-surface antigens (Sapre et al., 2014). Urinary biomarkers should predict the presence of both non-muscle invasive and muscle-invasive bladder cancers, as such will inform treatment response (Chakraborty et al., 2019). Surface markers are specific to each cell type furthermore, the determination of types of cell markers within particular cell membranes can be recorded.

The bladder urothelium is a transitional epithelium typically composed of three cell layers each with morphologically distinct cell types: basal precursor cells, intermediate cells, and large superficial umbrella cells (Volkmer et al., 2012). The germinal basal layer is identifiable with cell surface marker CD49f, urothelial cells defined by uroplakins (Moad et al., 2017), and cells of epithelial origin characterised by EpCAM (Brunner *et al.,* 2008). Determining cell surface and intracellular markers allows the stratification of NMIBC into molecular subtypes.

This aids cancer cell detection and is notably well established in routine clinical use (Pisitkun et al., 2006).

A tabular summary of molecular subtypes of NMIBC, histological features, and gene expression for each of the three bladder tumour classes are defined within Table 23. Mutations are identified in p53-like subtypes where infiltration of stromal fibroblasts is typically observed, basal classes with typical squamous features, and luminal sub-classes.

Tumour Class	Histological Features	Increased Protein Levels
1, 2	Luminal	E-CAD, HER2/3, Rab-25, UPKs
3	Basal	p63, CD49f, EGFR, Cyclin D1

Table 23 - Biological interpretation of Non-muscle Invasive Bladder Cancer molecular classes.

Human urinary tract epithelial cells were isolated and cultured from various parts of the urinary tract to enhance the understanding of the morphology of proliferating cells. Dörrenhaus et al provided an insight into the morphological variations within cells correlating to various locations in the urinary tract (Dörrenhaus et al., 2000). Cell culture is not instantaneous and takes a few days to yield confluent healthy cells as Erden and colleagues exhibited with epithelial morphology visible within isolated cells after day one coupled with a fibroblastic appearance discernible on day two, post cultivation (Erden Tayhan et al., 2017). Despite compelling evidence of the potential use of such methods for further in vitro clinical research, this does not yield an instant direct benefit to patients.

By contrast, cytological examination through evaluating cellular morphology is a standard reliable method for bladder cancer detection (Planz et al., 2005). With a specificity of ~86%, the sensitivity of detection is markedly lower at ~48% in High=Grade tumours and considerably lower at ~16% in Low-Grade tumours (Yafi et al., 2015). Importantly, such confirmed urinary cytology is a highly beneficial diagnostic tool for bladder cancer detection, yet despite this, cytology is not able to substitute cystoscopy (Leiblich, 2017). During cytological examination, cells visualised microscopically require human interpretation, introducing intra-observer bias as well as subjectivity. Nonetheless, due to the low specificity as well as invasive nature of cystoscopy the search for new detection tools is still relevant and highly required. Exploiting flow cytometry methods facilitates the appreciation of molecular

compositions within urine. Prospectively determining epithelial, basal, and urothelial compositions within matched patient voided urine allows an insight into the makeup and cellular composition of urine.

3.2.1 Cell Surface Markers

Epithelial cell extraction was undertaken, and urine cells were stained using cell surface marker EpCAM, a trans-membrane protein. EpCAM is often over-expressed by epithelial cancers and solely expressed in epithelia, therefore utilised as a cell surface maker within urine. Conjugated to Alexa Fluor 488, EpCAM detected epithelial-specific cells (as described in section 2.3.1) within each urine cell population of interest.

Basal cell detection within urine was completed using CD49f, a basal cell-specific cell surface marker. Employed as a differentiation marker, CD49f conjugated to Allophycocyanin (APC) fluorochrome was excited by far-red fluorescence lasers at a fluorescence emission peak of 660nm. CD49f-APC anti-human mouse antibody (clone GoH3) transmembrane glycoprotein specifically identified basal cells at the single cell level within the urine population of interest.

3.2.2 Intracellular Marker – Uroplakin 1b

Uroplakin Ib, a urothelial cell marker and member of the tetraspanin family identified urothelial-specific cells. Urine cells were fixed, and an intracellular cytokine stain Perm/Wash buffer was used to permeabilise cells before the addition of the Uroplakin Ib antibody (as described in section 2.3.2). Intracellular marker Uroplakin Ib was applied as a cytoplasmic stain. The unconjugated anti-human rabbit antibody and fluorescent secondary Alexa Fluor 647 dye-stained urothelial cells within the assessed urine population.

3.3 Hypothesis

I hypothesised that the identification of specific urothelial, basal, and epithelial cell populations could be determined within urine using a representative model of transitional cell carcinoma cell lines.

Within this chapter, I intended to distinguish specific cell populations within urine to elucidate molecular subtype composition within a representative model of NMIBC patients' urine. Initial authentication was completed using NMIBC cell lines spiked in healthy volunteers' urine. Undertaking epithelial, basal, and urothelial cell extraction using intracellular and cell surface markers enabled us to comprehend the molecular makeup of specific molecular subtypes within the urine and exclude inflammatory, erythrocytes, debris, and other renal filtered cells.

3.4 Aims

This investigation aimed to demonstrate cancer cells can be extracted from urine, with the intention to specifically identify:

a) Epithelial cell populations within urine, as non-invasive bladder cancers that originate from the transitional epithelium and innermost layer of urothelial cells.

b) Basal cell populations within urine.

c) Urothelial specific cell composition within urine.

Although an epithelial-specific marker would not have the ability to discriminate between renal tubular and urothelial cells, it would certainly identify transitional cells of epithelial origin.

3.5 Objectives

(1) Detect Class 1-2 epithelial-specific cell populations in urine spiked with transitional cell carcinoma lines.

(2) Identify Class 1-2 urothelial specific cells in urine from within the superficial and intermediate layers of the bladder.

(3) Characterise Class 3 basal specific cells within urine using a representative model of non-muscle invasive Bladder Cancer.

Moreover, the evaluation of cellular constituents in urine can provide an insight into the composition of cells in the liquid biopsy of bladder tumours. Similarly, this accelerates an understanding of the cellular molecular makeup within urine, providing the possibility of specifically isolating and characterising certain urinary cell types. Leukocytes are one of many cell types found in urine and appear morphologically similar to transitional epithelial cells, as both cell types have a granular appearance. The most distinctive features are the spindle, pyramidal cell shapes, and eccentric nuclei in transitional cell carcinoma.

3.6 Ethical Approval for healthy volunteer urine

Ethical approval was obtained, and healthy volunteer consent forms (see Appendix A) were completed by nine subjects who generously donated their urine sample, on three separate occasions, over eleven days for this part of the study. Volunteers were both a mixture of male and female, all between the ages of 23 and 63, as listed in Table 24. Each volunteer provided ~15ml urine that was spiked individually with 150, 000 cells/cm^2 either Transitional Cell Carcinoma (RT112/T24) or prostate (LNCaP) cells. Spiked cells with urine were left for two days at room temperature to reflect PHOTO-T home urine collection samples (as detailed in section 2.2.4). Confidentiality was maintained for each volunteer, as samples were anonymised, and my analysis had no clinical implications on participants' health.

3.6.1 Healthy Volunteer subject cohort for urine samples spiked with EpCAM, CD49f, and Uroplakin 1b cellular markers.

Healthy Volunteer	Gender	Age	Specimen Provided	Day Collected	Cell line spiked	Cell Marker Investigated
1	Male	41	~12 ml urine	Day 1	RT112	EpCAM
			~10 ml urine	Day 8	RT112	CD49f
			~15 ml urine	Day 11	RT112	Uroplakin Ib
2	Female	25	~8 ml urine	Day 1	T24	EpCAM
			~15 ml urine	Day 8	T24	CD49f
			~10 ml urine	Day 11	T24	Uroplakin Ib
3	Male	39	~12 ml urine	Day 1	LNCaP	EpCAM
			~10 ml urine	Day 8	LNCaP	CD49f
			~10 ml urine	Day 11	LNCaP	Uroplakin Ib
4	Male	58	~10 ml urine	Day 1	RT112	EpCAM
			~10 ml urine	Day 8	RT112	CD49f
			~10 ml urine	Day 11	RT112	Uroplakin Ib
5	Female	23	~15 ml urine	Day 1	T24	EpCAM
			~10 ml urine	Day 8	T24	CD49f
			~12 ml urine	Day 11	T24	Uroplakin Ib
6	Female	47	~8 ml urine	Day 1	LNCaP	EpCAM
			~12 ml urine	Day 8	LNCaP	CD49f
			~12 ml urine	Day 11	LNCaP	Uroplakin Ib
7	Male	63	~15 ml urine	Day 1	RT112	EpCAM
			~10 ml urine	Day 8	RT112	CD49f
			~10 ml urine	Day 11	RT112	Uroplakin Ib
8	Female	34	~15 ml urine	Day 1	T24	EpCAM
			~12 ml urine	Day 8	T24	CD49f
			~12 ml urine	Day 11	T24	Uroplakin Ib
9	Male	27	~12 ml urine	Day 1	LNCaP	EpCAM
			~10 ml urine	Day 8	LNCaP	CD49f
			~10 ml urine	Day 11	LNCaP	Uroplakin Ib

Table 24 – ~15ml urine spiked with epithelial cell marker EpCAM, basal cell marker CD49f, and intracellular urothelial cell marker Uroplakin 1b. Spiked urine cells were left at room temperature for two days before flow cytometry experiments.

3.6.2 RT112, T24, and LNCaP Cell Lines

As a representative model of cancer cells in normal urine, I manufactured a clinical analogue where I took fresh, healthy urine specimens and spiked them with cancer cells, and then investigated the cancer cells, (as described in section 2.3). I utilised bladder specific cell lines and LNCaP cells as a non-BC cell line, which served as an appropriate experimental control as the prostate is the male organ in closest proximity to the bladder. The human bladder transitional carcinoma cell lines RT112/84 and T24 (ATCC HTB-4) were used as an NMIBC tumour cell model. According to the description of the American Type Culture Collection, the T24 cell line was a transitional cell carcinoma isolated from the urinary bladder of an 81-year-old female. RT112 cell line supplied by the European Collection of Authenticated Cell Cultures was a human bladder carcinoma epithelial cell line (*ECACC Public Health England RT112)*. 90% of all bladder cancers are transitional cell carcinomas (Vriesema et al., 2001) and T24 and RT112 bladder cancer cell lines are a representative model of NMIBC. LNCaP (CRL-1740) cell lines derived from human epithelial prostate carcinoma were utilised as an appropriate control due to their nearby organ to the bladder's proximity. LNCaP clone FGC was isolated from a needle aspiration biopsy of the left supraclavicular lymph node from a 50-year-old Caucasian male with a confirmed diagnosis of metastatic prostate carcinoma.

LNCaP cells acted as a control cell line for the study and to represent the most common types of NMIBC, T24, and RT112 cell lines were thawed, cultured, and passaged (as described in section 2.2).

As patient samples are valuable and precious, particularly tissues from cancer patients as the nature of obtaining such material is often invasive, cell lines were used to gain an initial insight into the molecular characterisation of urine.

3.7 Representative transitional cell carcinoma model

Initially, 150,000 T24, RT112, and LNCaP cells were added respectively to ~15 ml urine obtained from healthy volunteers in a universal container. The urine sample spiked with cells was left at room temperature and analysed two days after voiding. Time of urine collection was standardised, ensuring the first urine sample upon waking was not utilised as urine is more concentrated in the morning due to dwelling time in the bladder for many hours overnight and, therefore, not representative of the participant’s urinary system. For routine clinical use, midstream urine is recommended and the most common collection method

clinically. This recapitulated cellular culture model of transitional cell carcinoma provided an *in vitro* model to mimic the PHOTO-T trial home urine collection (described in section 2.6.2).

3.8 Results

3.8.1 Urothelial cell surface detection in urine spiked LNCaP, T24, and RT112 cells

Urine cell pellets were prepared to specifically characterise cells of urothelial origin, as detailed in section 2.6.2 and various dilutions were prepared, as outlined in Table 25 below.

LNCaP cells spiked in urine	T24 cells spiked in urine	RT112 cells spiked in urine
Unstained	Unstained	Unstained
Secondary antibody only	Secondary antibody only	Secondary antibody only
1:50	1:50	1:20
1:100	1:100	1:50
1:200	1:200	1:200

Table 25 - Varying dilutions prepared for the isolation of urothelial cells for flow cytometric analysis in urine spiked with LNCaP, T24, and RT112 transition cells.

Urothelial-specific populations within T24 cells were plotted on bivariate dot plots and are displayed in Figure 20. Population means were not compared for statistically significant differences as cell sorting was undertaken to gain an appreciation of the molecular subtypes within urine. Considering each volunteer provided ~15ml urine spiked individually with 150, 000 cells/cm^2 either RT112, T24 or LNCaP, the return after flow cytometry analysis was not recorded and during each experiment the cell number far exceeded the number of minimum cells recorded. Dot plots were analysed using the FlowJo package with 10,000 events recorded in each experimental arm, meeting the minimum analysis requirements for flow cytometry (Hedley et al., 1993).

3.8.2 Optimising urothelial cell marker Uroplakin Ib staining in urine spiked with T24 cells

An unstained population of 89% T24 cells were identified and used as a negative control, as seen in scattergram (A) in Figure 20. To exclude background staining 0.74% of T24 cells were expressed with secondary antibody only (B). For optimal uroplakin Ib staining in urine spiked with T24 cells, various dilutions detailed in Table 25 were prepared for detection and quantification. As the 1:100 dilution identified a 99.9% positive detection of uroplakin Ib cells (D) this dilution was taken forward for subsequent urothelial cell detection within the T24 spiked urine population.

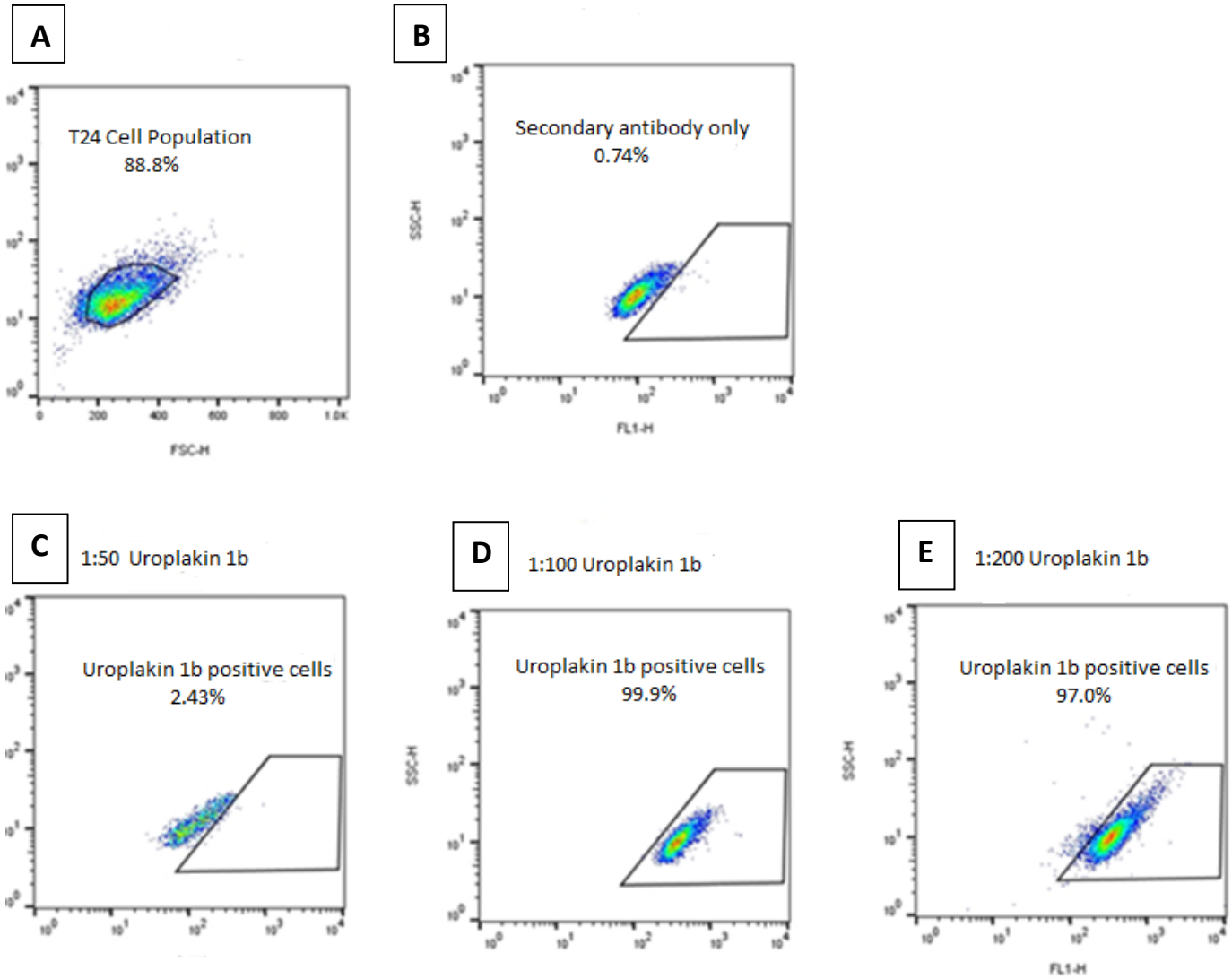

Figure 20 - Bivariate dot plots of T24 transitional carcinoma cells displaying (A) T24 unstained cells, (B) T24 cells with secondary antibody only, (C) 1:50 uroplakin 1b positive cells, (D) 1:100 uroplakin 1b positive cells, and (E) 1:200 uroplakin Ib positive cells.

3.8.3 Optimising urothelial cell marker Uroplakin Ib staining in urine spiked with RT112 cells

A set of RT112 cells spiked in urine were prepared for flow cytometric analysis with various dilutions of uroplakin Ib prepared (listed in Table 25), to quantify the population of urothelial-specific cells found in urine. 95.1% RT112 were identified and analysed (A), a secondary antibody was added and 5.22% RT112 cells were stained as background only (B). Varying dilutions of uroplakin Ib antibody were prepared, to optimise the most efficient dilution to efficiently pull down specific populations of urothelial cells. 68.9% of RT112 cells were detected as urothelial specific cells (C), 87.5% of RT112 cells were positively identified as of urothelial origin at 1:50 dilution (D), and 88% after staining at 1:200 dilution (E). Amounts of RT112 cells positively detected were similar, consequently, 1:200 dilution was chosen to take forward for urothelial specific staining in urine spiked with RT112 cells as preparing less antibody is more economical with a similar population of cells being captured after 1:50 and 1:200 dilutions were used during this antibody dilution optimisation.

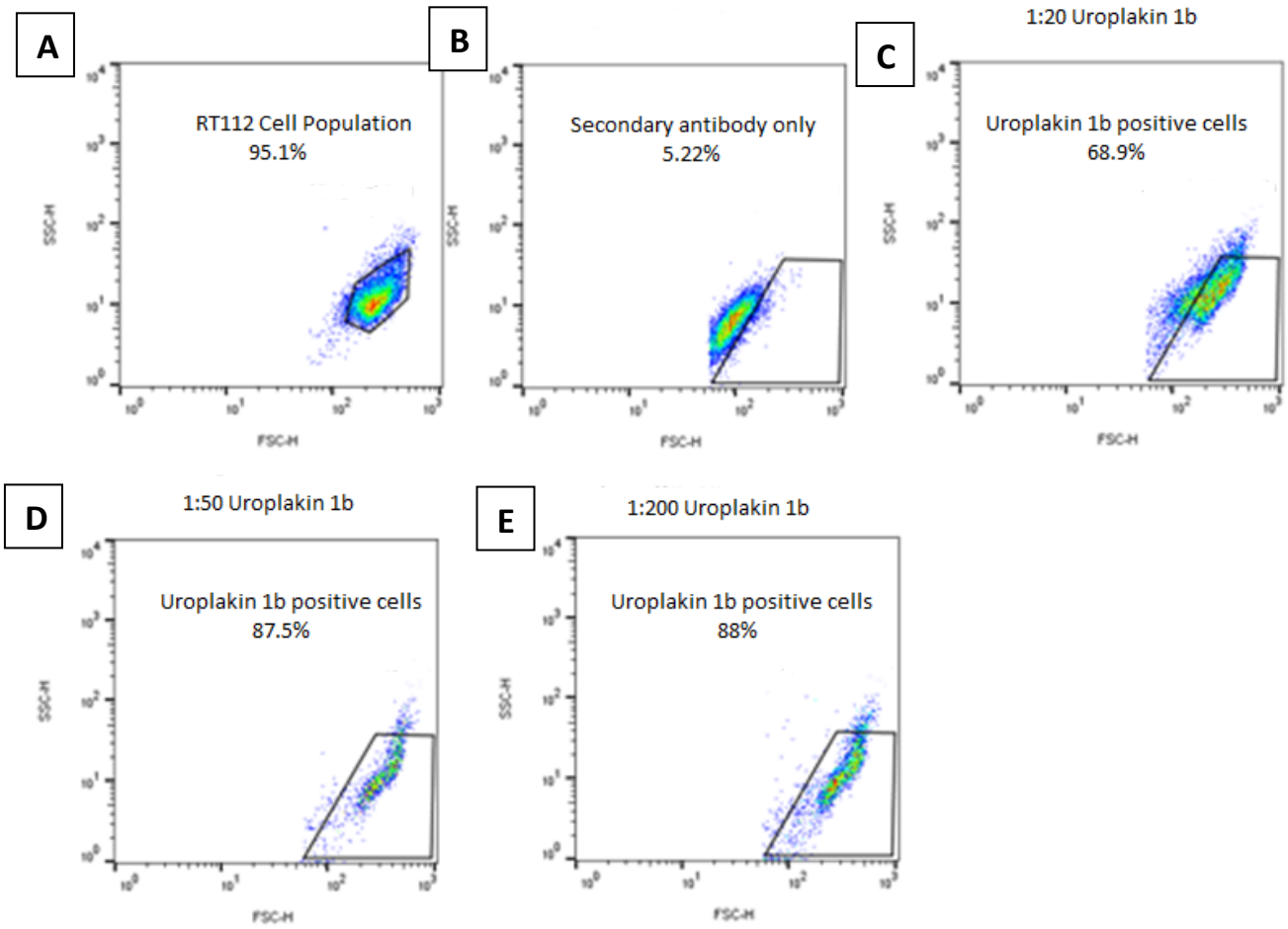

Figure 21 - Bivariate dot plots of RT112 transitional carcinoma cells displaying (A) RT112 unstained cells, (B) RT112 cells with secondary antibody added, (C) 1:20 uroplakin Ib positive cells, (D) 1:50 uroplakin Ib positive cells, and (E) 1:200 uroplakin Ib positive cells.

3.8.4 Optimising urothelial basal cell marker CD49f staining in urine spiked with RT112 and T24 cells

CD49f is a basal cell marker based on former findings within the bladder and prostate (Moad et al., 2017). A previously published dilution of 1:50 (Moad et al., 2017) detected multipotent basal stem cells from the whole prostate epithelium. This 1:50 dilution was taken forwarded as a starting point to capture basal cells within RT112 and T24 spiked urine. Typically, bladder tumours classified as Grade 3 presented with basal histological features, and an increased expression of CD49f was observed.

An 82.2% unstained population of RT112 cells were identified in Figure 22 (A), background staining detected 0.80% RT112 cells (B), and 83.5% RT112 cells were positively stained for CD49f after FACS analysis (C).

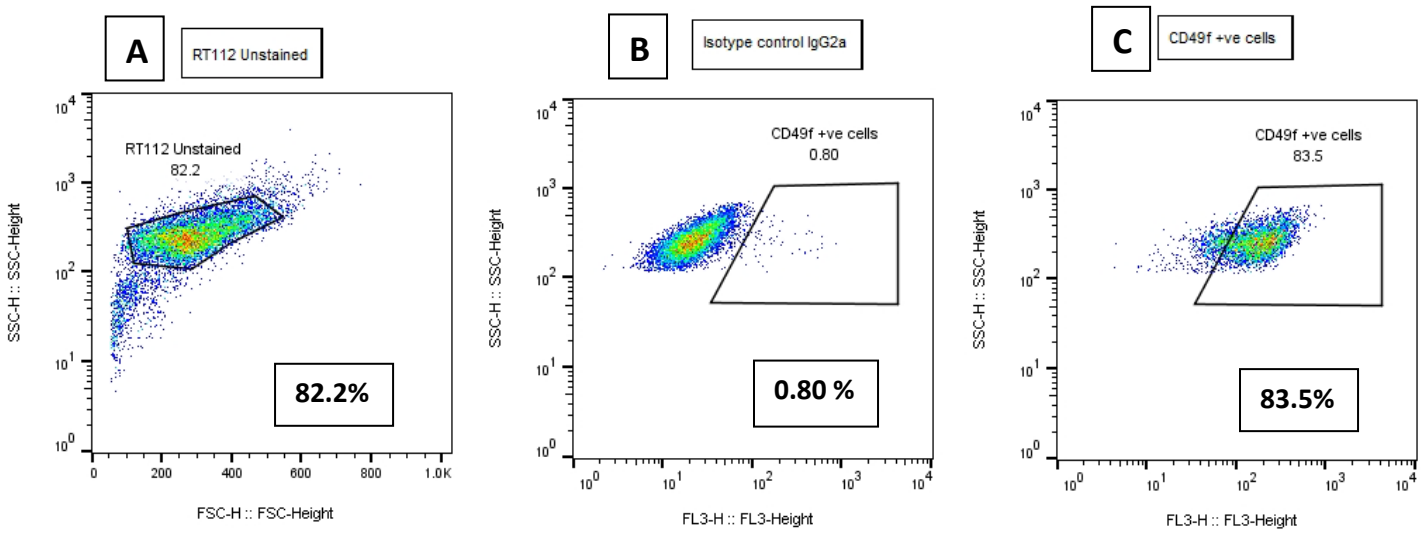

Figure 22 - Bivariate dot plots of RT112 transitional carcinoma cells displaying (A) RT112 unstained cells, (B) RT112 cells with secondary antibody added only, and (C) CD49f positive RT112 cells.

90.1% of the T24 cell population were identified (A) as seen below in Figure 23 and background staining identified 0.88% non-specific binding of the transitional cell population (B). After CD49f staining, 95% of T24 cells demonstrated Class 3 basal histological type features (C).

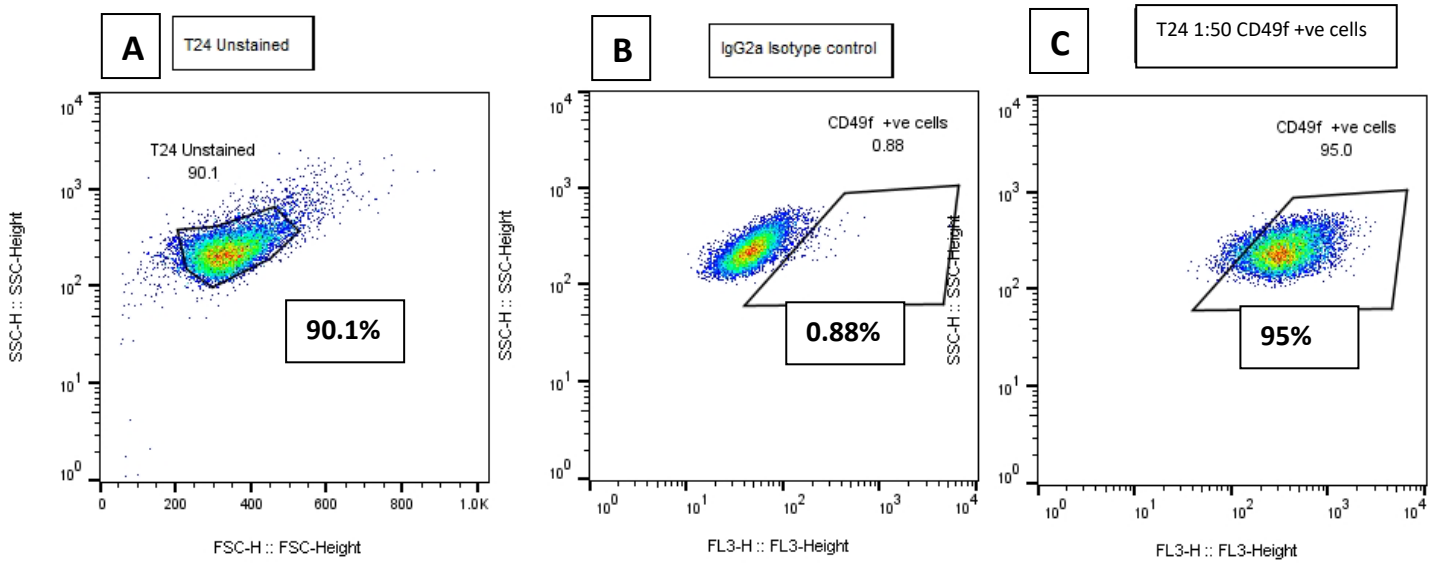

Figure 23 - Bivariate dot plots of T24 transitional carcinoma cells displaying (A) T24 unstained cells, (B) T24 cells with secondary antibody only added, and (C) CD49f positive T24 cells.

CD49f did not require further optimisation on either RT112 or T24 cells as I was confident that a 1:50 dilution of CD49f staining pulled down a sufficient proportion of cells with basal Class 3 histological features. For consistency, this 1:50 dilution was similarly prepared for basal cell isolation within LNCaP cells.

3.8.5 Epithelial surface cell detection in urine spiked RT112 and T24 cells

As described in section 2.6.2, urine cell pellets were spun, stained, and prepared to isolate cells of epithelial origin outlined in Table 26 below.

T24, RT112, and LNCaP cells spiked in urine	
Unstained	1:20 EpCAM
Secondary antibody only	Propidium Iodide

Table 26 -LNCaP, RT112, and T24 cells prepared to isolate EpCAM for flow cytometric analysis.

Compelling work has identified LNCaP cells, an established androgen sensitive human prostate cancer cell line of epithelial origin (BA.Michael J.Ackerman., 2008), and consequently, stain positive for EpCAM. LNCaP cells were expressed from the closest male

organ nearby to the bladder, adding strength to the validation of this study. As such, the LNCaP cell line was an ideal positive control for this investigation.

3.8.6 Epithelial surface cell detection in urine spiked LNCaP cells

The subsequent steps were to establish whether I could utilise LNCaP spiked in urine cells as an appropriate control, to specifically identify cells of epithelial origin as detailed in 3.4 aims.

EpCAM staining within LNCaP prostate adenocarcinoma cells spiked in urine.

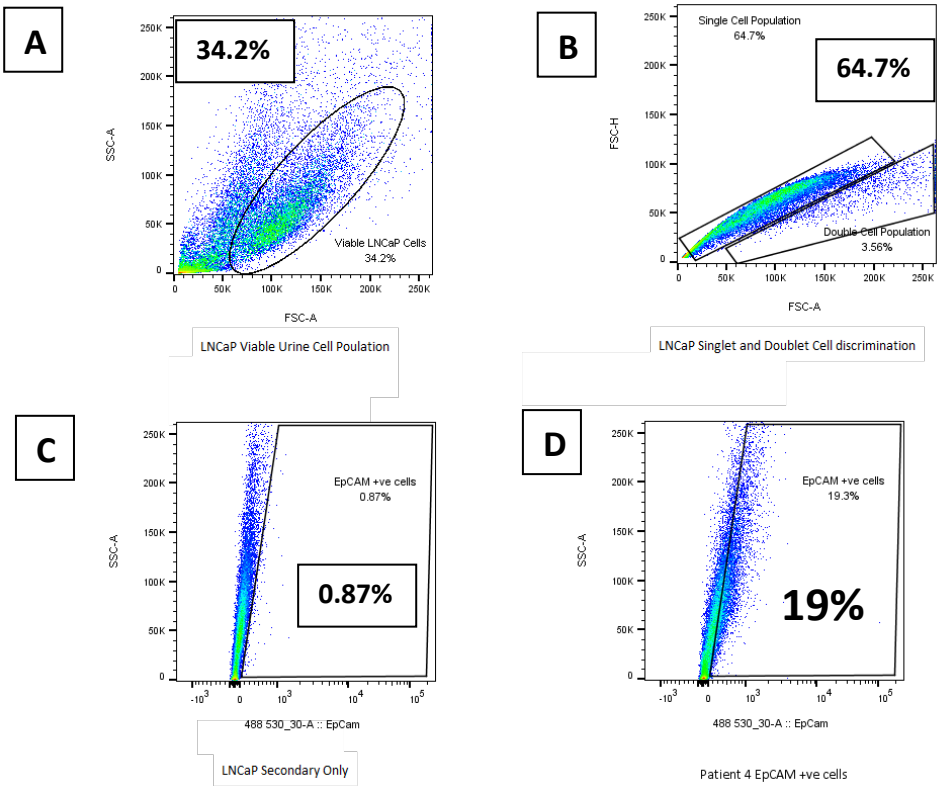

Figure 24 -Bivariate dot plots of LNCaP prostate cancer cells are displayed. Gating on forward and side scatter is based on cell size and granularity, and we can identify those cells that are viable as shown by the region that's highlighted in index (A). I have identified doublet discrimination (B) and I have gated those cells based on the area (FSC-A) vs height (FSC-H). Any cells that offer double the area, i.e., a duplication will correlate with a doublet event, which refers to the bottom gate 3.56% doublet cell population, and the upper gate refers to the single cell population. LnCaP cells with secondary antibody only added is displayed in (C), and we can see a clear shift of 19% EpCAM positive cells population within LNCaP cells in (D).

A cell population of 34.2% viable LNCaP cells were detected after flow cytometry analysis (A) as exhibited in Figure 24. To differentiate singlets from doublets 64.7% of the EpCAM positive LNCaP cells stained analysed were single cells and 3.56% were identified as double cell populations (B). To exclude background staining 0.87% of LNCaP cells were detected (C) and 19% of LNCaP cells were positively isolated by the epithelial surface marker EpCAM (D). 65.8% of LNCaP cells were non-viable, and every other cellular event recorded was excluded from the analysis.

3.8.7 Basal cell detection in urine spiked LNCaP cells

I then identified basal cells using CD49f cell surface marker, within LNCaP prostate adenocarcinoma cells spiked in urine. Basal cell positive populations are shown in Figure 25 after flow cytometric analysis.

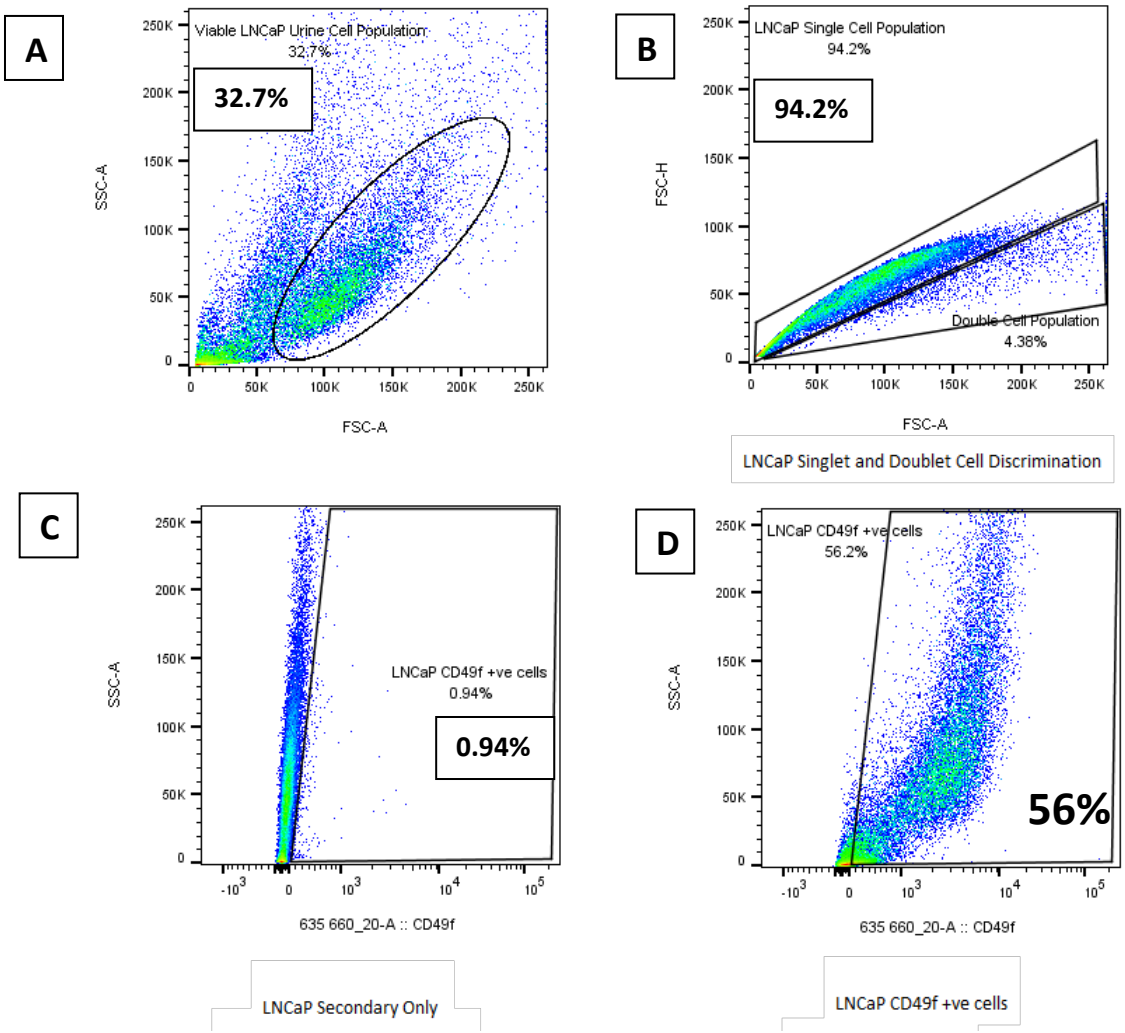

Figure 25 -Bivariate dot plots of LNCaP prostate cancer cells displaying (A) 32.7% LNCaP viable urine cell population, (B)94.2% LNCaP single and 4.38% doublet cell discrimination populations (C) 0.94% LNCaP cells with secondary antibody added only and (D) 56% LNCaP CD49f positive cell population.

LNCaP cells were analysed after 10, 000 recorded cellular events were examined and analysed by the flow cytometer. Unstained cells without the addition of primary antibody acted as a negative control. Figure 25 illustrates a 32.7% viable LNCaP population within urine (A) and a 94.2% single cell LNCaP population and a 4.38% doublet cell LNCaP population defined (B). 0.94% LNCaP cells stained positively with secondary antibody added only, to exclude background staining (C). 56% of LNCaP cells were positively stained with CD49f (D). 67.3% of LNCaP cells were non-viable, and every other cellular event recorded was excluded from analysis.

3.8.8 Urothelial cell detection in urine spiked LNCaP cells

Utilising intracellular marker Uroplakin 1b, I distinguished urothelial cell populations within LNCaP prostate adenocarcinoma cells, spiked in urine by flow cytometric analysis.

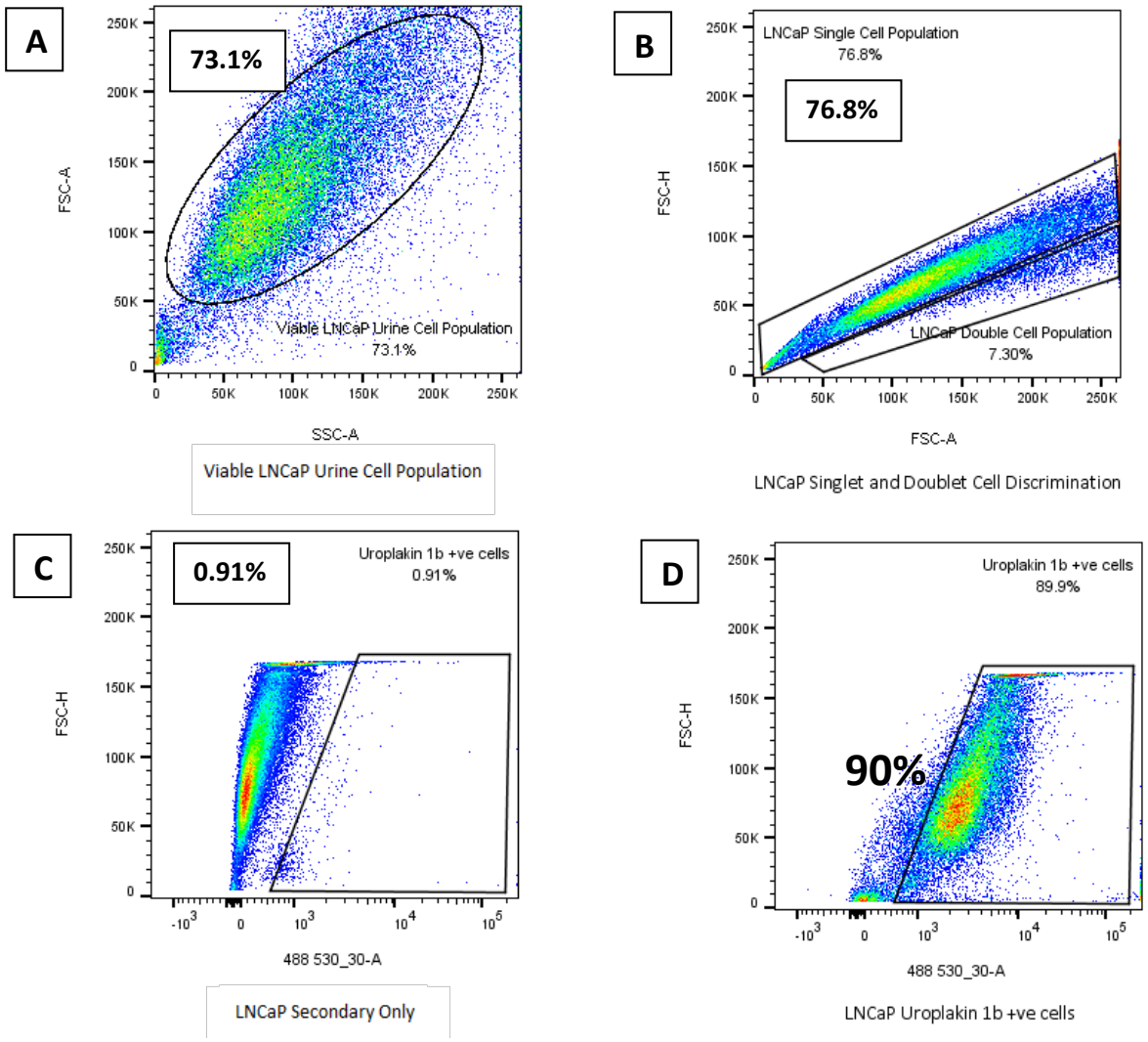

Figure 26 - Gating on forward and side scatter is based on cell size and granularity, and we can identify those cells that are viable as shown by the region that's highlighted in the index (A). I have identified doublet discrimination (B) and I gated those LNCaP cells based on the area (FSC-A) vs height (FSC-H). Any cells that offer double the area, i.e. a duplication will correlate with a doublet event, which refers to the bottom gate of 7.30% doublet cell population and the upper gate refers to the single cell population. LnCaP cells with secondary antibody only added is displayed in (C) and we can see a clear shift of 90% Uroplakin 1b positive cells population within LNCaP cells in (D).

A cell population of 73.1% viable LNCaP cells were detected after flow cytometry analysis (A) as displayed in Figure 26. To differentiate singlets from doublets 76.8% of the LNCaP positive cells stained analysed were single cells and 7.30% were identified as double cell populations (B). To exclude background staining 0.91% of LNCaP cells were detected (C) and 90% of LNCaP cells were positively isolated by the basal surface marker Uroplakin Ib (D). 26.9% of LNCaP cells were non-viable, and every other cellular event recorded was excluded from analysis.

3.8.9 Cell marker staining to identify NMIBC molecular subtypes in urine spiked LNCaP cells

Epithelial, basal, and urothelial specific cell types were observed in LNCaP cell urine populations. Data was collated in triplicate as three volunteers provided separate urine samples (as detailed in Table 24), that were spiked with LNCaP cells and displayed below in Figure 27. A high number of ~95% Uroplakin 1b cells on average were identified within LNCaP urine cell populations, which was expected as urothelial specific cells are shed into urine. An average of ~ 50% CD49f basal specific cells were detected within three LNCaP spiked urine samples and a lower average of ~25% EpCAM positive cells were identified in urine spiked with LNCaP prostate adenocarcinoma cells. Error bars were minimal but expected due to the unique and individual nature of each urine sample provided by three different urine sample volunteers.

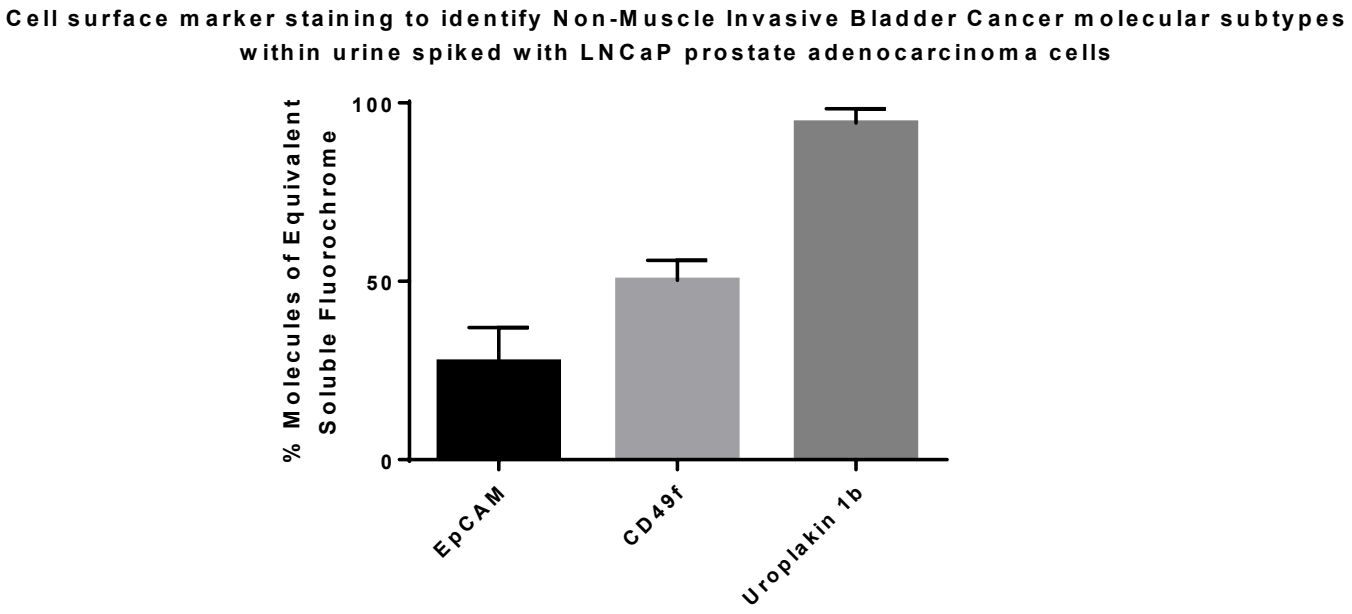

Figure 27 - Triplicate data with error bars to demonstrate cell surface marker staining within LNCaP cell spiked urine to supplement scattergrams displayed in Figures 24-26.

3.8.10 Epithelial cell detection in urine spiked T24 cells

Excluding cellular debris, Figure 28 illustrates a 27.1% viable population of unstained urine spiked with T24 cells identified (A). A 92.2% single cell T24 population and 5% doublet cell T24 population were defined within the urine (B). To exclude background fluorescence 0.63% of the cell population were isolated (C) and 25% of the T24 cell population were stained EpCAM positive (D). All other recorded cellular events outside the gates were excluded from analysis and assumed as cellular debris.

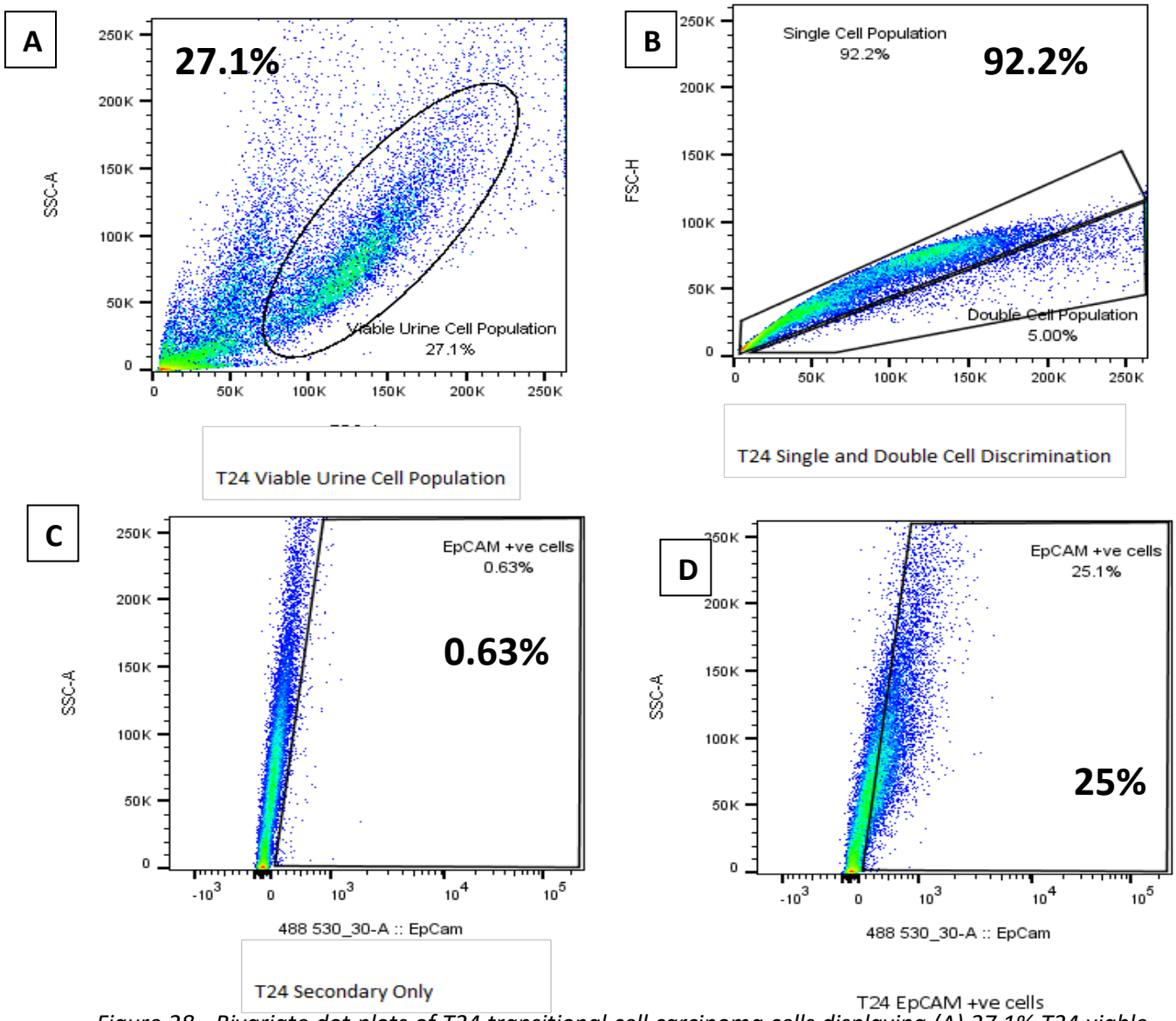

Figure 28 - Bivariate dot plots of T24 transitional cell carcinoma cells displaying (A) 27.1% T24 viable urine cell population, (B) 92.2% T24 single and 5% doublet cell discrimination populations (C) 0.63% T24 cells with secondary antibody added only and (D) 25% T24 EpCAM positive cell population.

3.8.11 Basal cell detection in urine spiked T24 cells

Utilising cell surface marker CD49f, I distinguished urothelial cell populations within transitional bladder cancer cell line T24 cells, spiked in urine. Basal cell positive populations identified by flow cytometry are displayed in Figure 29 below.

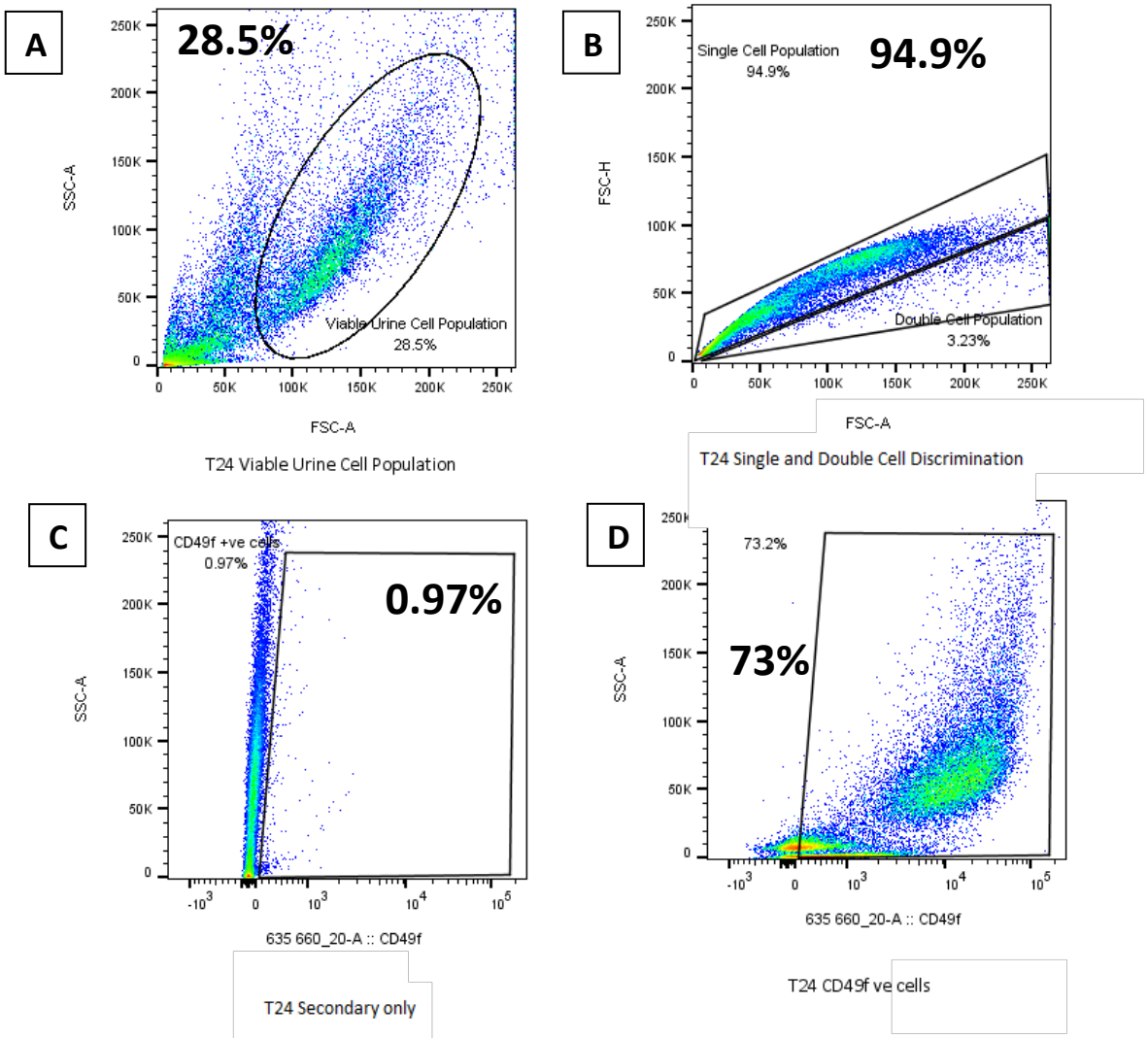

Figure 29 - Bivariate dot plots of T24 transitional cell carcinoma cells displaying (A) 28.5% T24 viable urine cell population, (B) 94.9% T24 single and 3.23% doublet cell discrimination populations (C) 0.97% T24 cells with secondary antibody added only and (D) 73% T24 CD49f positive cell population.

29% viable T24 cells were analysed after 10, 000 recorded cellular events were examined through the flow cytometer. Unstained cells without the addition of primary antibody acted as a negative control. Figure 29 illustrates that 29% of T24 cells were non-viable (A), a 95% single cell T24 population, and 3.23% double cell population (B). 0.97% T24 cells stained positively with secondary antibody added only (C) to exclude background staining. 73% of T24 cells were positively stained with CD49f (D) and defined as the basal cell population within urine. Every other cellular event recorded was excluded from the analysis.

3.8.12 Urothelial cell detection in urine spiked T24 cells

To identify urothelial specific cells within T24 transitional bladder cancer cells spiked in urine, Uroplakin 1b was utilised to distinguish and retrieve urothelial specific cell populations.

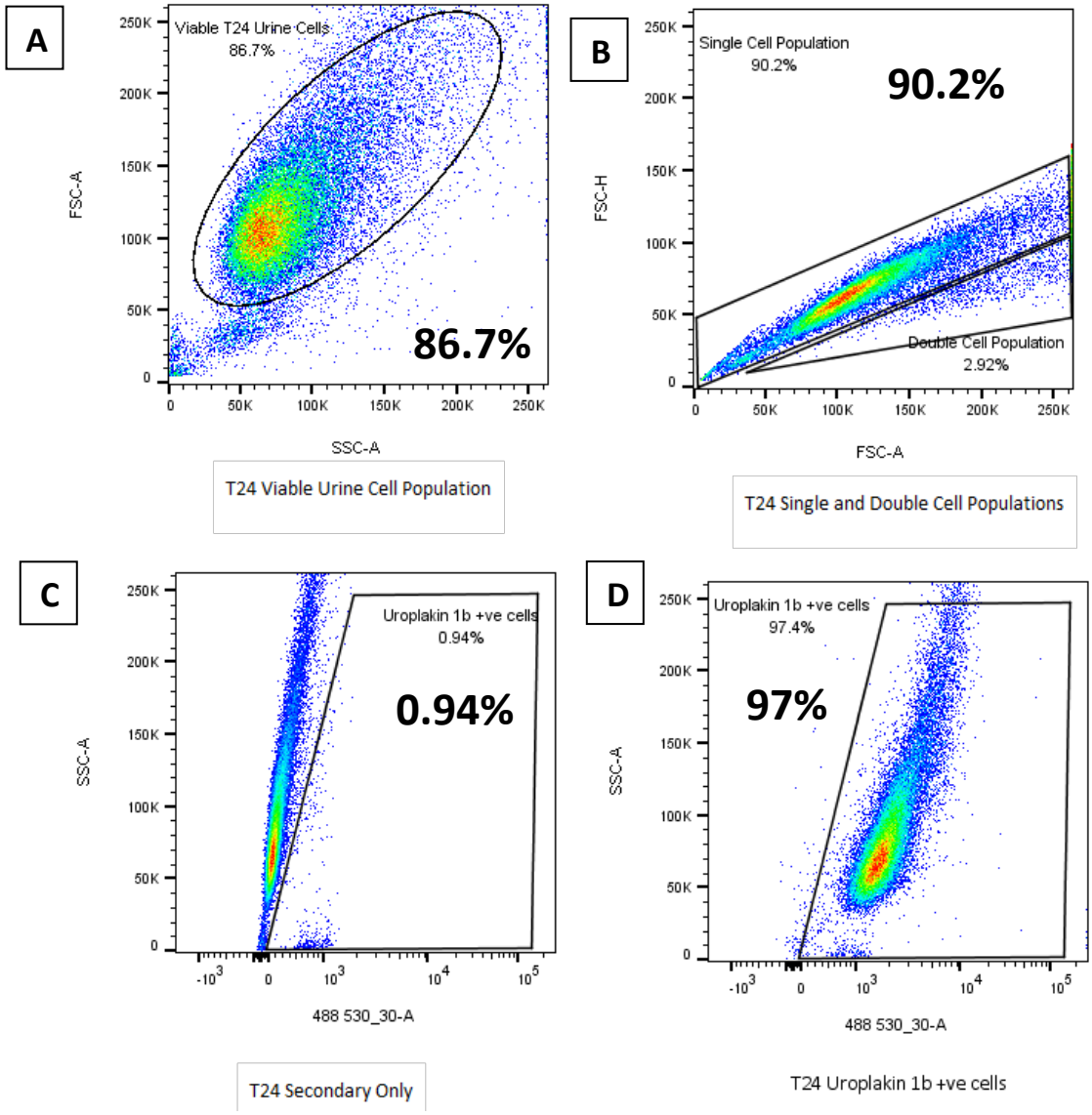

Figure 30 - Bivariate dot plots of T24 transitional cell carcinoma cells displaying (A) T24 viable urine cell population, (B) T24 single and doublet cell discrimination populations (C) T24 cells with secondary antibody added only, and (D) T24 Uroplakin Ib positive population.

To confirm cells analysed were viable propidium iodide staining identified 13.3% non-viable and 87% viable T24 cells (A). A 90.2% single cell T24 population and 3% doublet cell T24 population were defined within the urine (B). Unstained cells without the addition of primary antibody acted as a negative control. Figure 30 illustrates 0.94% T24 cells stained positively with secondary antibody added only (C) to exclude background staining. 97% of T24 cells were positively stained with Uroplakin Ib (D). Every other cellular event recorded was excluded from analysis.

3.8.13 Cell marker staining to identify NMIBC molecular subtypes in urine spiked T24 cells

Epithelial, basal, and urothelial specific cell types were observed in T24 cell urine populations. Data was collated in triplicate as three distinct urine samples were provided by volunteers (detailed in Table 24), spiked with T24 cells, and displayed in Figure 31. A high number of ~95% Uroplakin 1b cells on average were identified within T24 urine cell populations, which was anticipated as urothelial specific cells are shed into urine and T24 cells are NMIBC immortalised cell line authenticated. An average of ~ 80% CD49f Class 3 basal specific cells were detected within three T24 spiked urine samples and a lower average of ~20% EpCAM positive cells were identified in urine spiked with T24 cells. Error bars were minimal but expected as the variability of cellular components between each urine sample is anticipated, as specific amounts and cell types are variable in each human's urine.

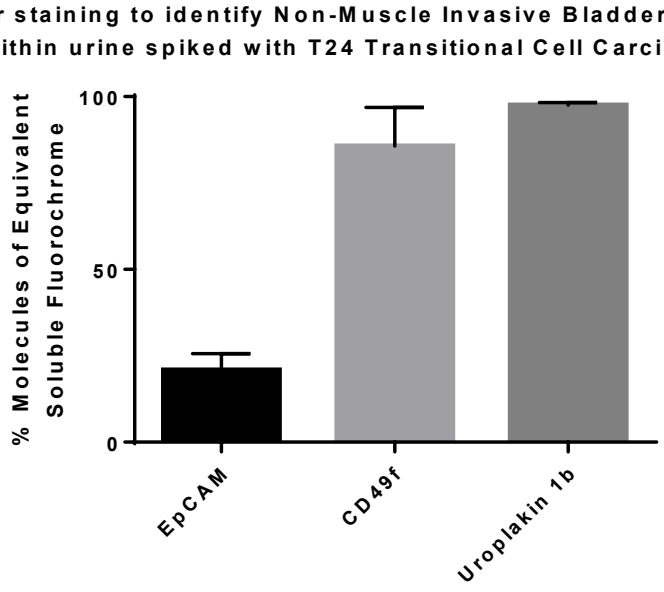

Figure 31 - Triplicate data with error bars to demonstrate cell surface marker staining within T24 cell spiked urine to supplement scattergrams displayed in Figures 28-30.

3.8.14 Epithelial cell detection in urine spiked RT112 cells

Moving on from the previous experiment having established the detection of urothelial, epithelial, and basal cells within urine spiked with T24 cells, I then isolated epithelial cell populations within urine spiked with RT112 cells.

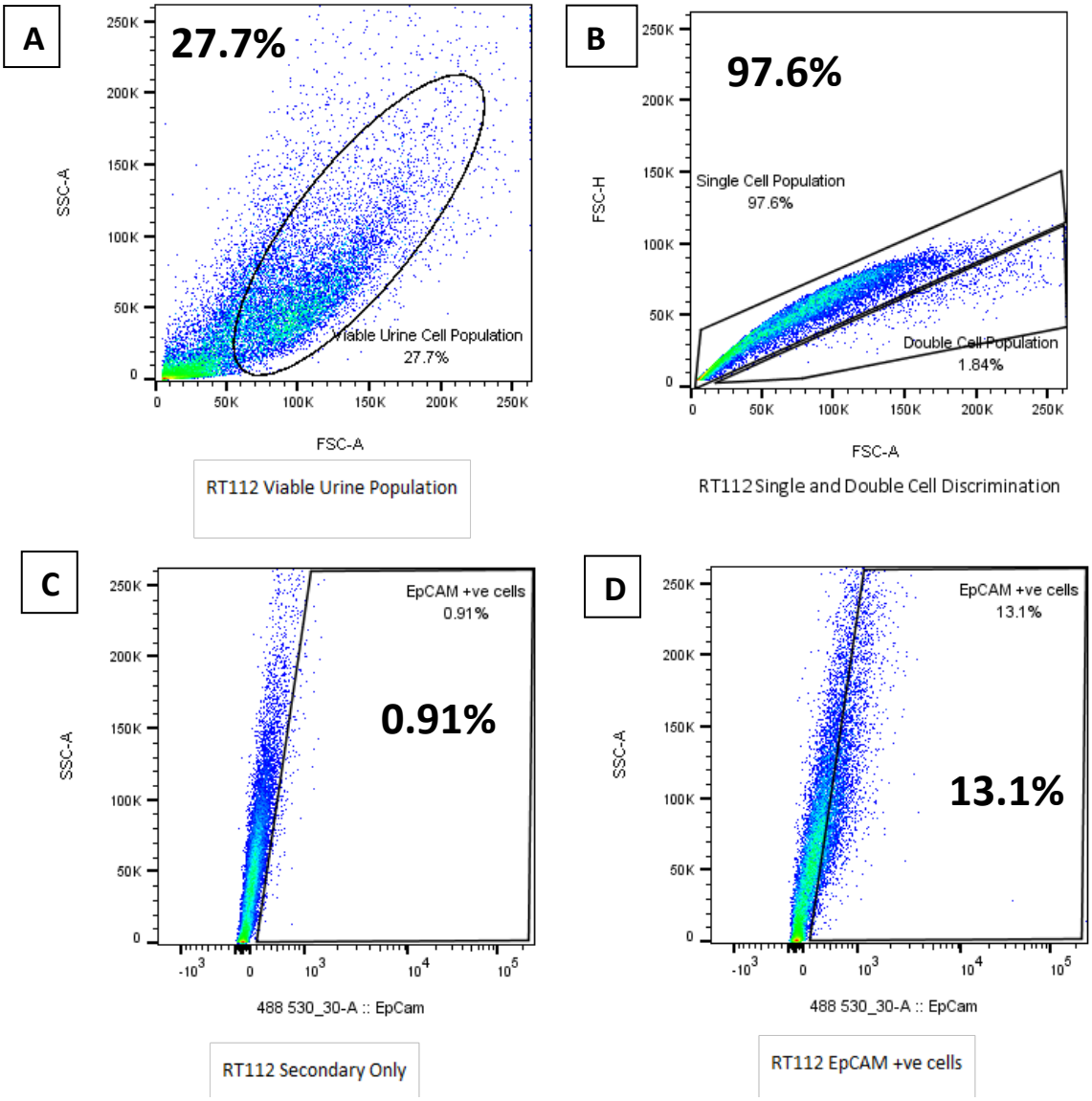

Figure 32 - Bivariate dot plots of RT112 transitional cell carcinoma cells displaying (A) 28% RT112 viable urine cell population, (B) 97.8% RT112 single and 1.84% doublet cell discrimination populations (C) 0.91% RT112 cells with secondary antibody added only and (D) 13% RT112 EpCAM positive cell population.

A cell population of 27.7% viable RT112 cells were detected after flow cytometry analysis (A) as exhibited in Figure 32. To differentiate singlets from doublets 97.6% of the EpCAM positive RT112 cells stained analysed were single cells and 1.84% were identified as double cell populations (B). To exclude background staining 0.91% of RT112 cells were detected (C) and 13.1% of RT112 cells were positively isolated by the epithelial surface marker EpCAM (D).

3.8.15 Basal cell detection in urine spiked RT112 cells

Having previously identified basal cell populations within urine spiked with T24 cells, I then attempted to utilise CD49f to isolate basal cells within RT112 transitional bladder cancer cells spiked in urine.

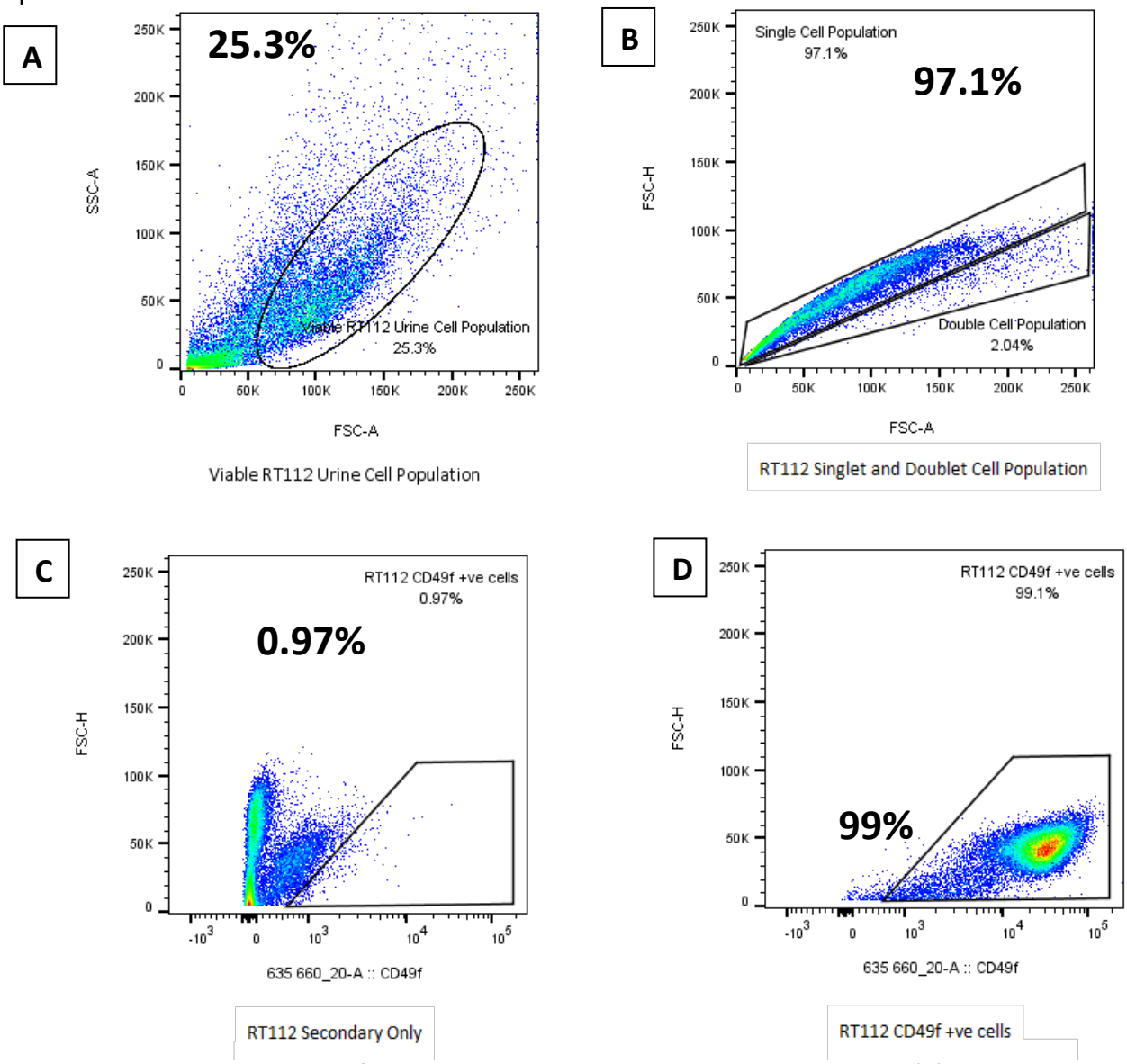

Figure 33 - Bivariate dot plots of RT112 transitional cell carcinoma cells displaying (A) 25.3% RT112 viable urine cell population, (B) 97.1% RT112 single and 2.04% doublet cell discrimination populations (C) 0.97% RT112 cells with secondary antibody added only and (D) 99% RT112 CD49f positive cell population.

A 25.3% unstained population of RT112 cells were identified (A), 97.1% single cell RT112 population, and 2.04% doublet cell RT112 cell population was observed (B). Background staining detected 0.97% non-specific binding within RT112 cells spiked in urine (C). After CD49f staining, 99% of RT112 cells demonstrated basal specific Class 3 histological type features (D) displayed in Figure 33.

3.8.16 Urothelial cell detection in urine spiked RT112 cell

Having established urothelial cell populations in T24 cells spiked in urine, I wanted to determine whether I can detect urothelial cells in another transitional bladder cancer cell line, RT112, spiked in urine.

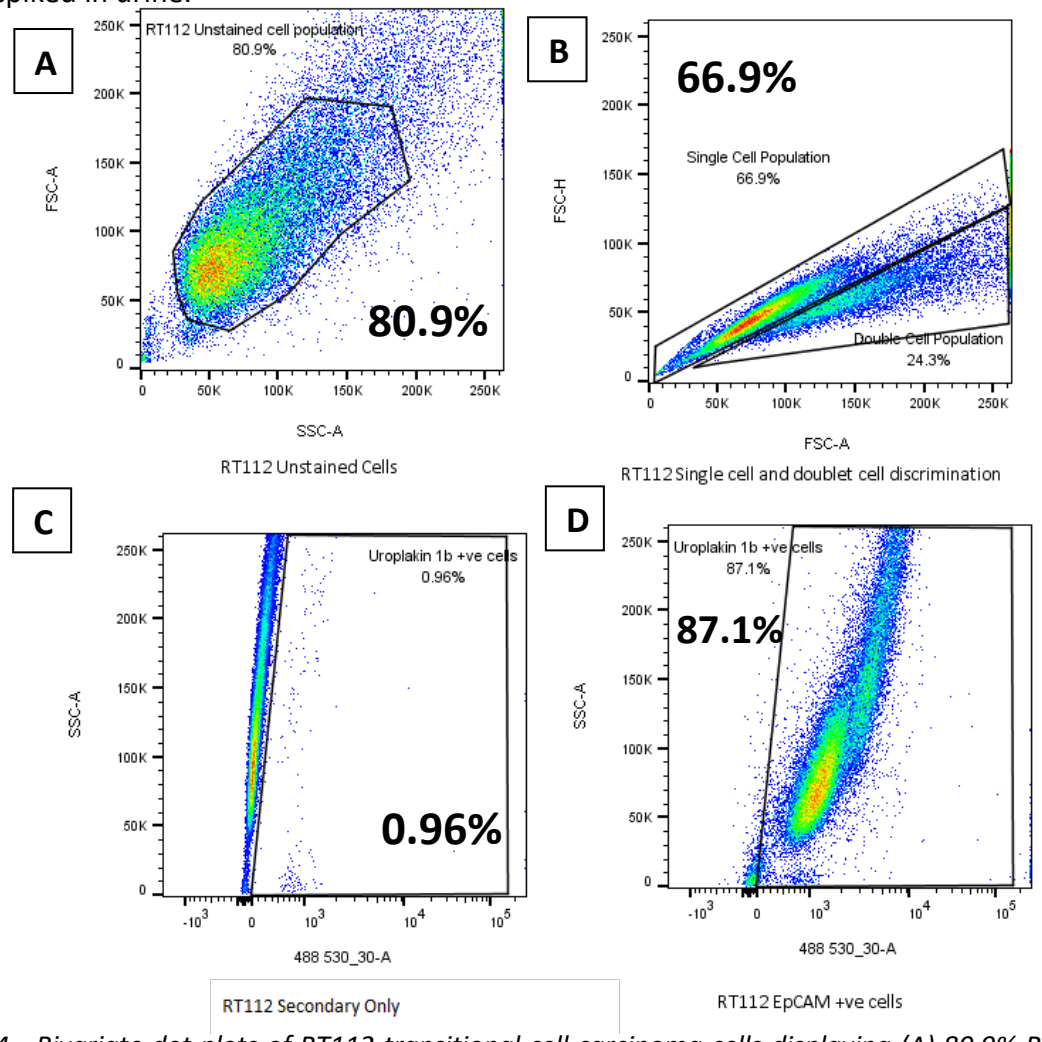

Figure 34 - Bivariate dot plots of RT112 transitional cell carcinoma cells displaying (A) 80.9% RT112 viable urine cell population, (B) 66.9% RT112 single and 24.3% doublet cell discrimination populations (C) 0.96% RT112 cells with secondary antibody added only and (D) 87.1% RT112 Uroplakin Ib positive cell population.

80.9% of viable RT112 cells were analysed after 30, 000 recorded cellular events were examined through the flow cytometer. Unstained cells without the addition of primary antibody acted as a negative control. Figure 34 illustrates, 19.1% of RT112 cells were non-viable (A), a 66.9% single cell RT112 population, and 24.3% double cell population (B). 0.96% Uroplakin Ib cells stained positively with secondary antibody added only (C) to exclude background staining. 87.1 % of RT112 cells were positively stained with Uroplakin Ib (D) and defined the urothelial specific cell population within urine. Every other cellular event recorded was excluded from the analysis.

3.8.17 Cell marker staining to identify NMIBC molecular subtypes in urine spiked RT112 cells

Epithelial, basal, and urothelial specific cell types were observed in RT112 cell urine populations. Data was collated in triplicate as three volunteers provided separate urine samples (as detailed in Table 24), that were spiked with RT112 cells and presented in Figure 35. A high number of ~90% Uroplakin 1b cells on average were identified within RT112 urine cell populations, which was expected as urothelial specific cells, of which RT112 cells are, are shed into urine. An average of ~ 99% CD49f basal specific cells were detected within three RT112 spiked urine samples and an average of ~95% EpCAM positive cells were identified in urine spiked with RT112 NMIBC transitional cells. Error bars were minimal but expected due to variability between three different urine sample volunteers.

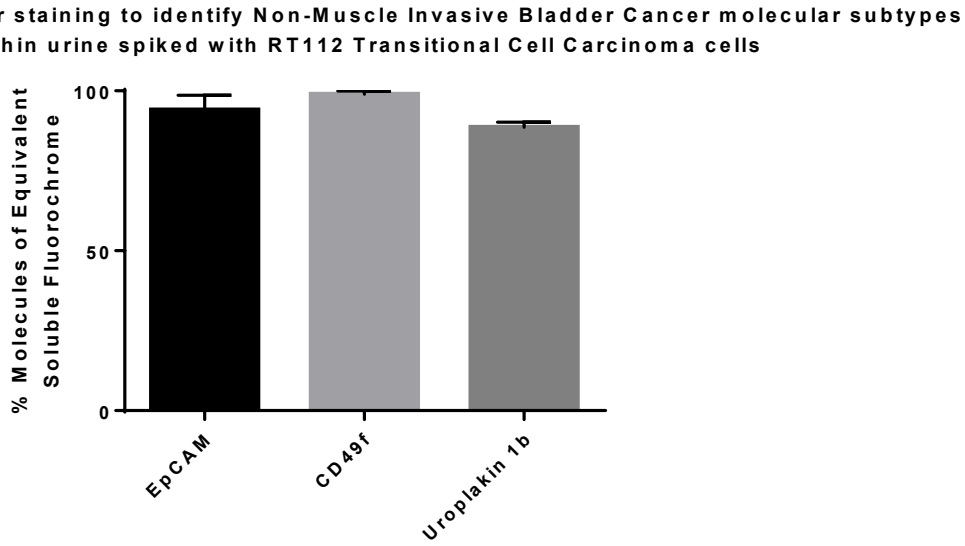

Figure 35 - Triplicate data (n=3) displaying error bars to demonstrate cell surface marker staining within RT112 cell spiked urine to supplement scattergrams displayed in Figures 32-34.

A graph to display positively identified EpCAM, Uroplakin 1b, and CD49f cells within LNCaP, T24, and RT112 cell lines.

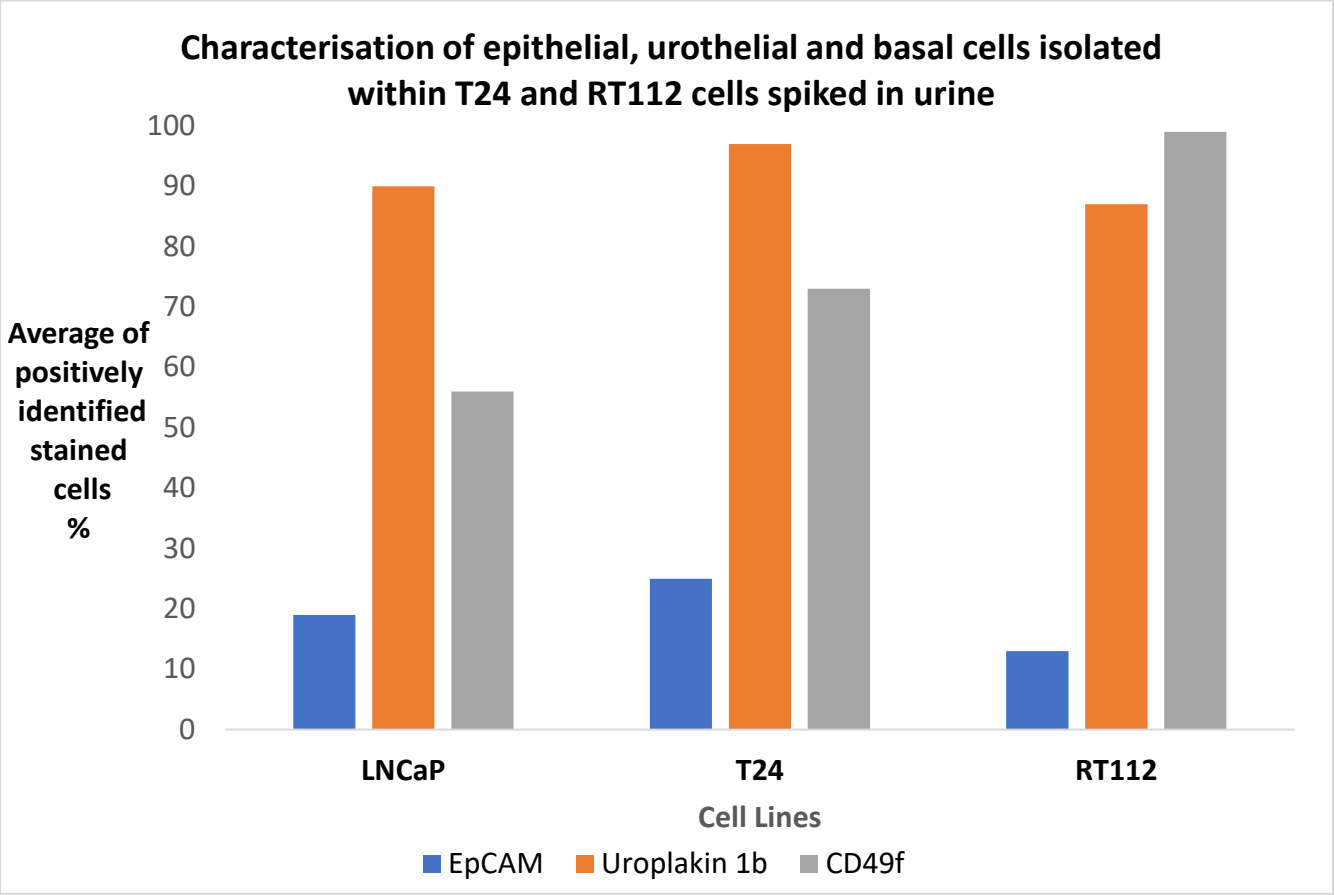

Figure 36 - A graph to illustrate collated average characterisation of epithelial (displayed in the blue bar), urothelial (represented by the orange bar), and basal cells (highlighted by the grey bar) in T24 and RT112 cells spiked in urine. Results in this figure are n=1. Each bar represents an average percentage of positively identified stained EpCAM, uroplakin 1b, and CD49f cells.

Overall, the largest number of cell types consistently isolated were urothelial specific cells and were observed in all three cell lines examined. This finding was predicted as the function of the bladder is to store urine and urothelial cells are shed during urination, as seen within the highest average positively identified Uroplakin Ib stained cells. Cells of basal layer origin were detected in all three cell types; expectedly as basal histological features are a molecular subtype component of both prostate and bladder cell classifications. Although each cell line is of epithelial origin, it is important to note that cell lines are immortalised, and epithelial integrity and cellular polarity may have been lost resulting in cells with more migratory phenotypes.

3.9 Discussion

FACS was performed to characterise the heterogeneous amalgamation of cells within the urine. Cell sorting was utilised through fluorescent features observed in each transitional cell and founded on the specific forward scattering and side scattering of light (Blanpain & Simons, 2013). Although large proportions of non-viable cells were observed, this was expected as epithelial cell shedding naturally occurs in the urine, attributing to large numbers of bacteria binding to bladder cell surfaces. As a result of this natural immune defence, cell viability between samples was not quantified, due to sample variability which was expected to differ between individual samples.

T24, RT112, and LNCaP cells were fixed prior to intracellular staining, ensuring uroplakin Ib was preserved in its original cytoplasmic cellular location. Transitional cells were permeabilised to detect intracellular surface antigens. Furthermore, there is evidence to suggest transitional cells were convincingly permeabilised as minimal non-specific binding variation was minimally visible in light scatter profiles, within the secondary only channel.

3.9.1 EpCAM

The ATCC states the morphological description of the T24 cell line is of epithelial origin, therefore T24 cells were anticipated to express EpCAM in abundance. Basal and luminal cells are the two main epithelial cell types of the human prostate and over 90% of prostate adenocarcinomas arise from prostatic epithelial cells. Surprisingly 19% LNCaP% (Figure 24), 25% T24 (Figure 28) and 13% RT112 cells (Figure 32) stained EpCAM positive which was markedly lower than expected. By contrast, increased urinary EpCAM levels have previously been described as indicative of muscle-invasive bladder cancer and previously reported to be specific to high-grade urothelial bladder cancer (Bryan et al., 2014). The low EpCAM expression (25%) observed in T24 cells illustrated in Figure 28, indicates the presence of an assortment of basal and luminal molecular phenotypes. Moreover, the bivariate dot plots of LNCaP EpCAM detection (Figure 24) and RT112 epithelial isolation (Figure 32) provide persuasive evidence in support of cellular consequences facilitating the transition from epithelial to a mesenchymal phenotype. Conceivably, if HT1376 or UM-UC-3 two muscle-invasive bladder cancer cell lines were stained with EpCAM, I propose similar low EpCAM expression would be detected, with a predicted increased N-Cadherin expression as cell adhesion decreases and cells lose polarity.

Due to a change in cell polarity, epithelial cells acquire a more migratory and mesenchymal phenotype as a result of uncontrolled activation (Lamouille et al., 2014). The change in cell polarity is a key element that induces the change from an epithelial apical-basal organisation to a mesenchymal phenotype as cells migrate and invade the extracellular matrix. This process Epithelial-Mesenchymal Transition first identified in embryonic development, not only occurs in other physiological functions such as wound healing yet is also known to promote tumour cell intravasation (Tsai, Donaher, et al. 2012). Despite this, the ability of cells to transit from one phenotype to another is essential for multicellular organisms, however, the bladder may suggest a more aggressive mesenchymal phenotype.

With this in mind, during EMT there is a down-regulation of epithelial markers and loss of cellular junctions causing epithelial cells to lose cell polarity (Clucas & Valderrama, 2015). Subsequently, cells then gain migratory and invasive properties acquiring an elongated mesenchymal phenotype. When secondary tumours form in the reverse process Mesenchymal-Epithelial transition promotes the formation of secondary tumours. (Li, Yang et al. 2014). Pathway signalling of EMT leads to cancer growth in prostate cancer and epithelial tumour cells with enhanced cell polarity degrade the extracellular matrix (Gong, Chippada-Venkata, et al. 2014). Nevertheless, this explains the remarkably low EpCAM positive T24, RT112, and LNCaP cells.

In light of the urinary model characterising transitional cells and recapitulating transitional cell carcinoma to the best of its ability, it does not display haematuria the most common symptom experienced by NMIBC patients as healthy volunteers' urine was obtained. Importantly (Bryan et al., 2014) observed an association between haematuria and EpCAM, however, haematuria did not significantly influence the detection of urinary EpCAM in bladder cancer patients adding strength to the use of this model as visible haematuria was not present within healthy volunteers urine.

The 19% EpCAM positively characterised LNCaP cells (displayed in Figure 24), 25% EpCAM positive T24 cells (highlighted in Figure 28), and the 13% EpCAM rich RT112 cells (visualised in Figure 32) confirms Wesseling and colleagues findings wherein a variety of malignant tumours derived from epithelial tissue overexpression and elevated EpCAM expression was identified in bladder CIS (Wesseling et al., 2009). Increased EpCAM levels found within urine are suggestive of Stage 2 or Grade 3 urothelial bladder cancer as described by (Bryan et al.,

2014). As increased epithelial cells are shed in urine with higher grade and staged bladder tumours this may, in turn, accelerate cell proliferation (Bryan et al. 2014). Higher levels of EpCAM may have been expected to be observed within the spiked urine samples, nevertheless, it is well known that cell-to-cell adhesion, cell polarity declines, and cells gain a more migratory function and exhibit invasive properties (Franzen et al., 2015).

3.9.2 T24 and Uroplakins

Urothelial specific marker Uroplakin Ib isolates urothelial cells and was explored in this investigation to eliminate all other cell types typically found in urine when the intracellular marker was applied to urine spiked cells.

Reflecting on the dot plots, viable urothelial cells can be convincingly quantified from urine as 100% T24 cells were detected at both 1:100 and 1:200 dilutions of uroplakin Ib optimisation staining. T24 cells were immortalised from the urinary bladder tissue of a female with a transitional cell carcinoma, and one can confidently assume T24 cells express the urothelial marker of interest.

3.9.3 RT112 and Uroplakins

Bivariate dot plots displayed in Figure 21 characterised 88% uroplakin Ib positive RT112 cells after staining with both 1:50 and 1:200 dilutions. Published work characterising uroplakins in the urinary tract showed RT112 cells had 3+ positive staining for Uroplakin Ib (Lee, 2011), confirming my data is robust as it verifies previously published findings.

Cell Line	Pathology	Origin	UPIa	UPIb	UPII	UPIII
RT4	Papilloma	Urinary Bladder	2+	3+	3+	2+
RT112	Carcinoma	Urinary Bladder	N	3+	N	N
HT1376	Carcinoma	Urinary Bladder	N	3+	N	N
Colo232	Carcinoma	Urinary Bladder	N	N	N	N
KK47	Carcinoma	Urinary Bladder	N	N	N	N
VM-CUB-3	Carcinoma	Urinary Bladder	2+	3+	2+	N

Table 27 - A Table characterising uroplakins in the urinary tract within the RT112 cell line.

Uroplakin 1b displayed 3+ positive staining within the urinary bladder and no positive staining was identified within Uroplakins Ia, II, and III. Table adapted from Demonstration of Uroplakins in the lower urinary tract Source: (Lee, 2011).

95% T24 cells (as shown in Figure 23) and 83.5% RT112 cells (displayed in Figure 22) detected with the basal surface marker CD49f, provide supportive evidence that a 1:50 dilution confidently identified basal cell populations within the two transitional cell lines. The above data confirmed published literature after the comprehensive transcriptional analysis of early-stage urothelial carcinoma demonstrated bladder T24 cells with basal histological features have increased CD49f expression (Cancer Genome Atlas Research Network, 2014). CD49f did not, therefore, require further optimisation for analysis, and I was confident CD49f at 1:50 dilution identified the basal subtype in T24 and RT112 bladder cancer cell lines and for standardisation was similarly used for LNCaP cell staining.

Basal cells were identified in all three cell lines at elevated levels reflecting the composition of the bladder and prostate. The basal cell layer encompasses the stem cell self-renewal population for epithelial prostate cells which complements the collated data average characterisation of basal cell populations within LNCaP cell urine. Basal cells were positive as CD49f stained cellular events and RT112 cells had the highest expression of basal cells isolated, out of the three cell lines observed.

3.10 Conclusion

Previously published data supported the aim of this investigation, and I am confident bladder cancer cell detection is inclusive of all the non-muscle invasive bladder cancer phenotypes required for this study. With the ability to isolate and characterise epithelial, urothelial, and basal cells from urine, all objectives outlined were met.

There are no liquid biomarkers to accompany NMIBC clinical-pathologic risk stratification (Lerner & Robertson, 2016). This investigation attempted to address the unmet need, highly required for NMIBC patients due to the economic burden of the reliance on cystoscopy (Health Technology Assess 2010), in addition to the uncomfortable, invasive, painful experience patients undergo during cystoscopy. Transcriptome-based analysis of 460 NMIBC identified three molecular subtypes associated with NMIBC risk progression (Hedegaard et al., 2016). In support of this, work in this study builds on the identification of specific molecular subtypes within urine by characterising specific cell populations, using a representative model of transitional cell carcinoma cell lines and an appropriate prostate adenocarcinoma cell line control.

Specificity within flow cytometry is determined by the ability to quantify the cellular population or antigen of interest (Selliah et al. 2019) and sensitivity is an essential requirement of a clinically effective screening process. A high number of 30 000 cellular events were acquired with this method, coupled with the ability to detect cellular populations demonstrated the high sensitivity of this assay providing a convincing, reliable, and informative representation of epithelial, urothelial, and basal cells in urine from cell lines spiked with urine as well as patient's urine following Radical Cystectomy. Published work has demonstrated bladder cancer in urine samples taken for screening after bladder irrigation, has a high sensitivity, yet low specificity with Flow Cytometry compared to urine cytology (Wheeless et al.1993).

Importantly, within a urine population, assessing individual T24 and RT112 cells characteristics contributes to our understanding of cellular patterns that are typical of individuals with NMIBC. I have determined whether urine spiked with T24 and RT112 cells express the epithelial, urothelial, and basal markers of interest, in turn, providing an insight into the molecular makeup of transitional cell lines used in non-muscle invasive bladder cancer research. Such can be applied to patient urine samples to gain an understanding of urothelial, epithelial, and basal cell type composition within urine.

Notably, relevant antibody staining was detected in each representative channel. In support of published literature, expected staining for both transitional cell lines were revealed in the bivariate dot plots. The data obtained from this investigation confirms published literature or at least provides an explanation such as EMT to explain the sparse numbers of EpCAM positive stained cells obtained than expected. Transitional cells within urine express the relevant markers of interest, the experimental procedure was robust as flow cytometric analysis was repeated three times for each cell marker of interest and the data is convincing and supports published literature. Above all, analysis performed with FlowJo analysis packages enables the analysis and interpretation of single-cell population data, therefore I would not recommend analysis to be performed in an alternative way.

Nevertheless, further work could be carried out to determine the quality of epithelial, urothelial, and basal cells capable to recover after cell sorting. From this, analysed cells could be further utilised for further downstream analysis. Potential future downstream analysis may involve Magnetic Activated cell sorting, and the use of highly specific antibodies tagged

with magnetic, fluorescent dyes to distinguish between cell types. Such would allow heterogeneous mixtures of urine cells to be sorted into different populations using an electromagnet.

Mixed cell populations can be differentiated and purified using bladder epithelium specific EpCAM and FACS established, to exclude inflammatory and other renal filtered cells. Subsequently, filtered urine could undergo mtDNA extraction and whole mtDNA genome sequencing performed with recovered cells separated into distinct populations. This would enable epithelial or urothelial specific cells to undergo mtDNA sequencing revealing mtDNA genotypes present in urine from specific cell types. Overall, I can confidently characterise molecular subtypes within urine using the markers chosen CD49f, Uroplakin Ib, and EpCAM and the use of appropriate negative isotype controls displayed satisfaction to negate all non-specific binding.

Chapter 4: Do Bladder tumours possess a unique mtDNA genotype?

In this section, I investigated clinical samples after Radical Cystectomy to comprehend whether there was a particular type of mtDNA genotype that was prevalent and associated with bladder cancers. The leading question I wanted to explore was whether bladder cancers at high frequencies have any type of mtDNA genotype. Consequently, in this chapter I asked the question do bladder tumours possess a unique mtDNA genotype?

4.1 Genomic sequencing advancements

Due to genomic advances, the ability to readily sequence malignant and normal tissue has upended our understanding of both cancer and ageing. Implications this has on how cancer genomics is applied, provides knowledge to clinical challenges of targeted treatment, understanding recurrence, directly relevant with NMIBC which has a high rate of >40% recurrence (Mowatt et al., 2011).

4.2 Hypothesis

With age, mtDNA alterations become more prevalent. As Bladder Cancer is a cancer associated with age, as individuals become older, I hypothesize that a unique mtDNA pathogenic variant mark is present and accumulates within bladder tumours.

4.3 Objectives

In this chapter I will:

1. Perform a histological assessment confirming the presence of tumour in each patient bladder tumour sample, in preparation for downstream whole mtDNA genome sequencing analysis.
2. Reliably amplify the mitochondrial genome in Non-Muscle Invasive Bladder Cancer patients undergoing Robotic Cystectomy.
3. Undertake whole mtDNA genome sequencing to identify tumour-specific mtDNA variants in bladder tumours from patients undergoing Robotic Cystectomy.

Consequently, the presence of clonally expanded mtDNA pathogenic variants in bladder tumours was investigated within this project, utilizing a cohort of patients undergoing Radical Cystectomy at Freeman Hospital, Newcastle, UK. The research question asked was can cancer genetics and sensitive sequencing technologies be applied to diagnose bladder cancer early

in tumour development OR detect BC recurrence? I investigated whether clonally expanded mtDNA pathogenic variants are present in bladder tumours and the extent they can aid our understanding of the genetic variants that are driving bladder cancer.

4.4 Materials and Methods

4.4.1 Sample Collection

Clinical samples were received from seventeen NMIBC patients undergoing Robotic Cystectomy within the Urology department at Freeman Hospital, Newcastle, UK. An assessment of a prospective cohort of clinical specimens as proof of principle was performed by collecting case clinical material of matched fresh resected NMIBC tissue. During cystoscopy, distinct biopsies were taken of the tumour and a separate biopsy was taken. When I compared normal and tumour urothelial biopsies, I was able to identify tumour-specific genotypes.

4.4.2 Methodology

Fresh resected NMIBC tissue: tumour and adjacent normal were collected from patients following radical cystectomy. Tumour content was scored by a Uropathologist, tumour-rich samples were sequenced and samples with no tumour present were not processed. Each bladder sample sequenced had a high tumour content of >80%, see Table 29, except patient 13 where the tumour was laser capture microdissected achieving 100% tumour (described in section 2.5 and section 4.5.11). The Uropathologist provided a clinical histopathological assessment detailed in Table 30.

Both FFPE H&E tissue sections and cryostat cut H&E tissue sections were prepared for tumour assessments. This ensured cellular detail was easily identifiable by the Uropathologist providing an accurate tumour evaluation. As illustrated in Figure 37, primary tissue was cut in half and two workflows were optimised and performed. Half the bladder biopsy was snap frozen in cold isopentane and liquid nitrogen and the other biopsy half was fixed in 10% formalin, processed, and embedded into an FFPE block. Genomic DNA was extracted from both the frozen and FFPE block and the whole mtDNA genome was amplified by long range PCR for Next Generation Sequencing.

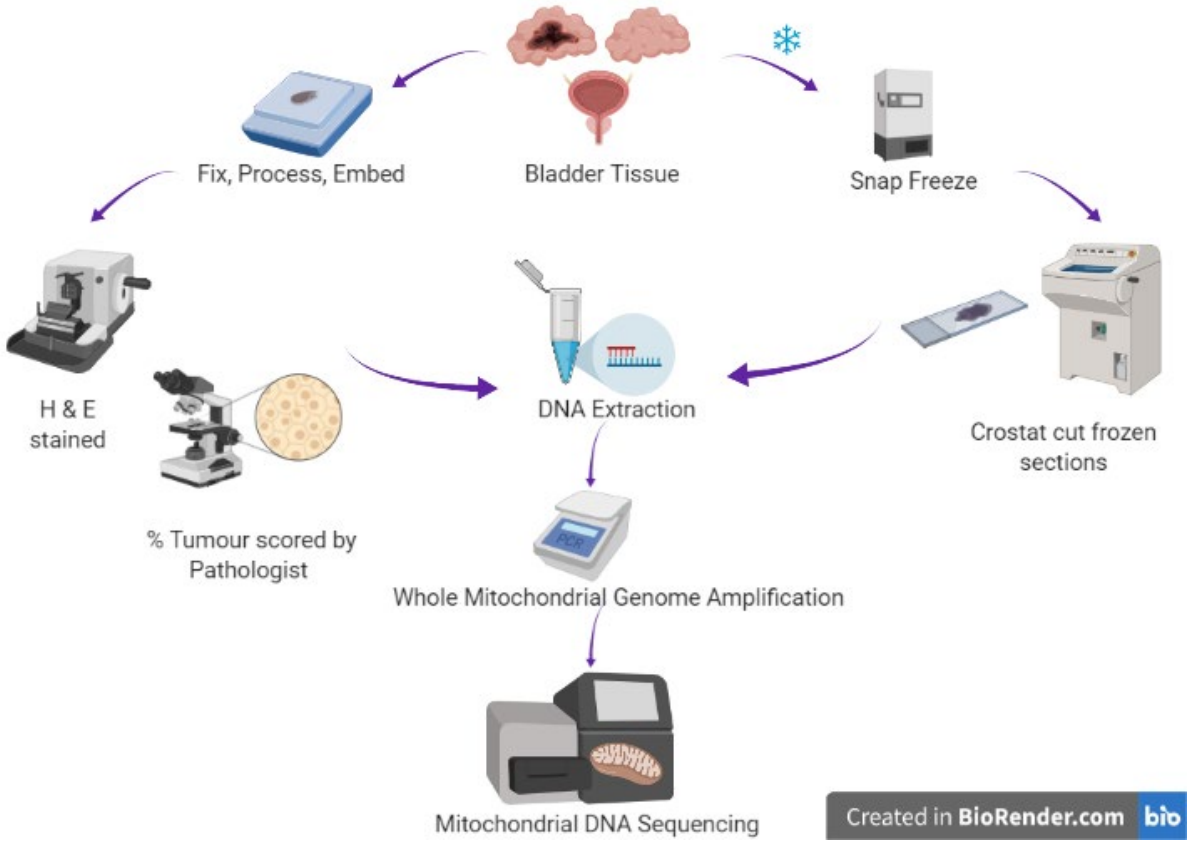

Figure 37 - Bladder tumour tissue and adjacent 'normal' bladder tissue sample processing workflow. Primary bladder tissue was cut in half, fixed in 10% formalin, and processed, whilst the other half was snap frozen and placed in the -80C freezer. Genomic DNA was extracted, the mitochondrial genome amplified and mtDNA sequencing performed by Next Generation Sequencing.

To determine and assess the tumour content in each bladder tumour sample, fresh frozen bladder tissue sections were cryosectioned at 4 µm, formalin-fixed sections were cut with the microtome at 4 µm, and sections H&E stained. Cellular detail and tissue architecture were identified after H&E staining enabling the characterisation of tumours by assessment.

Tumour rich bladder normal and tumour samples were digested by tissue lysis, DNA extracted, and PCR performed to amplify the entire mtDNA genome generating two overlapping long range PCR amplicons. Amplicons were pooled in equimolar amounts and fragmented using Ion Shear™ Plus [Life Technologies]. A 200bp library was prepared, libraries loaded onto sequencing chips and libraries sequenced using the Ion PGM and S5 next-generation sequencing systems to detect mtDNA genotypes specific to the bladder tumour.

A minimum sequence coverage depth of 1000x confidently detected mtDNA genotypes present in the bladder samples when aligned to the control hg19 and mtDNA reference genomes. Sequence coverage of this depth confidently detected variants that were only

present in the bladder tumour and not the patients' matched control sequence. Sequence alignment and analysis were performed using an established bioinformatics pipeline in Torrent Suite v5.0.4 utilising the Coverage Analysis [v5.0.4.0] and Variant Caller plug-in [v5.0.4].

4.5 Results

After optimisation following analysis of the first four patient bladder samples, the method of specimen cryopreservation was greatly improved as orientating bladder tissue pre cryosectioning ensured tumour rich regions were fully exposed. Bladder tissue was orientated (Figure 38), embedded onto OCT attached to filter paper (Figure 39), and frozen in liquid nitrogen (Figure 40). Orientating bladder tissue to expose macroscopic tumour rich regions ensured genomic DNA from tumour abundant areas was extracted and subsequently, the whole mtDNA genome sequenced.

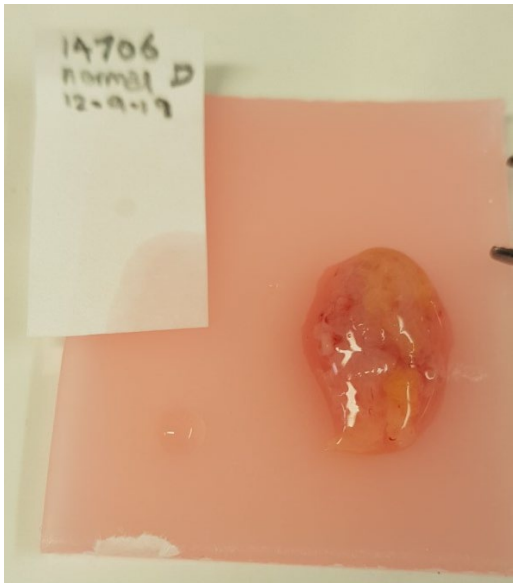

Figure 38 - Orientated patient 14 normal bladder tissue

Figure 39 - Orientated patient 14 tumour bladder tissue

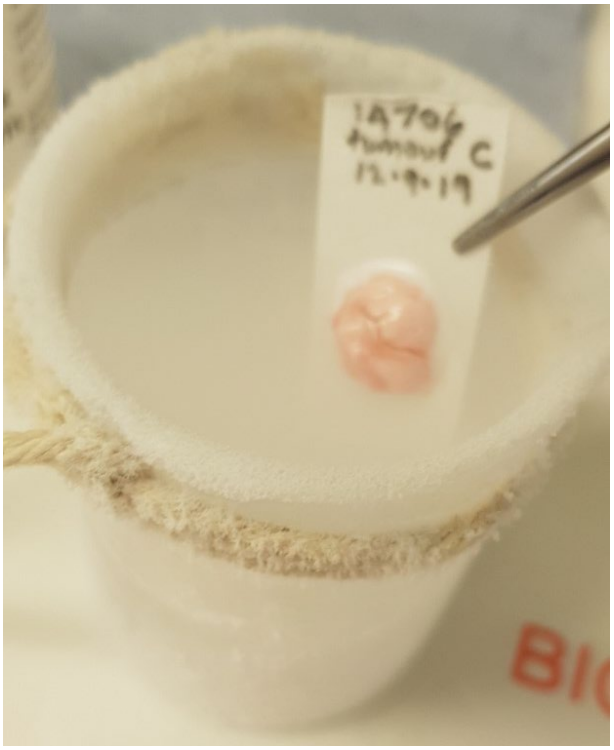

Figure 40 - Orientated patient 14 bladder tumour tissue specimen frozen in cold isopentane and liquid nitrogen.

4.5.1 Cryosectioning Bladder Tissue for lysis extraction and sequencing

Frozen bladder tissue was removed from the -80°C freezer and placed immediately on dry ice ready for cryosectioning. Bladder tissue was cryosectioned at 4 µm for H&E staining and 10x 15 µm cryosections cut and placed in a labelled sterile 1.5ml Eppendorf on dry ice for tissue lysis.

4.5.2 Tissue Lysis

20 µl proteinase K was added to 180 µl Buffer ATL, thoroughly mixed, and placed into sterile Eppendorf's on dry ice containing cryosectioned bladder tissue ready for complete lysis. Sufficient tissue lysis buffer was added to cover the tissue completely. The sample was mixed by vortexing and incubated at 56°C overnight in a rocking thermomixer at 800 rpm until the sample was completely lysed. During incubation where possible, the sample was vortexed occasionally to disperse the tissue and the rocking platform facilitated thorough lysis. Although solid tissue lysis is usually complete in 1–3 hrs, overnight lysis was achieved, and once complete, the 1.5 ml Eppendorf tube was briefly centrifuged to remove drops from the inside of the lid.

4.5.3 DNA Extraction

Genomic DNA was extracted and eluted into 50 µl AE buffer as described in section 2.7.1.

4.5.4 DNA Quantification

Genomic DNA was quantified for each sample using the nanodrop to determine sample quality and concentration as described in section 2.8. An example wavelength spectrum observed after quantification of patient 15 bladder tumour DNA is displayed in Figure 41 and patient 12 normal bladder DNA is displayed in Figure 42.

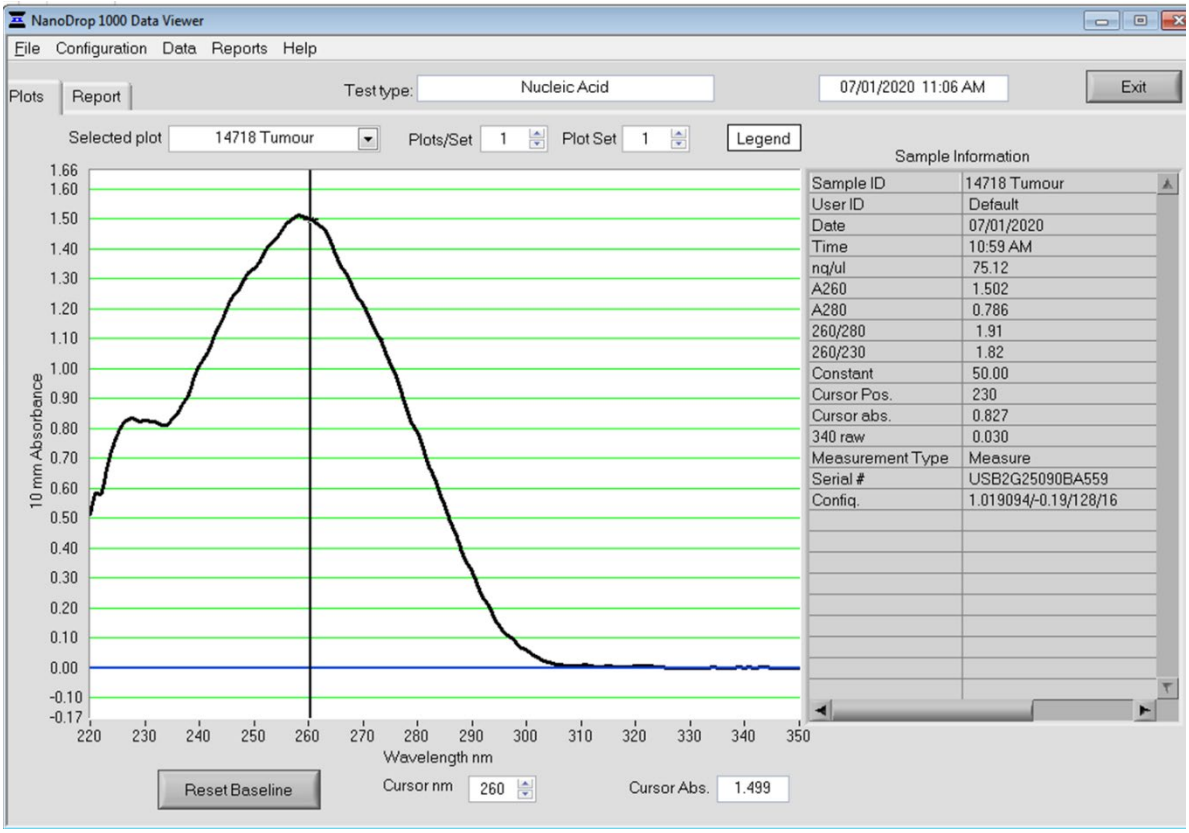

Figure 41 - Absorbance spectrophotometric graph displaying DNA quantification from patient 15 bladder tumour tissue.

The 260/280 ratio is used to assess DNA purity and a ratio of ~1.8 is generally regarded as 'pure DNA'. The 260/230 ratio is a secondary measure of nucleic acid purity and if the ratio is lower than 1.8, such indicates the presence of co-purified contaminants. The 260/280 ratio of 1.91 and 260/230 ratio of 1.82 show a fantastic nucleic acid extraction with high purity, ideal for downstream amplification and sequencing analysis.

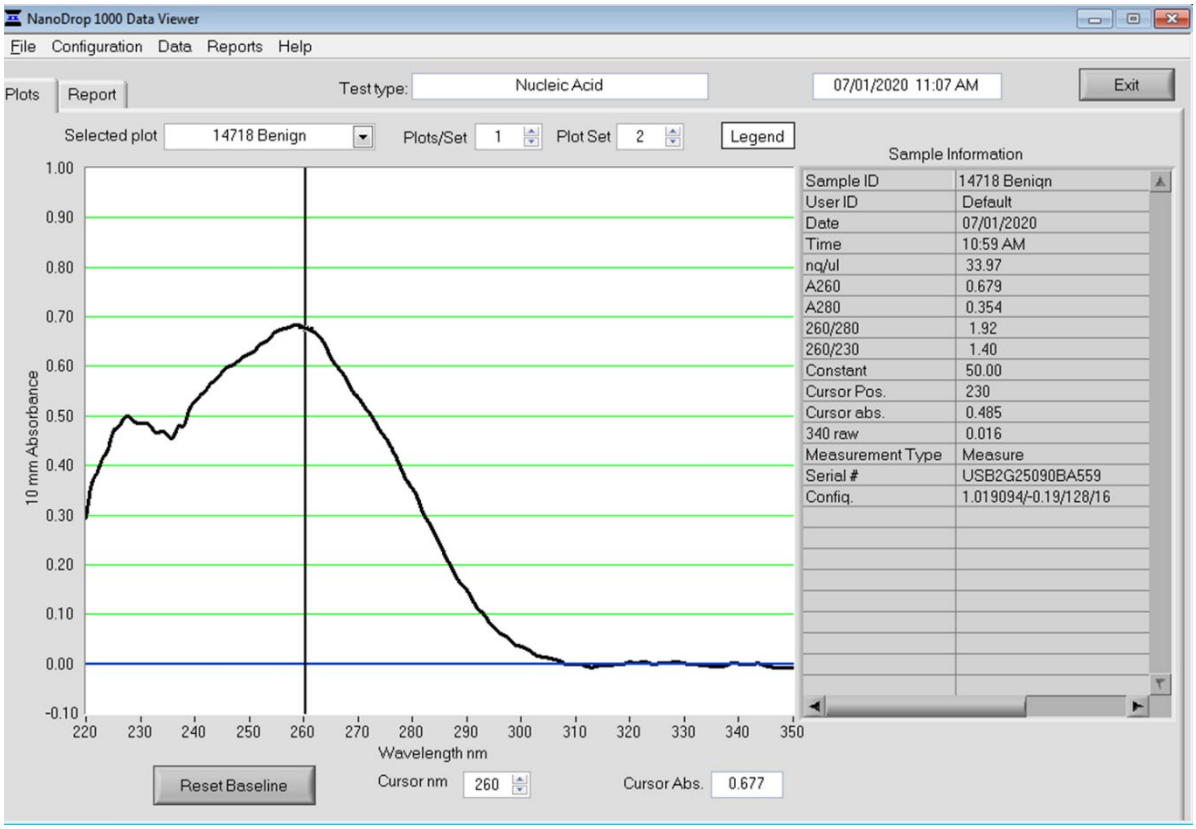

Figure 42 - Absorbance spectrophotometric graph displaying patient 15 DNA quantification from normal bladder tissue.

The 260/280 ratio of 1.92 and 260/230 ratio of 1.40 displayed in Figure 42 above indicates a good nucleic acid extraction with high purity, ideal for downstream amplification and sequencing analysis.

Table 28 below displays all nucleic acid purity results for each patient sample after nucleic acid was extracted, the whole mtDNA amplified and the whole mtDNA genome sequenced.

Patient	260/280	260/230	Nucleic Acid amount (ng/µl)
2 Benign	1.93	1.97	55.04
2 Tumour	1.93	1.21	23.23
4 Benign	1.03	0.42	117.55
4 Tumour	1.37	0.86	323.57
10 Benign	1.99	1.55	27.36
10 Tumour	1.92	1.95	8.91
11 Benign	1.98	1.90	42.78
11 Tumour	1.99	1.41	159.94
13 Benign	2.15	2.11	54.71
13 Tumour	1.81	1.69	24.77
15 Benign	1.92	1.40	33.97
15 Tumour	1.91	1.82	75.12
17 Benign	1.86	1.63	85.9
17 Tumour	1.89	1.93	102.6

Table 28 -Absorbance spectrums for cryostat cut sections of extracted genomic DNA from patients undergoing Radical Cystectomy.

4.5.5 mtDNA amplification

Post genomic DNA extraction, the whole mitochondrial genome was amplified using two overlapping primer pair sets 1AF'/R' and 1BF'/R', described in section 2.8.1 and displayed in Figure 43.

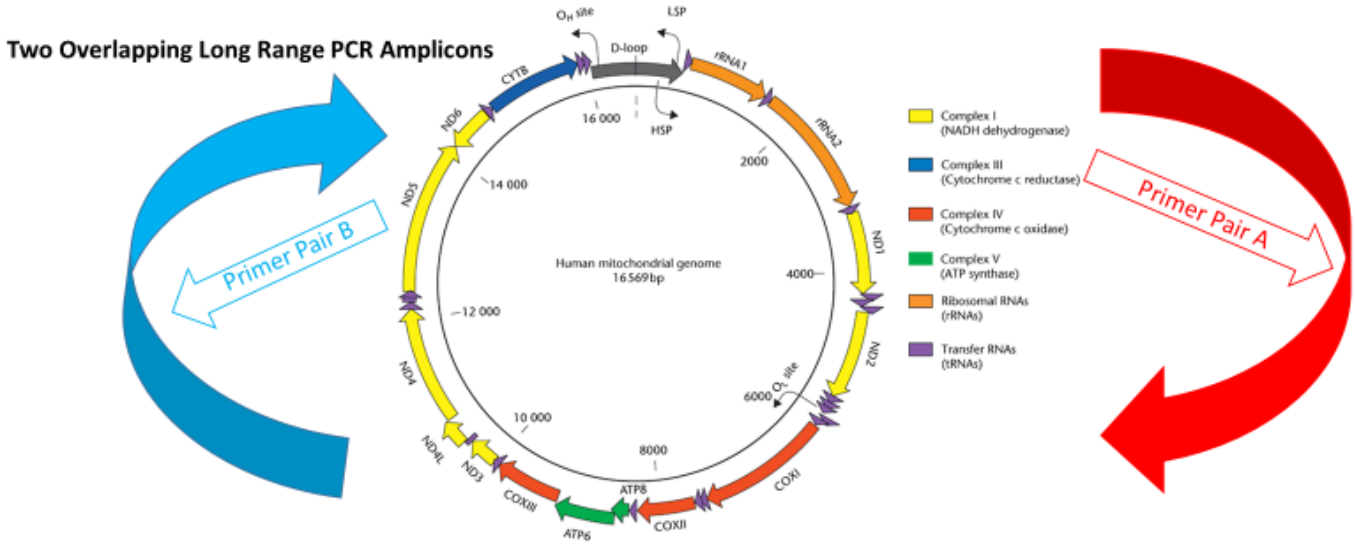

Bladder Tumour	Bladder 'Normal urothelium'	(Primer set)
F' 550-569 → expected product size 9289 base pairs R' 9839-9819		A
F' 9592-9611 → expected product size 7622 base pairs R' 645-626		B

Figure 43 - Two overlapping primer pair sets used to amplify the whole mtDNA genome in patient bladder tumours and normal bladder tissue following Radical Cystectomy, tissue lysis, and DNA extraction.

.

A 25µl reaction was prepared, with 1 µl DNA loaded. Reaction conditions were 94°C for 2 min, 35 cycles of 94°C for 30 secs, and 65°C for 16 mins. The final extension proceeded at 72°C for 16 mins. PCR products were then loaded and run onto a 0.7% agarose gel at 85V for 1.5hrs and visualised using the ChemiDoc Imaging system as seen in Figure 44.

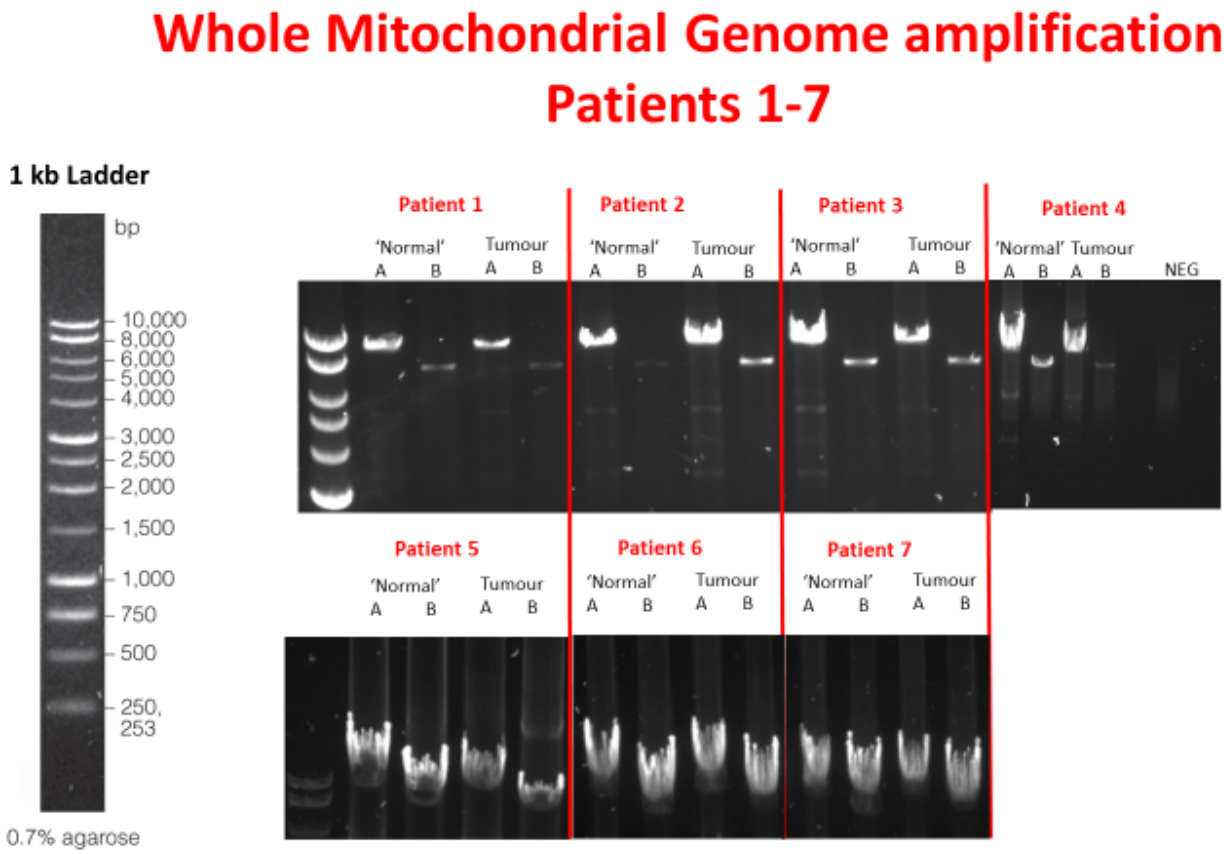

Figure 44 - Patients 1-7 whole mitochondrial genome amplified amplicons A and B visualised on agarose gels.

4.5.6 Library Construction

Amplicons were purified, as described in section 2.10, the molar concentration was quantified using the bionanalyser and an Agilent DNA 12 000 kit, detailed in 2.11.2. Samples underwent library construction, described in section 2.12, for full coverage of the mitochondrial genome. Template preparation was performed using the Ion Torrent PGM system and Ion Chef by emulsion PCR. Ion Sphere particles (ISPs) were enriched and subsequently deposited onto the 316 and 520 chips and library preparation and amplification were proceeded by sequencing on the Ion Torrent instrument.

Heat maps corresponding to the density of positive template ISPs were displayed after each sequencing run enabling the visualisation of the loading density of ISPs placed and sequenced on each chip, for every run.

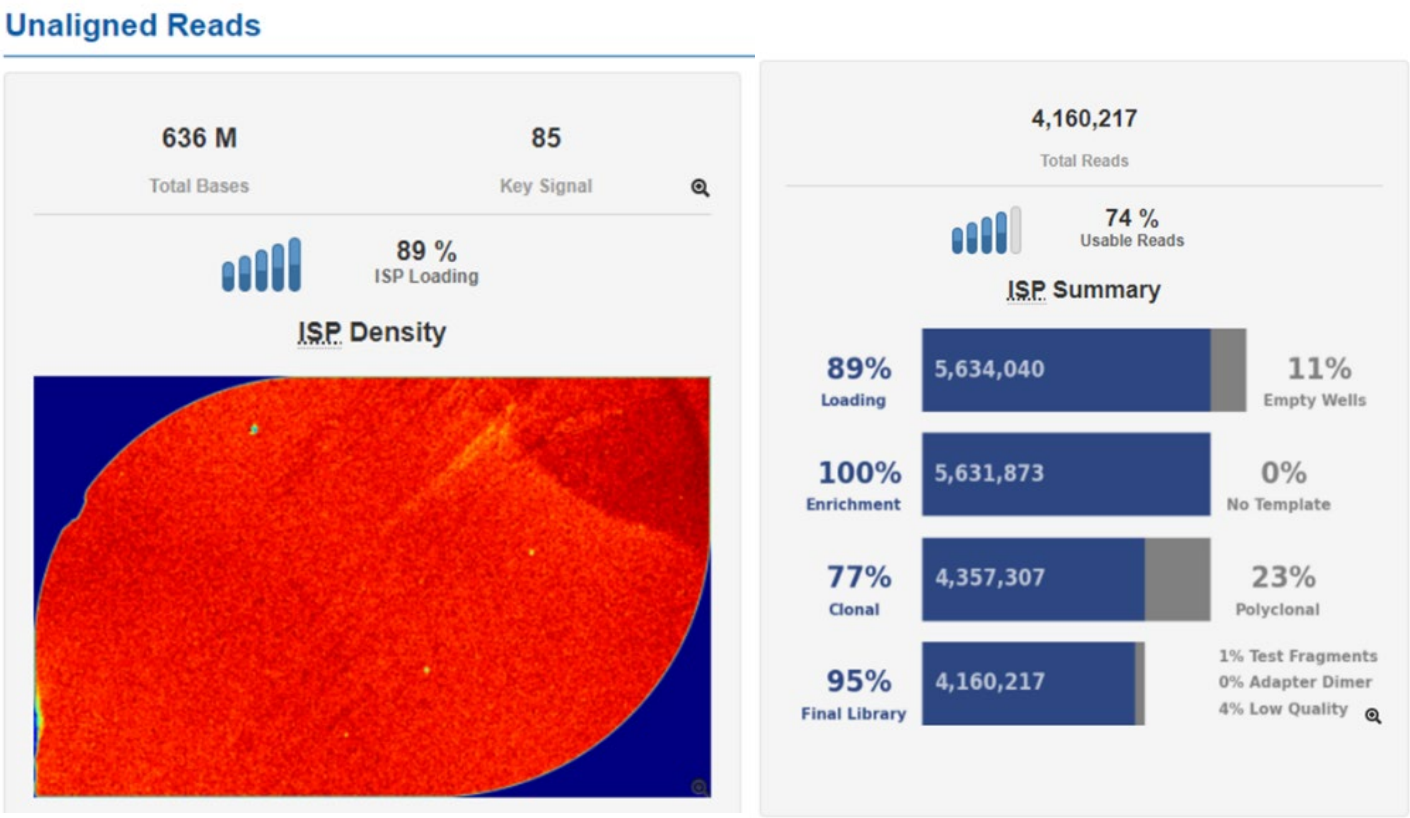

Figure 45 - Displays a heat map representing ISP density, ISP summary of wells loaded, enriched, and average total read length for one mtDNA sequencing run identifying tumour-specific mtDNA variants.

The blue zones within the heat map in Figure 45 signal empty wells, and the red zones signal a high density of beads loaded. With this particular mtDNA sequencing run, there was a high ISP loading of 89%, 100% bead enrichment, a total of 4,160,217 total reads obtained, and high fractions of amplified library fragments attached to ISPs, 95%.

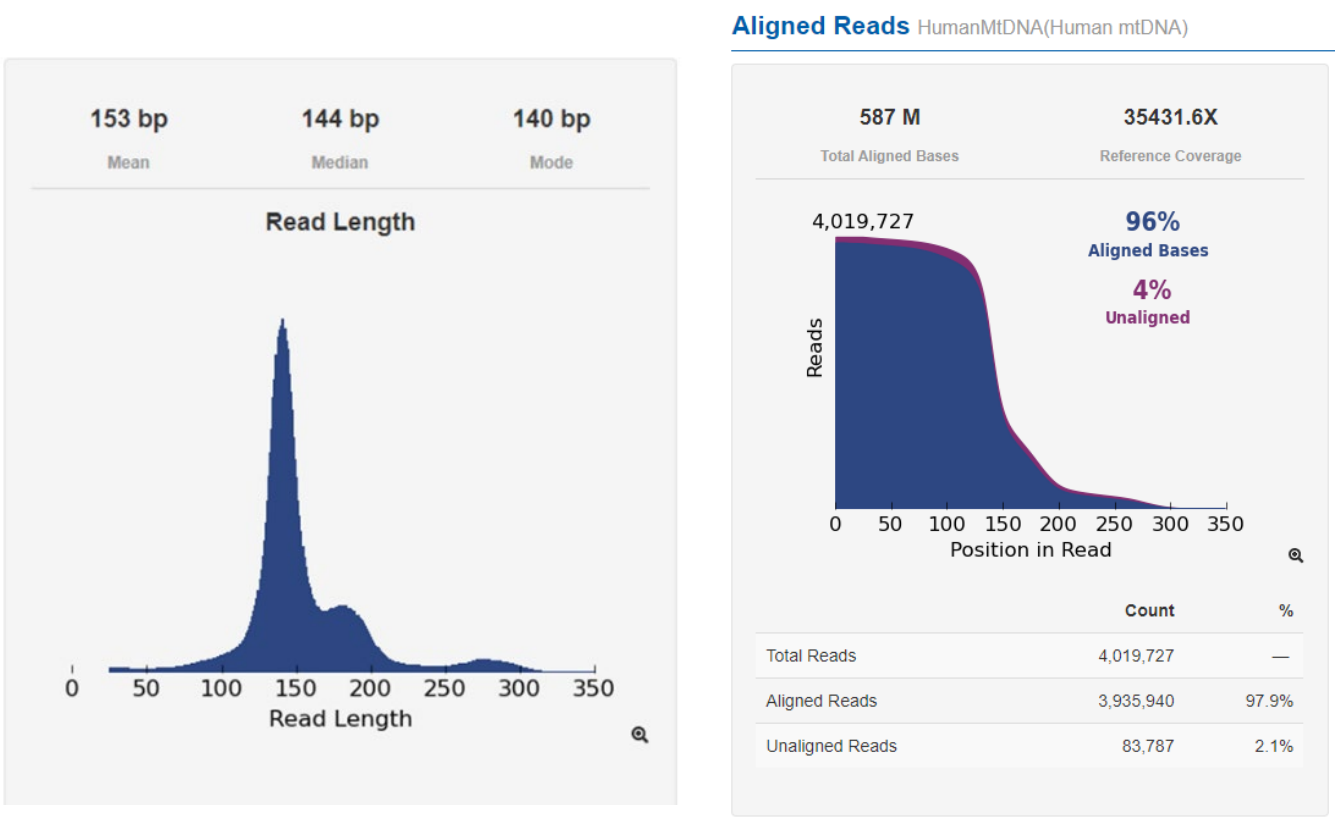

Figure 46 - Sequencing information summarising the average base pair read length and the total number of reads, both aligned and unaligned to the human mitochondrial genome.

Ligate adapters were ~50 base pairs long as seen in the horizontal line in Figure 47 below and a 99.4% mean raw accuracy was calculated during this mtDNA sequencing run.

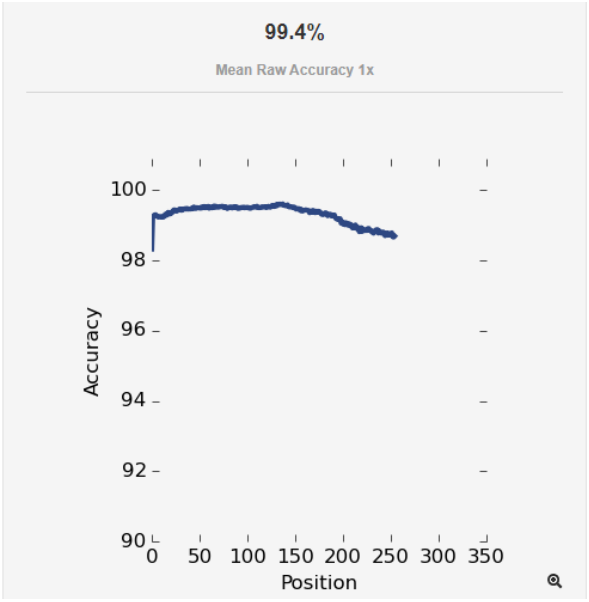

Figure 47 - Sequencing summary displaying percentage raw accuracy at various read length positions.

570 M

AQ17 Total Bases

Alignment Quality

	AQ17	AQ20	Perfect
Total Number of Bases [bp]	570 M	546 M	450 M
Mean Length [bp]	148	144	125
Longest Alignment [bp]	353	353	353
Mean Coverage Depth [x]	34385.1	32950.5	27174.5

Figure 48 - Sequencing summary of alignment quality including the total number of bases, mean length (bp), longest alignment (bp), and mean coverage depth (x).

AQ17 length of a read was the greatest length at which the read error rate is 2% or less and AQ20 length was the greatest length at which the error rate is 1% or less.

4.5.7 Tumour assessment of histological bladder tissue from Non-Muscle Invasive Bladder cancer patients undergoing Robotic Cystectomy.

Bladder tissue was sectioned, processed, and stained to sample the biopsy. Uropathologist review confirmed >75% of tumour rich cellular detail and only patients with high tumour content present in the tumour biopsy were subsequently analysed as displayed in Table 29 .

Bladder tissue with no presence of tumour was not prepared for mtDNA sequencing and only patients listed in Table 29 had a high presence of confirmed tumour after histopathological assessment. The whole mitochondrial genome was subsequently sequenced in these patient samples. To specifically obtain small but tumour rich material, patient 13's 10% tumour and normal bladder sample also underwent DNA extraction, mtDNA amplification, and mtDNA sequencing using a specific tumour rich capture method, Laser Capture Microdissection, and is described earlier in section 2.5.

Patient	Tumour Assessment (%)	TNM	Tumour Type
1	80	Grade 3 pT1 pN0	High Grade tumour
2	100	pT1 pN0 multifocal early	High Grade tumour
3	10	Grade 1	? CIS or early urothelial cancer
4	90	pT3b pN0 High Grade	Invasive High-Grade tumour
9	10	TNM8 PT0 Pn0	Low Grade papillary urothelial carcinoma
10	90	pta pN0 TNM 8	Papillary Low-Grade urothelial carcinoma
11	85-90	Grade 2/3 pN2	Invasive High-Grade urothelial carcinoma
13	10-15	Grade 3 pT2	5cm solid tumour High Grade solid invasive urothelial carcinoma
15	80-90	Grade 2 pT2 N0M0	Invasive solid tumour
17	80	Unable to obtain clinical information due to NHS COVID-19 restrictions	

Table 29 - Tumour assessment, TNM grade, staging, and tumour type of histological bladder malignant tissue from Bladder cancer patient cohort patients undergoing Robotic Cystectomy.

TNM staging: T= Size of the tumour, N= describes whether cancer has spread to lymph nodes. (N0) = no lymph nodes are affected. M= describes whether cancer has metastasised.

4.5.8 Demographic and Clinical characteristics of Bladder Cancer patient cohort

With ageing, an accumulation of mtDNA alterations is observed. Such was reflected in the BC patient cohort I investigated post Radical Cystectomy, as 25% of patients were females and 75% were males. Patients within our cohort had undergone Radical Cystectomy with a previous diagnosis determined, consequently their average age of diagnosis was not calculated, although their present age was determined from clinical notes. The average age of female patients studied within our BC patient cohort was 67.5 years and 71.6 years in male patients, reflecting the overall higher age of males suffering from BC compared to females.

Clinical reports available for all BC patients within our cohort were retrieved after initial TURBT samples were taken and analysed from NHS databases and assessed to determine the severity and diagnosis of the clinical disease course for each patient.

Patient ID	Age	Sex	Smoker	Clinical Presentation	Previous Diagnosis	Histopathological Diagnosis	Treatment	Initial TURBT date
1 NMIBC	64	Female	Never	Pain on micturition & visible haematuria	Not Known	Pathology for initial TURBT pT1 at least, G3 High Grade, CT and MDT suggest probable T4 disease from CT appearance (vaginal involvement) Cystectomy 11/10/2018 pathology pT1 pN0 no residual tumour and complete local excision.	Post initial TURBT but prior to cystectomy : downstaging chemotherapy Gemcitabine and Cisplatin 4 cycles from 06/2018 to 08/2018. Cystectomy 10/2018	26/03/2018- initial Bladder removal
2 MIBC	54	Male	Unknown	Haematuria 19/06/2018	Not Known	Bladder biopsy 13/08/2018, pathology CIS pathology pT1 pN0 multifocal early invasive High Grade G2 and widespread CIS local excision.	Surgery only. cystectomy 14/11/2018	Not Known
3 NMIBC	67	Female	Unknown	Visible Haematuria	Not Known	TCC. No papillary lesions or CIS are identified. Early urothelial carcinoma. G1. Lamina propria contains pigmented macrophages suggesting possible old biopsy site. Detrusor muscle is unremarkable.	TURBTs, BCG July 2009, Cystectomy Nov 2018, Chemotherapy (Gemcitabine and Cisplatin in combination with Avelumab (Javelin Study)	16/02/2009
4 NMIBC	64	Female	Unknown	Haematuria Clot retention Dec 2018	Not Known	Pathology pT1 G3 High Grade. Pathology pT3b pN0 local excision cannot be confirmed.	Radical Cystectomy 31/1/2019	01/12/2018
5 MIBC	71	Male	Yes	Haematuria Oct 2018	Acute cholecystitis since Nov 2018, suspicious for Prostate Ca from a PET scan	Pathology pT2 G3 High Grade. Radical cysto-prostatectomy 25/04/2019 pathology pT0 pN0/1 (left side lymph node has metastatic deposit)	Radical cysto-prostatectomy 25/04/2019 TURBT then Neo-adjuvant chemotherapy Gemcitabine and Cisplatin, 3 cycles from 01/2019 to 03/2019. Radical surgery.	06/11/2018

Patient ID	Age	Sex	Smoker	Clinical Presentation	Previous Diagnosis	Histopathological Diagnosis	Treatment	Initial TURBT date
6 MIBC	58	Male	Y	Microscopic Haematuria, Urgency, Frequency	Not Known	Extensive invasive urothelial carcinoma, large nested variant showing minimal tumour regression. Stage ypT4 YPN1	TURBT invasive of HG 2/3 urothelial carcinoma ,focal squamous differentiation stage pT2. HG muscle invasion.	Not Known
7 NMIBC	61	Male	Unknown	Haematuria	Not Known	Invasive HG urothelial carcinoma tumour invades through stroma but not to detrusor muscle. HG G2 Urothelial carcinoma. No dysplasia/malignancy. Laminia propria is edematous and contains pigmented macrophages suggesting previous hemorrhage.	Not Known	Not Known
8 NMIBC	67	Male	No	Haematuria & Clot retention	Grade 3 Invasive urothelial cancer of bladder	No evidence of residual in-situ or invasive malignancy, papillary lesions, CIS. New solid bladder tumour left lateral wall. Mx fragments of inflamed bladder wall. Atypical urothelial cells, HG nuclear changes. Invasive malignancy into detrusor muscle present.	Cisplatin & Gemcitabine chemotherapy. 3 cycles before CT scan.	19/11/18 2cm solid tumour Pt2 n0 m0 g3
9 NMIBC	66	Male	Not Known	LG NMIBC	Previous BCG. Significant lower UT symptoms (BCG related).	LG 2 papillary urothelial carcinoma. Multi-focal bladder tumours found. No evidence of residual in-situ or invasive malignancy. Scattered basal cells and loss of surface urothelium. No evidence of invasion and detrusor muscle is free from tumour. Familial history of Bladder Cancer brother died of it.	Single dose of mitomycin C given in bladder before urethral catheter removed. Complete local excision.	Not Known

Patient ID	Age	Sex	Smoker	Clinical Presentation	Previous Diagnosis	Histopathological Diagnosis	Treatment	Initial TURBT date
10 NMIBC	61	Male	Yes	Haematuria, pain on micturition	Extensive papillary lesion composed of complex branching & fused fibromuscular lobes.	LG G2 Papillary urothelial carcinoma stage pTa pN0. Features are of LG atypia, hemorrhage. Histology demonstrates NMIBC but due to hydronephrosis followed up with MRI, which shows MIBC. Staging confirms localized disease.	Radical Cystectomy. TNM 8 Complete local excision R0	Not Known
11 NMIBC	71	Male	Yes	Microscopic Haematuria, Urgency, Frequency, overactivity	Increased bladder sensation, bladder outflow obstruction, outflow blockage coming from prostate.	G2/3 PT1 TCC May require re-resection to rule out MIBC. HG invasive urothelial carcinoma. Fragments of bladder mucosa, but no detrusor muscle seen. IHC +ve for CK7,CK20+GATA3.	Beta-3-agonist did not change symptoms. Flexible cystoscopy performed. Cystectomy robotic minimally invasive approach.	12/19/19
12 MIBC	71	Male	No	Haematuria	Focal prostatic adenocarcinoma with is less than 5% of prostatic tissue therefore stage is pT1a	Total loss of surface urothelium with scattered basal cells throughout rest of bladder. No evidence of dysplasia, in-situ carcinoma or invasive malignancy.	Cisplatin & Gemcitabine chemotherapy.	Not Known
13 MIBC	64	Male	Ex Smoker Stopped 25 yrs ago	Haematuria Pain on micturition	TURBT –new 5cm solid bladder tumour. Resected.	Invasive HG carcinoma focally infiltrating in detrusor muscle. Dysplasia present. HG solid invasive urothelial carcinoma G3 Stage PT2. Tumour in left lateral wall of bladder.	Neoadjuvant cisplatin & gemcitabine chemotherapy. Bicalutamide monotherapy commenced.	Not Known

Patient ID	Age	Sex	Smoker	Clinical Presentation	Previous Diagnosis	Histopathological Diagnosis	Treatment	Initial TURBT date
14 MIBC	75	Female	No	Visible Hematuria & significant hydronephrosis	Flexible cystoscopy not done, underwent TURBT	HG Invasive urothelial carcinoma, G2 stage pT2. New solid tumour. Invasive. Histological examination shows fragments of bladder mucosa and detrusor muscle. Tumour is visibly focally invading into detrusor muscle. Irregular nests of atypical cells with large hyperchromatic nuclei.	Beta-3-agonist. Cisplatin & Gemcitabine chemotherapy.	07/2019
15 MIBC	62	Male	Yes	Haematuria, Urgency, Frequency	Invasive urothelial carcinoma	HG Invasive urothelial carcinoma which extensively involves detrusor muscle and focally extends to perivesical fat. Early invasive carcinoma is also seen within extramural ureters left & right. No definite CIS seen. G2 TNM8 PT2 PN2 Mx	Neoadjuvant cisplatin & gemcitabine chemotherapy. Bicalutamide monotherapy commenced.	Not Known
16 MIBC	78	Male	Not known	Haematuria & Clot Retention	Stage 2 sarcoma right testis Nov 2004. Chemotherapy received T2NM.	HG Invasive urothelial carcinoma with very focal squamous differentiation. Stage PT2	Chemotherapy 2004 Neoadjuvant cisplatin & gemcitabine chemotherapy 3 CYCLES 04/02/19	Nov 2018
17	Unable to obtain clinical information due to NHS COVID-19 restrictions.							

Table 30 - Demographic and Histopathological diagnosis of patients after TURBT within our cohort undergoing Radical Cystectomy. LG: Low Grade; HG: High Grade; CIS: Carcinoma-in-Situ.

4.5.9 Histological characterisation of patient 2 normal and tumour Bladder tissue H&E staining

Patient 2 Normal Bladder

The process of histological characterisation involved staining formalin-fixed normal and tumour bladder biopsies with H&E to identify measurable tumours. Demonstrated in figures 49 and 50 are examples of H&E stained bladder tissue normal and tumour sections from patient 2. From these H&E stained bladder tissue sections, additional tumours can be microscopically detected if resections were performed near the ureter.

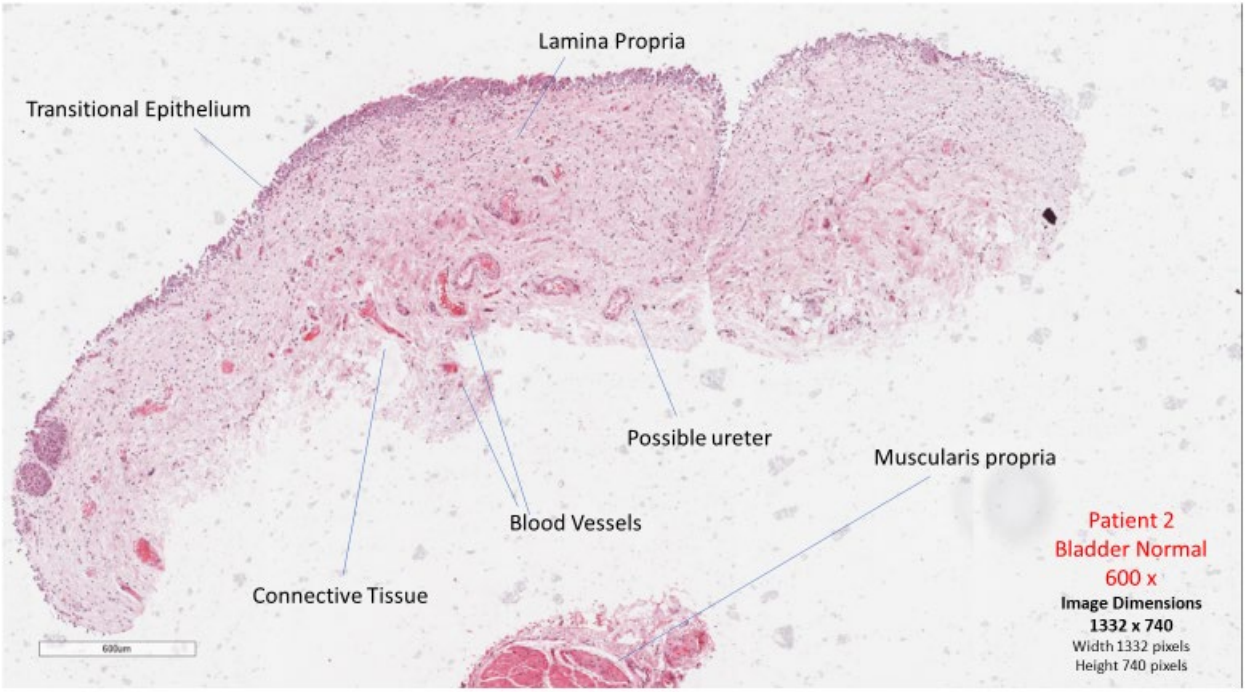

Figure 49 - - FFPE cut, H&E stained image of patient 2 adjacent normal urothelium, displaying urothelial surface with no visible tumour.

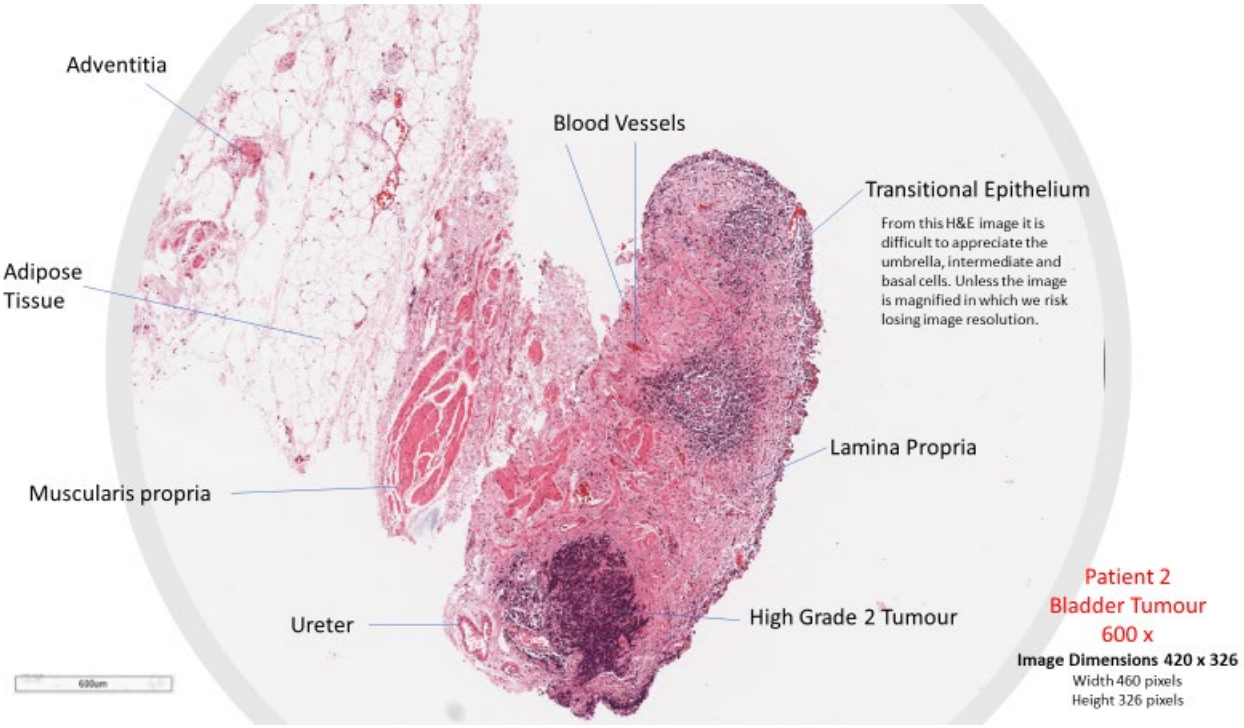

Figure 50 - FPPE cut, H&E stained image of patient 2 High-Grade Bladder Tumour, with 80% tumour identified within this tissue section.

4.5.10 Tumour-specific mtDNA variants are detectable in bladder tumours

Normal and tumour bladder biopsies underwent mitochondrial sequencing to identify mtDNA variants within the bladder tumour which were absent from the patients' normal urothelium. Generated sequence files were aligned both to the whole mitochondrial genome and the hg19 human complete genome. The mitochondrial genome was used as a reference genome to identify mtDNA variants and the hg19 human genome was used to verify these alterations and exclude NUMTS. No NUMTS were observed within the called variants.

Patient 1

Although 80% bladder tumour content was confirmed by the Uropathologist and a visible tumour was not observed in the normal urothelium, no tumour specific mtDNA variants were detected in patient 1. Consequently, no further downstream analysis was performed, or matched tissue was further investigated.

Patient 2

After histopathological examination patient 2, a 54-year-old male presented with multifocal early invasive High Grade BC and widespread CIS local excision. After Radical Cystectomy bladder tumour and normal tissue were assessed, and 100% bladder tumour was confirmed in patient 2 (see Figure 51). Following whole mtDNA sequencing, a tumour-specific mtDNA variant at a high heteroplasmy level of 90.1% was identified at position m.10404T>C in the mitochondrial genome. As I was interested in prevalent tumour-specific marks, I focussed on high level heteroplasmy, absent from the patients' normal urothelium as a tumour-specific mark from the founder tumour.

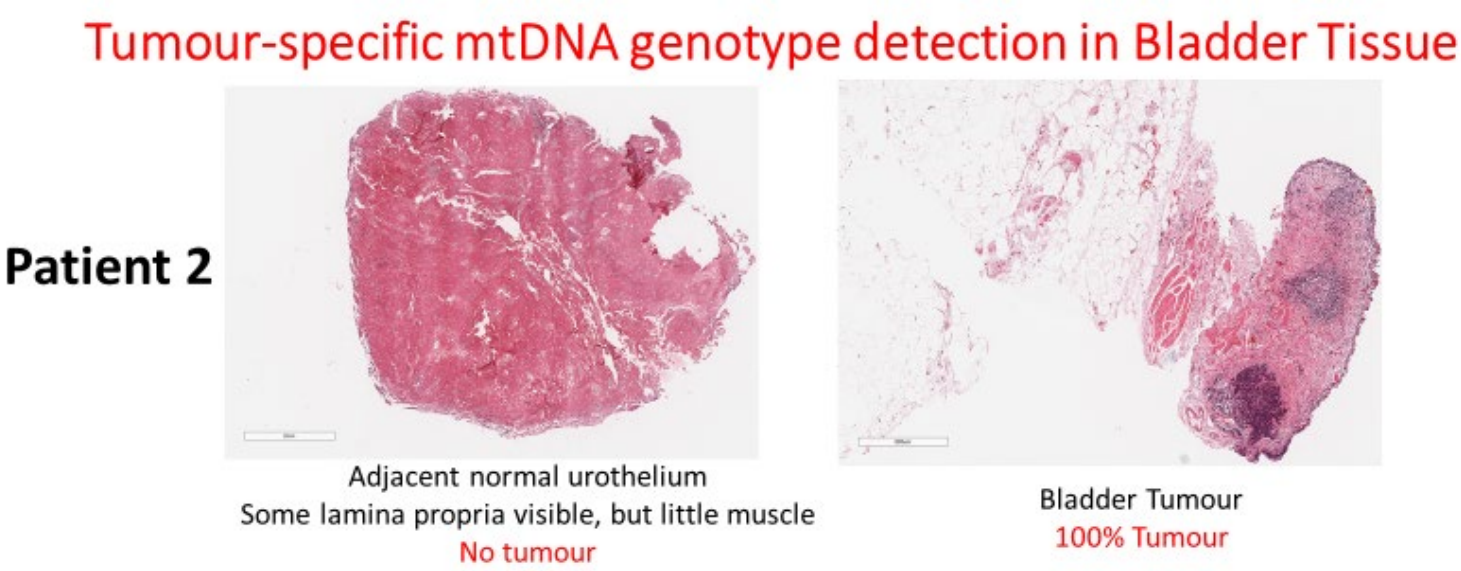

Figure 51 - H&E stained tissue sections of patient 2 normal urothelium and bladder tumour samples, produced on a microscopic slide.

Below is a table comprised of all mtDNA variants identified in patient 2 benign and tumour bladder biopsies. The majority of mtDNA modifications were detected in both normal and tumour bladder tissue at high heteroplasmy levels. Tumour-specific mtDNA alterations m.10404T>C were identified only in the tumour bladder biopsy at 90.1% heteroplasmy and m.14930G>A was observed at 90.4% heteroplasmy. m.14765AC>T was detected at a lower level heteroplasmy of 4% in the bladder tumour and at similar levels of 4.2% in the normal bladder sample. Only the tumour-specific mtDNA variants at high frequency were of interest, which highlights an index lesion at high prevalence.

mtDNA Variants detected in patient 2 bladder tumour tissue

Patient 2 Bladder Tumour (36 mtDNA Variants identified)					
Chrom	Position	Reference	Variant	Level of Heteroplasmy (%)	Quality
mtDNA	73	A	G	99.9	26035
mtDNA	153	A	G	99.9	33651.8
mtDNA	195	T	C	99.7	33708.8
mtDNA	225	GT	AC	100	33897.7
mtDNA	263	A	G	99.8	33769.3
mtDNA	311	-	C	97	18209.8
mtDNA	303	C	-	3	18209.8
mtDNA	750	A	G	99.8	33772.1
mtDNA	1438	A	G	99.8	33796.1
mtDNA	1719	G	A	99.7	33530.9
mtDNA	2706	A	G	99.9	33914.7
mtDNA	4769	A	G	100	33952.6
mtDNA	6221	T	C	99.7	33413.7
mtDNA	6371	C	T	99.1	33240.6
mtDNA	7028	C	T	99.5	33554.4
mtDNA	8393	C	T	94.5	30189.5
mtDNA	8860	A	G	99.9	33798.5
mtDNA	10404	T	C	90.1	27807.8
mtDNA	10532	A	G	99.9	33867.1
mtDNA	11719	G	A	99.8	33779.3
mtDNA	12705	C	T	99.7	33330.9
mtDNA	13251	C	T	99.8	33839.1
mtDNA	13708	G	A	99.8	32010.5
mtDNA	13966	A	G	99.6	33481.2
mtDNA	14470	T	C	99.9	25701.6
mtDNA	14766	C	T	96	30552.6
mtDNA	14765	AC	T	4	30552.6
mtDNA	14930	G	A	90.4	28005.5
mtDNA	15326	A	G	99.7	33736.6
mtDNA	15927	G	A	99.8	33762.8
mtDNA	16183	ACCCCCT	CCCCCC	24.8	21195.4
mtDNA	16183	ACCCCCT	CCCCCCC	69.6	21195.4
mtDNA	16223	C	T	99.6	24124.4
mtDNA	16278	C	T	99.4	32617
mtDNA	16519	T	C	99.9	33874.4
mtDNA	16566	G	A	97.4	29500.4

Patient 2 Normal Bladder Tissue (32 mtDNA Variants identified)					
Chrom	Position	Reference	Variant	Level of Heteroplasmy (%)	Quality
mtDNA	73	A	G	99.7	12792
mtDNA	153	A	G	99.4	20623.6
mtDNA	195	T	C	99.4	23285.8
mtDNA	225	GT	AC	99.6	23898.4
mtDNA	263	A	G	100	22306.8
mtDNA	750	A	G	99.9	25553.5
mtDNA	1438	A	G	99.8	28618.5
mtDNA	1719	G	A	99.7	21005.8
mtDNA	2706	A	G	99.4	25553.5
mtDNA	4769	A	G	99.8	22437.4
mtDNA	6221	T	C	99.3	24816.3
mtDNA	6371	C	T	98.3	20580.3
mtDNA	7028	C	T	99	25410.8
mtDNA	8393	C	T	92.7	10122.2
mtDNA	8860	A	G	99.9	15955.6
mtDNA	10532	A	G	99.8	32291.7
mtDNA	11719	G	A	99.7	33711.1
mtDNA	12705	C	T	99.7	33226.4
mtDNA	13251	C	T	99.7	33640.1
mtDNA	13708	G	A	99.8	13615.3
mtDNA	13966	A	G	99.2	27256.9
mtDNA	14470	T	C	99.3	9952.89
mtDNA	14766	C	T	95.4	14499.8
mtDNA	14765	AC	T	4.2	14499.8
mtDNA	15326	A	G	99.9	32740.4
mtDNA	15927	G	A	99.2	33297
mtDNA	16183	ACCCCCT	CCCCCC	18.2	9626.27
mtDNA	16183	ACCCCCT	CCCCCCC	66.8	9626.27
mtDNA	16223	C	T	98.9	12117.6
mtDNA	16278	C	T	98.8	16434.3
mtDNA	16519	T	C	99.5	24711.9
mtDNA	16566	G	A	95.3	15980.1

Figure 52 - mtDNA variants detected in patient 2 primary bladder benign and tumour tissue after mtDNA sequencing. Tumour-specific mtDNA variant m.10404T>C is detected at 90.1% and pathogenic variant m.14930G>A at 90.4% within the bladder tumour highlighted in yellow.

Patient 3

Patient 3, a 67 female whose smoking status was unknown presented clinically with visible haematuria, and after TURBT, early urothelial Transitional Cell Carcinoma was diagnosed histopathologically. The patient qualified for the 'JAVELIN Bladder 100' research study, funded by Pfizer, which provided Avelumab as maintenance therapy for advanced disease that was locally advanced and had not spread beyond the bladder. Patient 3 was administered chemotherapy, specifically Gemcitabine and Cisplatin in combination with Avelumab. Post mtDNA sequencing no tumour-specific mtDNA variants were detected in patient 3, hence no further downstream analysis was performed. Notably, both patients 1 and 3 had no high level heteroplasmy tumour-specific mtDNA variants detected, had mutually been administered Gemcitabine and Cisplatin, and subsequently I did not investigate these patients' samples further.

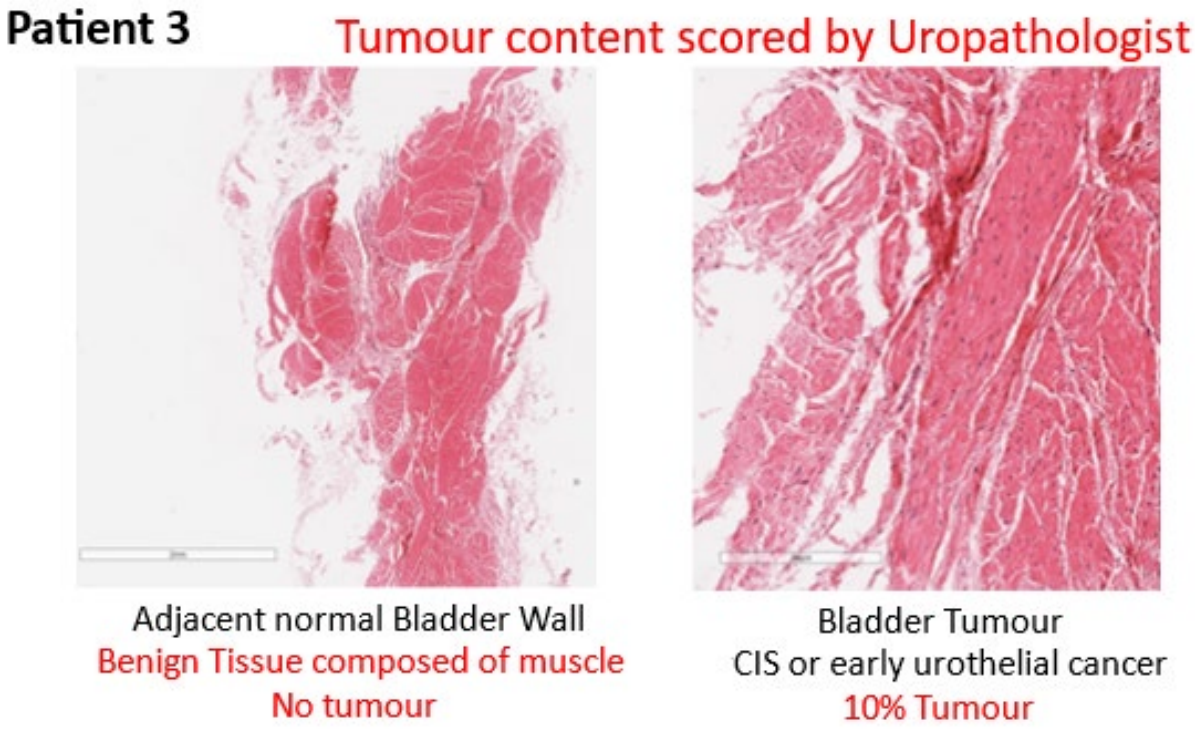

Figure 53 - Patient 3 bladder tumour content confirmed by Uropathologist. After H&E staining tumour content was scored as 'low' according to the cystectomy tumour content scoring sheet: High > 60%, medium 40-60%, and low <40%.

Patient 4

After undergoing Radical Cystectomy, post bladder tumour tissue DNA extraction, and whole mtDNA genome sequencing Single Nucleotide Polymorphisms (SNPs) were identified in patient 4. m.4841G>A mtDNA variant with the highest heteroplasmy level of 56% were observed in addition to the presence of variants m.5032G>A at 20% heteroplasmy and m.16147C>T at 53% heteroplasmy within the patients' bladder tumour post mtDNA sequencing.

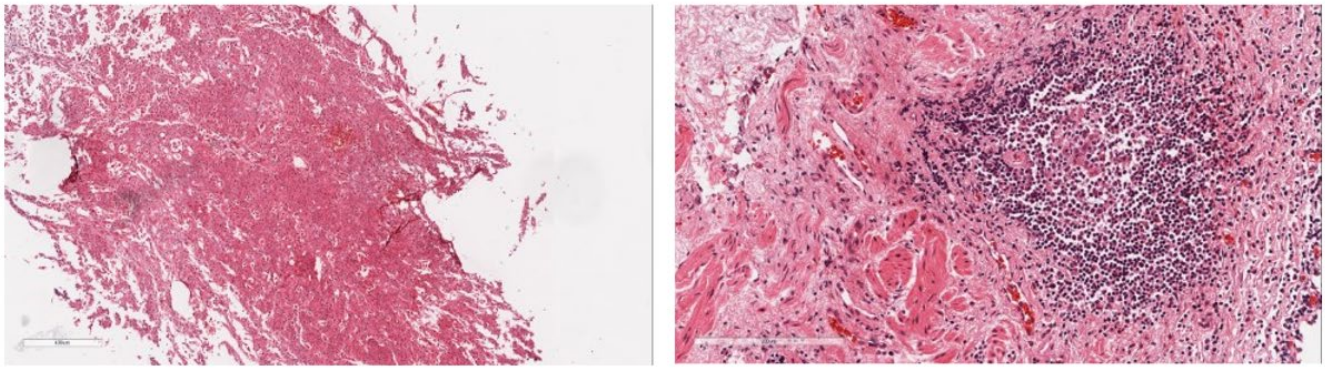

Figure 54 - Patient 4's bladder tumour content confirmed by Uropathologist. After H&E staining tumour content was assessed as 'high' according to the cystectomy tumour content scoring sheet High > 60%, medium 40-60%, and low <40%.

After undergoing Radical Cystectomy, post bladder tumour tissue DNA extraction and whole mtDNA genome sequencing Single Nucleotide Polymorphisms (SNPs) were identified in patient 4. m.4841G>A mtDNA variant with the highest heteroplasmy level of 56% were observed in addition to the presence of variants m.5032G>A at 20% heteroplasmy and m.16147C>T at 53% heteroplasmy within the patients' bladder tumour post mtDNA sequencing.

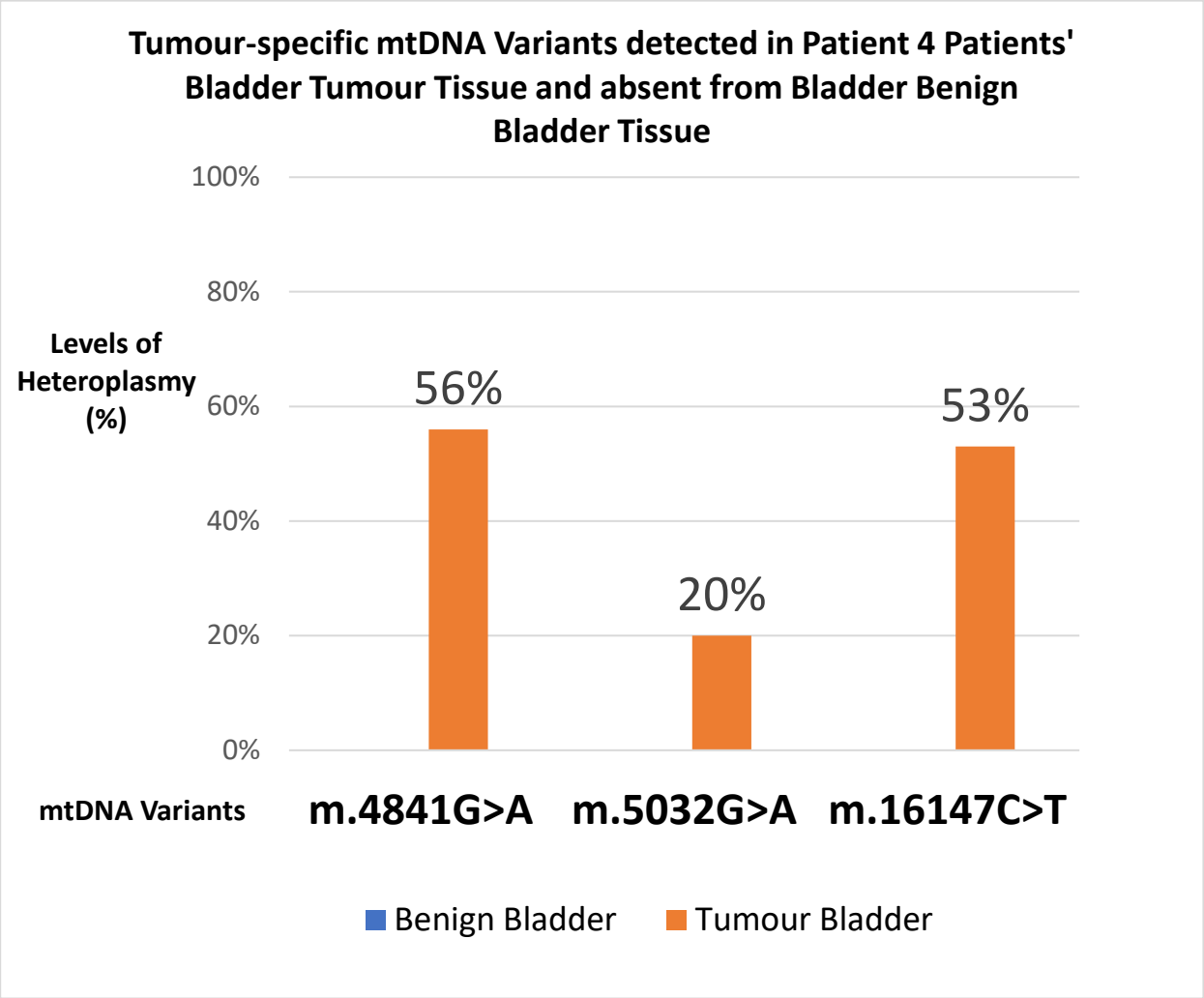

Figure 55 - Tumour-specific mtDNA variants detected in primary bladder tumour from patient 4 post cystectomy mtDNA sequencing data.

Patient 10

A 61-year-old smoker presented clinically with haematuria and pain on micturition. Pre-Radical Cystectomy, patient 10 had a previous histopathological diagnosis of an extensive papillary lesion within the bladder composed of complex branching and fused fibromuscular lobes. Histology demonstrated NMIBC and post MRI, evidence of muscle invasion was observed. After Radical Cystectomy, additional bladder tumour and normal tissue were obtained for the purposes of this research study. Post mtDNA sequencing a tumour-specific variant at m.1180T>C was detected at 69.2% heteroplasmy level.

mtDNA Variants detected in patient 10 bladder tumour tissue

Patient 10 Bladder Normal (13 mtDNA Variants identified)					
Chrom	Position	Ref	Variant	Level of Heteroplasmy (%)	Quality
mtDNA	263	A	G	99.7	20785.5
mtDNA	311	-	C	100	4506.9
mtDNA	750	A	G	100	44218.7
mtDNA	1438	A	G	99.8	45758.8
mtDNA	3010	G	A	99.6	45653.3
mtDNA	4769	A	G	99.9	45955.8
mtDNA	6272	A	G	99.6	45505.4
mtDNA	8764	G	A	99.9	22826.9
mtDNA	8860	A	G	99.9	27522.3
mtDNA	14869	G	A	99.8	45812.5
mtDNA	15326	A	G	99.8	45807.6
mtDNA	15736	A	G	99.5	45515.2
mtDNA	16519	T	C	99.6	22378.4

Patient 10 Bladder Tumour (16 mtDNA Variants identified)					
Chrom	Position	Ref	Variant	Level of Heteroplasmy (%)	Quality
mtDNA	263	A	G	100	17539
mtDNA	311	-	C	100	4092
mtDNA	750	A	G	99.9	20610.5
mtDNA	1180	T	C	69.2	12818.3
mtDNA	1438	A	G	99.9	21476
mtDNA	3010	G	A	99.9	26955.9
mtDNA	4769	A	G	100	15973.1
mtDNA	4866	T	C	15.7	1373.83
mtDNA	6272	A	G	99.7	27375.4
mtDNA	8764	G	A	99.8	10392.3
mtDNA	8860	A	G	100	13861.6
mtDNA	11577	G	A	23.6	3023.66
mtDNA	14869	G	A	99.7	27912.7
mtDNA	15326	A	G	99.9	27947.3
mtDNA	15736	A	G	99.8	23758.5
mtDNA	16519	T	C	100	16626.4

Figure 56 - Tumour-specific mtDNA variants detected in primary bladder benign and tumour from patient 10 post cystectomy sequencing data. Tumour-specific mtDNA variant m.1180T>C is detected at 69.2%, m.4866T>C 15.7% and pathogenic variant m.11577G>A at 23.6% within the bladder tumour highlighted in yellow.

Patient 11

A High Grade invasive urothelial carcinoma was diagnosed histopathologically within patient 11 and after being administered a Beta-3-agonist, unfortunately, this did not change symptoms and flexible cystoscopy was performed. A minimally invasive approach during Robotic cystectomy was undertaken and bladder tumour and normal tissue were assessed and sequenced for the whole mitochondrial genome. A tumour-specific mtDNA variant at position m.9098T>C was detected at a heteroplasmy level of 76%.

mtDNA Variants detected in patient 11 bladder tumour tissue

Patient 11 Bladder Normal (12 mtDNA Variants identified)				
mtDNA Position	Reference	Variant	Level of Heteroplasmy (%)	Quality
263	A	G	100	21493.9
456	C	T	97.5	6053.78
523	AC	-	99.4	3385.9
750	A	G	100	35152.5
1438	A	G	100	39485.1
4336	T	C	99.9	31810.8
4769	A	G	99.9	23617.4
4916	A	G	99.3	26691.6
8860	A	G	99.9	9991.34
15326	A	G	100	28750.5
15833	C	T	99.5	34659.7
16304	T	C	97.2	16987.7

Patient 11 Bladder NoTumour (14 mtDNA Variants identified)				
mtDNA Position	Reference	Variant	Level of Heteroplasmy (%)	Quality
263	A	G	100	8850.83
307	CCCT	TC	94.2	4530.48
456	C	T	100	2149.92
523	AC	-	98.5	1215.8
750	A	G	99.8	14517
1438	A	G	99.8	13460.2
4336	T	C	100	13264.3
4769	A	G	99.6	10044.3
4916	A	G	100	13675.2
8860	A	G	100	8016.17
9098	T	C	75.9	5940.33
15326	A	G	99.9	15098.7
15833	C	T	99.8	13050.4
16304	T	C	98.5	6928.41

Figure 57 - Tumour-specific mtDNA variants detected in primary bladder benign and tumour from patient 11 post cystectomy mtDNA sequencing data. Tumour-specific pathogenic variant m.9098T>C is identified at 75.9% within the bladder tumour highlighted in yellow above.

4.5.11 Laser Capture Microdissection

Patient 13

A minimal amount of tumour content was observed in patient 13 bladder tumour tissue (10%) and Laser Capture Microdissection (LCM), (as described in section 2.5) was completed to specifically acquire this tumour region for genome mtDNA sequencing. As the Uropathologist marked the 10% tumour-rich area (as seen in Figure 58 in blue) LCM generated 100% tumour material for DNA extraction and genome sequencing.

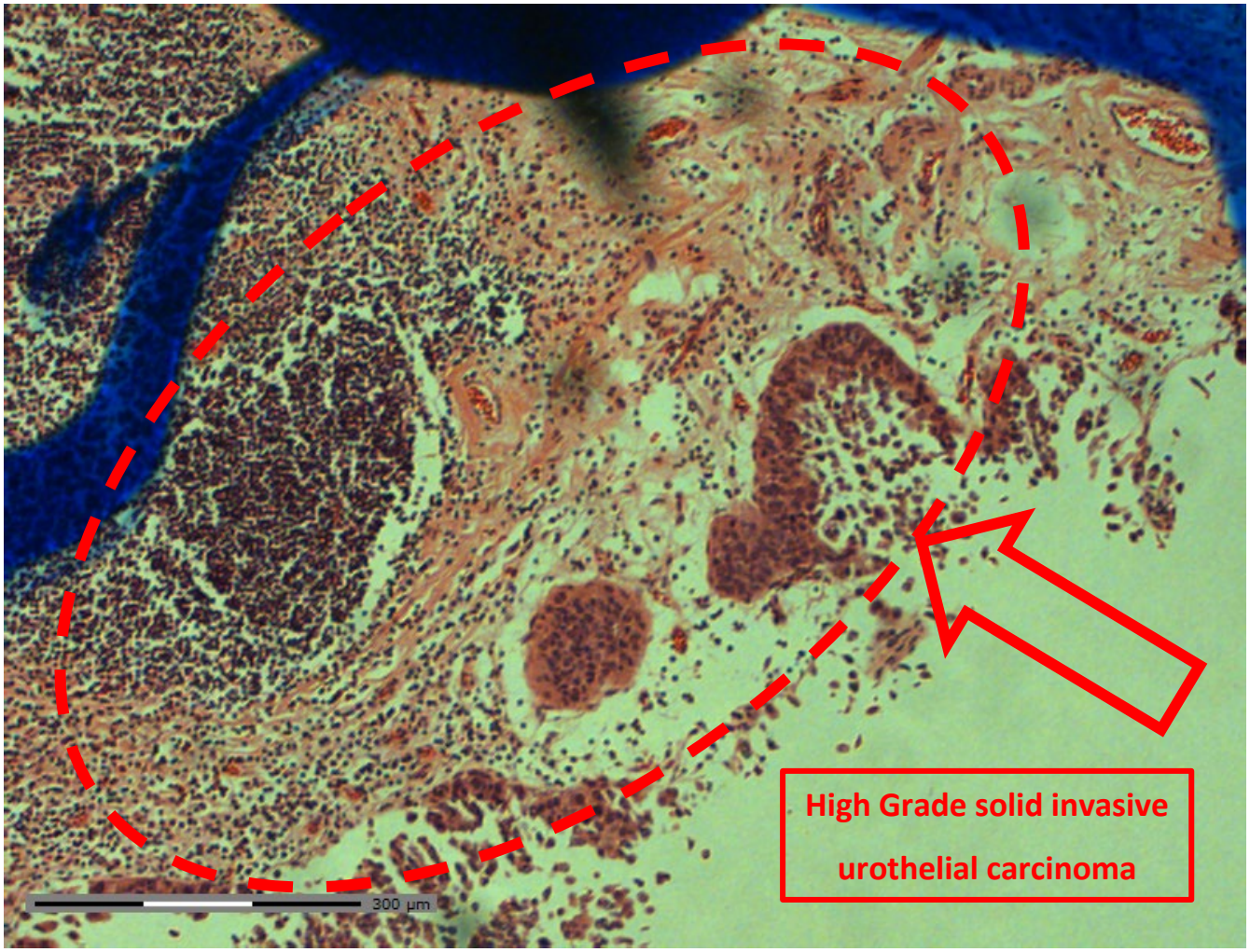

Figure 58 - 10 µm H&E stained cryostat cut bladder tumour section from patient 13. The cancerous area was marked blue and highlighted by the pathologist and the defined 10% tumour rich region is displayed within the red dotted line. Bladder tumour area at 5x magnification.

Optimising the laser settings and objective for bladder tissue was essential for extracting the tumour region, in preparation for downstream tissue lysis DNA extraction and whole mtDNA sequencing as described in 2.7.1. Optimal RoboLPC laser function settings used for patient 13 are listed in Table 31 below.

	Energy	RoboLPC laser function	Time
Cut	52 nm	20 delta	4ms
Focus	75 nm	5 delta	12 dB analog Gain

Table 31 - Microscopic laser settings used to LCM tumour rich region from patient 13 tumour tissue.

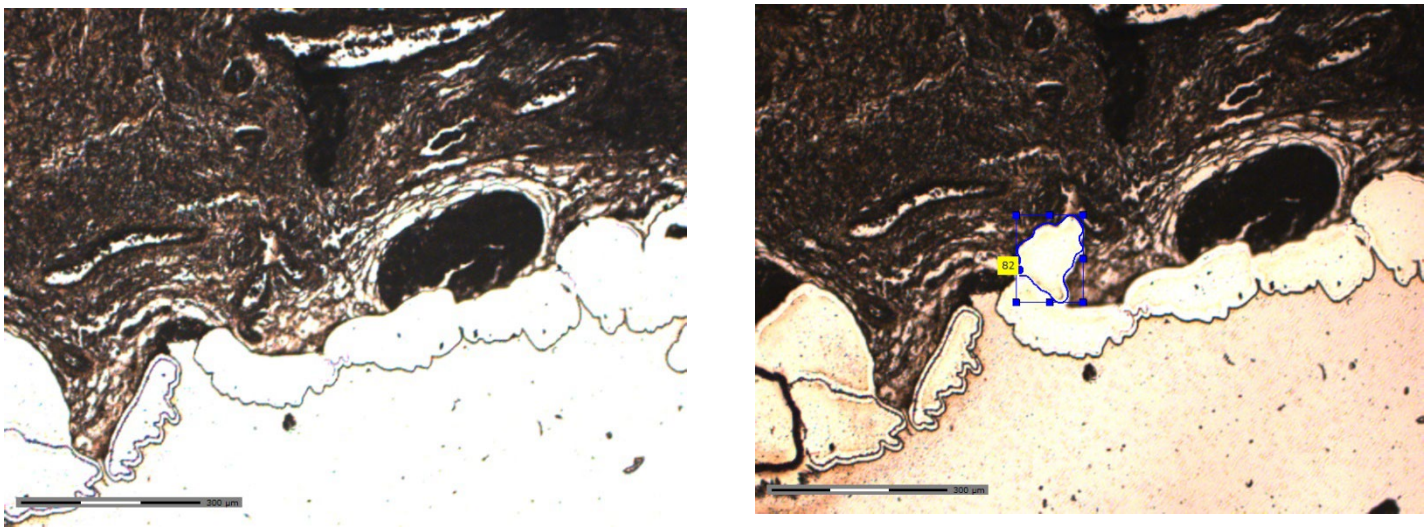

A **B**

Figure 59 - (A) Displays Patient 13 bladder tumour tissue ready to be cut using LCM and (B) displays a particular tumour-rich area of the same bladder tumour tissue cut by LCM (in blue).

A Graph to show m.3284G>A tumour specific mtDNA genotype identified in patient 13 bladder tumour tissue and absent from patients' matched normal urothelium.

Patient 13 Bladder Normal (31 mtDNA Variants identified)					
Chrom	mtDNA Position	Reference	Variant	Level of Heteroplasmy (%)	Quality
mtDNA	73	A	G	97	43367.3
mtDNA	153	A	G	96.7	42798.7
mtDNA	195	T	C	96.8	43226.1
mtDNA	225	GTA	ATG	97.6	43412.7
mtDNA	263	A	G	99.6	45276
mtDNA	310	T	C	4.4	20085
mtDNA	311	-	C	93.9	20085
mtDNA	750	A	G	99.3	44964.1
mtDNA	821	T	C	16.5	3764.92
mtDNA	1438	A	G	99.3	45280.6
mtDNA	1719	G	A	97.4	43461.3
mtDNA	2706	A	G	97.9	44057
mtDNA	3487	CTA	T	0.4	7.49562
mtDNA	4769	A	G	99.9	45742.4
mtDNA	6221	T	C	97.1	42504.8
mtDNA	6371	C	T	96.9	43404.7
mtDNA	7028	C	T	96.7	43270.8
mtDNA	8860	A	G	99.8	45527.4
mtDNA	9966	G	A	97.8	43942
mtDNA	11719	G	A	96.6	43114.4
mtDNA	12705	C	T	98.1	43624.3
mtDNA	13966	A	G	97.3	43330.7
mtDNA	14470	T	C	97.3	43483.2
mtDNA	14766	C	T	98.1	43866.2
mtDNA	15314	G	A	97.4	43669.8
mtDNA	15326	A	G	99.5	45248
mtDNA	16190	-	C	97.4	21852.1
mtDNA	16223	C	T	93.2	40408.5
mtDNA	16255	G	A	97.2	42559.8
mtDNA	16278	C	T	96.3	42904
mtDNA	16519	T	C	99.3	44183.4

Patient 11 Bladder Tumour (31 mtDNA Variants identified)					
Chrom	mtDNA Position	Reference	Variant	Level of Heteroplasmy (%)	Quality
mtDNA	73	A	G	99.6	45472.4
mtDNA	153	A	G	90.6	38759.1
mtDNA	195	T	C	99.4	45404.3
mtDNA	225	GTA	ATG	100	45431.2
mtDNA	263	A	G	99.8	45617.1
mtDNA	309	CT	TC	4.5	20515.1
mtDNA	311	-	C	95	20515.1
mtDNA	750	A	G	99.2	45076.9
mtDNA	1438	A	G	99.1	45072.5
mtDNA	1719	G	A	99.8	45719.8
mtDNA	2706	A	G	99.7	45692.1
mtDNA	3284	G	A	22.3	5716.59
mtDNA	4769	A	G	99.9	45827.9
mtDNA	6221	T	C	99.9	44599.1
mtDNA	6371	C	T	98.7	44804.2
mtDNA	7028	C	T	98.6	44722.9
mtDNA	8860	A	G	99.8	45430.9
mtDNA	9966	G	A	99.9	45791.8
mtDNA	11719	G	A	99	45020.7
mtDNA	12705	C	T	99.9	45159
mtDNA	13966	A	G	99.5	44914.6
mtDNA	14470	T	C	99.8	45466.5
mtDNA	14766	C	T	99.5	45178.1
mtDNA	15314	G	A	99.4	45328.9
mtDNA	15326	A	G	99.5	45330.9
mtDNA	15806	G	A	4.5	526.83
mtDNA	16190	-	C	36.5	5442.19
mtDNA	16223	C	T	97.2	43423.9
mtDNA	16255	G	A	99.8	44886.1
mtDNA	16278	C	T	98.9	44819
mtDNA	16519	T	C	99.6	44778.1

Figure 60- -Tumour-specific mtDNA variants detected in primary bladder benign and tumour from patient 13 post cystectomy mtDNA sequencing data. Tumour-specific pathogenic variant m.3284G>A was identified at 22.3% heteroplasmy level within the patient's bladder tumour, highlighted in yellow above.

A 64-year-old male ex-smoker presented clinically with haematuria and pain on micturition. After TURBT and resection, a 5cm solid bladder tumour was diagnosed and resected. Post resection an invasive High Grade 3 urothelial carcinoma was identified histopathologically and a tumour within the left lateral wall of the bladder was observed. The patient was administered neoadjuvant Cisplatin and Gemcitabine chemotherapy and Bicalutamide monotherapy commenced. Perhaps the patient responded to treatment as only 10% tumour was observed within the bladder tissue, collected post Radical Cystectomy, and whilst this was laser captured and microdissected, a tumour-specific mtDNA variant at position m.3284G>A was detected.

4.6 Discussion

In all the patient bladder tumours I investigated post cystectomy, with high (>80%) tumour content, there was at least one high frequency pathogenic variant identified after Next Generation Sequencing. Setting a threshold of 5% I found a high frequency pathogenic variant in every bladder tumour, the tumour-specific mtDNA variant was a unique variant and some mtDNA variants at lower heteroplasmy were also observed. Overall, relating to the original aims of this chapter investigation, I was interested in mtDNA pathogenic variants in bladder tumours to gain an insight as to whether tumour-specific mtDNA variants were present in

collected bladder tumours from BC patients attending Outpatients following Radical Cystectomy.

Bladder tissue post cystectomy provided a rich resource of abundant fresh tissue material enabling fundamental questions about mitochondrial biology within bladder tumours to be investigated. I found bladder tumours possess a unique mtDNA genotype or barcode, and a unique barcode was identified in ~40% of patients confirming published data.

Published data confirms that mtDNA pathogenic variants are common in NMIBC and tumour specific, therefore absent from cells in the patient's normal bladder lining (Shakhssalim et al., 2013). This is confirmed in our data as all mtDNA variants detected in patient 2: m.10404T>C, patient 4: m.4841G>A, m.5032G>A, m.16147C>T, patient 10: m.1180T>C, patient 11 m.9098T>C and patient 13 m.3284G>A are absent from the patients' normal urothelium and therefore tumour specific.

m.10404T>C detected in patient 2 bladder tumour tissue is situated on a gene MT-ND3 coding for subunit ND3 of complex I (NADH dehydrogenase), which is crucial for the transfer of electrons from NADH to the respiratory chain. Mitochondrial variants m.4841G>A and m.5032G>A identified in patient 4 primarily sit within the ND2 gene also affecting the complex I subunit of the oxidative phosphorylation system. A review of mtDNA pathogenic variants across BC studies found that mutations occur throughout the whole mtDNA genome, arise more frequently in complexes 1 and 4, and a potential explanation for this is that most mitochondrial base pairs cover these complexes (Swalwell et al., 2011).

Complex 1 is the first enzyme of the respiratory chain and is involved in the first step of the Electron Transport Chain process, the transfer of electrons from NADH to Ubiquinone (Riaz et al., 2016). Two electrons reduce ubiquinone to ubiquinol and defects of the mitochondrial respiratory chain may be caused by mutations in mtDNA (Swalwell et al., 2011). In mitochondrial disorders complex I deficiency is the most common enzyme defect in mitochondrial disorders. As mtDNA pathogenic variants accumulate, such transformations may be due to the accumulation of mtDNA in ageing cells (Greaves et al., 2014). Patient 2 was a 54-year-old male with a histological diagnosis of early invasive high grade 2 NMIBC and tumorigenesis can potentially be promoted and observed in this patient due to increased oxidative stress as a result of ETC dysfunction (Vyas et al., 2016). Complex I also plays a vital

role in energy metabolism (Robert W. Taylor & Turnbull, 2005) as such the bladder requires high energy requirements to contract and relax.

m.10404T>C detected in patient 2 affects the ND3 gene and produces a non-synonymous amino acid change due to the nucleotide change T-C. This is a missense variant, substitution within the protein-coding region. After whole-exome sequencing, m.10404T>C has been previously described to be involved with Ovarian Serous Cystadenocarcinoma and published in the Catalogue of Somatic Mutations in Cancer.

Point mutations, DNA duplication, deletion, or inversion are the main contributor to primary mtDNA diseases. Such mutations have a direct impact on the deregulation of OXPHOS function and encourage tumour growth. OXPHOS disorders exhibit respiratory chain deficiency displaying reduced enzymatic function in the respiratory chain complexes thus resulting in reduced ATP synthesis and oxygen consumption. Dysfunction in OXPHOS is reported to contribute to activating the AKT cell survival pathway. Activation of this pathway is driven by NADH resulting in the downregulation of apoptosis (Sun & St. John, 2016). This complements previous findings within human colonic crypts, where identified respiratory chain defects correlate with reduced complex subunit expression (Greaves et al., 2010).

With cancerous cells, however, it is recently reported that a normal amount of OXPHOS function is essential for optimal tumour viability conditions (Suzuki et al., 2011) suggestive of a functional impact relating to mtDNA pathogenic variants. This is directly relatable to our data where tumour-specific mtDNA are identified in patients 2, 4, 10, 11, and 13 with >80% tumour content.

Due to the oxidative microenvironment of mitochondria, mtDNA is vulnerable to oxidative damage from reactive oxygen species. Influencers are the proximity of mitochondria to the ETC, the lack of protective histones in the mtDNA, and the limited efficiency of the mtDNA repair mechanisms compared to nuclear DNA. A lack of protective histones and limited repair mechanisms enhance susceptibility to changes in mtDNA sequences (Suzuki et al., 2011). Although nucleoid composition may affect this, the mtDNA pathogenic variant rate is estimated at 5-50 x higher than nuclear DNA (Li et al., 2010). A high mtDNA mutation rate creates heteroplasmy and the process of cell division causes random segregation of both mutant and wild-type mtDNA (Blokzijl et al., 2016).

MtDNA pathogenic variants can act as single base pair variants and contribute to mtDNA population variability as mitochondrial nuclear transfers in the germline lineage cause pseudogenes, known as NUMTS (nuclear DNA sequences of mitochondrial origin) (Hazkani-Covo et al., 2010). Scientific evidence of nuclear DNA sequences of mitochondrial origin is known to accumulate through human evolution. Non-protein altering variants are more common. MtDNA deletions are associated with disease and these can be single often large-scale mtDNA deletions or multiple, usually smaller mtDNA deletions (Kirches, 2017).

Understanding somatic mutations in malignant tissues accelerate our understanding of how variants contribute to ageing. From our data, the detection of somatic mutations within cancerous material represents the expansion of a single cell as tissues are heterogeneous. Urothelial cancer cells are composed of multiple cell types, are sub-grouped into classes with basal, luminal, and p53-like characteristics, and although the transitional makeup of urothelial cells is simple in their composition they are heterogeneous genetically (Hedegaard et al., 2016).

Ageing leads to mitochondrial pathogenic variants which may lead to mitochondrial dysfunction.

DNA is transcribed into RNA which is translated to protein subunits and these subunits may come together to form complexes in the ETC and result in mitochondrial function. Nevertheless, if there are mtDNA pathogenic variants or alterations in downstream gene expression, this results in loss of core subunits and loss of complex stability resulting in eventual degradation of these unstable protein subunits affecting complexes and eventually functionally resulting in mtDNA dysfunction. This is observed within the mtDNA variants m.10404T>C identified in patient 2 and m.4841G>A detected in patient 4 affecting Complex 1 Respiratory Chain enzyme within bladder tumours, as presented in Table 32.

Patient	Variant	Gene	Locus	Respiratory Chain Enzyme	Locus Type	Amino acid change	Pathogenicity
2	m.10404T>C	ND3	MT-ND3	Complex I	Coding Sequence 1	Non-synonymous NADH dehydrogenase subunit 3 Stop → Gln, aa position 116	None
4	m.4841G>A m.5032G>A m.16147C>T	ND2 ND2 HVS1	MT-ND2 MT-ND2 MT-HV1	Complex I Complex I D-Loop	Coding Sequence 3	Synonymous L-L aa position 124	None
10	m.1180T>C	rRNA	MT-RNR1	12s rRNA	Coding for 12S ribosomal RNA	T-G identified on rRNA	None
11	m.9098T>C	ATP6	MT-ATP6	Complex V	Coding Sequence 2	L-T	Pathogenic
13	m.3284G>A	MT-TL1	MT-TL1	tRNA-LeuUUR	tRNA	LeuUUR	Low - Likely polymorphic
15	m..6052A>G	ND4	MT-CO1	Complex IV	Coding Sequence 2	Non-synonymous Asn → Ser	Low - Likely polymorphic

Table 32 - A Table to show tumour-specific mtDNA genotypes identified from patients from the Radical Cystectomy cohort in protein encoded genes. The mitochondrial gene in each tumour-specific pathogenic variant was identified in, the respiratory chain enzyme, amino acid change, and pathogenicity are all listed above.

The above table demonstrates bladder tumours do possess a unique genotype as mtDNA variants detected were absent from the patients' normal urothelium and identified in bladder tumours. Such highlights that mtDNA variants within this BC patient cohort are tumour-specific, suggesting a tumour-specific mark can be used as a baseline to lineage trace founder tumours in matched non-invasive patient material such as urine. As most patients clinically presented with haematuria, urine a non-invasive matched sample can be used to confirm the presence of these mtDNA variants.

mtDNA pathogenic variants

Colorectal cell lines and mtDNA pathogenic variants investigated by Vogelstein., *et al.,* found most mutations were somatic and homoplasmic (Polyak et al., 1998). Due to the diversity of the mitochondrial genome and the heterogeneity of mtDNA, the presence of a mtDNA pathogenic variant may assist in detecting tumour recurrence (He et al., 2010).

There were particular patients within the cohort I was interested in investigating further where residual tumour was visible within the bladder biopsy material at cystectomy, and after mtDNA sequencing, tumour-specific mtDNA variants were identified. I then went back to the original TURBT sample to map these pathogenic variants and determine if they were originally present after BC diagnosis (see Chapter 6). With the high 40% recurrence rates BC carries, the presence of tumour-specific mtDNA pathogenic variants detected in patients 2, 4, 10, 11, and 13 may highlight recurrence or presence of tumour within the clinical setting, as seen in Tables 29 and 30. NMIBC patients may achieve a complete response to neoadjuvant chemotherapy with little or no disease remaining, which may provide an explanation for tumour-specific mtDNA variants that were not detected in patient 1 despite a high tumour content (80%) visible in the bladder tumour sample.

Some evidence from a mutational level comes from studies where mtDNA pathogenic variants in prostate cancer were found to accumulate with advancing age and also observed to be associated with the nuclear genomic features of aggressive prostate cancer (McCrow et al., 2016). Some genes may be associated with a more favourable long-term outcome compared with other genes that may be associated with a more unfavourable outcome however a large number of these identified mutations were polymorphic variants, in non-coding regions with a small number of pathogenic mutations, similar to the above findings within the BC cohort. In the future with additional research downstream it would be insightful to determine the functionality of identified genes on a transcriptomic level.

Mitochondrial dysfunction plays several distinct roles in cancer (Schon et al., 2012). Respiratory functions occurring in the mitochondria may be compromised, NADH and pyruvate accumulating in the cytosol, and excess cytosolic pyruvate converted to lactate by lactate-dehydrogenase explaining the increased lactic acid found in many patients with mitochondrial diseases, particularly children. This facilitates tumour growth as tumours

suppress mitochondrial dysfunction in favour of increased secretion of lactate and uptake of glucose (Stefano & Kream, 2015).

Ishikawa *et al.* confirmed mtDNA dysfunction results in the overproduction of ROS affecting the ETC, which contributes to tumour cell metastasis (Ishikawa et al., 2008). ROS is produced at low levels during normal mitochondrial respiratory chain function and causes the development of somatic variants in mtDNA as reported by (Harman, 1992). The theory of ageing was extensively described in which mitochondria have a key role. Such mutations can impair the function of the respiratory chain, resulting in increased ROS production, thus the accumulation of more mitochondrial pathogenic variants. Particular pathogenic mitochondrial variants, for example, 8993T>G, lead to increased ROS production (Robert W. Taylor & Turnbull, 2005). ROS is known to be the source of oxidative impairment during ageing, subsequently affecting apoptosis, replicative senescence, and energy reduction all contributing to a loss of tissue and cellular function.

The flexibility that mitochondria confer to tumour cells, including alterations in fuel utilization, bioenergetics, cell death susceptibility, and oxidative stress, equally allows for survival in adverse environmental conditions such as starvation and during chemotherapeutic and targeted cancer treatments (Vyas et al., 2016).

As mitochondria have a separate genome to the human hg38, this adds to the unique complex biology of this organelle, as variants in mtDNA impact tumorigenesis. In addition to distinct mtDNA haplotypes that exist among different human populations, many germline and somatic mtDNA variants associated with cancer risk have been identified (van Gisbergen *et al.,* 2015). MtDNA inheritance is uniparental and although the functional consequence of many of these alterations is not well understood, some mutations occur in ETC genes and can result in increased oxidative stress due to ETC dysfunction to promote tumorigenesis.

This implies bladder tumours have a decreased dependence on mitochondrial metabolism to proliferate, directing mitochondrial therapies at enabling passenger mutations in genes such as DNA polymerase gamma needed for mtDNA copy number maintenance (Kamat et al., 2017).

Aerobic glycolysis-dependent metabolism is the primary energy source required for cellular growth and proliferation. Bladder cancer cells have been found to exhibit an increased

expression of genes coding for both glycolysis and the pentose phosphate pathway highlighting the robust role glycogen metabolism pathways play in BC development (Massari et al., 2016).

4.7 Conclusion

The hypothesis 'naturally occurring mtDNA pathogenic variants stochastically accumulate in normal ageing cells' has been confirmed after performing whole mtDNA genome sequencing on patient bladder tissue and it has been established that bladder tumours possess a unique mtDNA genotype. If these ageing cells become transformed, these mutations serve as inherent lineage tracing tumour-specific marks as seen with the tumour-specific mtDNA pathogenic variants identified in the BC patient cohort data above. Genome mtDNA sequencing of voided bladder cancer cells has defined the presenting index lesion and allows lineage tracing. As such, lineage tracing within accessible matched non-invasive patient samples such as urine can confirm tumour clearance and clonal recurrence.

Urinary mtDNA, presents a new concept in which longitudinal lineage tracing of specific mutational marks from the founder tumour afford excellent diagnostic performance and a unique translational opportunity as there are no bladder urinary biomarkers in routine clinical use. I now have a method of undertaking biomarker assessment to detect either macroscopic residual disease or early growth from the presentation of microscopic residual disease. This technique would transform clinical practice by confirming Bladder Cancer recurrence and relieving the reliance on surveillance cystoscopy. Non-invasive longitudinal urinary mtDNA analysis will aid diagnostic performance for quality assurance in complete tumour resection and, or non-invasive detection of early Bladder Cancer recurrence. I can conclude there may be various factors which influence the presence of tumour-specific mtDNA pathogenic variants including:

- Dwell time of urine in the bladder
- The size of tumour
- Whether the tumour has expanded deeper into the tumour

In the next chapter, I analysed matched patient urine samples from the BC patient cohort to confirm lineage tracing from founder bladder tumours.

Chapter 5: Is urine a valuable diagnostic tool for lineage tracing tumour-specific mtDNA genotypes detected in primary bladder tumours?

5.1 Urine has immediate contact with bladder tumours

In this chapter, I discussed the co-implementation of a diagnostic urine test in urology outpatients' settings and demonstrate that non-invasive liquid biopsy approaches are valuable tools for urological malignancy surveillance. Bladder Cancer patients require a non-invasive method of examination as undergoing a urine test is less painful than cystoscopy, consequently, I explored the cellular and non-cellular urine samples from the Bladder Cancer cohort. As urine has immediate contact with bladder tumours, an abundance of tumour derived material was investigated to understand the mtDNA pathogenic variant complexity of Bladder Cancer and aided as a non-invasive resource of bladder tumour material (Satyal et al., 2019). Tumours can be examined in a non-intrusive and inexpensive manner reducing the dependence on tumour monitoring, which is often painful for the patient (Kamat et al., 2014). The BC patient population expressed the requirement and personal importance of reducing discomfort experienced during a routine cystoscopic examination. Ultimately wider circles would benefit including the NHS and society, due to projected savings if a centralised mtDNA sequencing service were to be employed.

5.2 mtDNA genomic profile of Bladder Tumour material within urine

The genomic profile of bladder tumour biopsies has been informative in providing an understanding of the molecular basis of Bladder Cancer. Tumour-specific mtDNA genotypes were identified in fresh bladder tissue from patients undergoing Radical Cystectomy providing an index characterisation of the tumour's mtDNA for voided urine analyses. Urine is an abundant source of bladder tumour material, and the purpose of this investigation was to identify exclusive genetic signatures using the detection of frequently occurring molecular events within mtDNA in urine. Matched urine samples from the Bladder Cancer patient cohort were provided at the time of cystoscopy and I investigated whether the same tumour-specific genotypes were detectable in matched patients' cellular and cell-free urine compartments. genomic profile of bladder tumour biopsies has been informative in providing an understanding of the molecular basis of Bladder Cancer. Tumour-specific mtDNA genotypes were identified in fresh bladder tissue from patients undergoing Radical Cystectomy providing

an index characterisation of the tumour's mtDNA for voided urine analyses. Urine is an abundant source of bladder tumour material, and the purpose of this investigation was to identify exclusive genetic signatures by means of detection of frequently occurring molecular events within mtDNA in urine. Matched urine samples from the Bladder Cancer patient cohort were provided at the time of cystoscopy and I investigated whether the same tumour-specific genotypes were detectable in matched patients' cellular and cell-free urine compartments.

5.3 Sample collection

With approval from Newcastle Upton Tyne NHS trusts ethics committee, ethics were in place as described in Appendix B and approximately 15ml urine samples were received from six NMIBC patients undergoing Robotic Cystectomy within the Urology department at Freeman Hospital, Newcastle, UK. I undertook mtDNA sequencing within previously frozen matched patients' cellular and non-cellular urine samples (described in section 2.9.5). From each of the six patients I had previously detected tumour-specific mtDNA variants within their distinct bladder tumour biopsy, specific regions of the mtDNA genome (described in section 2.9), were sequenced by Next Generation Sequencing. Additionally, matched blood samples, ~7 ml for each patient, were also received, and mtDNA sequencing was undertaken, which provided a suitable control sample for germline assessment.

5.4 Aim

This analysis aimed to detect tumour-specific mtDNA genotypes within cellular and cell-free urine compartments. This would enable the detection of mtDNA pathogenic variants in patients presenting with residual disease at cystectomy and identify BC recurrence for longitudinal lineage tracing within patients with recurrent disease.

The exploration of mtDNA dysfunction by identification of mtDNA pathogenic variants present within cellular and cell-free urine compartments was interesting to investigate further. Cell-free urine compartments comprise of fragmented urothelial tumour nucleic acids and cellular urine contains exfoliated benign and malignant urothelial cells (Satyal et al., 2019), providing a non-invasive paradigm for Bladder Cancer surveillance. It was interesting to discover whether previously identified mtDNA pathological variants were also detected in the cellular and cell-free urine compartments.

cfDNA mtDNA within urine has a higher tumour genome burden and allows greater detection (90%) of key nuclear genomic biomarkers than the intact cellular fraction (61%) (Togneri et al., 2016). As published data has not confirmed if the detection of mtDNA in urine shadows comparable features, it was interesting to investigate both cellular and cell-free urine compartments.

5.5 Objectives

1) Reliably extract high quality genomic DNA from cellular and cell-free compartments of matched patients' urine from the Robotic Cystectomy Bladder Cancer patient cohort.
2) Amplify the mitochondrial genome within the cellular and cell-free compartments of matched patients' urine.
3) Evaluate index tumour-specific mtDNA genotypes in the cellular and cell-free compartments of matched patients' urine.

5.6 Methodology

Urine samples were processed and separated by centrifugation into cellular and cell-free compartments (as described in section 2.6.2 Urine Supernatant and Urine Cell Pellet Preparation). Genomic DNA was extracted from each derivative (detailed in section 2.7). Urine sample DNA was extracted and eluted in 50 µL AE buffer. After quantifying DNA (according to section 2.8 DNA quantification), long range mtDNA PCR amplicons (~4kb) were amplified (as described in section 2.9.1). Long Range PCR using five overlapping oligonucleotide primer pair sets was utilised for Next Generation Sequencing. To confirm mtDNA amplification, 0.7% agarose gels were prepared and ran for 90 minutes at 65V (as described in section 2.9.7 Gel Electrophoresis). Amplicons were purified (according to section 2.10) and libraries requiring fragmentation were prepared (detailed in section 2.11).

Separately, 1:20 EpCAM, 1:50 CD49f, and 1:200 Uroplakin Ib dilutions were prepared (as described in section 2.3) in previously frozen patients' cellular urine and examined on the flow cytometer for analysis. Cellular urine distinguished diverse types of epithelial, urothelial, and basal cells of interest. This investigation attempted to identify molecular subtypes within each patient's cellular urine samples following Robotic Cystectomy.

5.7 The analysis of mtDNA pathogenic variants in circulating free and cellular urine

As I previously outlined, once I had separated urine by centrifugation into separate cell-free and cellular compartments, genomic DNA was extracted and the whole mtDNA genome was amplified by long range PCR for Next Generation Sequencing. Figure 61 below displays the laboratory workflow undertaken for the processing of urine samples received from patients undergoing Radical Cystectomy.

A diagram to outline the laboratory workflow undertaken for patient urine sample processing from the Radical Cystectomy cohort.

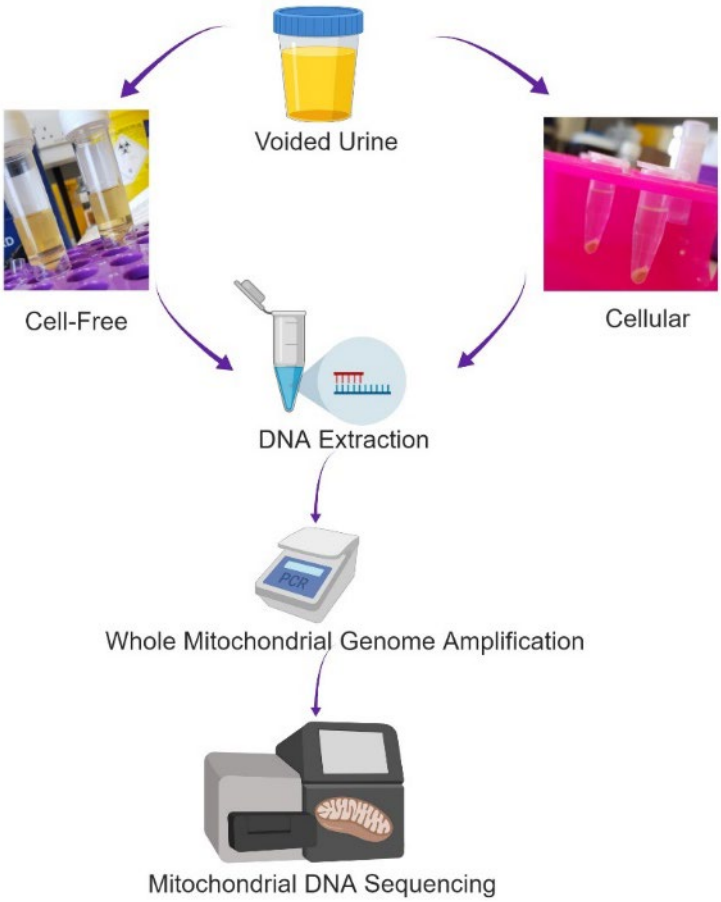

Figure 61 - Urine sample processing. Urine was separated by centrifugation into cellular and cell-free urine compartments. Genomic DNA was extracted from each urine compartment. The whole mtDNA genome was amplified by long range PCR, using five overlapping primer pairs for downstream application of Whole Genome mtDNA Sequencing (see section 2.9.2).

5.7.1 The analysis of mtDNA pathogenic variants as circulating free DNA in Blood as a reference for germline

Blood was separated by centrifugation into plasma, buffy coat, and red blood cells (as described in section 2.6.3 Buffy Coat sample preparation). From the buffy coat, DNA was extracted, quantified, (according to 2.7 DNA quantification) and long range mtDNA PCR amplicons (~9kb) were generated using five primer pairs (described in section 2.9.1 Long Range PCR). Libraries were prepared using amplified mtDNA amplicons for whole mtDNA genome sequencing (as detailed in section 2.11).

A diagram to outline the laboratory workflow performed for patient blood sample processing from the Radical Cystectomy Bladder Cancer cohort.

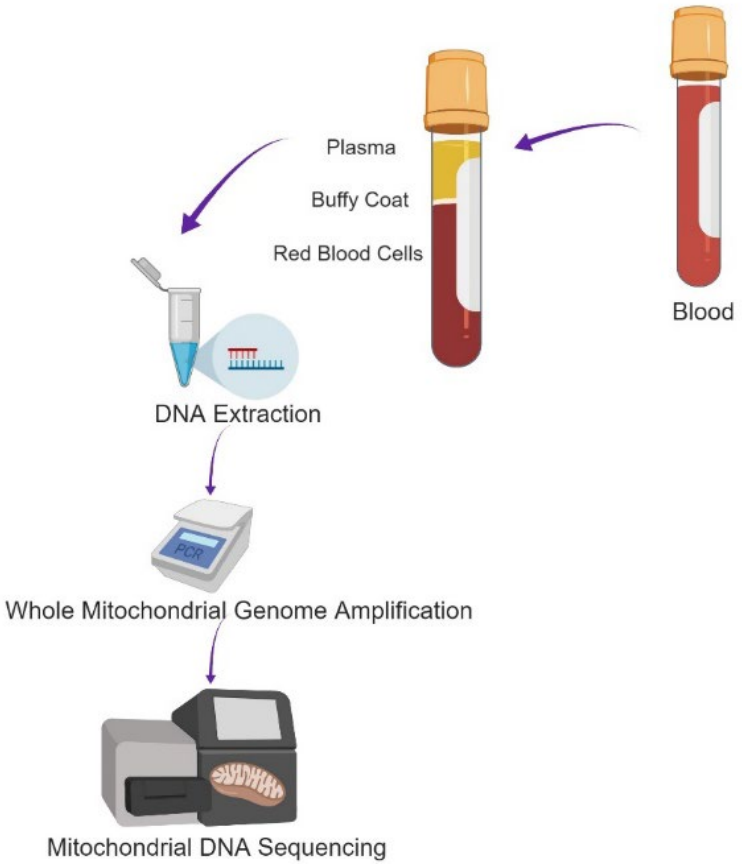

Figure 62 - A diagram to display blood sample processing laboratory workflow. Blood was centrifuged and separated into plasma, Buffy Coat, and red blood cells. The Buffy Coat compartment was utilised for whole DNA extraction and subsequent mtDNA sequencing.

Blood was separated by centrifugation into plasma, Buffy Coat, and red blood cells (detailed in section 2.6.3). Genomic DNA was extracted from the Buffy Coat sample (described in section 2.7). The mtDNA genome was amplified by long range PCR, using five overlapping primer pairs (see section 2.9.2) in preparation for downstream application of Next Generation Sequencing.

5.8 Results

5.8.1 Patient clinical parameter assessment

An assessment of clinical parameters including the presence of haematuria, Bladder Cancer stage, grade, morphology, and smoking status was evaluated from patients within the Bladder Cancer cohort undergoing Radical Cystectomy at Freeman Hospital, Newcastle, UK. Such clinical information provided an overview of individual patients' clinical factors.

A colour spectrum displaying patient clinical parameters from the Bladder Cancer cohort undergoing Radical Cystectomy at Freeman Hospital, Newcastle, UK.

Patient	Presence of Haematuria	Bladder Tumour Stage	Bladder Tumour Grade	Morphological assessment
2	**Yes**	pTis	High	CIS
4	**Yes**	pT2	High	Detrusor Muscle Involvement
10	**Yes**	pTis	Low	Papillary
11	**Yes**	pTis	High	Detrusor Muscle Involvement
13	**Yes**	pT2	High	Detrusor Muscle Involvement
15	**Yes**	pT2	High	Detrusor Muscle Involvement

Figure 63 - - Colour spectrum detailing clinical parameters of patients from the Bladder Cancer cohort undergoing Radical Cystectomy at Freeman Hospital, Newcastle, UK. A bladder tumour biopsy, normal urothelium biopsy, urine, and blood samples were obtained for *analysis for this research project, post Cystectomy.*

5.8.2 Urine sample and Buffy Coat DNA Extraction

High quality genomic DNA was extracted from 1ml Buffy Coat, 5ml cellular and 5ml cell-free compartments of matched patients' urine from the Robotic Cystectomy Bladder Cancer patient cohort (as described in section 2.7). DNA quality was measured (see section 2.8), DNA samples were used to create a PCR mastermix for mtDNA amplification (detailed in section 2.12.5) and confirm the presence of mtDNA genotypes. A minimum of 1 µl DNA was required in each mastermix PCR reaction, where nucleic acid extracted amounts provided low readings such as within patient 2 cell-free urine, I ensured the minimum of 1 µl DNA was applied for each reaction.

Patient	Sample	260/280	260/230	Nucleic Acid amount (ng/µl)
2	1ml Cellular urine	1.82	2.28	**447.64**
	1ml Cell-free urine	-0.35	0.35	**0.28**
	500 µl Buffy Coat	0.92	0.22	**65.24**
4	1ml Cellular urine	1.85	0.27	**1.01**
	5ml Cell-free urine	0.96	0.57	**12.45**
	500 µl Buffy Coat	1.09	0.26	**72.41**
10	1 ml Cellular urine	1.85	3.77	**151.05**
	5 ml Cell-free urine	2.01	2.44	**81.51**
	500 µl Buffy Coat	1.94	1.66	**39.75**
11	2 ml Cellular urine	1.89	2.37	**522.07**
	1ml Cell-free urine	0.81	-0.48	**0.48**
	500 µl Buffy Coat	1.71	1.43	**35.06**
13	1ml Cellular urine	1.85	2.36	**3.78**
	5ml Cell-free urine	1.91	2.58	**77.62**
	500 µl Buffy Coat	1.88	2.32	**43.12**
15	1ml Cellular urine	1.93	2.45	**18.84**
	1ml Cell-free urine	1.82	1.65	**0.92**
	250 µl Buffy Coat	1.97	1.93	**23.86**

Table 33 - A Table displaying nucleic acid amount and quality in six patients Buffy Coat, cellular and cell-free urine samples.

5.8.3 mtDNA genome amplification within cellular and cell-free compartments of matched patient 2 urine.

Having sequenced the whole mtDNA genome m.10404T>C tumour-specific mtDNA variant was detected in patient 2's bladder tumour biopsy and was absent from the patients' normal urothelium. The following matched samples: Urine cell pellet, Urine cell-free and Buffy Coat from blood underwent genomic DNA extraction, with mtDNA amplification in smaller fragments of ~ 4,000bp. The entire mitochondrial genome was sequenced by Next Generation Sequencing to identify pathogenic variant m.10404T>C and detect additional mtDNA genotypes.

Visualisation of whole mitochondrial genome amplification within the Buffy Coat, urine supernatant, urine cell pellet, bladder tumour, and bladder samples from patient 2 were displayed in Figure 64. The electrophoresis gel was prepared and imaged as detailed in section 2.9.7. Lane 1 was loaded with 5 µl 1Kb DNA ladder, lane 2 represented mtDNA amplified within nucleotide positions m.323-3574, lane 3 characterised mtDNA amplified within nucleotide positions m.3017-6944, lane 3 displayed mtDNA amplified within nucleotide positions m.6358-10147, lane 4 exhibited mtDNA amplified within nucleotide positions m.39607-13859, lane 5 presented mtDNA amplified within nucleotide positions m.9607-13859, lane 6 offered mtDNA amplified within nucleotide positions m.1365-771, lane 7 reflected the negative control and lane 8 the positive control.

Whole mitochondrial genome amplification from patient 2 Buffy Coat, urine supernatant, urine cell pellet, bladder tumour, and bladder normal DNA samples.

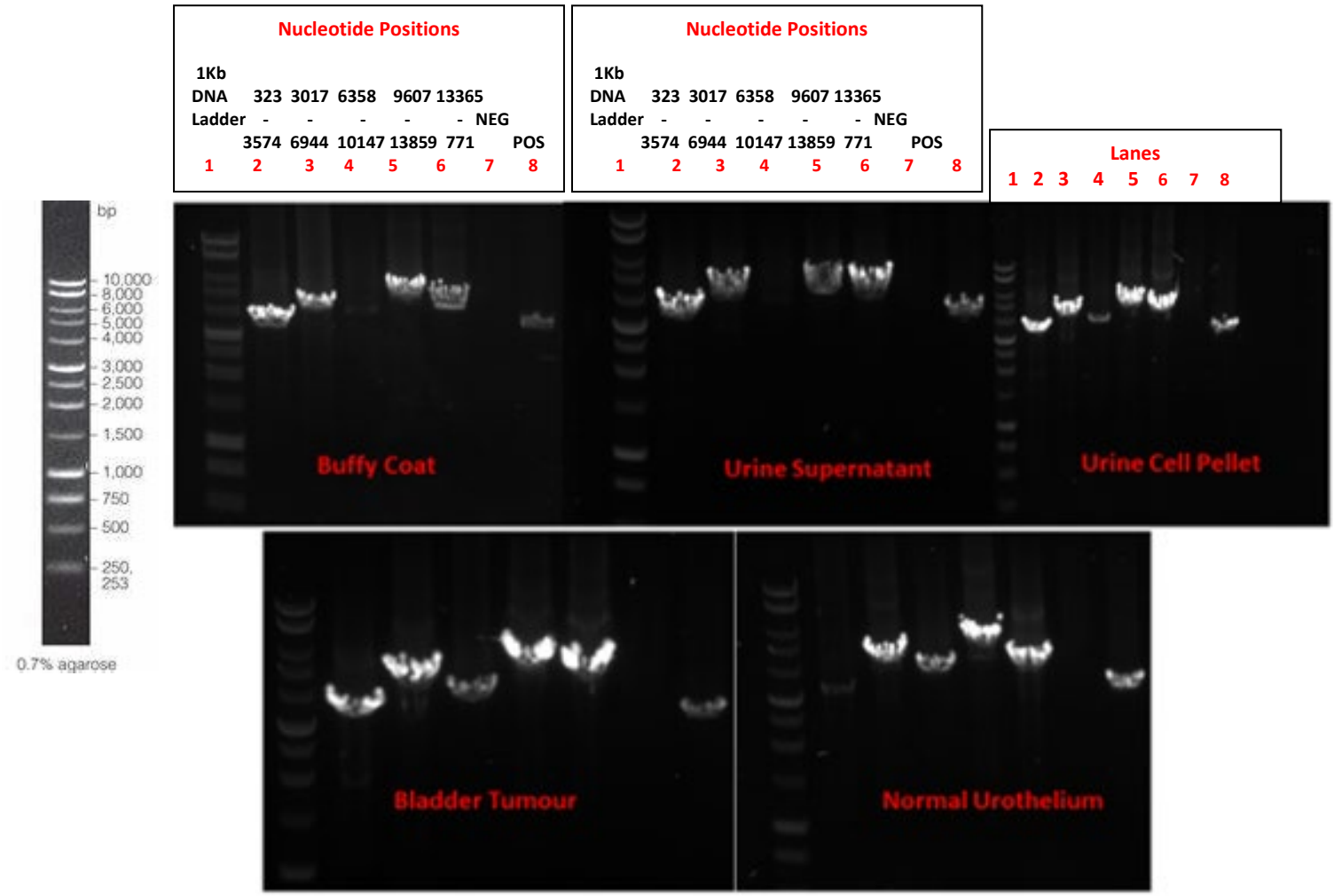

Figure 64 - Whole mitochondrial genome amplification using five overlapping primer pairs in patient 2 Buffy Coat, Urine supernatant, Urine Cell pellet, Bladder Tumour, and Bladder normal biopsies. A 1kbp DNA ladder was used to determine the size of generated target amplicons, negative control with no DNA within the mastermix (NEG) and positive control of known mtDNA amplified DNA (POS) were used when loading each patient sample. In the areas of the mitochondrial genome amplified weakly or did not appear to amplify (Buffy Coat Lane 4, Urine supernatant lane 4, normal urothelium lane 1), these specific regions were re-amplified with more than 1 µl DNA added to the mastermix.

5.8.4 mtDNA genome amplification within cellular and cell-free compartments of matched patient 4 urine.

Three tumour-specific pathogenic variants 4841G>A, m.5032G>A, m.16147C>T were detected in patient 4 bladder tumour biopsy and each mtDNA genotype was absent from the patients' normal urothelium. The following matched samples: urine cell pellet, urine cell-free and Buffy Coat from blood underwent genomic DNA extraction. After mtDNA amplification in smaller fragments of ~ 4,000bp, the entire mitochondrial genome was sequenced by Next Generation Sequencing.

Whole mitochondrial genome amplification from patient 4 buffy coat, urine supernatant, urine cell pellet, bladder tumour, and bladder normal DNA samples after Cystectomy.

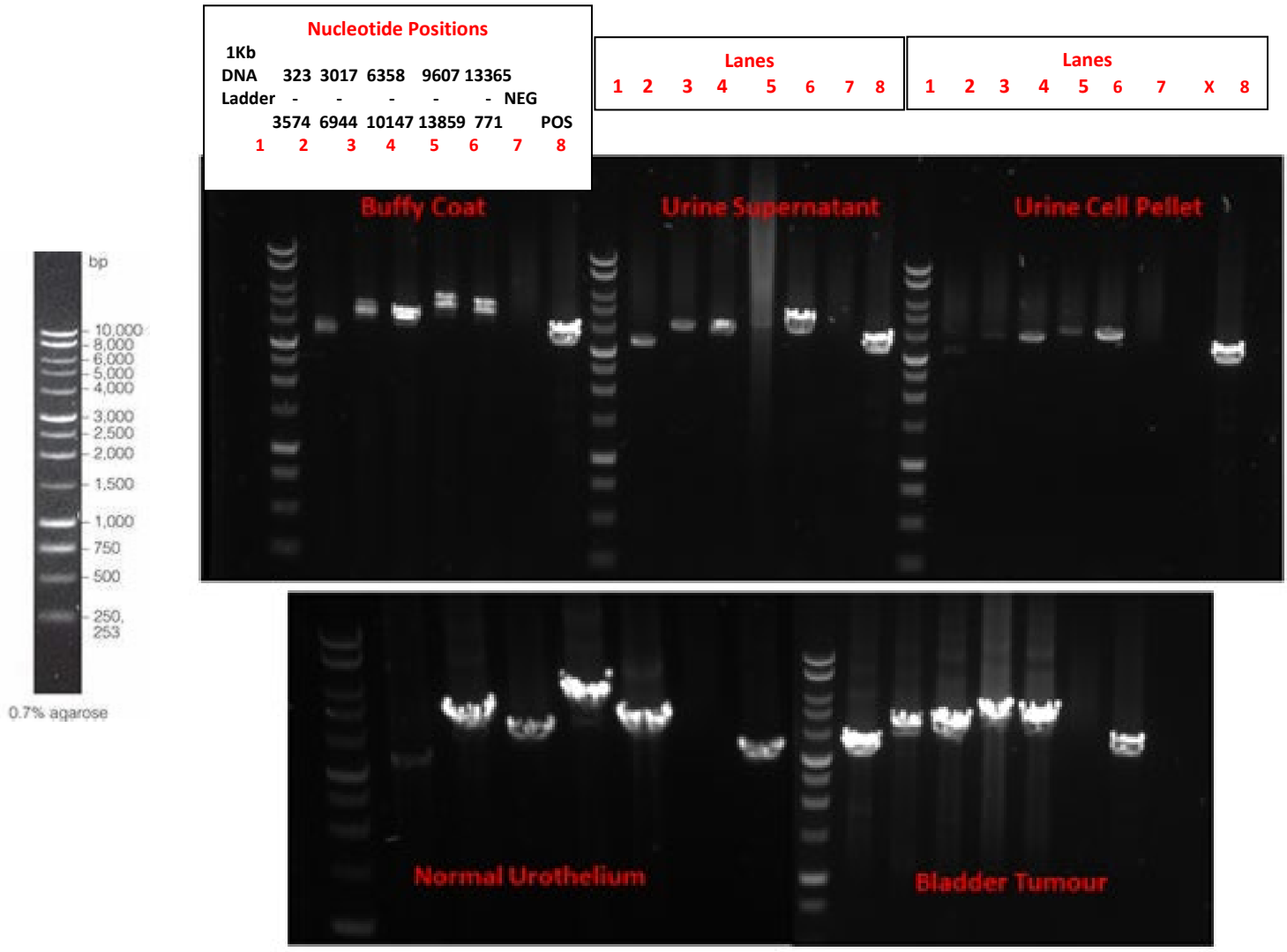

Figure 65 - Whole mitochondrial genome amplification using five overlapping primer pairs in patient 4 Buffy Coat, Urine supernatant, Urine Cell pellet, Bladder Tumour, and Bladder normal biopsies. X indicates no sample was loaded in this well. In the areas of the mitochondrial genome that amplified weakly or did not appear (Urine supernatant lane 4 and Urine cell pellet lanes 2 and 3), these specific regions were re-amplified and more than 1 µl DNA was added to the mastermix.

mtDNA amplification was repeated for each of the six patients where a tumour-specific mtDNA genotype was previously identified within their bladder tumour. Libraries were prepared on cellular and cell-free urine samples for mtDNA sequencing, additionally, Buffy coat was also sequenced for germline assessment.

5.8.5 mtDNA genotypes detected in patient 2 founder bladder tumour and normal biopsy, urine cellular and cell-free and Buffy Coat samples following Radical Cystectomy.

After mtDNA sequencing, I found pathogenic variant m.10404T>C within the founder bladder tumour. The presence of this tumour-specific mtDNA variant was also identified in the matched patients' cellular urine pellet, confirming the mtDNA alteration within non-invasive urine material is traceable. In terms of heteroplasmy levels, some variations occurred, however, it was consistent within the urine cell pellet and founder bladder tumour. m.10404T>C was detected at 90% in the patients' founder bladder tumour and the mtDNA genotype was confirmed in both the cellular urine compartment at 90% heteroplasmy level and 5% in the cell-free urine compartment (highlighted in yellow in Figure 66).

Additional mtDNA variants identified within the cellular urine were mtDNA pathogenic variants m.14582A>G at 100% heteroplasmy and m. 15524A>G at 9.5% heteroplasmy. The presence of germline mtDNA genotype m.13860CAA>GGT at 100% was observed within the Buffy Coat sample as highlighted in green. mtDNA variants specifically: m.14930G>A at 90.4% heteroplasmy was only observed within the bladder tumour biopsy and not identified in other matched patient samples.

Heteroplasmy levels of all mtDNA genotypes identified in patient 2 founder bladder tumour and normal biopsy, urine cellular and cell-free and Buffy Coat samples following Radical Cystectomy.

Patient 2 Tumour				Patient 2 Normal				Patient 2 Urine Cell Pellet				Patient 2 Urine Supernatant				Patient 2 Buffy Coat			
mtDNA Position	Reference	Variant	Heteroplasmy (%)	mtDNA Position	Reference	Variant	Heteroplasmy (%)	mtDNA Position	Reference	Variant	Heteroplasmy (%)	mtDNA Position	Reference	Variant	Heteroplasmy (%)	mtDNA Position	Reference	Variant	Heteroplasmy (%)
73	A	G	99.9	73	A	G	99.7												
								152	T	C	90.9								
153	A	G	99.9	153	A	G	99.4												
195	T	C	99.7	195	T	C	99.4												
								211	A	G	8.3								
225	GT	AC	100	225	GT	AC	99.6												
263	A	G	99.8	263	A	G	100	263	A	G	100								
311	-	C	97																
303	C	-	3																
								514	CA	-	100								
750	A	G	99.8	750	A	G	99.9	750	A	G	95.5								
1438	A	G	99.8	1438	A	G	99.8	1438	A	G	100								
								2880	A	G	22.2								
1719	G	A	99.7	1719	G	A	99.7												
								3243	A	G	64.3								
								3992	C	T	100								
2706	A	G	99.9	2706	A	G	99.4												
								4024	A	G	100								
4769	A	G	100	4769	A	G	99.8	4769	A	G	85.7								
								5004	T	C	81.8								
								5539	A	G	22.2								
6221	T	C	99.7	6221	T	C	99.3												
6371	C	T	99.1	6371	C	T	98.3												
7028	C	T	99.5	7028	C	T	99	8269	G	A	92.9								
8393	C	T	94.5	8393	C	T	92.7												
8860	A	G	99.9	8860	A	G	99.9	8860	A	G	100								
								9123	G	A	100								
												9595	C	G	100	9595	C	G	100
10404	T	C	90.1					10404	T	C	89.5	10404	T	C	4.9				
10532	A	G	99.9	10532	A	G	99.8	10532	A	G	98.8	10532	A	G	99.9	10532	A	G	99.1
11719	G	A	99.8	11719	G	A	99.7	11719	G	A	99.4	11719	G	A	99.8	11719	G	A	99.7
12705	C	T	99.7	12705	C	T	99.7	12705	C	T	99	12705	C	T	99.9	12705	C	T	99.2
																13230	C	A	2.9
13251	C	T	99.8	13251	C	T	99.7	13251	C	T	99.5	13251	C	T	100	13251	C	T	99.8
13708	G	A	99.8	13708	G	A	99.8	13708	G	A	99.7	13708	G	A	99.7	13708	G	A	99.8
13966	A	G	99.6	13966	A	G	99.2												
								14365	C	T	94.7								
14470	T	C	99.9	14470	T	C	99.3												
								14582	A	G	100								
14766	C	T	96	14766	C	T	95.4												
14765	AC	T	4	14765	AC	T	4.2												
14930	G	A	90.4					14956	T	C	96.3								
15326	A	G	99.7	15326	A	G	99.9	15326	A	G	100								
15927	G	A	99.8	15927	G	A	99.2	15524	A	G	9.5								
16519	T	C	99.9	16519	T	C	99.5												
16566	G	A	97.4	16566	G	A	95.3												

Figure 66 - A figure displaying all mtDNA genotypes detected in patient 2 samples. Tumour-specific mtDNA alteration m.10404T>C identified in the original bladder tumour at 90.1% heteroplasmy and additionally found in the non-invasive cellular urine at 89.5% heteroplasmy and cell-free urine at 5% heteroplasmy were highlighted in yellow. mtDNA variants specifically only found in each sample were highlighted in green: pathogenic variant m.14930G>A at 90.4% within the bladder tumour, m.14582A>G 100% and m.15524A>G 9.5% within the cellular urine, and m.13860CAA>GGT at 100% within the Buffy Coat.

5.8.6 Identification of urothelial and basal cell populations within patient 2 Cellular urine sample.

To identify urothelial and basal cell populations present within each patients' urine sample, class 1-2 urothelial specific cell populations were identified, and class 3 basal specific cells were characterised. Following gating for forward (FSC-A) and side scatter (SSC-A) as shown in Figure 67 (A), I then went on to discriminate doublet cell populations, shown in Figure 67 (B) looking at looking Forward scatter height (FSC-H) and area (FSC-A). Only those gated cells were then looked at according to controls for secondary only, presented in Figure 67 (C), to identify the total fraction of cells that were urothelial positive within the urine, which represented 41% as displayed in Figure 67 (D).

Bivariate plots to display urothelial specific cell populations within patient 2 urine sample after uroplakin Ib staining.

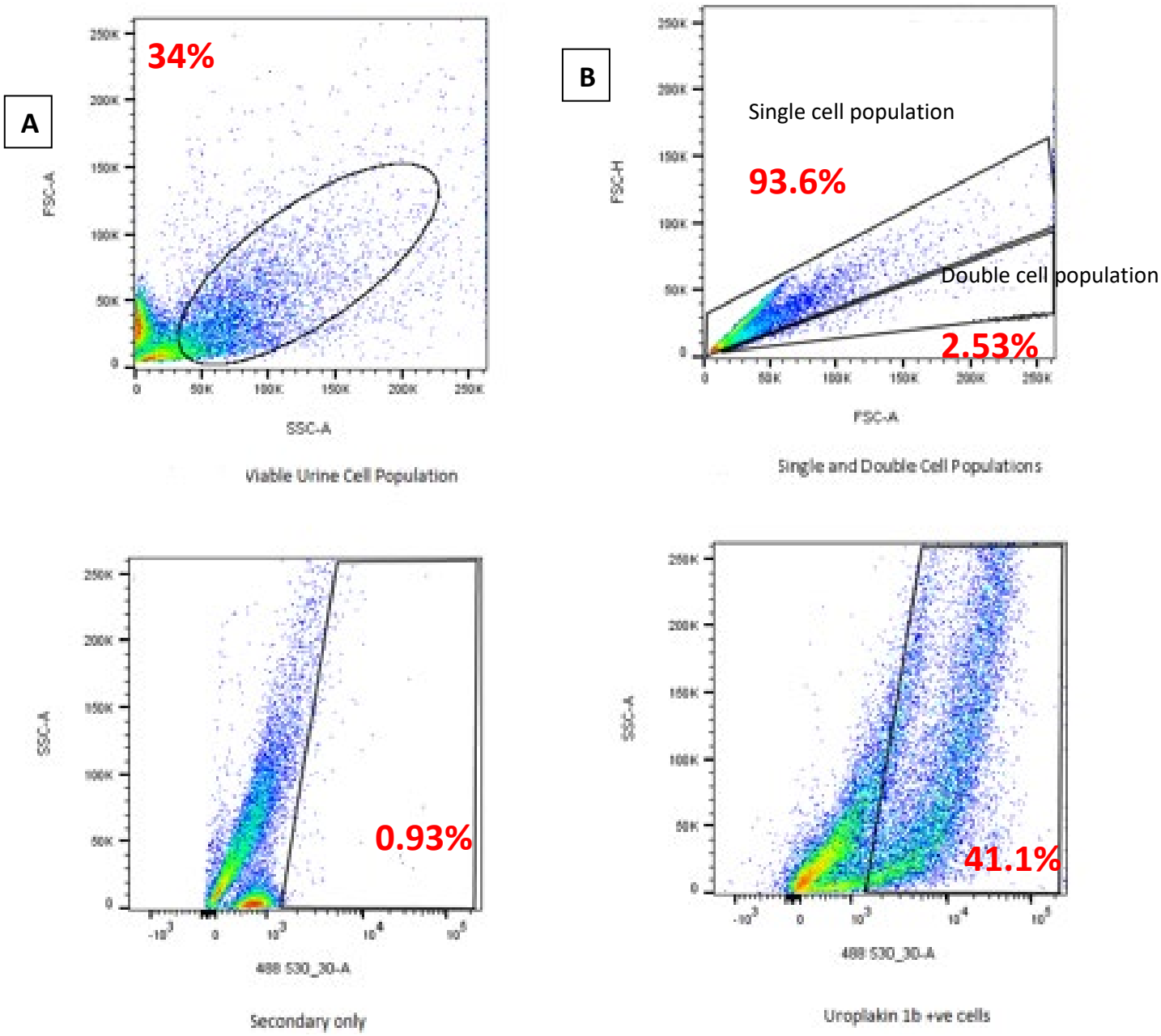

Figure 67 - Bivariate dot plots of patient 2's urine cells displaying (A) 34% viable urine cell populations, (B) 93.6% singlet population, 2.53% doublet cell discrimination populations, (C) 0.93% urine cells with secondary antibody only, and (D) 41.1% Urothelial positive cell population.

Of the 34% viable urine cells analysed, a 41% urothelial specific population was identified in patient 2's urine sample. The detection of m.10404T>C at 90% heteroplasmy in the cellular urine and 5% in the cell-free urine compartment demonstrates the mtDNA genotype was confirmed within the DNA of a mixture of urine cells that were not all urothelial specific, however, 41% were. 94% singlet and 2.53% doublet cells were distinguished within the patients' urine. Doublet cell populations were excluded from the analysis.

Bivariate plots to display basal cell populations within patient 2 urine sample after CD49f staining.

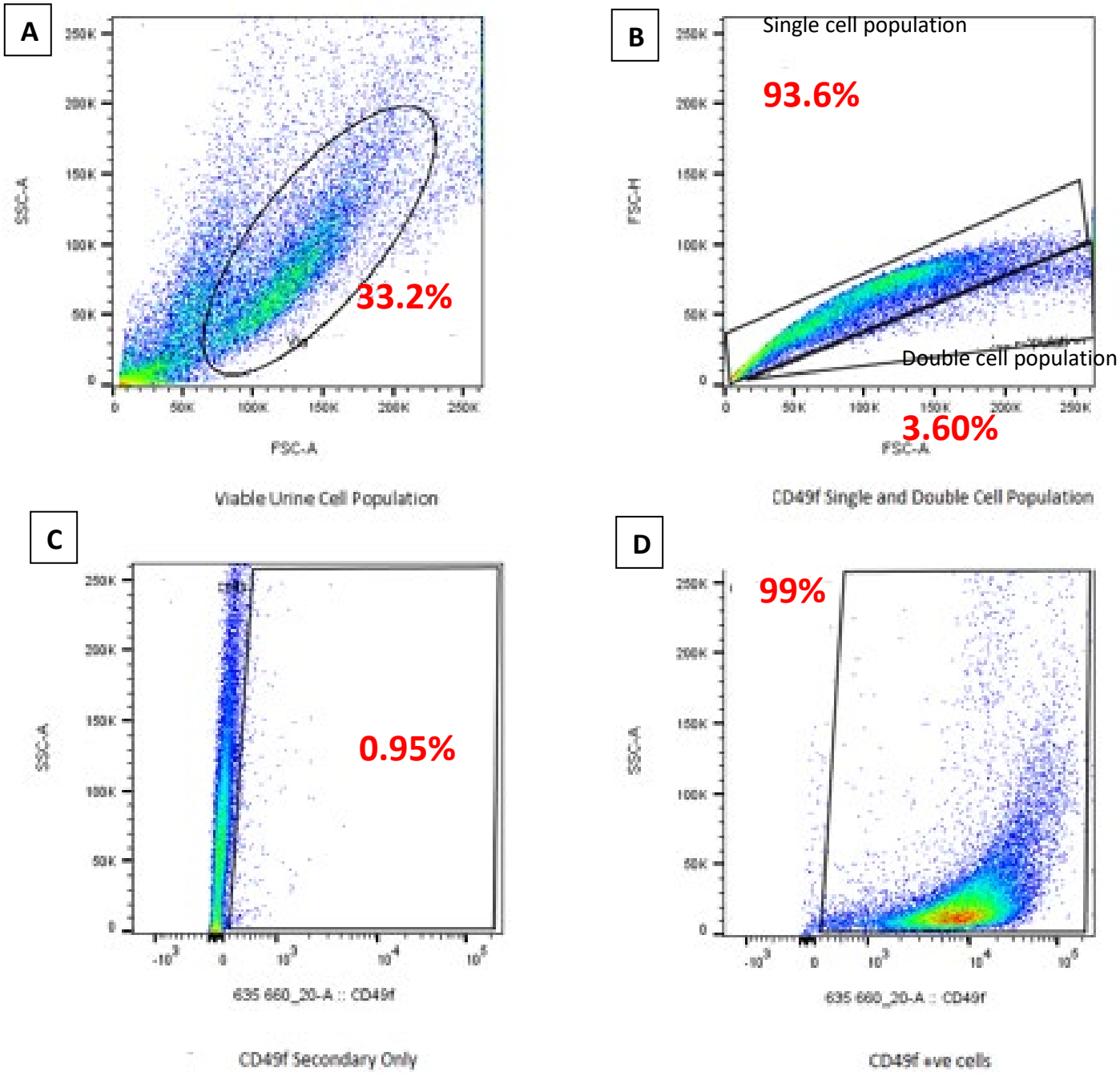

Figure 68 - Bivariate dot plots of patient 2's urine cells displaying (A) 33.2% viable urine cell population, (B) 93.6% singlet population, and 3.6% doublet cell discrimination populations, (C) 0.95% urine cells with secondary antibody only and (D) 99% Basal positive cell population.

33% viable urine cells were analysed, 94% singlet and 3.6% doublet cells were distinguished from the patients' urine sample and 99% were basal cell specific during the detection of the tumour-specific m.10404T>C genotype from within the patients' urine samples.

5.8.7 mtDNA genotypes detected in patient 4 founder bladder tumour and normal biopsy, urine cellular and cell-free and Buffy Coat samples following Radical Cystectomy.

Tumour-specific pathogenic variant m.4841G>A was identified in patient 4 founder bladder tumour at 56% heteroplasmy and in the matched non-invasive cellular urine compartment at 43% heteroplasmy and cell-free urine at 1% heteroplasmy. Tumour-specific mtDNA variants m.3971T>C, m.5032G>A, m.7308A>G, m.12952G>A, and m.16147C>T were not identified in the patients cellular and cell-free urine compartments. Additional mtDNA genotypes. m.6221T>C at 73.3% and m.6371C>T at 71.5% heteroplasmy was specifically observed within the cell-free urine of patient 4.

For both pathogenic variants m.10404T>C within patient 2 and m.4841G>A within patient 4, I spotted a pattern that these mtDNA alterations were detectable within both the cellular and cell-free urine compartments.

Heteroplasmy levels of all mtDNA genotypes identified in patient 4 founder bladder tumour and normal biopsy, urine cellular and cell-free and Buffy Coat samples following Radical Cystectomy.

Patient 4 Normal				Patient 4 Tumour				Patient 4 Urine Supernatant				Patient 4 Urine Cell pellet				Patient 4 Buffy Coat			
mtDNA Position	Reference	Variant	Heteroplasmy (%)	mtDNA Position	Reference	Variant	Heteroplasmy (%)	mtDNA Position	Reference	Variant	Heteroplasmy (%)	mtDNA Position	Reference	Variant	Heteroplasmy (%)	mtDNA Position	Reference	Variant	Heteroplasmy (%)
73	A	G	100	73	A	G	99.9					73	A	G	99.8	73	A	G	99.7
199	T	C	99.4	199	T	C	99.7					199	T	C	99.9	199	T	C	98.5
204	T	C	3.4									204	T	C	3.9	204	T	C	3.5
236	T	C	100	236	T	C	100					236	T	C	100	236	T	C	100
263	A	G	100	263	A	G	100					263	A	G	99.8	263	A	G	99.8
310	T	C	9.4	310	T	C	7.6					310	T	CCTC	98.2	310	T	CCTC	57
310	T	CCTC	86.6	310	T	CTC	88.7					310	T	CTC	1.3	310	T	CTC	40.7
750	A	G	99.9	750	A	G	99.9					750	A	G	99.8	750	A	G	99.2
1336	G	A	5.8	1336	G	A	55.7												
1438	A	G	99.8	1438	A	G	99.9												
3010	G	A	99.8	3010	G	A	99.9												
				3971	T	C	11.5												
3850	G	A	8.1																
4769	A	G	99.9	4769	A	G	100	4769	A	G	99.9	4769	A	G	99.9	4769	A	G	99.9
				4841	G	A	56.2	4841	G	A	1.3	4841	G	A	43.4				
				5032	G	A	20												
								6221	T	C	73.3								
								6371	C	T	71.5								
7013	G	A	99.6	7013	G	A	99.7												
				7308	A	G	4.3												
8821	T	C	74.7	8821	T	C	85.4												
8860	A	G	99.9	8860	A	G	100												
9097	A	G	100	9097	A	G	100												
9656	T	C	99.8	9656	T	C	99.7												
11654	A	G	99.9	11654	A	G	99.9												
11914	G	A	100	11914	G	A	99.9												
				12952	G	A	4												
15326	A	G	99.9	15326	A	G	99.8					15326	A	G	100	15326	A	G	99.7
16111	C	A	99.9	16111	C	A	99.9					16111	C	A	100	16111	C	A	99.6
				16147	C	T	52.9												
16519	T	C	99.7	16519	T	C	100	16519	T	C	100	16519	T	C	99.8	16519	T	C	99.6

Figure 69 - A table displaying all mtDNA genotypes detected in patient 4 samples. Tumour-specific mtDNA alteration m.4841G>A identified in the original bladder tumour at 56.2% heteroplasmy and additionally found in the non-invasive cellular urine at 43.4% and 1.3% heteroplasmy within the cell-free urine is highlighted in yellow. mtDNA variants specifically only found in each sample are highlighted in green: pathogenic variant m.3850G>A at 8.1% within the normal bladder sample, m.5032G>A at 20%, m.7308A>G at 4.3%, m.12952G>A at 4%, m.16147C>T at 52.9% heteroplasmy in the bladder tumour, m.6221T>C at 73.3% and m.6371C>T at 71.5% heteroplasmy within the cell-free urine.

5.8.8 Bivariate plots to display urothelial specific cell populations within patient 4 urine sample after uroplakin Ib staining.

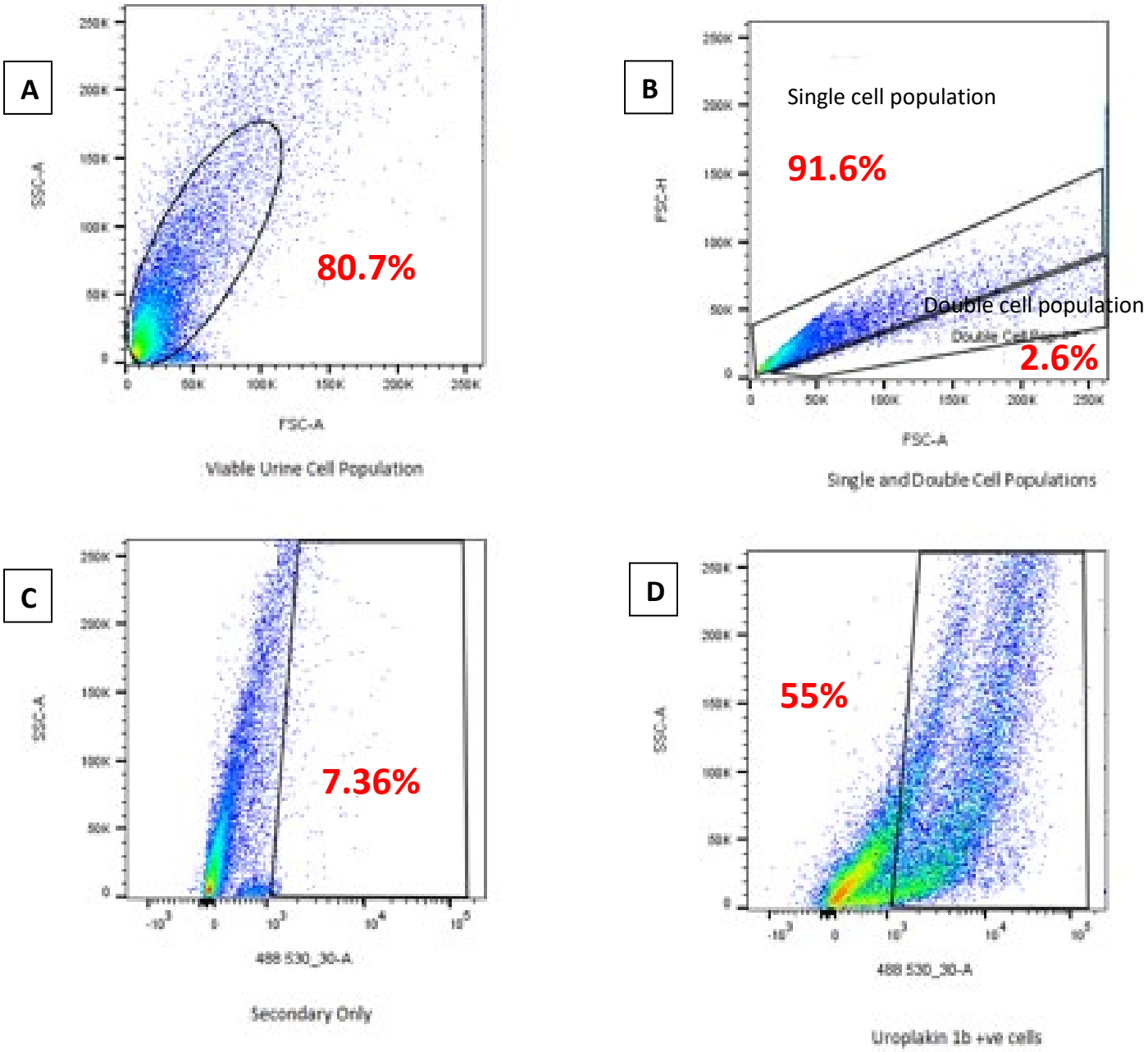

Figure 70 - Bivariate dot plots of patient 4's urine cells displaying (A) 80.7% viable urine cell population, (B) 91.6 singlet and 2.6% doublet cell discrimination populations, (C) 7.36% urine cells with secondary antibody were present and (D) 55% Urothelial positive cell population.

81% viable urine cells were analysed, 91.6% singlet and 2.6% doublet cells were distinguished from the patients' urine sample and 55% were urothelial cell specific during the detection of the tumour-specific m.4841G>A genotype in the patients' cellular and cell-free urine samples.

5.8.9 Bivariate plots to display basal cell populations within patient 4 urine sample after CD49f staining.

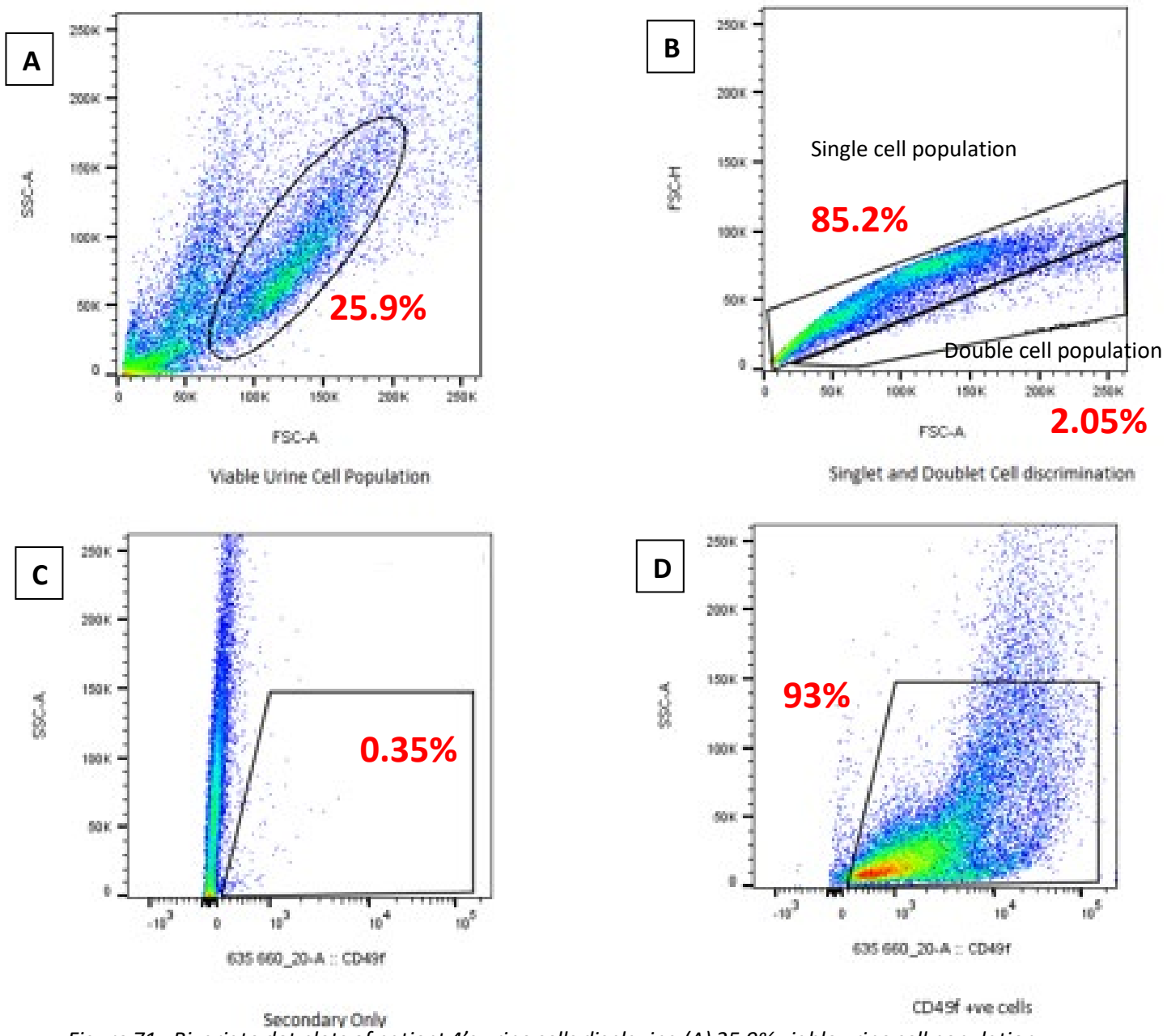

Figure 71 - Bivariate dot plots of patient 4's urine cells displaying (A) 25.9% viable urine cell population, (B) 85.2% single and 2.05% doublet cell discrimination populations, (C) 0.35% urine cells with secondary antibody only added and (D) 93% Basal positive cell population.

Of the 26% viable urine cells investigated, a 93% basal cell specific population was identified within patient 4's urine sample. The detection of tumour-specific m.4841G>C at 43% in the cellular urine and 1% in the cell-free urine compartment demonstrates the mtDNA genotype was observed within DNA from a mixture of urine cells, and 93% were of basal cell origin. 85.2% singlet and 2.05% doublet cells were distinguished within the patients' urine.

5.8.10 mtDNA genotypes detected in patient 10 founder bladder tumour and normal biopsy, urine cellular and cell-free and Buffy Coat samples following Radical Cystectomy.

Tumour-specific pathogenic variant m.1180T>C was identified at 69.2% heteroplasmy level in the patients' founder bladder tumour and confirmed at 54.2% in the cellular urine and 42% within the non-cellular urine compartments. Additional mtDNA genotypes m.4866T>C at 15.7% heteroplasmy and m.11577G>A at 23.6% were detected in the bladder tumour of patient 4, but not in any of the matched urine compartments. Each of the mtDNA variants was not observed in the Buffy Coat, therefore classified as tumour specific.

Heteroplasmy levels of all mtDNA genotypes identified in patient 10 founder bladder tumour and normal biopsy, urine cellular and cell-free and Buffy Coat samples following Radical Cystectomy.

Patient 10 Normal				Patient 10 Tumour				Patient 10 Urine Cell Pellet				Patient 10 Buffy Coat				Patient 10 Urine Supernatant			
mtDNA Position	Reference	Variant	Heteroplasmy (%)	mtDNA Position	Reference	Variant	Heteroplasmy (%)	mtDNA Position	Reference	Variant	Heteroplasmy (%)	mtDNA Position	Reference	Variant	Heteroplasmy (%)	mtDNA Position	Reference	Variant	Heteroplasmy (%)
263	A	G	99.7	263	A	G	100												
311	-	C	100	311	-	C	100												
750	A	G	100	750	A	G	99.9	750	A	G	99.1	750	A	G	99.1	750	A	G	99.1
				1180	T	C	69.2	1180	T	C	54.2					1180	T	C	42
1438	A	G	99.8	1438	A	G	99.9	1438	A	G	99.5	1438	A	G	99.4	1438	A	G	99.7
3010	G	A	99.6	3010	G	A	99.9	3010	G	A	99.9	3010	G	A	99.7	3010	G	A	99.3
4769	A	G	99.9	4769	A	G	100												
				4866	T	C	15.7												
6272	A	G	99.6	6272	A	G	99.7												
8764	G	A	99.9	8764	G	A	99.8												
8860	A	G	99.9	8860	A	G	100												
				11577	G	A	23.6												
14869	G	A	99.8	14869	G	A	99.7												
15326	A	G	99.8	15326	A	G	99.9												
15736	A	G	99.5	15736	A	G	99.8												
16519	T	C	99.6	16519	T	C	100												

Figure 72 - A figure displaying all mtDNA genotypes detected in patient 10 samples. Tumour-specific mtDNA alteration m.1180T>C identified in the original bladder tumour at 69.2% heteroplasmy and additionally found in the non-invasive cellular urine at 54.2% and 42% heteroplasmy within the cell-free urine is highlighted in yellow. mtDNA variants specifically only found in the bladder tumour sample were highlighted in green: pathogenic variant m.4866T>C at 15.7% and m.11577G>A at 23.6% heteroplasmy.

Heteroplasmy variability within patient 10 tissue sections

Patient 10's bladder tissue was further analysed by cryosectioning a further 600 µm, and every 150 µm, tissue was collected into a sterile Eppendorf and stored at -80°C. Whole genomic DNA was extracted from each sample (as described in section 2.7) and targeted mtDNA sequencing was performed using specific primer pair sets (as described in section 2.9.3) to confirm the presence of mtDNA variants within the patient sample.

Tumour-specific mtDNA genotypes detected in patient 10 bladder tumour after sequencing 600 µm depth of biopsy.

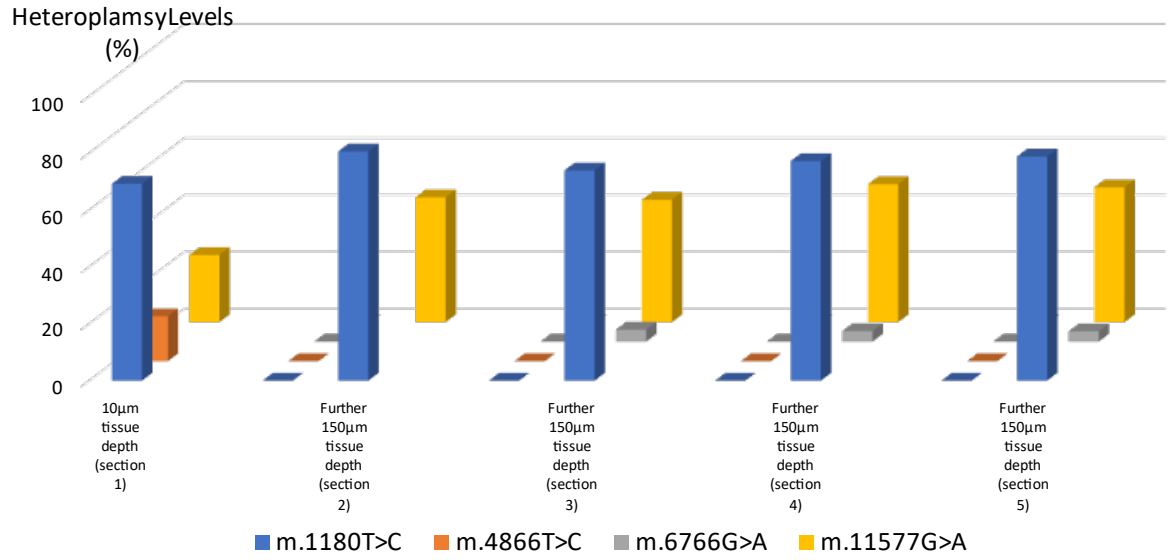

Figure 73 - Confirmation of the mtDNA genotypes m.1180T>C, m.4866T>C, m.6766G>A and m.11577G>A identified in patient 10 bladder tumour, after further sequencing every 150 µm totalling 600 µm within the depth of the bladder tissue.

Interestingly, the tumour-specific mtDNA genotype m.1180T>C originally identified at 69.2% heteroplasmy was detected throughout the depth of the bladder tissue sample, as well as m.11577G>A at 23.6% heteroplasmy at initial analysis. m.4866T>C was originally observed at 15.7% heteroplasmy in the primary bladder tumour sample analysed, however was not subsequently identified. m.6766G>A was not detected in the initial bladder tumour sample sequenced; however, this mitochondrial genotype was identified in each subsequent sample analysed. This additional analysis displays heteroplasmy variability within tissue sections from the sample, highlighting the importance of ensuring representative areas of the same sample are sequenced.

5.8.11 Bivariate plots to display urothelial specific cell populations within patient 10 urine sample after Uroplakin 1b staining.

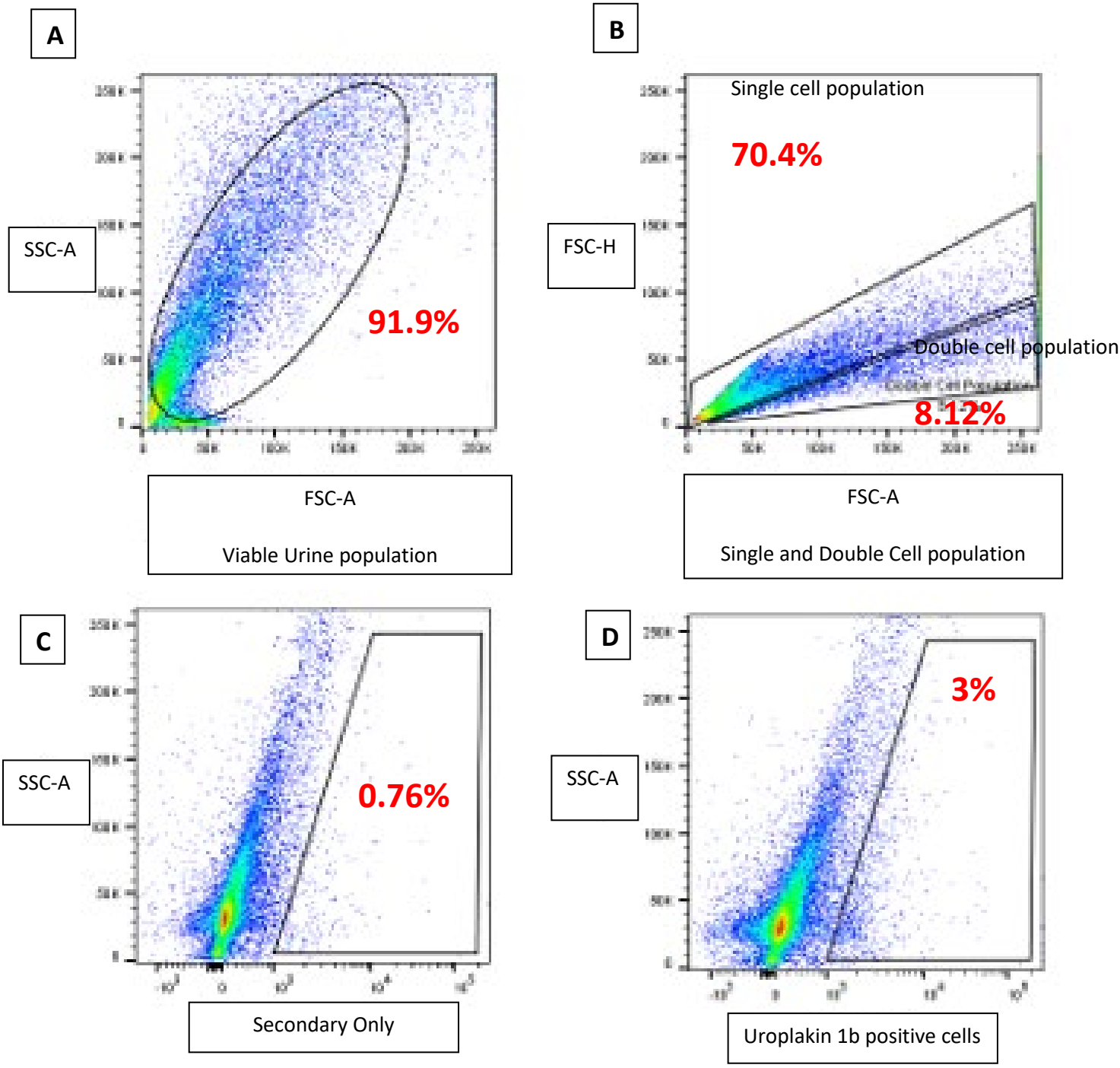

Figure 74 - Bivariate dot plots of patient 10's urine cells displaying (A) 91.9% viable urine cell populations, (B) 70.4% single and 8.12% doublet cell discrimination populations, (C) 0.76% urine cells with secondary antibody only added and (D) 3% Urothelial *positive cell population.*

92% viable urine cells were investigated, 70.4% singlet and 8.12% doublet cells distinguished from the patients' urine sample and 3% were urothelial cell specific.

5.8.12 Bivariate plots to display basal cell populations within patient 10 urine sample after CD49f staining.

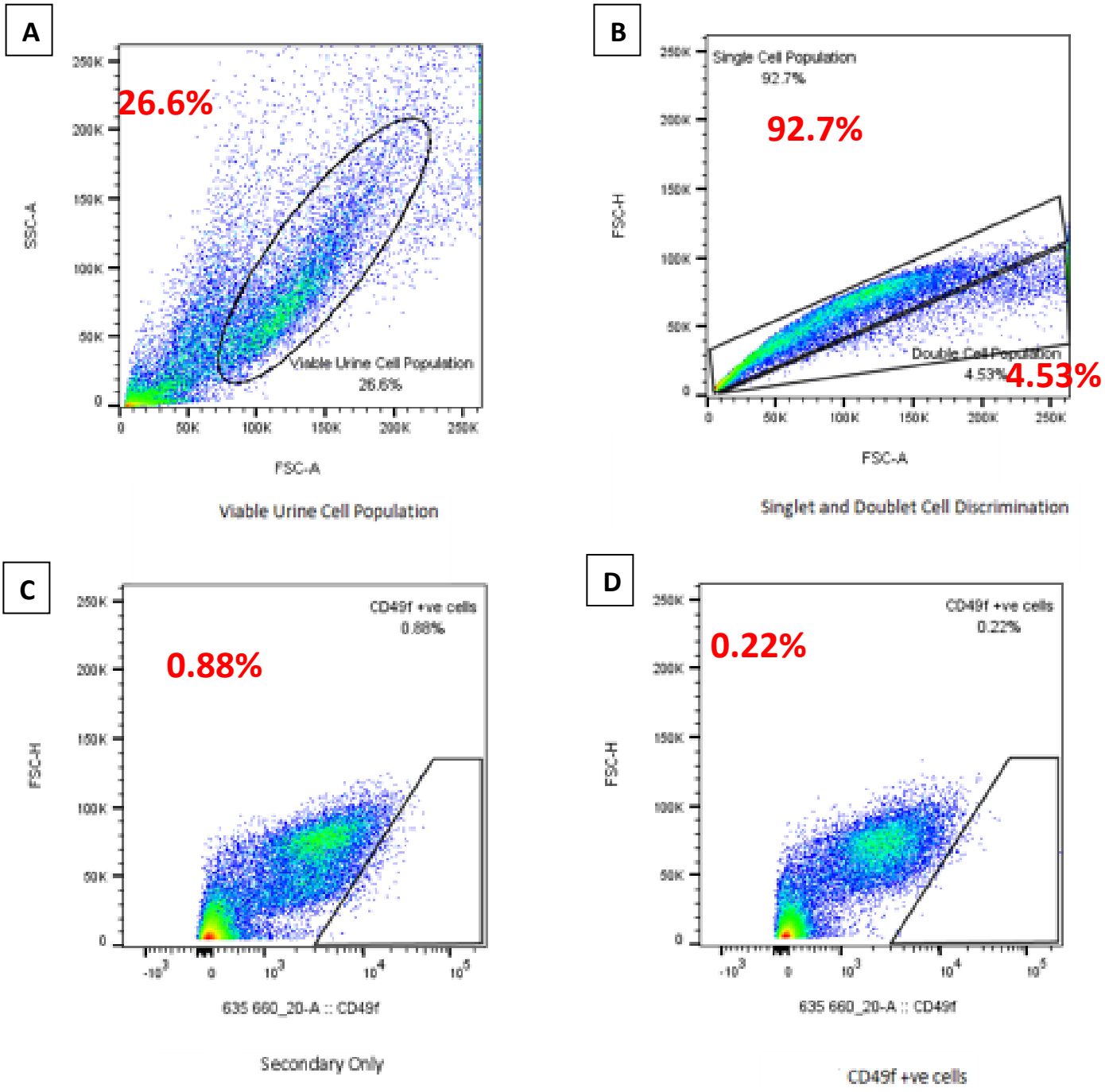

Figure 75 - Bivariate dot plots of patient 10's urine cells displaying (A) 26.6% viable urine cell populations, (B) 92.7% single and 4.53% doublet cell discrimination populations, (C) 0.88% urine cells with secondary antibody only added and (D) 0.22% Basal positive cell population.

26.6% viable urine cells were analysed, 92.7% singlet, 4.53% doublet cells distinguished from the patients' urine sample and 0.22% were basal cell specific.

Heteroplasmy levels of all mtDNA genotypes identified in patient 11 founder bladder tumour and normal biopsy, urine cellular and cell-free and Buffy Coat samples following Radical Cystectomy.

Patient 11 Normal				Patient 11 Tumour				Patient 11 Urine Cell Pellet				Patient 11 Urine Supernatant				Patient 11 Buffy Coat			
mtDNA Position	Reference	Variant	Heteroplasmy (%)	mtDNA Position	Reference	Variant	Heteroplasmy (%)	mtDNA Position	Reference	Variant	Heteroplasmy (%)	mtDNA Position	Reference	Variant	Heteroplasmy (%)	mtDNA Position	Reference	Variant	Heteroplasmy (%)
263	A	G	100	263	A	G	100												
				307	CCCT	TC	94.2												
456	C	T	97.5	456	C	T	100												
523	AC	-	99.4	523	AC	-	98.5												
750	A	G	100	750	A	G	99.8												
1438	A	G	100	1438	A	G	99.8												
4336	T	C	99.9	4336	T	C	100	4336	T	C	99.9	4336	T	C	99.8	4336	T	C	99.6
4769	A	G	99.9	4769	A	G	99.6	4769	A	G	99.9	4769	A	G	99.97	4769	A	G	99.6
4916	A	G	99.3	4916	A	G	100	4916	A	G	98.9	4916	A	G	99.6	4916	A	G	99
								5170	G	A	3.6								
								6409	T	C	5.2	6409	T	C	4.7				
8860	A	G	99.9	8860	A	G	100	8860	A	G	99.9	8860	A	G	99.9	8860	A	G	99.6
				9098	T	C	75.9	9098	T	C	93.2					9098	T	C	4.1
15326	A	G	100	15326	A	G	99.9												
15833	C	T	99.5	15833	C	T	99.8												
16304	T	C	97.2	16304	T	C	98.5												

Figure 76 - mtDNA genotypes detected in patient 11 urine samples collected following Robotic Cystectomy. m.9098T>C at 93% heteroplasmy was identified in the patients' cellular urine sample and additional mtDNA genotypes m.5170G>A at 4% and m..6409T>C at 5%.

m.9098T>C mtDNA variant identified at 76% heteroplasmy level in the patients' founder bladder tumour was confirmed in the non-invasive collected cellular urine compartment at a higher heteroplasmy level of 93%, however, was not present within the cell-free urine sample. m.9098T>C was not deemed as tumour specific as the mtDNA genotype was identifiable at 4% in the germline DNA Buffy Coat sample. mtDNA variants m.5170G>A at 4% and m.6409T>C at 5% were observed within the cellular urine sample only.

Heteroplasmy variability within patient 11 tissue sections

Patient 11's bladder tissue was further analysed by cryosectioning a further 600 µm, and every 150 µm tissue was collected into a sterile Eppendorf and placed at -80°C. Whole genomic DNA was extracted from each sample (as described in section 2.7) and targeted mtDNA sequencing was performed using specific primer pair sets (as described in section 2.9.5) to confirm the presence of mtDNA variants within the patient sample.

Tumour-specific mtDNA genotypes detected in patient 11 bladder tumour after sequencing 600 µm depth of biopsy

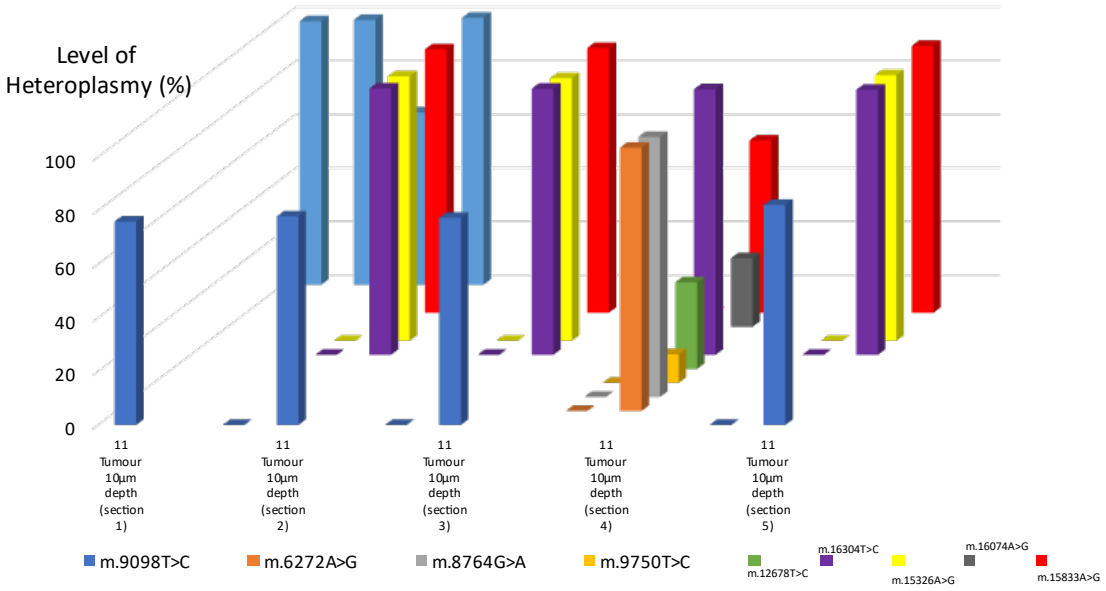

Figure 77 - Confirmation of the mtDNA genotypes and identified in patient 11 bladder tumour, after sequencing every 150 µm totalling 600 µm within the depth of the bladder tissue.

Interestingly, the tumour-specific mtDNA genotype m.9098T>C originally identified at 75.9% heteroplasmy was detected throughout the depth of the bladder tissue sample analysed. Other mtDNA genotypes including m.6272A>G, m.8764G>A, m.9750T>C, m. 12678T>C, m.16304T>C, m.15326A>G, m.16074A>G and m.15833A>G were detected at varying heteroplasmy levels confirming heteroplasmy variability in subsequent sections, within the same bladder tumour tissue sample.

5.8.13 Bivariate plots to display urothelial specific cell populations within patient 11 urine sample after uroplakin 1b staining.

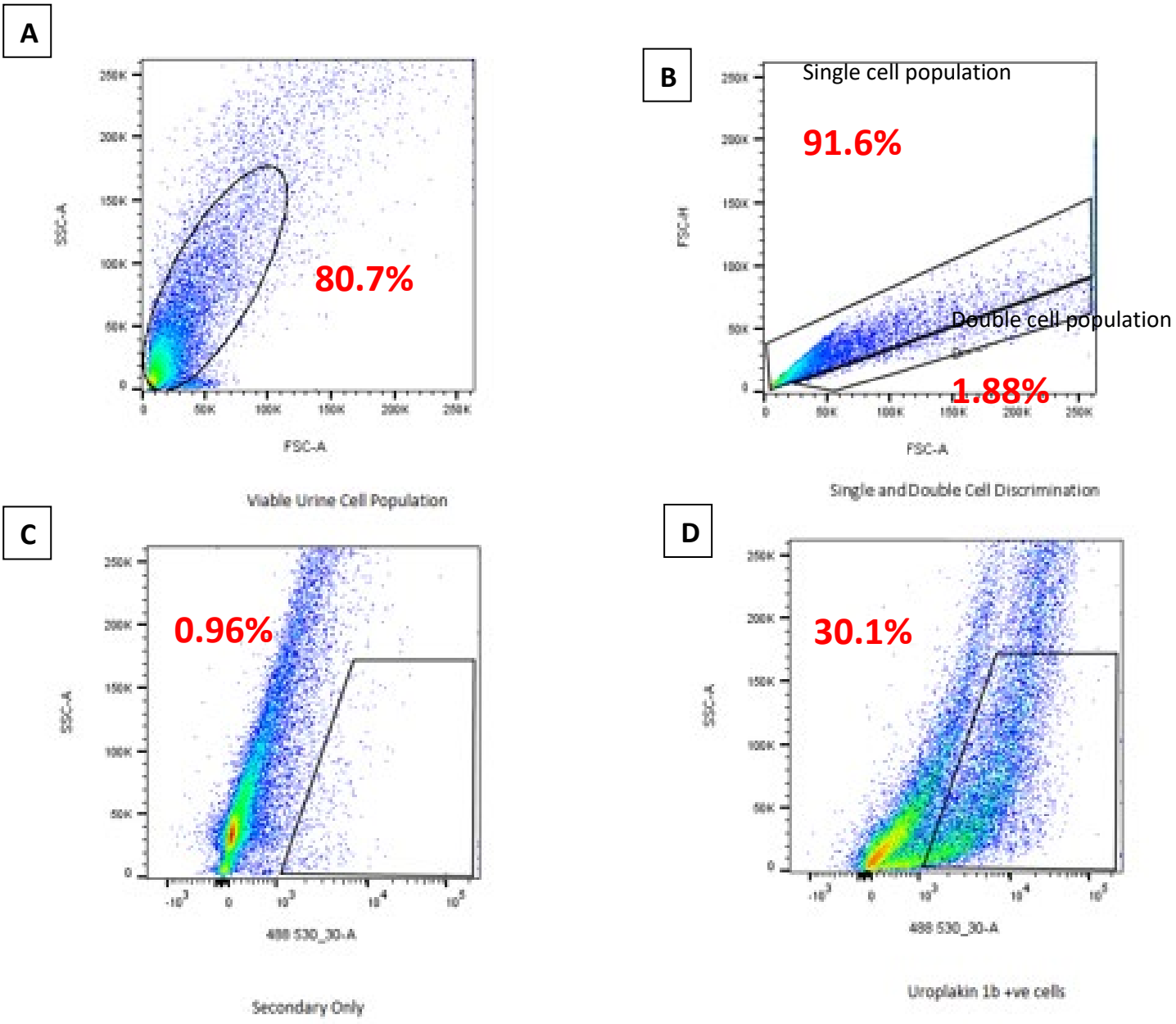

Figure 78 - Bivariate dot plots of patient 11's urine cells displaying (A) 80.7% viable urine cell populations, (B) 91.6% single and 1.88% doublet cell discrimination populations, (C) 0.96% urine cells with secondary antibody only added and (D) 30.1% Urothelial positive cell population.

80.7% viable urine cells were analysed, 91.6% singlet, and 1.88% doublet cells distinguished from the patients' urine sample. 30% of the urine cells investigated were epithelial cell specific during the detection of the tumour-specific m.9098T>C genotype in the patients' bladder tumour, urine cellular, and cell-free samples.

5.8.14 Bivariate plots to display basal cell populations within patient 11 urine sample after EpCAM staining.

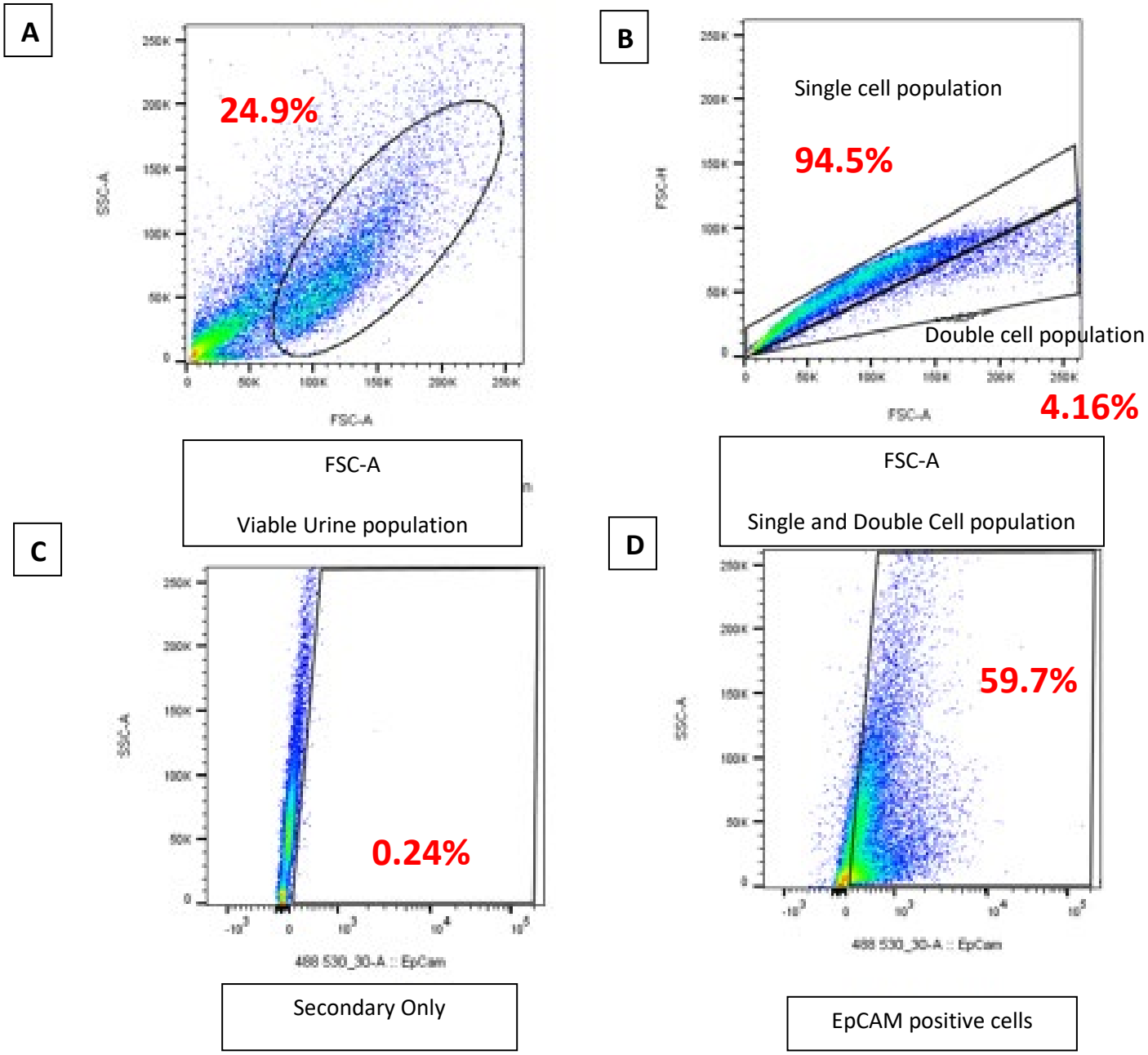

Figure 79 - Bivariate dot plots of patient 11's urine cells displaying (A) 24.9% viable urine cell populations, (B) 94.5% single and 4.16% doublet cell discrimination populations, (C) 0.24% urine cells with secondary antibody only added and (D) 59.7% EpCAM .positive cell population

24.9% viable urine cells were analysed, 94.5% singlet, and 4.16% doublet cells distinguished from the patients' urine sample. 59.7% of the urine cells investigated were epithelial cell specific.

5.8.15 mtDNA genotypes detected in patient 13 founder bladder tumour and normal biopsy, urine cellular and cell-free and Buffy Coat samples following Radical Cystectomy.

Pathogenic mtDNA variants m.3284G>A at 22.3% heteroplasmy and m.15806G>A at 4.5% were identified within the founder bladder tumour but not present in any other matched patient samples. Additional variants m.146T>C at 99.8% heteroplasmy, m150CCT>TCC at 100%, m.182CA>TG at 100%, m.204T>C at 100%, m.13590G>A at 99.5%, m.13650C>T at 97.7%, m.132926T>A at 3.5%, m.13986A>G at 99.5%, m.14059A>G at 99.7%, m.16129G>A at 99.7%, m.16114C>A at 99.7%, m.16213G>A at 99.4%, m.16274G>A at 99.3% and m.16390G>A at 98.6% heteroplasmy levels were observed only in the urine cell-free supernatant sample. Within the Buffy Coat specific pathogenic variants m.4104A>G at 100%, m. 4158A>G at 100%, m.5027C>T at 83.3%, m.5331C>A at 100%, m. 5814T>C at 66.7%, m.6614T>C at 91.7%, m.6713C>T at 91.7%, m. 7256C>T at 85.7%, m.8387G>A at 66.7%, m.12948A>G at 100%, m. 16039T>C at 28.6% Heteroplasmies were only identified within the germline.

Heteroplasmy levels of all mtDNA genotypes identified in patient 13 samples following Radical Cystectomy.

Patient 13 Normal				Patient 13 Tumour				Patient 13 Urine Cell pellet				Patient 13 Urine Supernatant				Patient 13 Buffy Coat			
mtDNA Position	Reference	Variant	Heteroplasmy (%)	mtDNA Position	Reference	Variant	Heteroplasmy (%)	mtDNA Position	Reference	Variant	Heteroplasmy (%)	mtDNA Position	Reference	Variant	Heteroplasmy (%)	mtDNA Position	Reference	Variant	Heteroplasmy (%)
73	A	G	97	73	A	G	99.6	73	A	G	96.8	73	A	G	100	73	A	G	99.8
												146	T	C	99.8				
												150	CCT	TCC	99.9				
153	A	G	96.7	153	A	G	90.6	153	A	G	97.1					153	A	G	99.3
												182	CA	TG	100				
195	T	C	96.8	195	T	C	99.4	195	T	C	96	195	TTAC	CTAT	100	195	T	C	98.9
												204	T	C	99.8				
225	GTA	ATG	97.6	225	GTA	ATG	100	225	GTA	ATG	97.8					225	GTA	ATG	100
263	A	G	99.6	263	A	G	99.8	263	A	G	99.8	263	A	G	99.7	263	A	G	99.4
310	T	C	4.4	309	CT	TC	4.5	310	T	CTC	23.2								
311	-	C	93.9	311	-	C	95	311	-	C	76.8					311	-	C	99.8
750	A	G	99.3	750	A	G	99.2	750	A	G	99.5	750	A	G	99.5	750	A	G	99.1
821	T	C	16.5					821	T	C	4.7	821	T	C	5.5				
1438	A	G	99.3	1438	A	G	99.1	1438	A	G	99.6	1438	A	G	99.7	1438	A	G	99.3
1719	G	A	97.4	1719	G	A	99.8	1719	G	A	99.9	1719	G	A	99.6	1719	G	A	99.5
2706	A	G	97.9	2706	A	G	99.7	2706	A	G	99.8	2706	A	G	99.6	2706	A	G	99.5
				3284	G	A	22.3												
																4104	A	G	100
																4158	A	G	100
4769	A	G	99.9	4769	A	G	99.9												
																5027	C	T	83.3
																5331	C	A	100
																5814	T	C	66.7
6221	T	C	97.1	6221	T	C	99.9												
6371	C	T	96.9	6371	C	T	98.7									6614	T	C	91.7
																6713	C	T	91.7
7028	C	T	96.7	7028	C	T	98.6												
																7256	C	T	85.7
																8387	G	A	66.7
8860	A	G	99.8	8860	A	G	99.8												
9966	G	A	97.8	9966	G	A	99.9	9966	G	A	83.3					8860	A	G	100
11719	G	A	96.6	11719	G	A	99									11719	G	A	100
12705	C	T	98.1	12705	C	T	99.9												
																12948	A	G	100
												13590	G	A	99.5				
												13650	C	T	98.8				
												13926	T	A	3.5				
13966	A	G	97.3	13966	A	G	99.5	13966	A	G	97.4					13039	T	C	28.6
												13986	A	G	99.5				
																13966	A	G	99.7
												14059	A	G	99.7				
14470	T	C	97.3	14470	T	C	99.8	14470	T	C	97.1					14470	T	C	99.8
14766	C	T	98.1	14766	C	T	99.5	14766	C	T	97.5	14766	C	T	100	14766	C	T	99.5
												15110	G	A	99.8				
												15217	G	A	99.5				
												15301	G	A	99.8				
15314	G	A	97.4	15314	G	A	99.4	15314	G	A	97.9					15314	G	A	99.8
15326	A	G	99.5	15326	A	G	99.5	15326	A	G	99.5	15326	A	G	99.8	15326	A	G	99.7
				15806	G	A	4.5												
												16129	G	A	99.7				
												16114	C	A	99.7				
												16213	G	A	99.4				
16223	C	T	93.2	16223	C	T	97.2	16223	C	T	94	16223	C	T	95.7	16223	C	T	95.5
16255	G	A	97.2	16255	G	A	99.8	16255	G	A	97.5					16255	G	A	99.6
												16274	G	A	99.3				
16278	C	T	96.3	16278	C	T	98.9	16278	C	T	96.2	16278	C	T	99.1	16278	C	T	97.9
												16390	G	A	98.6				
16519	T	C	99.3	16519	T	C	99.6	16519	T	C	99.5					16519	T	C	99.5

Figure 80 - A Table displaying mtDNA genotypes detected in patient 13 founder tumour, cellular and cell-free urine samples, and buffy coat collected following Robotic Cystectomy. mtDNA variants only found in each patient tissue sample were highlighted in green.

5.8.16 Bivariate plots to display urothelial specific cell populations within patient 13 urine sample after Uroplakin 1b staining.

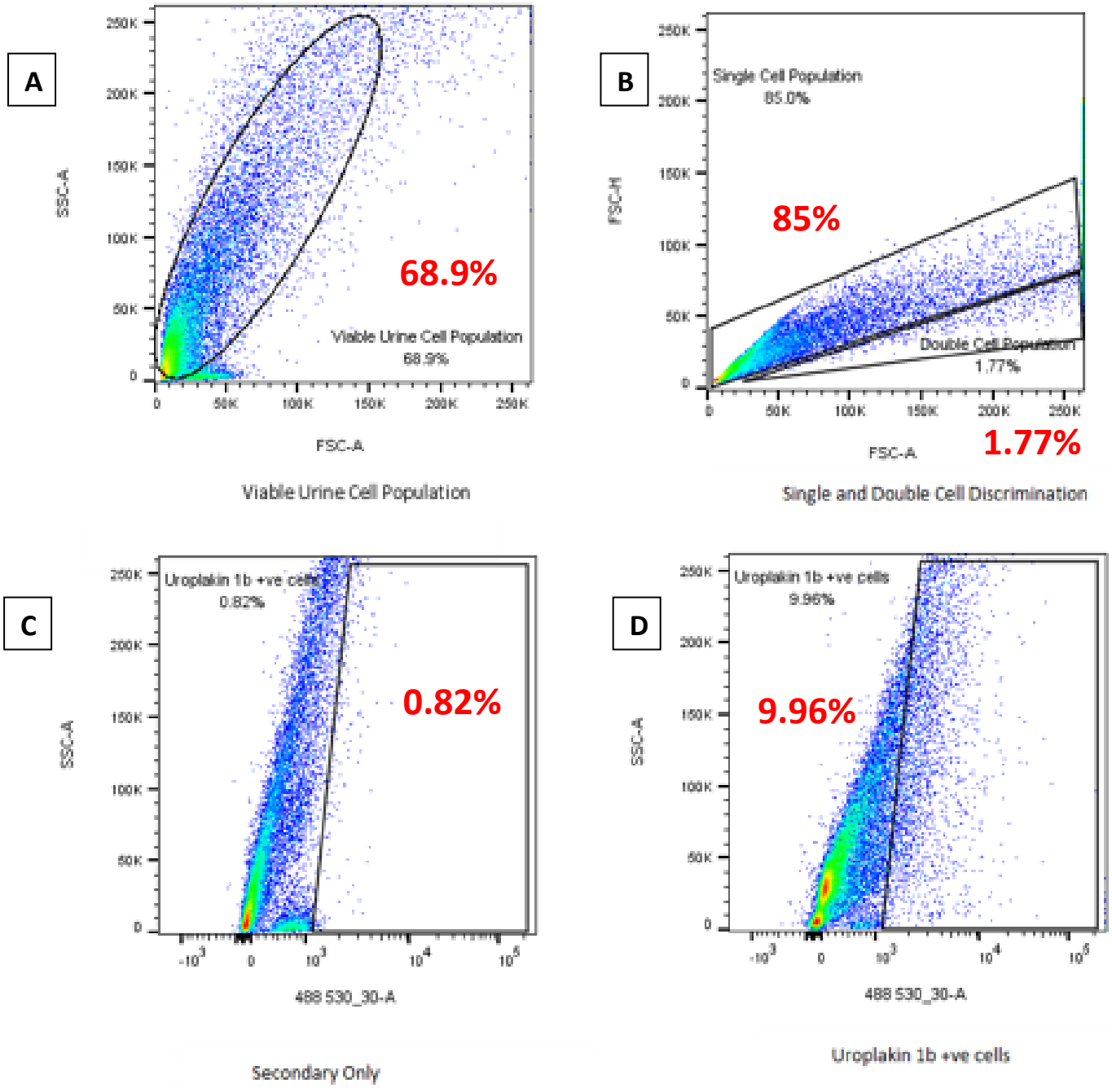

Figure 81 - Bivariate dot plots of patient 13's urine cells displaying (A) 68.9% viable urine cell population, (B) 85% single and 1.77% doublet cell discrimination populations, (C) 0.82% urine cells with secondary antibody only added and (D) 9.96% Urothelial positive cell population.

68.9% viable urine cells were analysed, 85% singlet and 1.77% doublet cells were distinguished from the patients' urine sample, and 9.96% of the urine cells from patient 13 were urothelial cell specific.

5.8.17 Bivariate plots to display urothelial specific cell populations within patient 13 urine sample after CD49f staining.

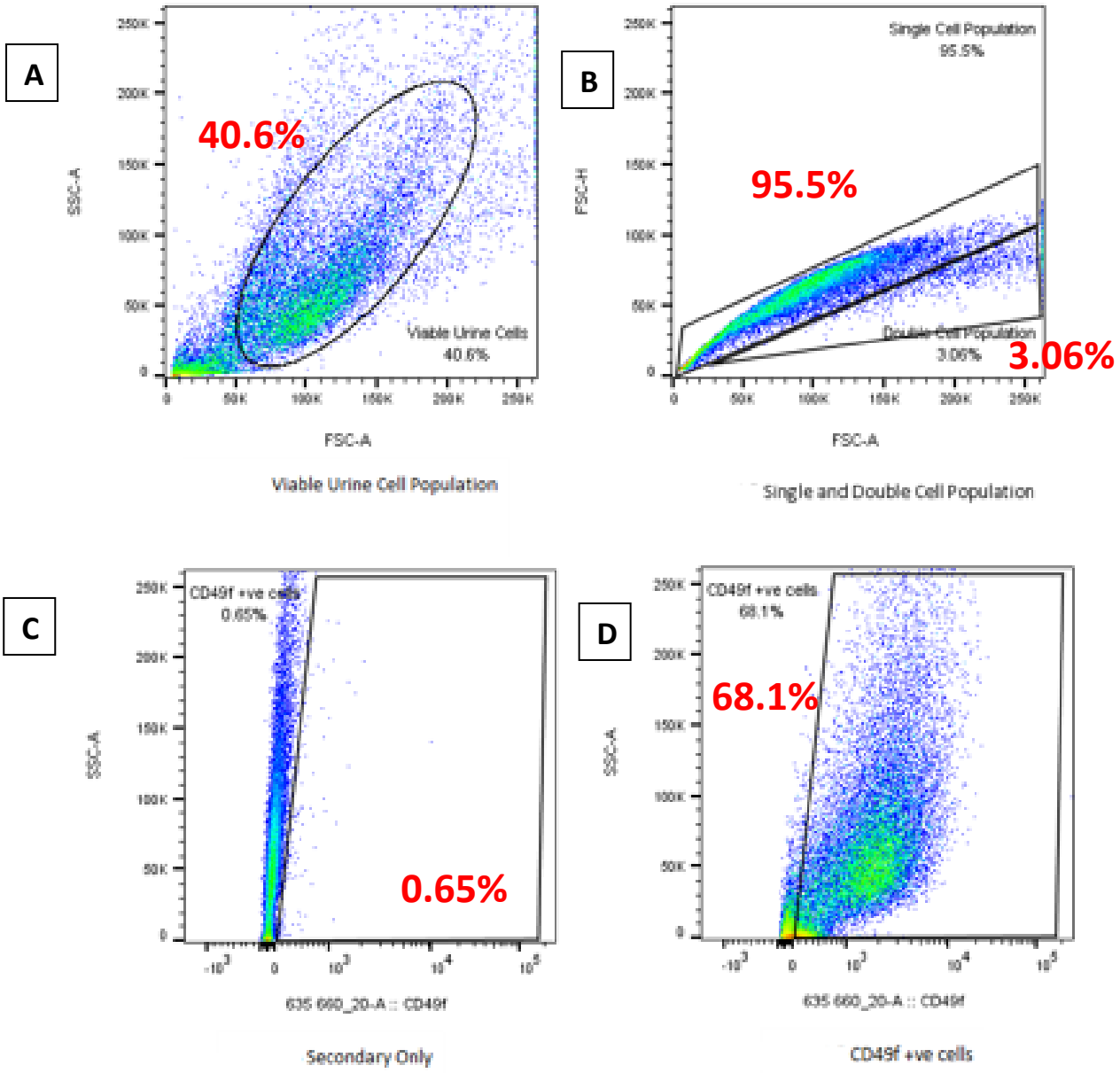

Figure 82 - Bivariate dot plots of patient 13's urine cells displaying (A) 40.6% viable urine cell population, (B) 95.5% single and 3.06% doublet cell discrimination populations, (C)0.65% urine cells with secondary antibody only, and (D) 68.1% Basal positive cell population.

40.6% viable urine cells were investigated, 95.5% singlet, and 3.06% doublet cells distinguished from the patients' urine sample. 68.1% of the urine cells analysed were basal cell specific during the detection of the mtDNA insertion. MtDNA genotypes m.146T>C, m.150CCT>TCC, m.182CA>TG, m.204T>C, m.13590G>, m.13650C>T and m.132926T>A observed only in the urine cell-free supernatant sample.

5.8.18 Bivariate plots to display urothelial specific cell population mtDNA genotypes detected in patient 15 founder bladder tumour and normal biopsy, urine cellular and cell-free and Buffy Coat samples following Radical Cystectomy.

m.6052A>G mtDNA variant was identified at 51.7% heteroplasmy level in the patients' buffy coat and 80% in the founder bladder tumour, highlighted in Figure 83. The mtDNA genotype was also detected in the cellular urine compartment at a higher heteroplasmy level of 93% and in the cell-free urine compartment at 96%. As m.6052A>G was additionally found in the germline DNA the mtDNA genotype was not deemed as tumour specific. Additional mtDNA variants m.6945T>GG at 100% heteroplasmy, m.6949CCGTAGGTGG>TAGCTGTTT at 100% heteroplasmy, m.9595C>G at 92.9% heteroplasmy, and m.9598TCCTAAACA>GACGGCCAGT at 36.4% heteroplasmy was observed in the Buffy Coat.

Heteroplasmy levels of all mtDNA genotypes identified in patient 15 samples following Radical Cystectomy.

Patient 15 Normal				Patient 15 Tumour				Patient 15 Urine Supernatant				Patient 15 Urine Cell Pellet				Patient 15 Buffy Coat			
mtDNA Position	Reference	Variant	Heteroplasmy (%)	mtDNA Position	Reference	Variant	Heteroplasmy (%)	mtDNA Position	Reference	Variant	Heteroplasmy (%)	mtDNA Position	Reference	Variant	Heteroplasmy (%)	mtDNA Position	Reference	Variant	Heteroplasmy (%)
311	-	C	58.7	311	-	C	88.7									2540	C	A	44.4
												2706	A	G	97.4	2706	A	G	98.8
3594	C	T	99.8	3594	C	T	99.7					3594	C	T	98.6	3594	C	T	99.6
4104	A	G	99.2	4104	A	G	99.2					4104	A	G	99.5	4104	A	G	99.3
4370	T	C	99.6	4370	T	C	98.9					4370	T	C	99.7	4370	T	C	98.7
4767	ATA	GTG	100	4767	ATA	GTG	100					4767	ATA	GTG	100	4767	ATA	GTG	100
5027	C	T	99.4	5027	C	T	99.7	5027	C	T	99	5027	C	T	99.7	5027	C	T	98.7
5553	T	C	4.9																
5814	T	C	99.7	5814	T	C	99.8	5814	T	C	100	5814	T	C	100	5814	T	C	100
6052	A	G	46.6	6052	A	G	80.4	6052	A	G	95.7	6052	A	G	93.3	6052	A	G	51.7
6580	G	A	3.5																
6614	T	C	98.3	6614	T	C	98.9	6614	T	C	98.3	6614	T	C	99.3	6614	T	C	99
				6713	C	T	99.7	6713	C	T	99.7	6713	C	T	99.7	6713	C	T	100
				6806	A	G	99.6	6806	A	G	99.7	6806	A	G	99.1	6806	A	G	99.6
6713	C	T	99.7	7028	C	T	98.9												
6806	A	G	99.7	7256	C	T	99.6												
																6945	T	GG	100
																6949	CCGTAGGTGG	TAGCTGTTT	100
7028	C	T	98.7					7028	C	T	99.5								
								7256	C	T	99.4								
7521	G	A	99.7	7521	G	A	99.4	7521	G	A	99.6								
8080	C	T	97.6	8080	C	T	98.8	8080	C	T	98.6								
8206	G	A	99.5	8206	G	A	99.8	8206	G	A	100								
								8233	A	-	4.9								
8387	G	A	99.6	8387	G	A	99.9	8387	G	A	99.8								
8503	T	C	98.5	8503	T	C	99	8503	T	C	96.7								
8701	A	G	98.8	8701	A	G	98.8	8701	A	G	99.1								
8860	A	G	99.8	8860	A	G	99.7	8860	A	G	99.8								
9221	A	G	99.8	9221	A	G	99.8												
9899	T	C	99.6	9899	T	C	99.4	9899	T	C	99.2	9899	T	C	99.5	9899	T	C	98.7
10115	T	C	99.3	10115	T	C	99.3	10115	T	C	99.6	10115	T	C	99	10115	T	C	99.2
10589	G	A	99.9	10589	G	A	99.8	10589	G	A	99.8	10589	G	A	99.6	10589	G	A	99.5
10873	T	C	99.8	10873	T	C	99.9	10873	T	C	96.6	10873	T	C	100	10873	T	C	97.9
11719	G	A	99	11719	G	A	99	11719	G	A	98.3	11719	G	A	100	11719	G	A	98.7
				11944	T	C	99.5	11944	T	C	99.2	11944	T	C	100	11944	T	C	99.5
				12236	G	A	99.6	12236	G	A	99.8	12236	G	A	99.7	12236	G	A	99.7
								12705	C	T	100	12705	C	T	100	12705	C	T	99.9
								12948	A	G	99.3	12948	A	G	99	12948	A	G	99
13590	G	A	99.8					13590	G	A	99.8	13590	G	A	98.3	13590	G	A	97.1
13650	C	T	99.1					13650	C	T	98.3	13650	C	T	97.9	13650	C	T	98.8
13986	A	G	99.5	13986	A	G	99.8												
14059	A	G	99.5	14059	A	G	99.9												
14766	C	T	99.7	14766	C	T	99.9												
15110	G	A	99.7	15110	G	A	99.8												
15217	G	A	98.3	15217	G	A	99												
15301	G	A	99.6	15301	G	A	99.7												
15326	A	G	99.6	15326	A	G	99.6												
16114	C	A	99.5	16114	C	A	99.5												
16129	G	A	98.9	16129	G	A	98.4												
16213	G	A	99.2	16213	G	A	99.3												
16223	C	T	95.3	16223	C	T	97.7												
16274	G	A	99.3	16274	G	A	99												
16390	G	A	98.7	16390	G	A	99.3												

Figure 83 - A Table displaying mtDNA genotypes detected in patient 15 founder tumour, cellular and cell-free urine samples, and buffy coat collected following Robotic Cystectomy. m.6052A>G was identified at 80% heteroplasmy in the founder bladder, tumour, confirmed at 93% within the urine cell pellet, 96% in the cell-free urine, and at 51.7% within the Buffy Coat sample, highlighted in yellow. mtDNA variants only found in each sample were highlighted in green.

5.8.19 Bivariate plots to display urothelial specific cell specific populations within patient 15 urine sample after Uroplakin 1b staining.

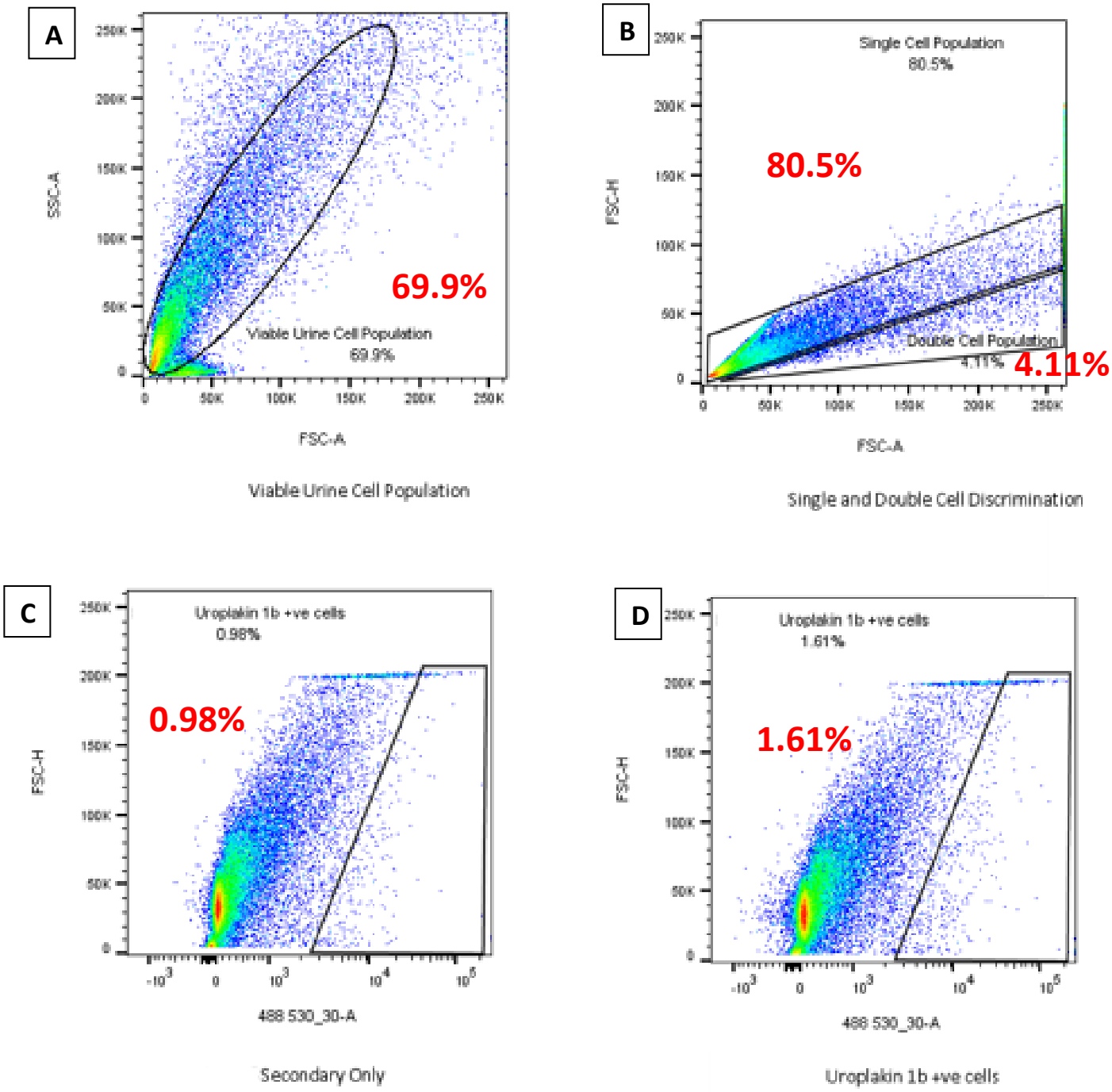

Figure 84 - Bivariate dot plots of patient 15's urine cells displaying (A)69.9% viable urine cell population, (B) 80.5% single and 4.11% doublet cell discrimination populations, (C)0.98% urine cells with secondary antibody only added and (D) 1.61% Urothelial positive cell population.

69.9% viable urine cells were analysed, 80.5% singlet and 4.11% doublet cells distinguished from the patients' urine sample and 1.61% of this urine cell population were urothelial cell specific.

5.8.20 Bivariate plots to display basal cell populations within patient 15 urine sample after CD49f staining.

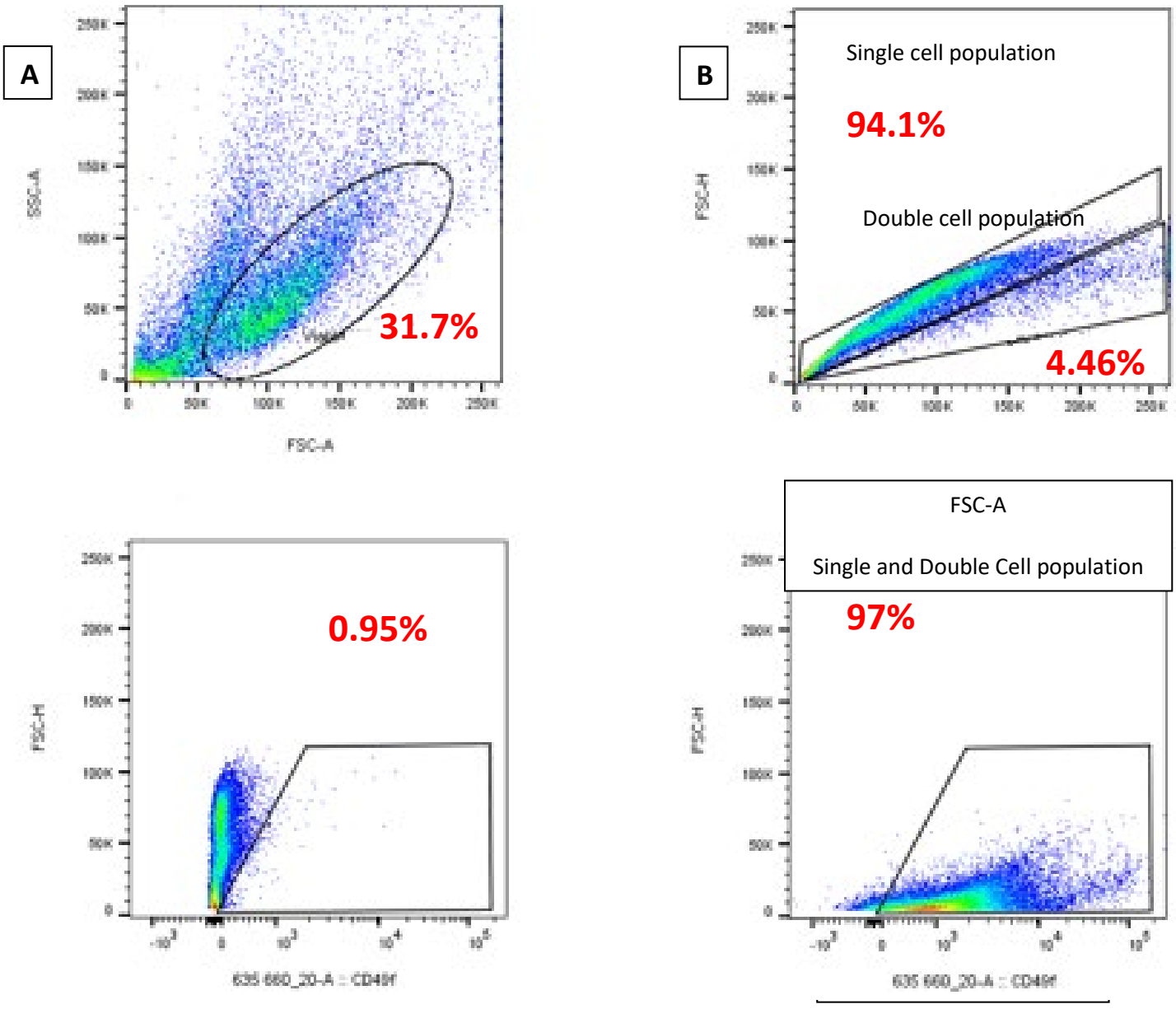

Figure 85 - Bivariate dot plots of patient 15's urine cells displaying (A) 31.7% viable urine cell populations, (B) 94.1% single and 4.46% doublet cell discrimination populations, (C)0.95% urine cells with secondary antibody only, and (D) 97% Basal positive cell population.

31.7 % viable urine cells were analysed, 94.1% singlet and 34.46% doublet cells distinguished from the patients' urine sample and 97% were basal cell specific during the detection of the mtDNA m.6052A>G genotype in the patients' bladder tumour, urine cellular, cell-free, and buffy coat.

5.9 Discussion

This proposed urinary mtDNA test provides a significant competitive advantage over urinary DNA biomarkers developed for the initial diagnosis of bladder cancer. The approach is uniquely positioned to tackle incomplete resection and recurrence by using a definitive lineage tracing method. Alternative methodologies are limited or provide no data on their utility in surveillance (Goodison et al., 2013). Cystoscopy is the main approach to monitor BC surveillance; however, this is uncomfortable, painful, time consuming, and puts a burden on the NHS due to the high cost of follow-up cystoscopy.

Examining genetic alterations within urine offers clinical utility with the identification of tissue-specific mutations. This allows the molecular stratification of tumours and an understanding of the response to treatment therapies. Such is exhibited clinically where cell-free DNA amplification for *EGFR* mutations is utilised for targeted therapy for non-small cell lung adenocarcinoma patients (Berz et al., 2016). In discussing my data, I will consider the results obtained in all the patients studied.

5.9.1 Mitochondrial pathogenic variants detected in patient 2 samples following cystectomy

Patient 2 initially presented with haematuria, a HG multifocal urothelial carcinoma confirmed after histopathological evaluation and 100% tumour was present in the founder bladder tumour biopsy. As urine is an abundant source of bladder tumour material it was hypothesised, that the tumour-specific mtDNA genotype was detected at a high heteroplasmy level (92%), and pathogenic variant m.10404T>C would be identified in the patients' matched urine samples. Cellular urine specimen confirmed the presence of the tumour-specific mtDNA variant at 91% heteroplasmy and pathogenic variant m.10404T>C was confirmed at an exceptionally low, but detectable 5% within the cell-free urine compartment. Given the mtDNA was obtained from the cells, the heteroplasmy in the urine supernatant was lower than expected . This may be due to PCR based NGS that can contribute towards allele dropout, where, if confirmed by Sanger sequencing the validation of the mtDNA variant could be confirmed. This validated the ability to lineage trace a tumour-specific mtDNA mutation in a non-invasive manner in urine, reflecting the bladder tumour abundant material composition of urine. Pathogenic variant m.10404T>C was not observed in the adjacent normal' bladder tissue or the Buffy Coat of the patient as expected, confirming

the presence of a tumour-specific variant, absent from the patients' normal urothelium, identifiable at high heteroplasmy in the cellular urine compartment (90%) and lower heteroplasmy in the matched patients' cell-free urine sampled (5%). As primer pair 4 was used to amplify the specific area of the mitochondrial genome covering m.10404T>C, the primer pairs utilised covered nucleotide positions m.9607-m.13859, which clarifies why some variants are not listed in the patients supernatant and Buffy Coat, compared to patients' primary bladder tumour and normal tissue and urine cell pellet.

Identifying pathogenic variant m.10404T>C within the cell-free urine compartment was expected as tumour cell-free DNA extracted from the urine of NMIBC patients has a higher tumour genome burden and allows greater detection (90%) of key nuclear genomic biomarkers than the intact cellular fraction (61%) (Togneri et al., 2016).

The phenomenon of the detection of mtDNA in urine previously remained unknown, however, the identification of a tumour-specific mtDNA genotype within both urine compartments in patient 2 suggests such follows similar characteristics. The 5% level of heteroplasmy at which pathogenic variant m.10404T>C was detected was surprisingly low as the targeted mtDNA variant was highly specific to the tumour, although this confirmation within urine provides confidence of limits of sensitivity within detection and robustness of the assay. Additional mtDNA variants identified within the urine pathogenic variants m.152T>C, m211A>G, m.3243A>G, m.3992C>T, m.4024A>G, m.5004T>C, m.5539A>G and m.8269G>A were also observed and pathogenic variant m.13860CAA>GGT within the buffy coat as displayed in Figure 66.

Using the basal cellular surface marker CD49f, 99% of cells were epithelial, as the urothelium is a stratified epithelium comprised of basal cells. Based on the bivariate plot data I have presented in Figure 68 of the basal cell populations within patient 2 urine sample after CD49f staining, the epithelial layer will give rise to basal cells. Urothelial specific cells were observed at 41% in urine, confirming the number of urothelial cells sequenced and verifying the mixed composition of various cell types present in urine. With additional time, I would look within the cell-free urine compartment and identify the diverse cell populations specific to the urine supernatant.

As the m.10404T>C pathogenic variant was identified in the primary bladder tumour and both cellular and cell-free urine compartments of patient 2, I can validate urine is a non-invasive liquid biopsy approach for urological malignancy surveillance. Bladder tumours can be examined in a non-intrusive and inexpensive manner reducing the dependence on invasive tumour monitoring for the patient.

5.9.2 Mitochondrial pathogenic variants detected in patient 4 samples following cystectomy

90% tumour was observed in patient 4's solid bladder tumour biopsy and a histopathological diagnosis of invasive HG tumour with the patient initially presenting with haematuria. Positively an intact epithelial and basal cell layer was observed as 93% CD49f positive cells were detected, and 55% urothelial specific cells were analysed for the confirmation of pathogenic variant m.4841G>A mtDNA specific genotype identification by whole mtDNA genome sequencing.

The tumour-specific mtDNA genotype pathogenic variant m.4841G>A was confirmed in both the patients' cellular urine at 43% heteroplasmy and cell-free urine at an exceptionally low heteroplasmy of 1%, confirming urine as a non-invasive approach to detect mtDNA variants. Tumour-specific mtDNA variants pathogenic variants m.5032G>A and m.16147C>T previously identified in the founder bladder tumour were not observed within the cellular and cell-free urine compartments. A single lineage can initiate from a single cell that has evolved towards cancer but has not yet become malignant. A single lineage is the smallest cancerised field, a cell evolving towards cancerous tendencies, although the cell is not in a malignant state. This concludes that every cancer arises from a likely detectable cancerised condition (Braakhuis et al., 2003). It can be proposed that pathogenic variants m.5032G>A and m.16147C>T were separate clones formed by initial single lineages that had not acquired lineage tracing abilities within the cellular and cell-free urine obtained from this patient, affording an explanation for the mtDNA variants not observed within the cellular and cell-free urine.

Published data confirms that mtDNA mutations are common in NMIBC, and are tumour specific, therefore absent from cells in the patient's normal bladder lining (Shakhssalim et al., 2013). This is confirmed in our data as all mtDNA variants detected pathogenic variants m.4841G>A, m.5032G>A, m.10404T>C and m.16147C>T were absent from the patients' normal urothelium.

Dominant mtDNA mutations may become established in a clonal cell population (Kassouf et al., 2015) suggesting an explanation for mtDNA variants seen in patient 4 that were not detectable within the patients' urine, particularly pathogenic variants m.5032G>A and m.16147C>T. Varying other cells are being shed into the urine, not just tumour cells, therefore perhaps there was a dilutional effect observed, as it may be that some of the tumour cells may be more sticky, more robust, and not shed as easily, explaining the pathogenic mtDNA genotype not being detectable within the urine, considering the tumour content was scored at 90%. Additionally, due to clonal expansion, it can prove difficult to distinguish driver mutations from passenger mutations within cancer (Ding et al., 2012). Across cancer types, it is still not clearly understood the order and timing in which mutations occur and whether a progression mutation can supersede a founder mutation (Bailey et al., 2018). This provides a probable explanation for the mtDNA variant m4841G>A being confirmed in patient 4's urine, although it is important to note the absence of the other mtDNA variants m.5032G>A and m.16147C>T from the patients' urine.

As primer pair 2 covering nucleotide positions m.3017-6944 and primer pair 5 covering nucleotide positions m.13365-771 were utilised to amplify the specific area of the mitochondrial genome covering m.4841G>A, m.5032G>A and m.16147C>T providing an explanation as to the reason some variants are not listed in the patients urine supernatant, cell pellet and Buffy Coat, compared to patients' primary bladder tumour and normal tissue.

5.9.3 Mitochondrial pathogenic variants detected in patient 10 samples following cystectomy

3% urothelial specific cells were determined from the patients' urine sample, suggesting the various other cell types comprising the composition of urine were analysed by whole mtDNA genome sequencing. As urine samples were acquired during Robotic Cystectomy, excessive saline washes were required during surgery, and it is probable, this may have contributed to the lack of urothelial specific cells observed by flow cytometry. On the contrary, from the bivariate dot plot, each dot represents a cellular event, and a clear presence of numerous cells were visible. Potentially, the identified cells were not of urothelial origin and were other cell types including glomerular, lymphocytes, and squamous cells. Macroscopically the urine sample appeared straw coloured and saline would emerge as clear, suggesting the urine sample analysed was not an entire sample of saline. CD49f is downregulated during

differentiation, and after CD49f staining, only 0.22% basal cells were observed, posing the biological question of basal cell differentiation occurring within the urothelium layers of this patient.

mtDNA pathogenic variant m.1180T>C was identified at 69.2% heteroplasmy level in the patients' founder bladder tumour and confirmed at 54.2% in the cellular urine, and at 42% within the non-cellular urine compartments, therefore I can conclude this mtDNA variant is tumour specific. Additional mtDNA genotypes m.4866T>A at 15.7% and m.11577G>A at 23.6% heteroplasmy were detected in the bladder tumour of patient 4 but not in any of the matched urine compartments. As pathogenic variants m.4866T>A and m.11577G>A were not observed in the Buffy Coat, these mtDNA genotypes are classified as tumour specific.

Pathogenic variant m.1180T>C was identifiable in the original bladder tumour and lineage traced within the cellular and cell-free urine samples; this confirms urine as a non-invasive method of detecting tumour-specific mtDNA variants.

Primer pair 1 covering nucleotide positions m.323-3574 was used to confirm the presence of m.1180T>C, which confirms why some variants are not listed in the patients urine supernatant, cell pellet and Buffy Coat, compared to patients' primary bladder tumour and normal tissue.

5.9.4 Mitochondrial pathogenic variants detected in patient 11 samples following cystectomy

An 85-90% invasive HG tumour was determined in patient 11 and after EpCAM staining 60% epithelial-specific cells were observed within the urine sample. 30% urothelial specific cells were identified, as bladder urothelium regenerates from basal and intermediate cells and the basal layer is composed of two layers of cuboidal cells ensuing the basement membrane (Guo et al., 2020).

Pathogenic variant m.9098T>C mtDNA variant was identified at 76% heteroplasmy level in the patients' founder bladder tumour and detected in the non-invasive collected cellular urine compartment at a higher heteroplasmy level of 93%, although, interestingly, the mtDNA genotype was not present within the cell-free urine sample. This may be due to the cell-free DNA yield being low (0.48 ng/µl), perhaps the variant was present, however, it may have been beyond the limit of what I could detect.

Pathogenic variant m.9098T>C was not classified as tumour specific as the mtDNA genotype due to the presence of the mtDNA genotype in the germline DNA buffy coat sample. Urine samples can identify mtDNA variants not observed in the other matched tumour samples (bladder tumour and cell-free urine) with pathogenic variants m.6409T>C at 5% and m.5170G>A at 4% identified within the cellular urine sample in patient 11 only.

Primer pair 3 covering nucleotide positions m.6358-10147 was utilised to confirm the presence of m.9098T>C, providing an explanation as to the reason some variants are not listed in the patients urine supernatant, cell pellet and Buffy Coat, compared to patients' primary bladder tumour and normal tissue.

5.9.5 Mitochondrial pathogenic variants detected in patient 13 samples following cystectomy

10-15% tumour was identified by the Uropathologist and after Laser Capture Microdissection of this area, the tumour content became 100% for analysis. Following microscopic H&E examination, a 5cm solid HG urothelial carcinoma was previously confirmed after histopathological assessment. Within the patients' matched urine 68% of cells were positively confirmed as basal cells and 10% were urothelial cell specific.

Additional mtDNA variants m.3284G>A at 22.3% heteroplasmy and m.15806G>A at 4.5% were detected within the founder bladder tumour but not present in any other matched patient samples suggesting clonal expansion within matched sample types has not occurred. Further pathogenic variants m.146T>C at 99.8% heteroplasmy, m.182CA>TG at 100% heteroplasmy, m.204T>C at 100% heteroplasmy, m.13590G>A at 99.5% heteroplasmy, m.13650C>T at 98.8% heteroplasmy, m.13926T>A at 3.5% heteroplasmy, m.13986A>G at 99.5% heteroplasmy, m.14059A>G at 99.7% heteroplasmy, m.16129G>A at 99.7% heteroplasmy and m.16114C>A at 99.7% heteroplasmy levels were observed only in the urine cell-free supernatant sample confirming the potential use of cell-free nucleic acids as biomarkers as cell-free nucleic acids have previously been identified as biomarkers in cancer patients (Schwarzenbach et al., 2011).

Primer pairs 1 covering nucleotide positions m.323-3574, primer pair 4 covering nucleotide positions m.9607-13859 and primer pair 5 covering m.13365-771 were used to identify mtDNA variants in the urine supernatant and cell pellet which confirms why some variants

are not listed in these partitions of patient 13's samples compared to patients' primary bladder tumour, bladder normal tissue and Buffy Coat.

5.9.6 Mitochondrial pathogenic variants detected in patient 15 samples following cystectomy

An 80-90% invasive solid tumour was confirmed after histopathological examination and 15% of urine cells were epithelial cell specific. 97% basal specific cell populations were detected and only 2% urothelial specific cells were positively identified within the urine population. Other cell types that make up the composition of urine were sequenced as only 2% of urothelial cells were observed within the patient's urine sample, although 15% of these were epithelial in origin.

Clonal expansion of germline variant m.6052A>G mtDNA variant was observed after detection at 51.7% heteroplasmy level in the patients' buffy coat. Within the patients' founder bladder tumour, the mtDNA genotype was detected at 80% heteroplasmy and additionally identified within both urine compartments, at a higher heteroplasmy level of 93% in the cellular urine and in the cell-free urine compartment at 96%. Additional mtDNA variant m.204T>C at 44.4% heteroplasmy was observed in the buffy coat and at 100% in the founder bladder tumour sample highlighting the clonal expansion of another germline mtDNA variant.

I have observed mtDNA pathogenic variants within patients' bladder tumour and matched urine. This provides confidence in my hypothesis and the intention of developing a urine test for the non-invasive detection of mtDNA pathogenic variants. Within the urine, other mtDNA pathogenic variants were identified and further investigations as to where these variants are from would be of interest to me. They may be variants shed from other cells that make it into the urine, additionally, there may be the presence of other clonal expansions within the bladder.

Primer pairs 1 covering nucleotide positions m.323-3574, primer pair 2 covering m.3017-6944, primer pair 4 covering m.9607-13859 and primer pair m.13365-771 was utilised to confirm the presence of m.6052A>G, providing an explanation as to the reason some variants are not listed in the patients urine cell pellet and Buffy Coat, compared to patients' primary bladder tumour, bladder normal tissue and urine cell pellet.

5.10 Conclusion

Complete mitochondrial genome sequencing of voided bladder cancer cells has defined the presenting index lesion. Lineage tracing within accessible matched non-invasive patient samples such as urine can therefore offer urological malignancy surveillance and confirms tumour clearance and clonal recurrence.

Although mtDNA variants present in the normal tissue, but absent from the tumour were detected, such is still an interesting finding. It is unknown if m.3850G>A identified at 8.1% heteroplasmy in patient 4 normal bladder tissue and m.5553T>C detected at 4.8% heteroplasmy in patient 15 normal bladder tissue, contribute to transformation in normal epithelium from which tumours evolve. In a larger patient cohort mtDNA drivers of benign clonal expansions present in normal tissue could be investigated to further understand prevalent mtDNA pathogenic mutational driver genes.

Non-invasive liquid biopsy approaches offer an inexpensive alternative to current clinical practice and reduce the dependence on tumour monitoring. The nature of BC high recurrence rates (>40%), mandates frequent long-term cystoscopy, which is invasive for patients and makes the disease one of the most expensive cancers to manage. Urine affords non-invasive liquid biopsy of bladder tumours and to access large clinical trial related archives (NIHR HTA PHOTO and CRUK BCPP) allows rapid translation of any emerging biomarkers. From the results presented in this Chapter, I have shown proof of principle for a new biomarker of recurrence – urinary mtDNA variants, which now lays the foundations for a larger translational trial utilising the PHOTO and BCPP tissue archives.

Chapter 6: Are tumour-specific mtDNA genotypes identifiable in patients matched bladder tissue following TURBT?

6.1 Transurethral resection of the bladder (TURBT)

Current clinical processes for suspected BC sufferers involve patients undergoing a pipeline from which they receive a diagnosis, undergo TURBT, and then proceed to cystectomy (as described in section 1.71). Within the Bladder Cancer patient cohort I explored, residual tumour was detected at cystectomy and tumour-specific mtDNA variants were identified in patients' primary bladder tumour biopsies. The aim of the investigation in this chapter was to map back to original patient TURBT samples and identify any detectable mitochondrial DNA variants where residual tumour was confirmed post cystectomy.

Transurethral bladder resection is the first-line surgical treatment of NMIBC (Kassouf et al., 2015). The procedure utilises a resectoscope to access the bladder via the urethra to remove all macroscopically visible papillary non-muscle invasive tumours. TURBT material is routinely sent for histopathological analysis offering the ability to diagnose, stage, and treat visible bladder tumours. The histopathological type, size, grade, depth of tumour invasion, and extent of disease are determined from the TURBT sample, patients are then evaluated and placed on an appropriate treatment pathway accordingly. Patients' survival rates can be severely impacted if misdiagnosis occurs, specifically, if tumours are under staged (van der Heijden & Witjes, 2009).

Repeat TURBT is proposed in patients with HG or T1 staged tumours, providing pathologists had not identified the presence of muscle in the original resection (Qie et al., 2016). The quality and results of transurethral resection of the bladder can be improved by repeat TURBT. If widespread and multiple tumours are identified during resection, repeat TURBT is advised as often urologists cannot be sure if the initial resection was completed (Babjuk, 2009).

All surgical procedures carry risks due to the invasive nature of practices coupled with the threat of complications. Risks of perforations in the bladder during surgery are low, if such does occur a catheter is left in the bladder to allow healing and is removed when recovery has taken place (Qie et al., 2016).

Histopathology laboratories produce FFPE for most tissues processed offering a wealth of resourceful material and access to archival FFPE blocks. Obtaining reliable mtDNA sequencing reads from FFPE material, enables mtDNA variants to be investigated and identified from TURBT samples routinely processed within Histopathology. DNA damage, particularly fragmentation is induced by formalin fixation, which can result in low amounts of amplifiable template for PCR amplification, however using this approach I have been able to amplify mtDNA using five primer pairs to gain full coverage of the mitochondrial genome. DNA can be prone to fragmentation due to fixation; however, technologies are improving to provide long reads from FFPE material.

In this chapter I went on to look at matched TURBT samples, reliably amplify the mitochondrial genome, and confirmed previously detected mitochondrial DNA variants from the cystectomy cohort, by Next Generation Sequencing.

6.2 Materials and Methods

TURBT samples were received from five NMIBC patients undergoing Robotic Cystectomy within the Urology department at Freeman Hospital, Newcastle, UK. Genomic DNA was extracted from the original TURBT block (as described in section 2.7.2), and DNA quantified as described in section 2.8. To specifically amplify a targeted area of the mitochondrial genome, specific primer pair sets ~200bp were utilised to generate amplicons to investigate the presence of an mtDNA genotype previously detected within the primary bladder tumour biopsy, post cystectomy.

I performed targeted amplification and mtDNA sequencing of the mitochondrial genome, taking the most prevalent pathogenic variant detected as seen in Table 34, and I looked to target amplification from the original biopsy of the tumour to the TURBT sample.

Patient	Targeted mtDNA Variant	Nucleotide Positions	Primer sequences (5' > 3')	Amplicon Size (bp)
2	m.10404T>C	10354-10558	CCCTAAGTCTGGCCTATGAGTG - AGGGAGGATATGAGGTGTGAG	204
4	m.4841G>A	4783-4974	AACTAGGAATAGCCCCCTTTCAC - CACCTCAACTGCCTGCTATG	191
4	m.5032G>A	4953-5147	ATCATAGCAGGCAGTTGAGGT - CGTGGTGCTGGAGTTTAAGTTG	194
4	m.16147C>T	16046-16252	TGGGTACCACCCAAGTATTGAC - TGGAGTTGCAGTTGATGTGTG	206
10	m.1180T>C	1127-1318	ACTGCTCGCCCAGAACACTAC - TTACGTGGGTACTTGCGCTT	191
11	m.9098T>C	8196 - 9201	TGTAAAACGACGGCCAGTACAGTTTCA TGCCCATCGTC - CAGGAAACAGCTATGACCGTTGTCGT GCAGGTAGAGG	1005
		9127 - 10147	TGTAAAACGACGGCCAGTATCCTAGA AATCGCTGTCGC - CAGGAAACAGCTATGACCTAGCCGTT GAGTTGTGGTAG	1020

Table 34 - Oligonucleotide primer pairs used to amplify targeted areas of the mitochondrial genome, with reads aligned directly to the revised Cambridge reference sequence.

Amplicons underwent PCR (as described in section 2.9.6), 1.5% agarose gels were prepared to visibly confirm mtDNA amplification (described in section 2.9.7), amplicons purified (described in section 2.10) and amplicon libraries without fragmentation were prepared (described in section 2.11) for Next-Generation Sequencing. A minimum coverage of 200x was applied and sequence alignment to the mtDNA reference genome was carried out using the

variant plug-in Torrent Suite Variant Caller v5.10.1.20 (mtDNA custom settings). Analysis was performed on Torrent Suite version 5.10.2, utilising the coverage analysis and variant Caller plugin. 1% heteroplasmy cut-off detection limits were applied to call confident mtDNA variants in each TURBT sample.

6.3 Results

6.3.1 DNA Quantification

Genomic DNA was quantified using the nanodrop to determine sample quality and nucleic acid concentration for each TURBT sample. An example wavelength spectrum observed after quantification of DNA extracted from patient 10 TURBT sample is displayed in Figure 86 below.

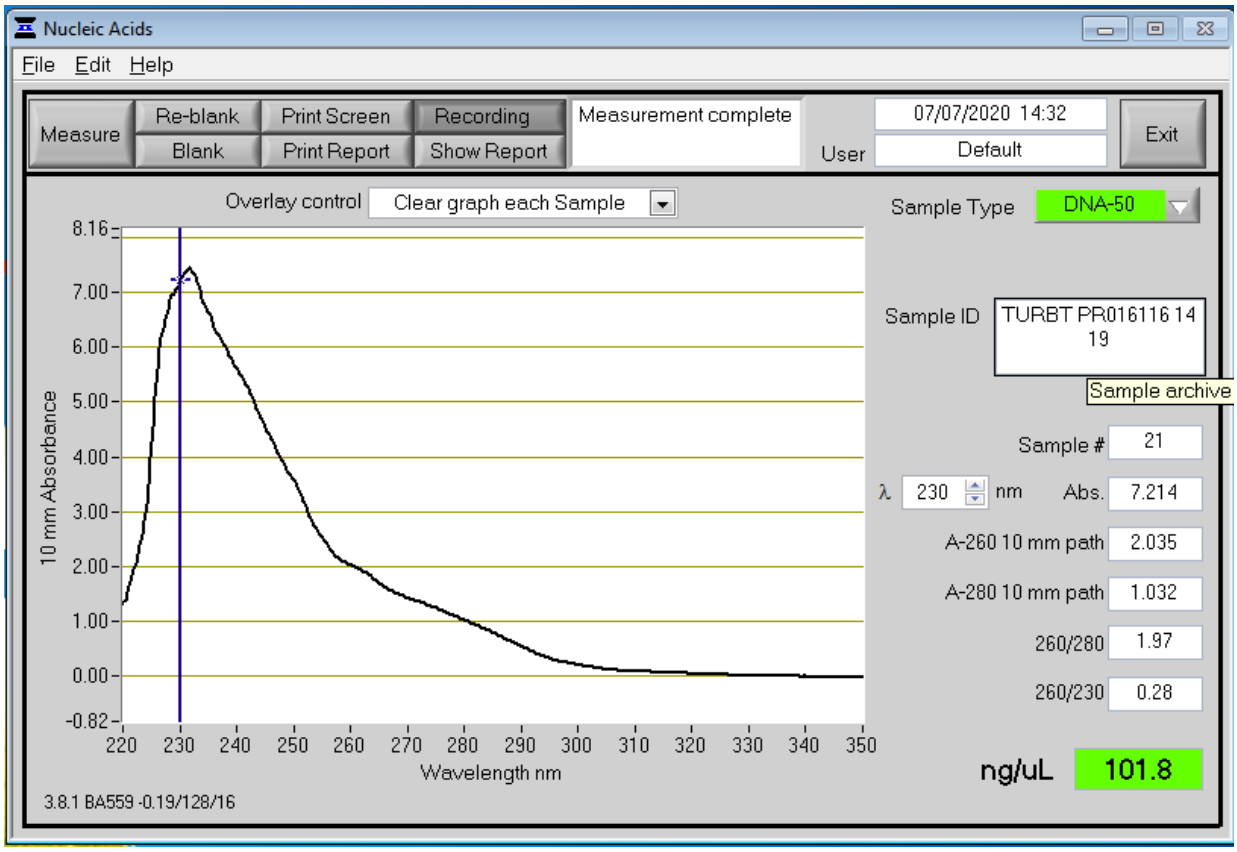

Figure 86 - Absorbance spectrophotometric graph displaying DNA quantification from patient 10 TURBT bladder tumour tissue.

The 260/280 ratio of 1.97 shows a good nucleic acid extraction with high purity, ideal for downstream targeted mtDNA amplification and mtDNA sequencing analysis. The 260/230 ratio of 0.28 signifies the presence of co-purified contaminants, expected due to the nature

of fragmented and damaged DNA induced by formalin fixation. Such is the nature of formalin-fixed material, with fixation routinely performed to preserve the cellular architecture and nature of tissues removed from the body for histopathological investigation.

Table 35 below, displays all nucleic acid purity results for each patient sample after nucleic acid extraction. A selected ~200bp area of the mitochondrial genome was amplified and targeted areas of the mtDNA genome were sequenced.

Nature of sample	Patient	260/280	260/230	Nucleic Acid amount (ng/µl)
FFPE TURBT Block	**2**	1.73	0.26	81.4
	4	1.66	0.24	71.6
	10	1.97	0.28	101.8
	11	1.77	0.25	85.3
	13	2.00	0.30	76.8

Table 35 - Absorbance spectrums displaying extracted genomic DNA from patients matched TURBT samples. 10x10 µm sections were microtome cut from FFPE TURBT blocks and utilised for mtDNA analysis.

6.3.2 mtDNA amplification

Post genomic DNA extraction, selected areas of the whole mitochondrial genome were amplified using specifically targeted primer pair sets described in section 2.9.. Gels were run at 65 V for 90 minutes and visualised on the ChemiDoc GelDoc system, selecting the illuminator which could excite SYBR Safe (as described in section 2.9.8).

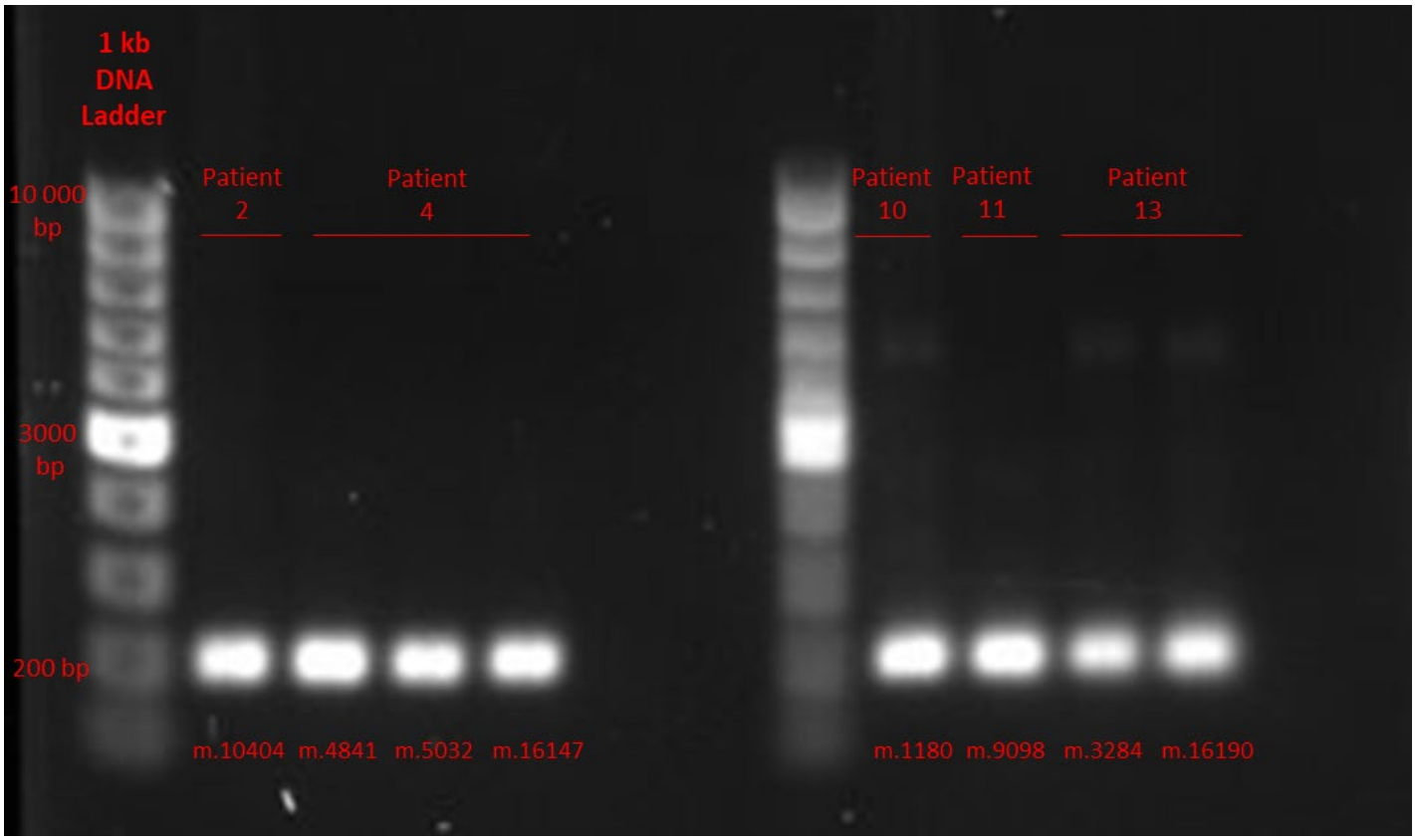

Figure 87 - Patient TURBT samples amplified with specific targeted mitochondrial genome primers amplicons visualised on 1.5% agarose gel. mtDNA amplification was confirmed in patient 2 at mtDNA position m.10404, patient 4 at mtDNA positions m.4841, m.5032 and m.16147, patient 10 at mtDNA position m.1180, patient 11 at mtDNA position m.9098, and patient 13 at mtDNA position m.3284.

6.3.3 Confirmation of mtDNA Variants detected within patient TURBT samples after targeted mtDNA sequencing

I went on to sequence the identical tumour-specific mtDNA variants detected within the bladder tumour post cystectomy within matched TURBT bladder samples and the data within section 6.3.4 suggested reliable mtDNA sequencing reads were obtained from FFPE bladder tumour material. This confirmed the presence of mtDNA genotypes within the original TURBT, with generated sequence files aligned to the whole mitochondrial genome.

6.3.4 Tumour-specific mtDNA variant m.10404T>C detected in patient 2's primary bladder tumour post cystectomy is detectable and confirmed in patients' matched TURBT sample.

mtDNA Pathogenic Variants detected in patient 2 TURBT sample within targeted mitochondrial genome positions m.10354-m.10558						
mtDNA Position	Reference	Variant	Allele Call	Level of Heteroplasmy (%)	Quality	Type
10404	T	C	Heterozygous	6.1	94.4219	SNP
10532	A	G	Homozygous	99.8	10933.4	SNP

Figure 88 - Detectable mitochondrial variants identified in patient 2 TURBT sample after mtDNA amplification utilising specific targeted mitochondrial genome primers spanning mitochondrial genome positions m.10354 – m.10558. Tumour-specific mtDNA variant m.10404T>C previously detected within patient 2's primary bladder tumour biopsy at 90.1%, urine cell pellet at 89.5% and urine supernatant at 4.9% heteroplasmy level is shown in blue.

The m.10404T>C variant was identified at 90.1% heteroplasmy in patient 2's bladder tumour biopsy and this tumour-specific mtDNA variant was also detected in the patient's original TURBT sample at 6.1% heteroplasmy. Other mtDNA variants were identified from the patients' TURBT sample within the targeted mitochondrial genome positions m.10354 – m.10558. The m.10532A>G variant was observed at homoplasmic levels within the patient's original TURBT sample, however as this mitochondrial DNA variant was also detected within the Buffy Coat at 99.1% heteroplasmy 99.9% in urine supernatant, 98.8% heteroplasmy in urine cell pellet, 99.8% in bladder normal tissue and 99.9% in bladder tumour tissue indicating the m.10532A>G variant is not a germline mutation (as displayed in Figure 88).

6.3.5 The m.4841G>A, m.16111C>A, and m.16147C>T mtDNA variants detected in patient 4's bladder tumour biopsy post cystectomy are identifiable in patients' original TURBT sample.

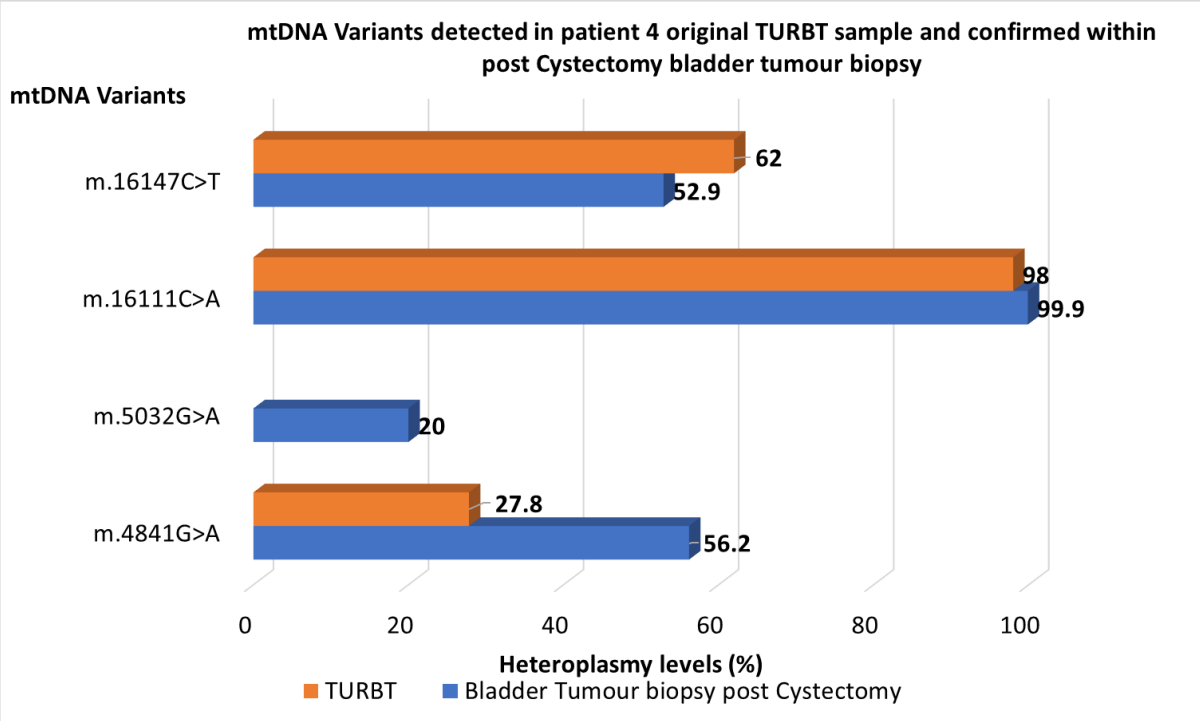

Figure 89 - mtDNA variants identified in patient 4 TURBT sample after mtDNA amplification within specific targeted mitochondrial genome primers spanning three mitochondrial genome positions m.4783-m.4974, m.4953-m.5147 and m.16046-m.15252. mtDNA genotypes detected in TURBT samples are indicated in orange and mtDNA variants previously detected within the primary bladder tumour biopsy are shown in blue.

A tumour-specific m.4841G>A mtDNA variant was identified in the patients' original TURBT sample at 27.8% heteroplasmy and observed at higher levels (56.2%) within the bladder biopsy investigated post cystectomy. The m.16111C>A variant was detected at similar levels (98%) in the original TURBT sample and confirmed as being homoplasmic within the bladder tumour biopsy post cystectomy. This mtDNA variant was not tumour specific as the mtDNA genotype was also present in the patients' normal biopsy. Tumour-specific pathogenic variant m.16147C>T observed in the original TURBT sample at 62% heteroplasmy, was also identifiable in the bladder tumour biopsy post cystectomy at levels of 52.9% heteroplasmy. The m.5032G>A variant was observed only within the bladder biopsy obtained at cystectomy at levels of 20% heteroplasmy and not within the original TURBT.

6.3.6 A tumour-specific m.1180T>C mtDNA variant detected in patient 10's bladder post cystectomy is confirmed in the original TURBT sample.

mtDNA Pathogenic Variants detected in patient 10 TURBT sample within targeted mitochondrial genome positions m.1127-m.1318						
mtDNA Position	Reference	Variant	Allele Call	Level of Heteroplasmy (%)	Quality	Type
1180	T	C	Heterozygous	63.1	15688.4	SNP

Figure 90 - Tumour-specific mtDNA variant identified in patient 10 TURBT sample after mtDNA amplification with specific targeted mitochondrial genome primers spanning mitochondrial genome positions m.1127 – m.1318. m.1180T>C detected within the patients' TURBT sample at 63.1% heteroplasmy level *is highlighted in yellow.*

The m.1180T>C variant was observed at 63.1% heteroplasmy level in patient 2's TURBT sample, and this tumour-specific mtDNA genotype was also detected in the patients' bladder tumour biopsy post cystectomy sample at a slightly increased (69.2%) level of heteroplasmy. No other mtDNA variants were identified within the targeted region spanning positions m.1127 to m.1318 of the mitochondrial genome.

I further investigated tumour heterogeneity within the patients' bladder tumour sample to confirm the tumour specific mitochondrial alteration m.1180T>C identified within the original TURBT sample. Interestingly, m.1180T>C was identified after further sectioning and sequencing deeper within the patients bladder tumour tissue. 10 µm deeper into the sample m.1180T>C was detected at 69% level of heteroplasmy within section 1, 81% level of heteroplasmy 50µm further into the tissue in section 2, 74% level of heteroplasmy in section 3, 77% level of heteroplasmy in section 4 and 79% level of heteroplasmy in section 5. Other mtDNA pathogenic variants (m.4866T>C, m.6766G>A and m.11577G>A) were identified at lower heteroplasmy levels, as displayed in Figure 91.

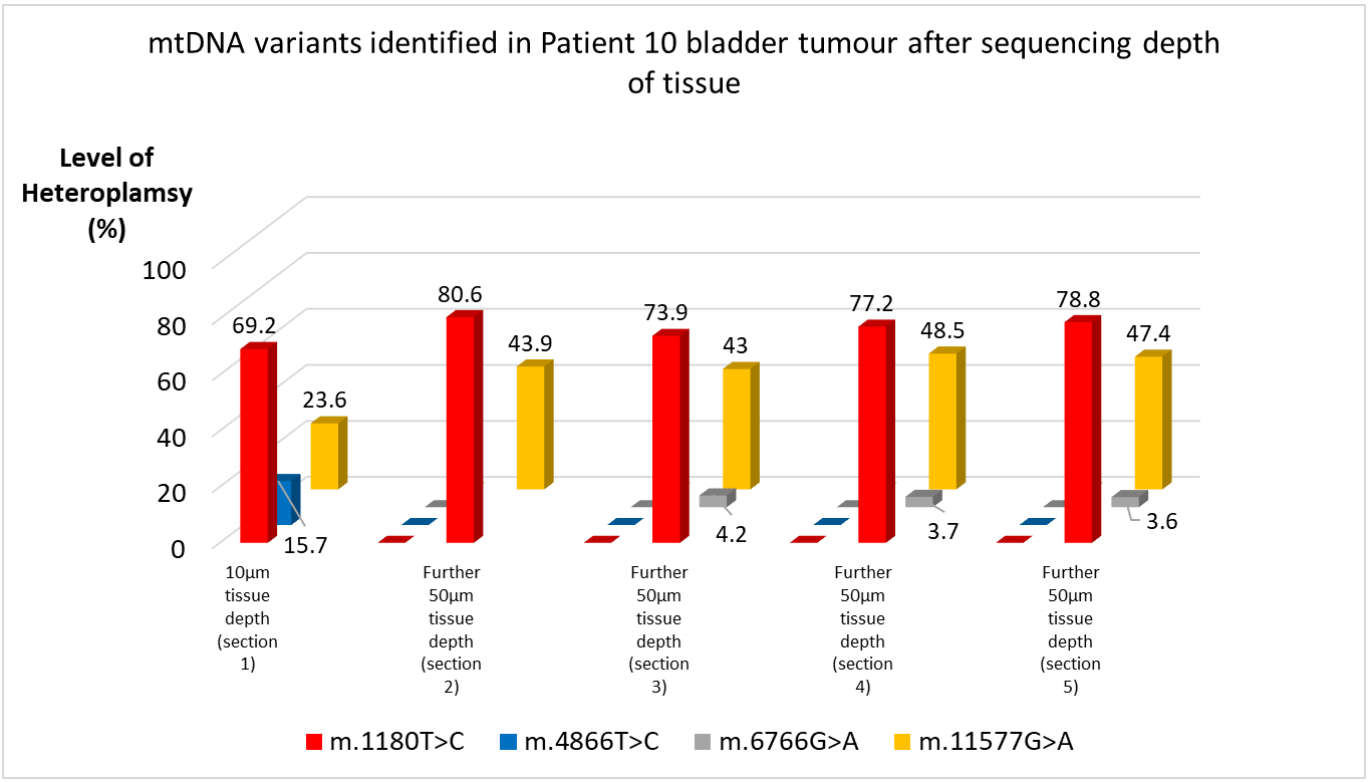

Figure 91 - mtDNA pathogenic variants identified after sampling 210 µm deep within patients' bladder tumour tissue.

6.3.7 mtDNA variant m.9098T>C detected in patient 11's bladder tumour post cystectomy are identifiable in the patients' original TURBT sample.

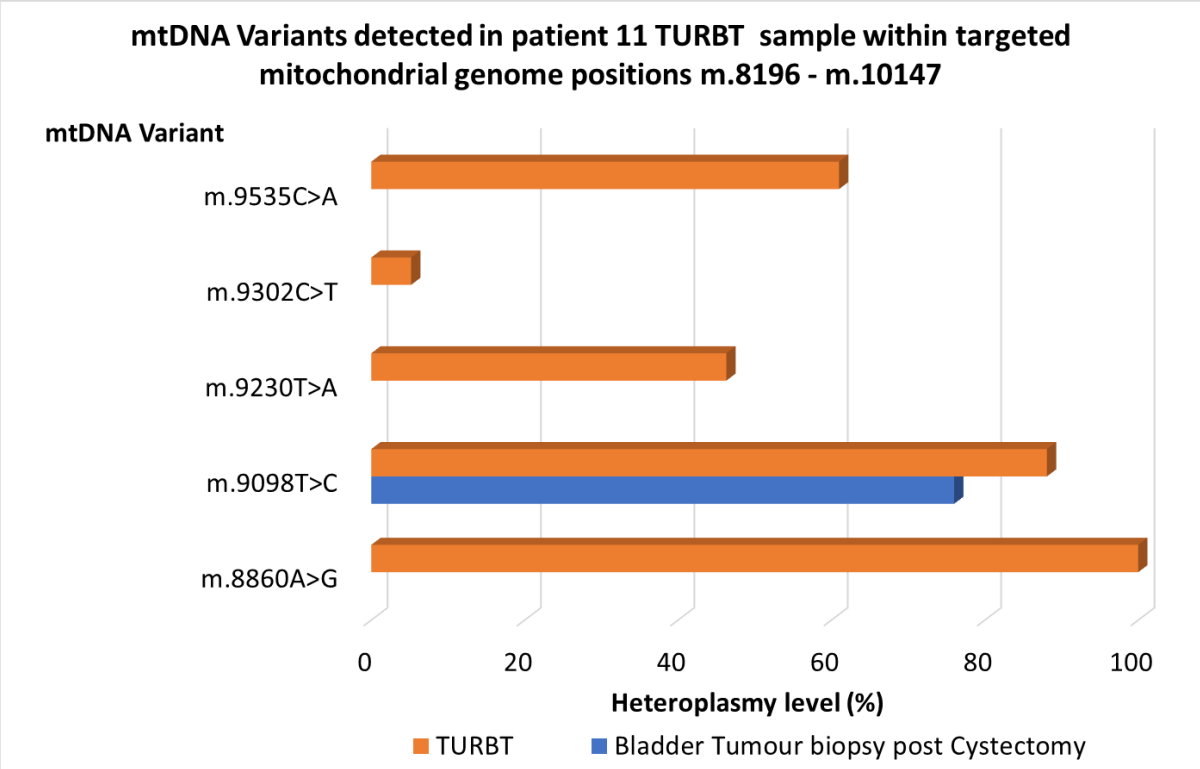

Figure 92 - mtDNA variants identified in patient 11 TURBT sample after mtDNA amplification with specific targeted mitochondrial genome primers spanning two mitochondrial genome positions m.8196 - m.9201 and m.9127-m.10147. mtDNA genotypes observed in TURBT samples are indicated in orange, and mtDNA variants previously detected within the primary bladder tumour biopsy are shown in blue.

The m.8860A>G variant was detected at homoplasmic levels in the original TURBT sample and the bladder tumour biopsy post cystectomy. The tumour-specific m.9098T>C variant observed in the original TURBT sample at 88.1% heteroplasmy, was also identifiable in the bladder tumour biopsy post cystectomy at 75.9% heteroplasmy. Other mtDNA variants were detected within the TURBT sample only, including m.9230T>A (46.3% heteroplasmy), m.9302C>T (5.2% heteroplasmy), and m.9535C>A (61% heteroplasmy) however, each of these mtDNA genotypes were not identified within the bladder biopsy investigated post cystectomy.

The tumour-specific mitochondrial alteration m.9098T>C was confirmed and identified after further sectioning and sequencing deeper within the patients' bladder tumour tissue. Ten microns deeper into the tissue, mitochondrial pathogenic variant m.9098T>C was detected at 77% level of heteroplasmy within section 1, 82% level of heteroplasmy in section 3, 77% level of heteroplasmy in section 4 and 79% level of heteroplasmy in section 5. Other mtDNA pathogenic variants (m.6272A>G, m.8764G>A, m.9750T>C, m.14348T>C, m.11577G>A and m.16074A>G) were identified at lower heteroplasmy levels within the 210 µm depth of bladder tumour tissue sequenced.

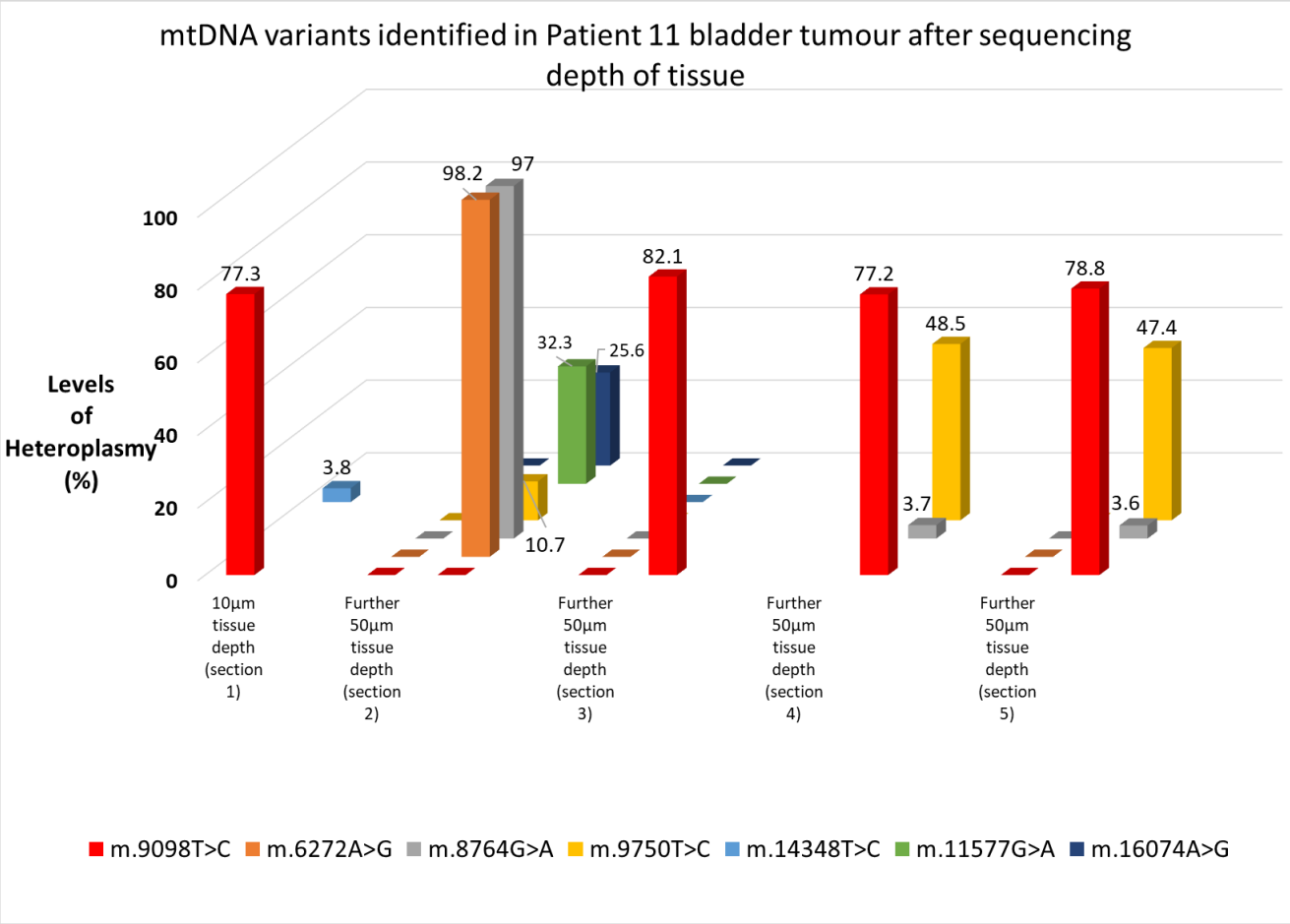

Figure 93 - mtDNA pathogenic variants identified after sampling 210 µm deep within the patients' bladder tumour tissue.

6.3.8 mtDNA pathogenic variants detected in patient 13's TURBT sample within targeted mitochondrial genome positions m.16015 – m.16223.

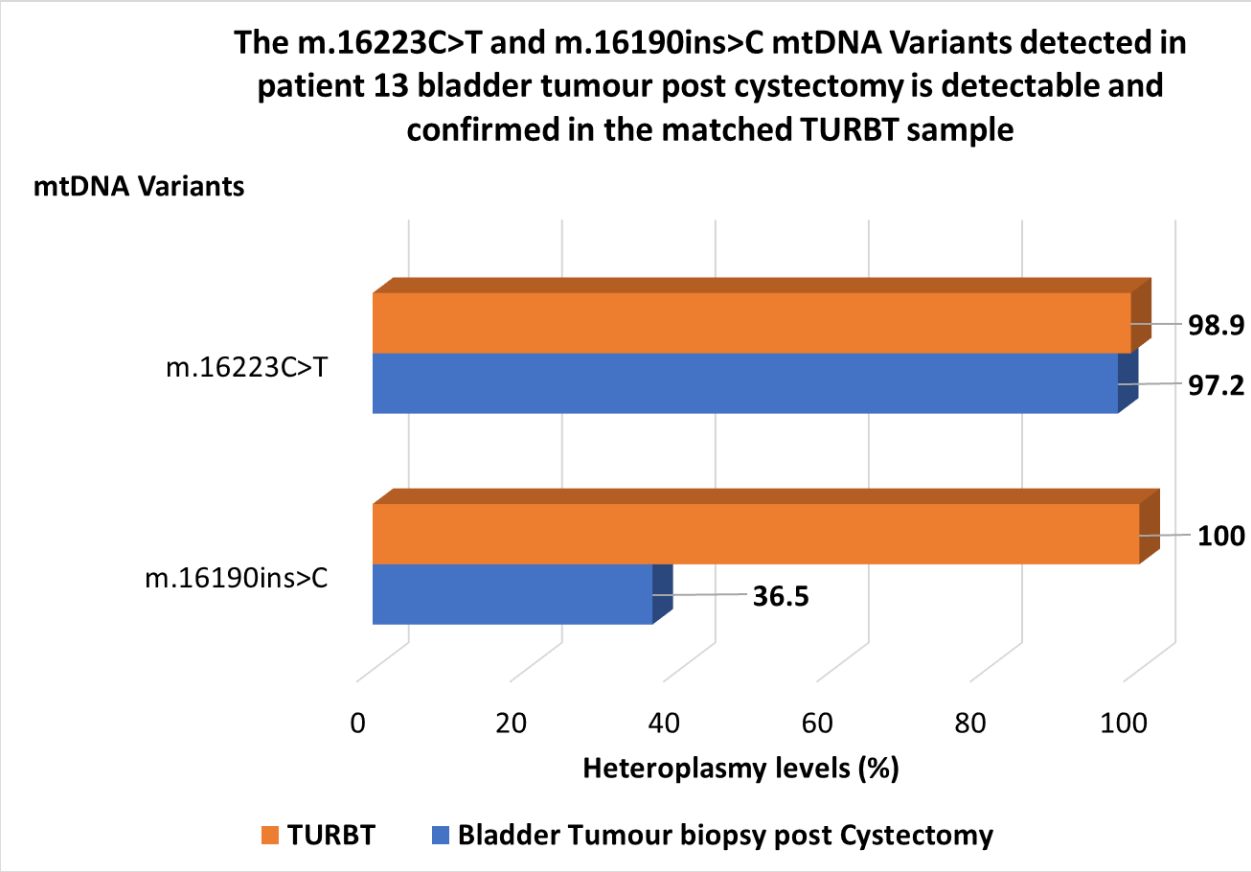

Figure 94 - mtDNA variants identified in patient 13 TURBT sample after mtDNA amplification with specific targeted mitochondrial genome primers spanning mitochondrial genome positions m.16015 – m.16223. mtDNA genotypes identified in TURBT samples are indicated in orange and mtDNA variants previously detected within the primary bladder tumour biopsy are shown in blue.

The m.16223C>T variant was detected at 98.9% heteroplasmy within the patients TURBT sample and within the primary bladder biopsy post cystectomy. Remarkably, m.16223C>T was observed at homoplasmic levels within both the original TURBT and in the primary bladder biopsy post cystectomy.

6.4 Discussion

6.4.1 Sequence artefacts in DNA from formalin-fixed tissue

This investigation has proven reliable long reads of ~200 bp can be obtained from patient FFPE TURBT material. Confirming mtDNA variants previously identified within fresh clinical patient bladder samples following cystectomy demonstrates the increasing use of FFPE material to obtain further molecular genetic information after the initial presentation of bladder cancer within TURBT samples. This unfolds a wealth of resourceful FFPE material within histopathology that can be investigated to further urologists, researchers, research nurses, and the wider community's genomics understanding of mtDNA variants within Bladder Cancer.

Often, greater sequence variants are observed in FFPE tissues compared to frozen tissues (Petrackova et al., 2019), reducing accuracy when calling pathogenic variants. Accurately detecting transformations is imperative, and this motivated our rationale for a targeted (~200bp) sequencing approach to confirm the presence of mtDNA variants within TURBT samples, originally detected in primary bladder tumour biopsies. Sequence artefacts enhance the risk of false positive mutation calls due to DNA damage from fixation (Blokzijl et al., 2016). To prevent this, validation of variant calls is advisable, as seen with this investigation by the confirmation of identifying mtDNA variants across patients' matched bladder tissues.

In the field of nuclear DNA sequencing, this has been a recognised challenge, mitochondrial DNA, with its abundance, seems less vulnerable, nevertheless, I sought to explore the suitability of FFPE material for DNA sequencing. After extensive protocol optimisation, I obtained good quality DNA from each TURBT sample, the 260/280 ratio within this TURBT sample cohort ranged between 1.66-2.00 (as described in Table 35), and a ratio of ~1.8 is largely regarded as 'pure DNA'. This suggests good nucleic acid extraction, particularly from FFPE material. The 260/230 ratio, a secondary measure of nucleic acid purity indicates the presence of co-purified contaminants if the ratio is lower than 1.8. The 260/230 ratio is a secondary measure of nucleic acid purity and if the ratio is lower than 1.8, such indicates the presence of co-purified contaminants. Commonly, each sample had a significantly low 260/230 ratio, varying between 0.24 and 0.30 indicating the presence of co-purified contaminants. This is expected due to fragmented and damaged DNA induced by formalin fixations confirming the natural landscape of fixed material.

No error bars were calculated or presented on any of the figures displayed above, as extracted DNA was only amplified once within specific targeted regions of the mitochondrial genome where tumour-specific mtDNA variants had previously been identified. Additionally, only one TURBT FFPE block was provided for each patient, and 10x10 μm sections were taken for targeted genomic DNA extraction.

6.4.2 mtDNA genotypes detected in patient 2 TURBT sample

I expected the variants identified from within the cystectomy bladder tumour, cellular and cell-free urine samples to be present in the TURBT. The TURBT samples part of the tumours, and if the patient presents with large tumours, the TURBT may not have sampled specifically that area of the tumour. With the TURBT sample, not all the material may have been tumour in my analysis. Therefore, if sub-clonal expansions are present, they may not be overlapping between cystectomy and TURBT, as I sampled different areas, and one could perform multi-regional sequencing. However, with truncal mutations that occurred early and then subsequently transmitted to all the tumour, I would still expect these to be detectable, and it appears that I observed that with the high-frequency m.10353G>C, m.10404T>C, and m.10532A>G variants that were detected. Precision medicine relies on identifying pathogenic variants with confidence, and m.10532A>G was detected at identical heteroplasmy levels in both samples, suggesting reliable mtDNA sequencing reads were obtained from this investigation.

Interestingly the m.10404T>C variant was observed in both the original TURBT at 6.1% and a markedly increased heteroplasmy level of 91% in the bladder tumour biopsy post-cystectomy. After presenting with a pT1 multifocal early HG tumour, the patient did not take any medication and undertook cystectomy surgery only. The 40% risk of recurrence within 3 years and the high recurrence rate is known to reflect incomplete resection of tumours (Mowatt et al., 2011)). Although urologists do their utmost best, often tumours are missed beyond their control, and tumours remain after resection. Wide resection is advised during surgery as there is a substantial risk of tumour reoccurrence at the original site. With a high grade 2 tumour and widespread CIS local excision, the extensive nature of bladder tumours visible within this patients' biopsies may explain the clonal expansion of the m.10404T>C variant observed in the bladder tumour post cystectomy. The identification of tumour-specific m.10404T>C mtDNA variant in both the TURBT and bladder tumour biopsy post cystectomy

can confirm that the detection of mtDNA variants may indicate bladder tumour recurrence in patients.

Although the m.10353G>C variant was only detected within the TURBT sample and not the primary bladder tumour, routinely employing mtDNA sequencing for each cystoscopy replaced in surveillance can identify recurrence, minimise discomfort for the patient and provide savings on the NHS.

6.4.3 mtDNA variants identified in patient 4 TURBT sample

The tumour-specific m.4841G>A and m.16147C>T mtDNA variants were observed in both the original TURBT and primary bladder tumour biopsy. The m.4841G>A variant was identified at 27.8% in the original TURBT and an increased heteroplasmy of 56.2% in the bladder tumour indicating the clonal expansion of the mtDNA genotype. This supports the suggestion of undertaking mtDNA sequencing on TURBT samples to identify bladder cancer recurrence early within the patient. Comparable heteroplasmy levels of 98% in the TURBT sample and 100% in the primary bladder biopsy were observed in the variant m.16111C>A confirming this as a reliable mtDNA sequencing approach. Similar heteroplasmy levels at the m.16147C>T variant were identified at 62% heteroplasmy in the TURBT sample and 52.9% heteroplasmy in the primary bladder tumour biopsy, again confirming confidence when calling out these mitochondrial variants. From the histopathological diagnosis, local excision could not be confirmed, HG tumour was present, and although there were two mtDNA variants only identified in the TURBT sample m.5148A>G, and m.9098T>C, yet again this demonstrates the aims of this investigation have been met and TURBT samples could provide a reliable biomarker for bladder cancer recurrence.

6.4.4 mtDNA genotype detected in patient 10 TURBT sample

The tumour-specific m.1180T>C variant was observed at 63.1% heteroplasmy in the original TURBT and 69.2% heteroplasmy level in the primary bladder tumour, within the targeted m.1127 to m.1318 mitochondrial genome region that was sequenced. Other lower level mtDNA variants were not detected in this targeted mitochondrial region sequenced within the TURBT sample. Such may be associated with the LG papillary urothelial carcinoma patient 10 originally presented with, and as this is a feasibility study a direct correlation between the identification of mtDNA variants and grade and stage of Bladder Cancer cannot be inferred.

Interestingly, after further sequencing a 240 µm depth of patient 10's bladder tumour tissue, the m.1180T>C pathogenic variant was detected at 81%, 74%, 77% and 79% heteroplasmy. This suggests clonal expansion of the tumour specific mtDNA genotype, validating the reliability of the sequencing method used and confirms the correlation of smoking and bladder cancer diagnosis, as the patient investigated was a smoker. Although m.4866T>C was not identified after further sequencing the bladder tumour, m.11577G>A was detected at 24% in the original bladder tumour, at 44% heteroplasmy level a further 50 µm into the tissue, 43% a further 50 µm, 49% an additional 50 µm and 47% a further 50 µm, again suggesting the presence of clonal expansion of this mtDNA genotype within the tumour.

6.4.5 mtDNA variants detected in patient 11 TURBT sample

One mtDNA variant m.9098T>C was observed at similar heteroplasmy levels in both the original TURBT (88.1%) and primary bladder tumour biopsy (75.9%) within the targeted mitochondrial genome positions m.8196 to m.10147 regions sequenced. m.8860A>G was identified at 100% homoplasmy in the TURBT sample. With similar heteroplasmy levels of m.9098T>C mtDNA genotype observed in two distinct matched samples, confidence is provided in the detection of mtDNA variants within FPPE bladder material. As a result, it can be inferred that the primary aim of this investigation was completed as we have the ability to map back to original TURBT samples and identify mtDNA pathogenic variants in patients from the Bladder Cancer cohort where residual tumour was detected at cystectomy. Eight mtDNA genotypes were identified within the original TURBT sample m.1189T>C at 15.8% heteroplasmy level, m.1944C>G at 27.3%, m.7478G>A at 28.6%, m.7959C>T at 33.3%, m.9302C>T at 5.2%, m.9535C>A at 61% and m.16256C>T at 88.9% heteroplasmy. It is encouraging low-level mtDNA variants can be reliably identified within the selected mitochondrial genome region sequenced completing a proof of principle for the potential of an outstanding novel biomarker of Bladder Cancer recurrence. Patient 11's original histopathological diagnosis post TURBT suggested re-resection may be required to rule out MIBC, highlighting the presence of residual tumour being missed and left at the residual tumour site.

Interestingly, after further sequencing a 240 µm depth of patient 11's bladder tumour tissue, the m.9098T>C pathogenic variant was detected at 82%, 77% and 79% suggesting tumour-specific mtDNA genotype clonal expansion within the bladder tumour. Other mtDNA

genotypes were identified when the depth of the tumour was analysed, including m.9750T>C detected at 11% heteroplasmy level 60 µm deeper within the bladder tumour tissue, at 49% heteroplasmy level 160 µm deeper and at 47% heteroplasmy level a further 50 µm deeper into the tissue, again proposing a tumour specific mtDNA mark expanded within the tumour.

6.4.6 mtDNA variants detected in patient 13 TURBT sample

An invasive solid HG urothelial carcinoma was observed after TURBT, and following mtDNA sequencing, m.16223C>T was observed at similar heteroplasmy levels of 98.9% in the original TURBT sample and 97.2% in the primary bladder tumour biopsy. This implies a reliable methodological approach was applied, and certainty in the detection of mtDNA variants from within FFPE material was achieved.

6.5 Conclusion

To summarise mtDNA TURBT profiling, I found some pathogenic variants that were not consistently shared across both cystectomy and TURBT matched patient samples, however, these were generally identified at low frequency. I did detect some truncal mutations that were shared, which implies, as long as truncal variants are identified, this approach will be reliable. The main aim of this part of the investigation was to demonstrate that I can pick up mtDNA variants from the matched TURBT samples, confirming longer term this methodology can be employed for lineage tracing to detect BC recurrence in time. Hypothetically this, therefore, is an appropriate method to use.

Encouragingly, feasibility has been ensured for future investigations of other patient cohorts, including the largest patient randomised controlled Bladder Cancer clinical trial, PHOTO-T, as potentially mtDNA profiling can be performed on matched FFPE blocks and urine samples. In the future, I would have aimed to investigate additional Bladder Cancer patient cohorts of FFPE bladder tumour material from the Royal Victoria Hospital, Newcastle.

To conclude, I was able to confirm that reliable sequencing reads can be obtained from formalin-fixed bladder samples with cut-off detection limits of 1% heteroplasmy, providing confidence in identifying and confirming mtDNA genotypes present in FFPE TURBT material. Freshly collected bladder tumour material is not easy to obtain without ethical approval, material transfer agreements, huge efforts from research nurses and urologists time during surgery, whilst being faced with providing critical care for their patients under anaesthetic.

FPPE samples, therefore, provide a resource of material to be further studied, where actionable detectable variants can be identified enhancing mutational analysis within urothelial carcinomas.

Chapter 7: Conclusion

Bladder Cancer is a common urological disease; having described high rates of recurrence urologists have previously been unable to reliably detect relapse, a current relevant area of urological research. Within the results sections of this body of work, I demonstrated I could detect epithelial, urothelial, and basal cell populations of bladder cancer cells within urine. I went on to show that after histological assessment, whole mitochondrial genome sequencing can be undertaken, mitochondrial mutation marks identified, and I demonstrated that a portion were present within the patients' primary bladder tumour urine and TURBT sample. I performed validation work with matched patient tissue analysis, and this research now lays a platform for further clinical testing, particularly with the PHOTO-T cohort.

The PHOTO-T cohort consists of blood and urine samples collected serially at baseline, 3, 12, 24 and 36 months or recurrence, and FFPE tissue collected at baseline and recurrence only. Within this cohort of around 100 patients, mtDNA mutations that accumulate with age can be defined using protocols I have optimised for the detection of mtDNA in matched urine, bladder tissue biopsies, blood and TURBT samples. Patient matched primary tumour bladder biopsies, and control germline blood can undergo mtDNA sequencing, as shown in this study, and unique index mutations evaluated within urine. Furthermore, archival paraffin embedded patient bladder samples collected can be utilised for immunohistopathological analysis and longitudinal assessment of unique mtDNA mutations.

An understanding of the functional consequences on the various mitochondrial complexes through oxidative phosphorylation from detected mtDNA pathogenic variants would provide further insight into the role mitochondrial variants play in influencing bladder cancer cell growth, contributing to recurrence. Applying single cell sequencing approaches would accelerate our understanding of mtDNA variants within individual bladder cancer cells. Additionally, distinct cell-to-cell variability within the tumour microenvironment could be identified on a single cell level and not only within populations of cells.

Smoking is the leading risk factor for NMIBC, and as incidences are higher in males than females, this provided the rationale to deeply investigate patient 10 and 11's bladder tumour samples as both patients were smokers and male. Tumour specific mtDNA genotype

m.1180T>C was identified in the TURBT, bladder tumour, urine cell pellet and urine cell-free samples within patient 10, and m.9098T>C within the same samples investigated in patient 11. Additionally, evidence of clonal expansion and tumour heterogeneity were observed when whole genome mtDNA sequencing was performed throughout their 220 µm depth of bladder tumour sample studied confirming reliability of the proposed methodology to be applied within the urology clinical setting.

I have demonstrated evidence of tumour-specific mtDNA marks expanding within the bladder tumours after sampling original TURBT and matched bladder tumour samples. The mtDNA genes I have reported were exclusively within the amplified segment of the mitochondrial genome, and reads were called at 1% specificity. This 1% threshold was chosen to filter out background noise, and analysis of the program and filtering out low quality reads confirmed validity of the data.

References

Abedini, A., Zhu, Y. O., Chatterjee, S., Halasz, G., Devalaraja-Narashimha, K., Shrestha, R., S. Balzer, M., Park, J., Zhou, T., Ma, Z., Sullivan, K. M., Hu, H., Sheng, X., Liu, H., Wei, Y., Boustany-Kari, C. M., Patel, U., Almaani, S., Palmer, M., … Susztak, K. (2021). Urinary Single-Cell Profiling Captures the Cellular Diversity of the Kidney. *Journal of the American Society of Nephrology*, *32*(3), 614 LP – 627. https://doi.org/10.1681/ASN.2020050757

Andersson, E., Steven, K., & Guldberg, P. (2014). Size-based enrichment of exfoliated tumor cells in urine increases the sensitivity for DNA-based detection of bladder cancer. *PLoS ONE*, *9*(4). https://doi.org/10.1371/journal.pone.0094023

Andersson, S. O., Rashidkhani, B., Karlberg, L., Wolk, A., & Johansson, J. E. (2004). Prevalence of lower urinary tract symptoms in men aged 45-79 years: A population-based study of 40 000 Swedish men. *BJU International*. https://doi.org/10.1111/j.1464-410X.2004.04930.x

BA.Michael J.Ackerman., 2013 John R.Giudicessi. (2008). 基因的改变NIH Public Access. *Bone*, *23*(1), 1–7. https://doi.org/10.1038/jid.2014.371

Babjuk, M. (2009). Transurethral Resection of Non-muscle-invasive Bladder Cancer. *European Urology, Supplements*, *8*(7), 542–548. https://doi.org/10.1016/j.eursup.2009.06.003

Babjuk, M., Böhle, A., Burger, M., Capoun, O., Cohen, D., Compérat, E. M., Hernández, V., Kaasinen, E., Palou, J., Rouprêt, M., Van Rhijn, B. W. G., Shariat, S. F., Soukup, V., Sylvester, R. J., Zigeuner, R., & Catto, J. (2017). *EAU Guidelines on Non–Muscle-invasive Urothelial Carcinoma of the Bladder: Update 2016*. *4*(2), 4–7. https://doi.org/10.1016/j.eururo.2016.05.041

Babjuk, M., Oosterlinck, W., Sylvester, R., Kaasinen, E., Böhle, A., & Palou-Redorta, J. (2008). EAU Guidelines on Non-Muscle-Invasive Urothelial Carcinoma of the Bladder. *European Urology*, *54*(2), 303–314. https://doi.org/10.1016/J.EURURO.2008.04.051

Bailey, M. H., Tokheim, C., Porta-Pardo, E., Sengupta, S., Bertrand, D., Weerasinghe, A., Colaprico, A., Wendl, M. C., Kim, J., Reardon, B., Ng, P. K. S., Jeong, K. J., Cao, S., Wang, Z., Gao, J., Gao, Q., Wang, F., Liu, E. M., Mularoni, L., … Karchin, R. (2018). Comprehensive Characterization of Cancer Driver Genes and Mutations. *Cell*, *173*(2), 371-385.e18. https://doi.org/10.1016/j.cell.2018.02.060

Baltaci, S., Bozlu, M., Yildirim, A., Gökçe, M. I., Tinay, I., Aslan, G., Can, C., Türkeri, L., Kuyumcuoɬlu, U., & Mungan, A. (2015). Significance of the interval between first and second transurethral resection on recurrence and progression rates in patients with high-risk non-muscle-invasive bladder cancer treated with maintenance intravesical Bacillus Calmette-Guérin. *BJU International*.

Barlogie, B., Raber, M. N., Schumann, J., Johnson, T. S., Drewinko, B., Swartzendruber, D. E., Göhde, W., Andreeff, M., Freireich, E. J., Barlogie, B., Raber, M. N., Schumann, J., Johnson, T. S., Drewinko, B., Swartzendruber, D. E., Göhde, W., Andreeff, M., Freireich, E. J., Barlogie, B., … Freireich, E. J. (1983). Flow Cytometry in Clinical Cancer Research. *Cancer Research*, *43*(9), 3982–3997.

Berz, D., Raymond, V. M., Garst, J. H., & Erlander, M. G. (2016). Non-invasive urine testing of EGFR activating mutation and T790M resistance mutation in non-small cell lung cancer. *Experimental Hematology and Oncology*, *5*(1), 1–6. https://doi.org/10.1186/s40164-016-0052-3

Blanpain, C., & Simons, B. D. (2013). Unravelling stem cell dynamics by lineage tracing. *Nature Publishing Group*, *14*. https://doi.org/10.1038/nrm3625

Blokzijl, F., De Ligt, J., Jager, M., Sasselli, V., Roerink, S., Sasaki, N., Huch, M., Boymans, S., Kuijk, E., Prins, P., Nijman, I. J., Martincorena, I., Mokry, M., Wiegerinck, C. L., Middendorp, S., Sato, T., Schwank, G., Nieuwenhuis, E. E. S., Verstegen, M. M. A., … Van Boxtel, R. (2016). Tissue-specific mutation accumulation in human adult stem cells during life. *Nature*. https://doi.org/10.1038/nature19768

Bolla SR, Odeluga N, Amraei R, et al. Histology,Bladder (2023). Figure, benign urothelial cells, histology

Braakhuis, B. J. M., Tabor, M. P., Kummer, J. A., Leemans, C. R., & Brakenhoff, R. H. (2003). A Genetic Explanation of Slaughter's Concept of Field Cancerization: Evidence and Clinical Implications. *CANCER RESEARCH*, *63*, 1727–1730.

Breyer, J., Wirtz, R. M., Otto, W., Erben, P., Kriegmair, M. C., Stoehr, R., Eckstein, M., Eidt, S., Denzinger, S., Burger, M., Hartmann, A., & on behalf of the BRIDGE Consortium. (2017). In stage pT1 non-muscle-invasive bladder cancer (NMIBC), high KRT20 and low KRT5 mRNA expression identify the luminal subtype and predict recurrence and survival. *Virchows Archiv*. https://doi.org/10.1007/s00428-017-2064-8

Bryan, R. T., Shimwell, N. J., Wei, W., Devall, A. J., Pirrie, S. J., James, N. D., Zeegers, M. P., Cheng, K. K., Martin, A., & Ward, D. G. (2014). Urinary EpCAM in urothelial bladder cancer patients: Characterisation and evaluation of biomarker potential. *British Journal of Cancer*, *110*(3), 679–685. https://doi.org/10.1038/bjc.2013.744

Cancer Genome Atlas Research Network, T. (2014). Comprehensive molecular characterization of urothelial bladder carcinoma. *Nature*, *507*. https://doi.org/10.1038/nature12965

Carpenter, A. R., Becknell, M. B., Ching, C. B., Cuaresma, E. J., Chen, X., Hains, D. S., & McHugh, K. M. (2016). Uroplakin 1b is critical in urinary tract development and urothelial differentiation and homeostasis. *Kidney International*. https://doi.org/10.1016/j.kint.2015.11.017

Chakraborty, A., Dasari, S., Long, W., & Mohan, C. (2019). Urine protein biomarkers for the detection, surveillance, and treatment response prediction of bladder cancer. *American Journal of Cancer Research*, *9*(6), 1104–1117. http://www.ncbi.nlm.nih.gov/pubmed/31285945%0Ahttp://www.pubmedcentral.nih.gov/articlerender.fcgi?artid=PMC6610049

Choi, W., Porten, S., Kim, S., Willis, D., Plimack, E. R., Hoffman-Censits, J., Roth, B., Cheng, T., Tran, M., Lee, I. L., Melquist, J., Bondaruk, J., Majewski, T., Zhang, S., Pretzsch, S., Baggerly, K., Siefker-Radtke, A., Czerniak, B., Dinney, C. P. N., & McConkey, D. J. (2014). Identification of Distinct Basal and Luminal Subtypes of Muscle-Invasive Bladder Cancer with Different Sensitivities to Frontline Chemotherapy. *Cancer Cell*. https://doi.org/10.1016/j.ccr.2014.01.009

Clucas, J., & Valderrama, F. (2015). Correction to ERM proteins in cancer progression [J. Cell Sci. 127, (2015), 267-275]. *Journal of Cell Science*, *128*(6), 1253. https://doi.org/10.1242/jcs.170027

Cormio, A., Musicco, C., Pesce, V., Villani, R., Antonelli, A., & Barret, E. (2018). Age, mitochondria and bladder cancer. In *Journal of Gerontology and Geriatrics* (Vol. 2018, Issue 4, pp. 260–264). Pacini Editore S.p.A.

Cormio, Antonella, Sanguedolce, F., Musicco, C., Pesce, V., Calò, G., Bufo, P., Carrieri, G., & Cormio, L. (2017). Mitochondrial dysfunctions in bladder cancer: Exploring their role as disease markers and potential therapeutic targets. In *Critical Reviews in Oncology/Hematology*. https://doi.org/10.1016/j.critrevonc.2017.07.001

Croft, W. A., & Nelson, C.-E. (1979). Collection and Evaluation of Normal Exfoliated Urinary Bladder Cells in Man Using Scanning Electron Microscopy. *Scandinavian Journal of Urology and Nephrology*, *13*(1), 43–48. https://doi.org/10.3109/00365597909179998

Curtius, K., Wright, N. A., & Graham, T. A. (2017). An evolutionary perspective on field cancerization. In *Nature Reviews Cancer*. https://doi.org/10.1038/nrc.2017.102

Czerniak, B., Dinney, C., & McConkey, D. (2016). Origins of Bladder Cancer. *Annual Review of Pathology: Mechanisms of Disease*. https://doi.org/10.1146/annurev-pathol-012513-104703

D'Erchia, A. M., Atlante, A., Gadaleta, G., Pavesi, G., Chiara, M., De Virgilio, C., Manzari, C., Mastropasqua, F., Prazzoli, G. M., Picardi, E., Gissi, C., Horner, D., Reyes, A., Sbisà, E., Tullo, A., & Pesole, G. (2015). Tissue-specific mtDNA abundance from exome data and its correlation with mitochondrial transcription, mass and respiratory activity. *Mitochondrion*. https://doi.org/10.1016/j.mito.2014.10.005

Ding, L., Ley, T. J., Larson, D. E., Miller, C. A., Koboldt, D. C., Welch, J. S., Ritchey, J. K., Young, M. A., Lamprecht, T., McLellan, M. D., McMichael, J. F., Wallis, J. W., Lu, C., Shen, D., Harris, C. C., Dooling, D. J., Fulton, R. S., Fulton, L. L., Chen, K., … Dipersio, J. F. (2012). Clonal evolution in relapsed acute myeloid leukaemia revealed by whole-genome sequencing. *Nature*, *481*(7382), 506–510. https://doi.org/10.1038/nature10738

Dörrenhaus, A., Müller, J. I. F., Golka, K., Jedrusik, P., Schulze, H., & Föllmann, W. (2000). Cultures of exfoliated epithelial cells from different locations of the human urinary tract and the renal tubular system. *Archives of Toxicology*, *74*(10), 618–626. https://doi.org/10.1007/s002040000173

Elson, J. L., Samuels, D. C., Turnbull, D. M., & Chinnery, P. F. (2001). Random intracellular drift explains the clonal expansion of mitochondrial DNA mutations with age. *American Journal of Human Genetics*, *68*(3), 802–806. https://doi.org/10.1086/318801

Erden Tayhan, S., Tezcan Keleş, G., Topçu, İ., Mir, E., & Deliloğlu Gürhan, S. İ. (2017). Isolation and in vitro cultivation of human urine-derived cells: An alternative stem cell source. *Turkish Journal of Urology*, *43*(3), 345–349. https://doi.org/10.5152/tud.2017.93797

Erichsen, H., & Chanock, S. (2004). SNPs in cancer research and treatment. *British Journal of Cancer*, *90*, 747–751. https://doi.org/10.1038/sj.bjc.6601574

Franzen, C. A., Blackwell, R. H., Todorovic, V., Greco, K. A., Foreman, K. E., Flanigan, R. C., Kuo, P. C., & Gupta, G. N. (2015). Urothelial cells undergo epithelial-to-mesenchymal transition after exposure to muscle invasive bladder cancer exosomes. *Oncogenesis*, *4*(8), e163–e163. https://doi.org/10.1038/oncsis.2015.21

Giaretti, W. (1997). Flow cytometry and applications in oncology. *Journal of Clinical Pathology*, *50*(4), 275–277. https://doi.org/10.1136/jcp.50.4.275

Goodison, S., Rosser, C. J., & Urquidi, V. (2013). Bladder Cancer Detection and Monitoring: Assessment of Urine- and Blood-Based Marker Tests. *Molecular Diagnosis & Therapy*, *17*(2), 71–84. https://doi.org/10.1007/s40291-013-0023-x

Greaves, L. C., Barron, M. J., Plusa, S., Kirkwood, T. B., Mathers, J. C., Taylor, R. W., & Turnbull, D. M. (2010). Defects in multiple complexes of the respiratory chain are present in ageing human colonic crypts. *Experimental Gerontology*, *45*(7–8), 573–579. https://doi.org/10.1016/j.exger.2010.01.013

Greaves, L. C., Nooteboom, M., Elson, J. L., Tuppen, H. A. L., Taylor, G. A., Commane, D. M., Arasaradnam, R. P., Khrapko, K., Taylor, R. W., Kirkwood, T. B. L., Mathers, J. C., & Turnbull, D. M. (2014). Clonal Expansion of Early to Mid-Life Mitochondrial DNA Point Mutations Drives Mitochondrial

Dysfunction during Human Ageing. *PLoS Genetics*, *10*(9), 1–10. https://doi.org/10.1371/journal.pgen.1004620

Guo, C. C., Bondaruk, J., Yao, H., Wang, Z., Zhang, L., Lee, S., Lee, J. G., Cogdell, D., Zhang, M., Yang, G., Dadhania, V., Choi, W., Wei, P., Gao, J., Theodorescu, D., Logothetis, C., Dinney, C., Kimmel, M., Weinstein, J. N., … Czerniak, B. (2020). Assessment of Luminal and Basal Phenotypes in Bladder Cancer. *Scientific Reports*, *10*(1), 1–14. https://doi.org/10.1038/s41598-020-66747-7

Hanahan, D., & Weinberg, R. A. (2011). Hallmarks of cancer: The next generation. In *Cell*. https://doi.org/10.1016/j.cell.2011.02.013

Harman, D. (1992). Free radical theory of aging. *Mutation Research/DNAging*. https://doi.org/10.1016/0921-8734(92)90030-S

Hazkani-Covo, E., Zeller, R. M., & Martin, W. (2010). Molecular poltergeists: Mitochondrial DNA copies (numts) in sequenced nuclear genomes. In *PLoS Genetics*. https://doi.org/10.1371/journal.pgen.1000834

He, Y., Wu, J., Dressman, D. C., Iacobuzio-Donahue, C., Markowitz, S. D., Velculescu, V. E., Diaz, L. A., Kinzler, K. W., Vogelstein, B., & Papadopoulos, N. (2010). Heteroplasmic mitochondrial DNA mutations in normal and tumour cells. *Nature*. https://doi.org/10.1038/nature08802

Health Technology Assesement 2010, 14:1-331, iii---iv

Hedegaard, J., Lamy, P., Nordentoft, I., Algaba, F., Høyer, S., Ulhøi, B. P., Vang, S., Reinert, T., Hermann, G. G., Mogensen, K., Thomsen, M. B. H., Nielsen, M. M., Marquez, M., Segersten, U., Aine, M., Höglund, M., Birkenkamp-Demtröder, K., Fristrup, N., Borre, M., … Dyrskjøt, L. (2016). Comprehensive Transcriptional Analysis of Early-Stage Urothelial Carcinoma. *Cancer Cell*. https://doi.org/10.1016/j.ccell.2016.05.004

Hedley, D. W., Clark, G. M., Cornelisse, C. J., Killander, D., Kute, T., & Merkel, D. (1993). Consensus review of the clinical utility of DNA cytometry in carcinoma of the breast. *Breast Cancer Research and Treatment*, *28*(1), 55–59. https://doi.org/10.1007/BF00666357

Hertweck, K. L., & Dasgupta, S. (2017a). The Landscape of mtDNA Modifications in Cancer: A Tale of Two Cities. *Frontiers in Oncology*. https://doi.org/10.3389/fonc.2017.00262

Hertweck, K. L., & Dasgupta, S. (2017b). The Landscape of mtDNA Modifications in Cancer: A Tale of Two Cities. *Frontiers in Oncology*, *7*(November), 1–12. https://doi.org/10.3389/fonc.2017.00262

Hwang E.C., Choi H.S., Jung S., II, Kwon D.D., Park K., Ryu S.B. Use of the NMP22 BladderChek test in the diagnosis and follow-up of urothelial cancer: A cross-sectional study. *Urology.* 2011;77:154–159.

Ishikawa, K., Hashizume, O., Koshikawa, N., Fukuda, S., Nakada, K., Takenaga, K., & Hayashi, J. I. (2008). Enhanced glycolysis induced by mtDNA mutations does not regulate metastasis. *FEBS Letters*. https://doi.org/10.1016/j.febslet.2008.09.024

Ju, Y. S. (2016). Intracellular mitochondrial DNA transfers to the nucleus in human cancer cells. *Current Opinion in Genetics and Development*, *38*, 23–30. https://doi.org/10.1016/j.gde.2016.02.005

Kamat, A. M., Bağcıoğlu, M., & Huri, E. (2017). What is new in non-muscle-invasive bladder cancer in 2016. In *Turk Uroloji Dergisi*. https://doi.org/10.5152/tud.2017.60376

Kamat, A. M., Hahn, N. M., Efstathiou, J. A., Lerner, S. P., Malmström, P. U., Choi, W., Guo, C. C., Lotan, Y., & Kassouf, W. (2016). Bladder cancer. In *The Lancet*. https://doi.org/10.1016/S0140-6736(16)30512-8

Kamat, A. M., Vlahou, A., Taylor, J. A., Hudson, M. A., Pesch, B., Ingersoll, M. A., Todenhöfer, T., Van Rhijn, B., Kassouf, W., Grossman, H. B., Behrens, T., Chandra, A., Goebell, P. J., Palou, J., Sanchez-Carbayo, M., & Schmitz-Dräger, B. J. (2014). Considerations on the use of urine markers in the management of patients with high-grade non–muscle-invasive bladder cancer. *Urologic Oncology: Seminars and Original Investigations*, *32*, 1069–1077. https://doi.org/10.1016/j.urolonc.2014.06.017

Kassouf, W., Traboulsi, S. L., Kulkarni, G. S., Breau, R. H., Zlotta, A., Fairey, A., So, A., Lacombe, L., Rendon, R., Aprikian, A. G., Siemens, D. R., Izawa, J. I., & Black, P. (2015). CUA guidelines on the management of non-muscle invasive bladder cancer. *Canadian Urological Association Journal*, *9*(9–10), 690. https://doi.org/10.5489/cuaj.3320

Khan, L. B., Read, H. M., Ritchie, S. R., & Proft, T. (2017). Artificial Urine for Teaching Urinalysis Concepts and Diagnosis of Urinary Tract Infection in the Medical Microbiology Laboratory †. *Journal of Microbiology & Biology Education*, *18*(2), 1–6. https://doi.org/10.1128/jmbe.v18i2.1325

Kirches, E. (2017). MtDNA As a Cancer Marker: A Finally Closed Chapter? *Current Genomics*. https://doi.org/10.2174/1389202918666170105093635

Lamouille, S., Xu, J., & Derynck, R. (2014). Fakultas Psikologi Dan Sosial Budaya Universitas Islam Indonesia Yogyakarta. *Nature Reviews Molecular Cell Biology*, *15*(3), 178–196. https://doi.org/10.1038/nrm3758.Molecular

Lee, G. (2011). Uroplakins in the lower urinary tract. In *International Neurourology Journal*. https://doi.org/10.5213/inj.2011.15.1.4

Leiblich, A. (2017). Recent Developments in the Search for Urinary Biomarkers in Bladder Cancer. *Current Urology Reports*, *18*(12). https://doi.org/10.1007/s11934-017-0748-x

Lerner, S. P., & Robertson, A. G. (2016). Molecular Subtypes of Non-muscle Invasive Bladder Cancer. In *Cancer Cell*. https://doi.org/10.1016/j.ccell.2016.06.012

Li, M., Schönberg, A., Schaefer, M., Schroeder, R., Nasidze, I., & Stoneking, M. (2010). Detecting heteroplasmy from high-throughput sequencing of complete human mitochondrial DNA genomes. *American Journal of Human Genetics*. https://doi.org/10.1016/j.ajhg.2010.07.014

Lobban, E. D., Smith, B. A., Hall, G. D., Harnden, P., Roberts, P., Selby, P. J., Trejdosiewicz, L. K., & Southgate, J. (1998). Uroplakin Gene Expression by Normal and Neoplastic Human Urothelium. *The American Journal of Pathology*. https://doi.org/10.1016/S0002-9440(10)65709-4

López-Otín, C., Blasco, M. A., Partridge, L., Serrano, M., & Kroemer, G. (2013). The hallmarks of aging. In *Cell*. https://doi.org/10.1016/j.cell.2013.05.039

Lu, Tian and Jinming Li. “Clinical applications of urinary cell-free DNA in cancer: current insights and promising future.” *American journal of cancer research* 7 11 (2017): 2318-2332

Mack, E. (2007). Flow Cytometry controls, instrument setup and the determination of positivity. *Cytometry. Part A : The Journal of the International Society for Analytical Cytology*, *71*(1), 8–15. https://doi.org/10.1002/cyto.a

Maecker, T., Todd, C., & Levy, S. (1997). The tetraspanin facilitators. *The FASEB Journal*, *11*(6), 428–442.

Martincorena, I., Roshan, A., Gerstung, M., Ellis, P., Van Loo, P., McLaren, S., Wedge, D. C., Fullam, A., Alexandrov, L. B., Tubio, J. M., Stebbings, L., Menzies, A., Widaa, S., Stratton, M. R., Jones, P. H., & Campbell, P. J. (2015). High burden and pervasive positive selection of somatic mutations in normal human skin. *Science*, *348*(6237), 880–886. https://doi.org/10.1126/science.aaa6806

Massari, F., Ciccarese, C., Santoni, M., Iacovelli, R., Mazzucchelli, R., Piva, F., Scarpelli, M., Berardi, R., Tortora, G., Lopez-Beltran, A., Cheng, L., & Montironi, R. (2016). Metabolic phenotype of bladder cancer. *Cancer Treatment Reviews*, *45*, 46–57. https://doi.org/10.1016/j.ctrv.2016.03.005

Matuszewski, M. A., Tupikowski, K., Dołowy, Ł., Szymańska, B., Dembowski, J., & Zdrojowy, R. (2016). Uroplakins and their potential applications in urology. *Central European Journal of Urology*, *69*(3), 252–257. https://doi.org/10.5173/ceju.2016.638

McCrow, J. P., Petersen, D. C., Louw, M., Chan, E. K. F., Harmeyer, K., Vecchiarelli, S., Lyons, R. J.,

Bornman, M. S. R., & Hayes, V. M. (2016). Spectrum of mitochondrial genomic variation and associated clinical presentation of prostate cancer in South African men. *Prostate*, *76*(4), 349–358. https://doi.org/10.1002/pros.23126

Mitsuzuka, K., Handa, K., Satoh, M., Arai, Y., & Hakomori, S. (2005). A specific microdomain ("glycosynapse 3") controls phenotypic conversion and reversion of bladder cancer cells through GM3-mediated interaction of α3β1 integrin with CD9. *Journal of Biological Chemistry*, *280*(42), 35545–35553. https://doi.org/10.1074/jbc.M505630200

Moad, M., Hannezo, E., Buczacki, S. J., Wilson, L., El-Sherif, A., Sims, D., Pickard, R., Wright, N. A., Williamson, S. C., Turnbull, D. M., Taylor, R. W., Greaves, L., Robson, C. N., Simons, B. D., & Heer, R. (2017). Multipotent Basal Stem Cells, Maintained in Localized Proximal Niches, Support Directed Long-Ranging Epithelial Flows in Human Prostates. *Cell Reports*, *20*(7), 1609–1622. https://doi.org/10.1016/j.celrep.2017.07.061

Moll, R., Lowe, A., Laufer, J., & Franket, W. W. (1992). Cytokeratin 20 in Human Carcinomas A New Histodiagnostic Marker Detected by Monoclonal Antibodies. *American Journal of Pathology*, *140*(2).

Mowatt, G., N'Dow, J., Vale, L., Nabi, G., Boachie, C., Cook, J. A., Fraser, C., & Griffiths, T. R. L. (2011). Photodynamic diagnosis of bladder cancer compared with white light cystoscopy: Systematic review and meta-analysis. *International Journal of Technology Assessment in Health Care*, *27*(01), 3–10. https://doi.org/10.1017/S0266462310001364

Oldfors, A., Larsson, N. G., Holme, E., Tulinius, M., Kadenbach, B., & Droste, M. (1992). Mitochondrial DNA deletions and cytochrome c oxidase deficiency in muscle fibres. *Journal of the Neurological Sciences*, *110*(1–2), 169–177. http://www.ncbi.nlm.nih.gov/entrez/query.fcgi?cmd=Retrieve&db=PubMed&dopt=Citation&list_uids=1324295

Pathol, C. (1981). *of patients with grade I and grade*. 612–615.

Pérez-Amado CJ, Bazan-Cordoba A, Hidalgo-Miranda A, Jiménez-Morales S. Mitochondrial Heteroplasmy Shifting as a Potential Biomarker of Cancer Progression. *International Journal of Molecular Sciences*. 2021; 22(14):7369

Petrackova, A., Vasinek, M., Sedlarikova, L., Dyskova, T., Schneiderova, P., Novosad, T., Papajik, T., & Kriegova, E. (2019). Standardization of Sequencing Coverage Depth in NGS: Recommendation for Detection of Clonal and Subclonal Mutations in Cancer Diagnostics. *Frontiers in Oncology*, *9*(September), 1–6. https://doi.org/10.3389/fonc.2019.00851

Pisitkun, T., Johnstone, R., & Knepper, M. A. (2006). Discovery of urinary biomarkers. *Molecular and Cellular Proteomics*, *5*(10), 1760–1771. https://doi.org/10.1074/mcp.R600004-MCP200

Planz, B., Jochims, E., Deix, T., Caspers, H. P., Jakse, G., & Boecking, A. (2005). The role of urinary cytology for detection of bladder cancer. *European Journal of Surgical Oncology*, *31*(3), 304–308. https://doi.org/10.1016/j.ejso.2004.12.008

Polyak, K., Li, Y., Zhu, H., Lengauer, C., Willson, J. K., Markowitz, S. D., Trush, M. A., Kinzler, K. W., & Vogelstein, B. (1998). Somatic mutations of the mitochondrial genome in human colorectal tumours. *Nat Genet*, *20*(3), 291–293. https://doi.org/10.1038/3108

Qie, Y., Hu, H., Tian, D., Zhang, Y., Xie, L., Xu, Y., & Wu, C. (2016). The value of extensive transurethral resection in the diagnosis and treatment of nonmuscle invasive bladder cancer with respect to recurrence at the first follow-up cystoscopy. *OncoTargets and Therapy*. https://doi.org/10.2147/OTT.S103703

Raitanen MP; FinnBladder Group. The role of BTA stat Test in follow-up of patients with bladder cancer: results from FinnBladder studies. World J Urol. 2008 Feb;26(1):45-50. doi: 10.1007/s00345-007-0230-3. Epub 2008 Jan 8. PMID: 18180926.

Reznik, E., Miller, M. L., Şenbabaoğlu, Y., Riaz, N., Sarungbam, J., Tickoo, S. K., Al-Ahmadie, H. A., Lee, W., Seshan, V. E., Hakimi, A. A., & Sander, C. (2016). Mitochondrial DNA copy number variation across human cancers. *ELife*. https://doi.org/10.7554/eLife.10769

Riaz, N., Wolden, S. L., Gelblum, D. Y., & Eric, J. (2016). *HHS Public Access*. *118*(24), 6072–6078. https://doi.org/10.1002/cncr.27633.Percutaneous

Sapre, N., Anderson, P. D., Costello, A. J., Hovens, C. M., & Corcoran, N. M. (2014). Gene-based urinary biomarkers for bladder cancer: An unfulfilled promise? *Urologic Oncology: Seminars and Original Investigations*, *32*(1), 48.e9-48.e17. https://doi.org/10.1016/j.urolonc.2013.07.002

Satyal, U., Srivastava, A., & Abbosh, P. H. (2019). Urine Biopsy—Liquid Gold for Molecular Detection and Surveillance of Bladder Cancer. *Frontiers in Oncology*, *9*(November), 1–9. https://doi.org/10.3389/fonc.2019.01266

Schon, E. A., Dimauro, S., & Hirano, M. (2012). Human mitochondrial DNA: Roles of inherited and somatic mutations. *Nature Reviews Genetics*, *13*(12), 878–890. https://doi.org/10.1038/nrg3275

Schwarzenbach, H., Hoon, D. S. B., & Pantel, K. (2011). Cell-free nucleic acids as biomarkers in cancer patients. In *Nature Reviews Cancer*. https://doi.org/10.1038/nrc3066

Sfakianos, J. P., Kim, P. H., Hakimi, A. A., & Herr, H. W. (2014). The effect of restaging transurethral resection on recurrence and progression rates in patients with nonmuscle invasive bladder cancer treated with intravesical bacillus Calmette-Guérin. *Journal of Urology*. https://doi.org/10.1016/j.juro.2013.08.022

Shakhssalim, N., Houshmand, M., Kamalidehghan, B., Faraji, A., Sarhangnejad, R., Dadgar, S., Mobaraki, M., Rosli, R., & Sanati, M. H. (2013). The mitochondrial C16069T polymorphism, not mitochondrial D310 (D-loop) mononucleotide sequence variations, is associated with bladder cancer. *Cancer Cell International*. https://doi.org/10.1186/1475-2867-13-120

Shariat, S. F., Karam, J. A., Lotan, Y., & Karakiewizc, P. I. (2008). Critical Evaluation of Urinary Markers for Bladder Cancer Detection and Monitoring. *REVIEWS IN UROLOGY*, *120*(2).

Skinner, E. C. (2007). The best treatment for high-grade T1 bladder cancer is cystectomy. In *Urologic Oncology: Seminars and Original Investigations*. https://doi.org/10.1016/j.urolonc.2007.05.023

Stefano, G. B., & Kream, R. M. (2015). Cancer: Mitochondrial Origins. *Medical Science Monitor*. https://doi.org/10.12659/MSM.895990

Stewart, C. M., Kothari, P. D., Mouliere, F., Mair, R., Somnay, S., Benayed, R., Zehir, A., Weigelt, B., Dawson, S.-J., Arcila, M. E., Berger, M. F., & Tsui, D. W. (2018). The Value of Cell-free DNA for Molecular Pathology. *The Journal of Pathology*. https://doi.org/10.1002/path.5048

Sun, X., & St. John, J. C. (2016). The role of the mtDNA set point in differentiation, development and tumorigenesis. *Biochemical Journal*. https://doi.org/10.1042/BCJ20160008

Suzuki, T., Nagao, A., & Suzuki, T. (2011). Human Mitochondrial tRNAs: Biogenesis, Function, Structural Aspects, and Diseases. *Annual Review of Genetics*. https://doi.org/10.1146/annurev-genet-110410-132531

Swalwell, H., Kirby, D. M., Blakely, E. L., Mitchell, A., Salemi, R., Sugiana, C., Compton, A. G., Tucker, E. J., Ke, B. X., Lamont, P. J., Turnbull, D. M., McFarland, R., Taylor, R. W., & Thorburn, D. R. (2011). Respiratory chain complex i deficiency caused by mitochondrial DNA mutations. *European Journal of Human Genetics*, *19*(7), 769–775. https://doi.org/10.1038/ejhg.2011.18

Sylvester, R. J., Van Der Meijden, A. P. M., Oosterlinck, W., Witjes, J. A., Bouffioux, C., Denis, L., Newling, D. W. W., & Kurth, K. (2006). Predicting recurrence and progression in individual patients with stage Ta T1 bladder cancer using EORTC risk tables: A combined analysis of 2596 patients from seven EORTC trials. *European Urology*. https://doi.org/10.1016/j.eururo.2005.12.031

Taylor, R W, Taylor, G. A., Durham, S. E., & Turnbull, D. M. (2001). The determination of complete

human mitochondrial DNA sequences in single cells: implications for the study of somatic mitochondrial DNA point mutations. *Nucleic Acids Research*, *29*(15), E74–E74. https://doi.org/10.1093/nar/29.15.e74

Taylor, Robert W., & Turnbull, D. M. (2005). Mitochondrial DNA mutations in human disease. In *Nature Reviews Genetics*. https://doi.org/10.1038/nrg1606

Togneri, F. S., Ward, D. G., Foster, J. M., Devall, A. J., Wojtowicz, P., Alyas, S., Vasques, F. R., Oumie, A., James, N. D., Cheng, K. K., Zeegers, M. P., Deshmukh, N., O'Sullivan, B., Taniere, P., Spink, K. G., McMullan, D. J., Griffiths, M., & Bryan, R. T. (2016). Genomic complexity of urothelial bladder cancer revealed in urinary cfDNA. *European Journal of Human Genetics*, *24*(8), 1167–1174. https://doi.org/10.1038/ejhg.2015.281

Urology Today, UK, Diagram illustrating the different T-stages of bladder cancer. (© 2021 The University of Texas MD Anderson Cancer Center)

van der Heijden, A. G., & Witjes, J. A. (2009). Recurrence, Progression, and Follow-Up in Non-Muscle-Invasive Bladder Cancer. In *European Urology, Supplements* (Vol. 8, Issue 7, pp. 556–562). https://doi.org/10.1016/j.eursup.2009.06.010

Volkmer, J.-P., Sahoo, D., Chin, R. K., Ho, P. L., Tang, C., Kurtova, A. V., Willingham, S. B., Pazhanisamy, S. K., Contreras-Trujillo, H., Storm, T. A., Lotan, Y., Beck, A. H., Chung, B. I., Alizadeh, A. A., Godoy, G., Lerner, S. P., van de Rijn, M., Shortliffe, L. D., Weissman, I. L., & Chan, K. S. (2012). Three differentiation states risk-stratify bladder cancer into distinct subtypes. *Proceedings of the National Academy of Sciences*. https://doi.org/10.1073/pnas.1120605109

Vriesema, J. L. J., Aben, K. K. H., Witjes, J. A., Kiemeney, L. A. L. M., & Schalken, J. A. (2001). Superficial and metachronous invasive bladder carcinomas are clonally related. *International Journal of Cancer*. https://doi.org/10.1002/ijc.1402

Vyas, S., Zaganjor, E., & Haigis, M. C. (2016). Mitochondria and Cancer. In *Cell*. https://doi.org/10.1016/j.cell.2016.07.002

Weinstein, J N, Akbani, R., Broom, B. M., Wang, W., Verhaak, R. G. W., McConkey, D., Lerner, S., Morgan, M., Creighton, C. J., Smith, C., Cherniack, a D., Kim, J., Pedamallu, C. S., Noble, M. S., Al-Ahmadie, H. a, Reuter, V. E., Rosenberg, J. E., F.Bajorin, D., Bochner, B. H., … Eley, G. (2014). Comprehensive molecular characterization of urothelial bladder carcinoma. *Nature*, *507*(7492), 315–322. https://doi.org/10.1038/nature12965

Weinstein, John N., Akbani, R., Broom, B. M., Wang, W., Verhaak, R. G. W., McConkey, D., Lerner, S.,

Morgan, M., Creighton, C. J., Smith, C., Cherniack, A. D., Kim, J., Pedamallu, C. S., Noble, M. S., Al-Ahmadie, H. A., Reuter, V. E., Rosenberg, J. E., F.Bajorin, D., Bochner, B. H., … Eley, G. (2014). Comprehensive molecular characterization of urothelial bladder carcinoma. *Nature*, *507*(7492), 315–322. https://doi.org/10.1038/nature12965

Wesseling, J., Franchi, G., Guddo, F., Naspro, R., Macchi, R. M., Giunta, P., Pasquale, M. Di, Parente, M., Arizzi, C., Roncalli, M., & Campo, B. (2009). *of Carcinoma In situ of the Bladder :* 99–106.

Wiggins, R., Horner, P. J., Whittington, K., & Holmes, C. H. (2009). Quantitative analysis of epithelial cells in urine from men with and without urethritis: Implications for studying epithelial: Pathogen interactions in vivo. *BMC Research Notes*, *2*. https://doi.org/10.1186/1756-0500-2-139

Williams, S. B., Ye, Y., Huang, M., Chang, D. W., Kamat, A. M., Pu, X., Dinney, C. P., & Wu, X. (2015). Mitochondrial DNA Content as Risk Factor for Bladder Cancer and Its Association with Mitochondrial DNA Polymorphisms. *Cancer Prevention Research*. https://doi.org/10.1158/1940-6207.CAPR-14-0414

Wu, X. R., Kong, X. P., Pellicer, A., Kreibich, G., & Sun, T. T. (2009). Uroplakins in urothelial biology, function, and disease. In *Kidney International*. https://doi.org/10.1038/ki.2009.73

Yafi, F. A., Brimo, F., Steinberg, J., Aprikian, A. G., Tanguay, S., & Kassouf, W. (2015). Prospective analysis of sensitivity and specificity of urinary cytology and other urinary biomarkers for bladder cancer. *Urologic Oncology: Seminars and Original Investigations*, *33*(2), 66.e25-66.e31. https://doi.org/10.1016/j.urolonc.2014.06.008

Yang M, Zheng Z, Zhuang Z, Zhao X, Xu Z, Lin H. ImmunoCyt™ and cytology for diagnosis of bladder carcinoma: a meta analysis. Chin Med J (Engl). 2014;127(4):758-64. PMID: 24534237

Appendix A – Healthy Volunteer Consent Form

Northern Institute for Cancer Research

Please initial the boxes for each section:

1. I have read and understood the attached healthy volunteer information sheet and have been given a copy to keep. I have been informed by the doctor and senior member of staff (see below) as to the nature of the analysis that will be performed with my sample. I have had sufficient opportunity to ask questions and have no further questions at this time. I understand why the research is being done and any risks involved. ☐

2. I agree to give a sample for research purposes and if this consent is for giving a blood sample, I have not donated blood for research purposes within the last thirty days. ☐

3. I understand that I will not benefit financially if this research leads to the development of a new treatment or medical test. ☐

4. I understand that as my sample is anonymous it is untraceable and so cannot be withdrawn at a future date. ☐

5. I agree that the samples I have given can be stored in the NICR. ☐

6. I can confirm that I have no known underlying conditions or recent infections that would make me unsuitable as a healthy volunteer. ☐

Healthy Volunteer
Printed name…….
Signature ……Date ……..……

Doctor
Printed name……
Signature …… Date ……..……

Researcher

Printed name……

Signature …… Date ……..…….

PLEASE RETURN COMPLETED FORM TO QUALITY ASSURANCE MANAGER

Appendix B – Ethical approval for research involving human participants

Newcastle University

APPLICATION FOR APPROVAL OF A RESEARCH PROGRAMME INVOLVING HUMAN PARTICIPANTS IN A NON-CLINICAL SETTING

Registration No. *(office use only)* ☐☐☐☐☐☐

This application form is to be used by **STAFF** and **STUDENTS** seeking ethical approval for an **individual research project or programme** involving the study of human subjects in a non-clinical setting. Where the study involves a clinical setting or material derived from a clinical setting (e.g. tissue, blood or other bodily fluids, patient records, intervention procedures etc.) ethical approval or advice must be sought through the systems operated by the Central Office for Research Ethics Committees (COREC) – see http://www.corec.org.uk .

A completed version of this document should be emailed to the Secretary of your appropriate Ethics Committee in the University. *Applications must be completed on this form; attachments will not be accepted other than those requested on this form. This form has been designed to be completed electronically; no handwritten applications will be accepted.*

Research must NOT begin until approval has been received from the appropriate Ethics Committee.

CATEGORY: UNDERGRADUATE research *NO*
POSTGRADUATE research *YES*
STAFF research YES

PROGRAMME TITLE: Collection of blood, plasma and urine samples from healthy volunteers.

NAME OF RESEARCHER(S): Professor Andy Hall and Professor Craig Robson.
On behalf of all Northern Institute for Cancer Research Principal Investigators using samples from healthy volunteers.

NAME OF SUPERVISOR(S) (for student research): N/A

DATE: 20th JULY 2009

DECLARATION BY RESEARCHERS
The information contained in this application is accurate. I have attempted to identify all risks that may arise in conducting this research and acknowledge my obligations and the rights of the participants.

Researcher(s)
Professor Andy Hall — Name: ANDY HALL — Date 20/7/09

Professor Craig Robson — Name: CRAIG ROBSON — Date 20/7/09

(Office Use Only)

The appropriate Ethics Committee has considered the ethical aspects of this proposal. The committee recommends that the programme/project be:

☐ approved ☐ deferred ☐ not approved

Signed: **Print Name:** **Date** ...../...../.....

Page 1

Ethics Committee concerned:

PART A

1. YOUR CONTACT DETAILS

Please provide contact details for all researchers named on this application:

NAME	EMAIL	PHONE
Prof. Andy Hall Director of NICR	a.g.hall@newcastle.ac.uk	0191 246 4411
Prof. Craig Robson Prof. of Molecular Urology	c.n.robson@ncl.ac.uk	0191 246 4426

2. TYPE OF PROGRAMME/PROJECT

Please mark ONE box to indicate the predominant nature of this programme/project.

a) Questionnaire/Survey ☐
e.g., surveys of members of particular groups/organisations, mail out questionnaires, street surveys

b) Experiment ☐
e.g., participants completing tasks under controlled conditions, use of tasks/methods other than or in addition to questionnaires/surveys.

c) Observational ☐
e.g., observing people behave in a natural setting or in a laboratory

d) Other YES
Please describe: Collection of blood, plasma and urine samples donated by healthy volunteers recruited from NICR staff and postgraduate students.

3. PARTICIPANTS

		YES	NO	N/A
a)	Will you inform participants that their participation is voluntary?	YES	☐	
b)	Will you inform participants that they may withdraw from the research at any time and for any reason?	☐		N/A
c)	Will you inform participants that their data will be treated with full confidentiality and that, if published, it will not be identifiable as theirs?	YES	☐	

d)	Will you obtain written consent for participation?	YES	☐	
e)	Will you debrief participants at the end of their participation (i.e., give them an explanation of the study and its aims and hypotheses)?	☐	☐	N/A
f)	Will you provide participants with written debriefing (i.e., a sheet that they can keep that shows your contact details and explanations of the study)?	YES	☐	
g)	If using a questionnaire, will you give participants the option of omitting questions they do not want to answer?	☐	☐	N/A
h)	If an experiment, will you describe the main experimental procedures to participants in advance, so that they are informed about what to expect?	☐	☐	N/A
i)	If the research is observational, will you ask participants for their consent to being observed?	☐	☐	N/A

IMPORTANT If you have marked **NO** to any of the questions above and have marked **BOX A** below, please give an explanation (no more than 300 words):

4. ETHICAL ISSUES

a)	Will this programme/project involve deliberately misleading participants in any way?	YES ☐	NO NO
b)	Is there any realistic risk of any participant experiencing any degree of physical or psychological harm, distress or discomfort?	YES	☐
c)	Will you be administering drugs or other substances to your participants, or taking fluid or other samples from them?	YES TAKING SAMPLES	NO GIVING DRUGS
d)	Will your participants fall into any of the following special groups?		
	Schoolchildren (under 18 years of age)	☐	NO
	People with learning or communication disabilities	☐	NO
	People in custody	☐	NO
	People engaged in illegal activities (e.g., drug-taking)	☐	NO
	Other vulnerable people	☐	NO

IMPORTANT If you have marked **YES** to any of the questions above, then you must mark **BOX B** below and complete **PART B** of this form.

5. ETHICAL ASSESSMENT

Please mark ONE box:

A I consider that this programme has **NO** significant ethical implications to be brought before an Ethics Committee.

PROGRAMME/PROJECT SUMMARY. *Please provide a brief description of your programme/project. This should be sufficient for reviewers of this application to ascertain exactly what your research involves. For instance, it should include information about the aims of the programme/project, and also the sources of your participants (i.e., target group/s) and how you will be recruiting them. Also include a brief summary of what participants will be required to do*

(e.g., main procedures, tasks, tests). This description must be in simple, everyday language that is free from unnecessary technical terms and no more than 300 words. Please also attach a copy of your consent form. Also attach a copy of any questionnaires (if using them in this research). You do not need to complete Part B of this form.

B	I consider that this programme/project **MAY** have ethical implications that should be brought before the Ethics Committee, and/or it will be carried out with children or other vulnerable populations. *If you have marked this box, you **must** complete **PART B** of this form.*	**YES**

PART B

You need only complete this part if you believe that your programme/project may have ethical implications (e.g., use of deception) and you have marked **BOX B** above, or your programme/project will be carried out with children or other vulnerable populations.

1. PROGRAMME DETAILS

1.1 PROPOSED DURATION OF PROGRAMME From: JULY 2009 To: JULY 2014

1.2 PROGRAMME/PROJECT OUTLINE AND AIMS: (300words)

Several studies performed in the Northern Institute for Cancer Research involve the use of blood, plasma or urine collected from normal healthy volunteers. These samples are used as part of an assay or assay development as controls or standards. For example, in the Pharmacology laboratory, drug concentrations in patient samples are measured following drug administration. Analysis requires the extraction of drug from blood, plasma or other body fluids. To optimise conditions for these methods, expired plasma from the National Blood Transfusion Service is routinely used. However, it is sometimes necessary to use fresh blood or plasma that has not been frozen or stored for long periods. In this case, blood is obtained from healthy volunteers, with no drug administration, who work in the laboratory or the department. This is on a strictly voluntary basis, with no compulsion or coercion involved. Samples are always taken by a medically qualified member of staff, and appropriate precautions are taken to safeguard the donor and other members of staff from potential risk.

1.3 PROPOSED METHOD: *Provide an outline of the proposed method, including where and how data will be collected, and all tasks that participants will be asked to complete. Present this outline of the method in a step-by-step chronological order, and avoid using jargon and technical terms as much as possible (No more than 700 words).*

Where fresh samples are required from healthy volunteers they will be collected from volunteers recruited from staff and students of the Northern Institute for Cancer Research. To minimize the slight risk of compulsion or coercion volunteers will be requested to come forward in response to an e.mail request, sent to all staff and students on the institute mailing list.
Blood will always be taken by a medically qualified member of staff, and appropriate precautions taken to safeguard the donor and other members of staff from potential risk.
The maximum volume of blood taken on any one day will be less than 60ml and volunteers must not donate blood more than once a month. The blood or plasma is used solely as a means of mimicking samples taken from patients.
The analysis has no clinical implications for the donor, in terms of either health or exposure to chemicals or drugs. The samples are anonymous to protect donor confidentiality, so no information from the analysis can be communicated back to the donor. No electronic records will be kept identifying the donor and signed consent forms will be stored in a safe and secure location and only accessed by staff with a NHS trust confidentiality agreement or honorary contract.

1.4 DOES THIS PROGRAMME/PROJECT REQUIRE APPROVAL FROM AN EXTERNAL ETHICS COMMITTEE?

NO

IF YES, HAS APPROVAL ALREADY BEEN GRANTED?

☐ YES *(please attach a copy of the approval letter)*

☐ NO *(please submit a copy of the approval letter as soon as it becomes available. Note that you cannot proceed with data collection until approval has been granted by **all** relevant ethics committees)*

2. PARTICIPANT DETAILS

2.1 NUMBER OF PARTICIPANTS REQUIRED: 20 per annum on average, based on previous numbers.

AGE RANGE OF PARTICIPANTS: 20-65 years.

2.2 DOES THE RESEARCH SPECIFICALLY TARGET: *(Select as many as applicable)*

		YES	NO
a)	students or staff of this university	YES☐	☐
b)	adults (over the age of 18 years and competent to give consent)	YES☐	☐
c)	children/legal minors (anyone under the age of 18 years)	☐	NO
d)	the elderly	☐	NO☐
e)	people from non-English speaking backgrounds	☐	NO☐
f)	pensioners or welfare recipients	☐	NO☐
g)	anyone who is intellectually or mentally impaired to the extent that they cannot provide consent	☐	NO☐
h)	anyone who has a physical disability	☐	NO☐
i)	patients or clients of professionals	☐	NO☐
j)	anyone who is a prisoner or parolee	☐	NO☐
k)	any other person whose capacity to consent may be compromised	☐	NO☐
l)	any groups where a leader or council of elders may need to give consent on behalf of the participant	☐	NO☐

2.3 SOURCE AND MEANS BY WHICH PARTICIPANTS ARE TO BE RECRUITED

Please provide specific details as to how you will be recruiting participants. Where will your participants be sourced? How will people be told you are doing this research? How will they be approached and asked if they are willing to participate? If you are mailing or phoning people, please explain how you have their names and contact details. Also mention any specific criteria for choosing participants (i.e., exclusion/inclusion criteria) and whether you will provide incentives for participation (e.g., payment). If a recruitment advertisement is to be used for this programme/project, please attach a copy to this application.

Volunteers will be recruited from staff and students based in the Northern Institute for Cancer Research.
Requests for volunteers will be made via the NICR internal mailing list for staff and students. This general request system is to reduce the inclusion of reluctant volunteers responding to direct approaches from colleagues to donate samples.
There will be no specific inclusion/exclusion criteria.
No incentives will be provided.

3. MANAGEMENT OF ETHICAL ISSUES

3.1 POTENTIAL RISK TO PARTICIPANTS AND RISK MANAGEMENT PROCEDURES

Identify, as far as possible, all potential risks (small and large) to participants (e.g. physical, psychological, social, legal or economic, etc.) that are associated with the proposed research. Also explain any risk management procedures that will be put in place. Volunteers will be recruited on a strictly no coercion basis.

The risks associated with this procedure are low.
Slight physical discomfort may be caused by the venopuncture; there is a very low risk of fainting by some subjects and some individuals may develop bruising.
The method of recruitment is designed to eliminate any element of coercion (see 2.3).

3.2 DEBRIEFING

It is a researcher's obligation to ensure that all participants are fully informed of the aims and methodology of the programme/project, and to ensure that participants do not experience any level of distress, discomfort, or unease following a research session. Please describe the debriefing that participants will receive following the study and the exact point at which they will receive the debriefing. Also describe any particular provisions or debriefing procedures that will be in place to ensure that participants feel respected and appreciated after they leave the study. Please attach a copy of the written debriefing sheet that you will give to participants. If you do not plan to provide a written debriefing sheet, please explain why.

Donors will be given an information sheet describing the procedure (see attached document).

4. INFORMED CONSENT

4.1 PLEASE DESCRIBE THE ARRANGEMENTS YOU ARE MAKING TO INFORM PARTICIPANTS, BEFORE PROVIDING CONSENT, OF WHAT IS INVOLVED IN PARTICIPATING IN YOUR STUDY? *If you will be providing participants with a written information sheet, please attach it to this application.*

Information sheet attached.

4.2 PLEASE DESCRIBE THE ARRANGEMENTS YOU ARE MAKING FOR PARTICIPANTS TO PROVIDE THEIR FULL CONSENT BEFORE DATA COLLECTION BEGINS? *Participants should be able to provide written consent. Please attach the consent form that you will be using in your programme/project. If you think that gaining consent in this way is inappropriate for your programme/project, then please explain how consent will be obtained and recorded.*

Consent form attached

You have now completed this form. Please email this form to the Secretary of your Ethics Committee.